Exploration Systems Mission Directorate
NASA Advanced Capabilities Division
ISS Research

Science Requirements Definition (SRD)

The Zero Boil-Off Tank (ZBOT) Experiment

Version 3.9

May 7, 2008

Principal Investigator:
Dr. Mohammad Kassemi
National Center for Space Exploration Research (NCSER)
NASA Glenn Research Center, 21000 Brookpark Rd., Mail Stop 110-3
Cleveland, Ohio 44135
(216) 433-5031 (phone)
(216) 433-5033 (fax)
Email: Mohammad.Kassemi@nasa.gov

Co-Investigator:
Dr. David Chato
NASA Glenn Research Center
Cleveland, Ohio 44135
Email: David.J.Chato@nasa.gov

ZBOT Science Team:

PI: Dr. M. Kassemi (NCSER)
CoI: Dr. D. Chato (GRC)
PS: David Plachta (GRC)
RA: Steve Barsi (NCSER)

ZBOT Project Management:

PM: B. Sheredy (GRC)

Signature Page

Title of Experiment: ZBOT

Date: May 7, 2008

Revision: 3.9

Dr. Mohammad Kassemi Principal Investigator		Signature		Date
Dr. David Chato Co-Investigator		Signature		Date

CONCURRENCES
NASA Glenn Research Center

David Plachta ZBOT Project Scientist		Signature		Date
Bill Sheredy ZBOT Project Manager		Signature		Date
Dr. Fred Kohl Project Manager: ISS Research		Signature		Date
Dr. Francis Chiaramonte Program Executive: ISS Research		Signature		Date

Summary

NASA's projected exploration program includes a series of human and robotic expeditions to low and high earth orbit, Moon, Mars, and possibly the asteroids and moons of other planets. Integral to all phases of these space and planetary expeditions is *affordable* and *reliable* cryogenic fluid storage for use in the propellant or life support systems. Without safe, efficient, and flexible cryogen storage, economically justified human missions may not be possible.

Cryogen vaporization caused by various heat leaks into the tank from its surroundings is the main cause of storage tank self-pressurization. This has led to the development of innovative pressure control designs based on mixing of the bulk liquid with or without active cooling. Unfortunately, both tank pressurization and pressure control are governed by intricate and complicated dynamic interactions among the forced mixing, the various gravity dependent transport mechanisms in the vapor and liquid phases, and the condensation/evaporation process at the interface. Consequently, effective implementation and optimization of a dynamic pressure control system for space applications cannot be accomplished empirically, especially, since there is a serious scarcity of relevant microgravity data.

The aerospace engineering community feels that a large-scale in-space technology validation test or demonstration of the cryogenic storage tank prototype will be ultimately necessary. But with the budgetary and time constraints of the current lunar architecture design process, this is not a possibility. In any case, before such an ambitious technology validation space experiment becomes possible, small-scale targeted microgravity simulant fluid experiments and state-of-the-art two-phase flow CFD storage tank models that have been validated with the microgravity data can be used to first understand the underlying physical phenomena influencing tank pressurization in space and then to optimize and scale-up the pressure control mechanism for microgravity and/or on-surface applications. In this manner, the risks associated with the design of space-based storage tanks using only 1-g testing of the technology can still be greatly reduced. In this light, the objectives of the ZBOT project are four-fold:

1. Develop a small-scale simulant-fluid experiment for both preliminary ground-based testing and subsequent ISS flight experiments to obtain valuable microgravity empirical data for tank pressure control design and archival science data for model validation.
2. Build a science base for future space storage tank engineering efforts by elucidating the roles of the various interacting transport and phase change phenomena that impact tank pressurization and pressure control in variable gravity through systematic 1g and microgravity scientific investigation.
3. Develop, validate, and verify two-phase CFD models for tank pressure control that can be used to aid the future scale-up tank design.
4. Show the feasibility of Zero-Boil-Off (ZBO) pressure control scheme for microgravity and variable gravity applications by examining the effect of forced mixing of the bulk liquid on destratification and pressure reduction in a ventless Dewar.

The products of this research will be: a small-scale simulant-fluid tank pressurization flight experiment; validated and verified two-phase CFD models for cryogenic storage tanks; valuable microgravity stratification, mixing, and pressure reduction data obtained under controlled conditions conducive for model validation and benchmarking; a science document containing valuable 1g and microgravity experimental data and parametric simulations; and finally an engineering document with important empirical correlations for future storage tank design.

It is anticipated that the availability of relevant microgravity data and the development of the much-needed empirical correlations for mixing and destratification in space, together with

verification and validation of the CFD codes that will be used in the scale-up design of the future storage tank prototype will all contribute significantly to reduce the uncertainties associated with the development of cryogenic upper stages for flight. If the results of this research are brought to fruition they will ultimately contribute to reducing the risk and costs of future space expeditions in line with the needs of the NASA Exploration Initiative in preserving and sustaining human life and human habitats in space.

Table of Acronyms

ALLVT	Active Liquid Lumped Vapor Tank (model)
CFD	Computational Fluid Dynamics
CFM	Cryogenic Fluid Management
CoI	Co-Investigator
EDS	Earth Departure Stage
ISS	International Space Station
ISRU	In-situ Resource Utilization
LCH4	Liquid methane
LEO	Low Earth Orbit
LHe	Liquid helium
LH2	Liquid hydrogen
LN2	Liquid nitrogen
LOX	Liquid oxygen
LLAM	Lunar Lander Ascent Module
LLDM	Lunar Lander Descent Module
LVLH	Local Vertical Local Horizontal
MOP	Maximum Operating Pressure
MSG	Microgravity Science Glovebox
PI	Principal Investigator
PNP	Perfluoro-N-Pentane
PS	Project Scientist
RA	Research Associate
SRD	Science Requirements Definition
TTP	Thermodynamic Tank Pressurization (model)
TVS	Thermodynamic Vent System
XPOP	X-axis Perpendicular to Orbital Plane
XVV	X-axis Velocity Vector
YVV	Y-axis Velocity Vector
ZBO	Zero Boil Off
ZBOT	Zero Boil Off Tank (experiment)

Table of Contents

1. Introduction

The extension of human space exploration from low earth orbit into the solar system will be NASA's biggest challenge for the future. The projected exploration programs include a series of human and robotic expeditions to low and high earth orbit, Moon, Mars, and possibly the asteroids and other planetary moons. Integral to all phases of these space expeditions is *affordable* and *reliable* cryogenic fluid storage for use in the propulsion and life support systems.

The NASA Exploration Vision (Bush, 2004) for return to the Moon and travel to Mars has shaped NASA's short- and long-term technological needs in this area. NASA's short term propellant requirements are dictated by the robotic and human exploration of the Moon where NASA's Exploration Systems Architecture Study (NASA, 2005) has several important elements that are base-lined cryogenic propellant tanks for short- to moderate-duration storage. These include the Earth Departure Stage (EDS), the Lunar Lander Descent Module (LLDM) and the Lunar Lander Ascent Module (LLAM). The long-term NASA propellant requirements are determined by the Mars mission where there is a prominent need for efficient and long-duration cryogenic storage. Long term cryogenic tank systems are also needed for storage of both propellant and life support fluids in several In-Situ Resource Utilization (ISRU) options under consideration as parts of the Lunar and Mars architectures.

As a result of these technological needs, a Cryogenic Fluid Management (CFM) Program has been formed by NASA to address the key engineering and development issues associated with storage and transfer of cryogenic fluids in support of the Lunar and Mars architectures. A central aspect of this program is focused on the development of efficient tank pressure control systems.

1.1 Storage Tank Pressure Control

Effective pressure control for future cryogenic storage tanks is needed in order to ensure their structural integrity in withstanding self-pressurization without need for excessive venting that result in cryogen mass loss. Heat leaks through the tank thermal protection system and into the tank fluids is the main cause of liquid vaporization and self-pressurization of the tank (Salerno and Kittel, 1999; Kittel and Plachta, 2000). Ordinarily, direct venting to the outside surrounding can relieve the excess pressure. Unfortunately, in the microgravity environment, the position of the vapor-liquid interface is not well defined and direct venting is undesirable due to the possibility of expelling liquid along with vapor unless the propellant is first settled by firing the engine. In-Space venting is also undesirable because it prohibits manned flight operations around the storage tanks. In on-surface applications, the position of the vapor is better defined. Nevertheless continuous venting over a significant length of time still results in considerable loss of propellant or life support fluids.

Conventional passive storage technologies mainly rely on efficient insulation to minimize the heat leaks into the tank and periodic venting to relieve the tank pressure. Naturally, when these conventional storage technologies are used, larger tanks are required to account for the cryogen losses. For moderate and long-term missions, the added mass of propellant needed to compensate for the boil-off and the weight of the larger tanks required to accommodate the extra mass can render the use of cryogenic propellants prohibitive, causing mission planners to consider propellants with much lower specific impulses or ventless but dynamic pressure control.

Dynamic pressure control is, in general, accompanied with some form of forced mixing of the bulk liquid to promote thermal destratification. This can be achieved by the following four design options:

1. Settled venting with mixing of the bulk liquid.
2. Venting with mixing and *passive* cooling.
3. Ventless storage with mixing of the bulk liquid.
4. Zero-Boil-Off (ZBO) storage with mixing and *active* cooling.

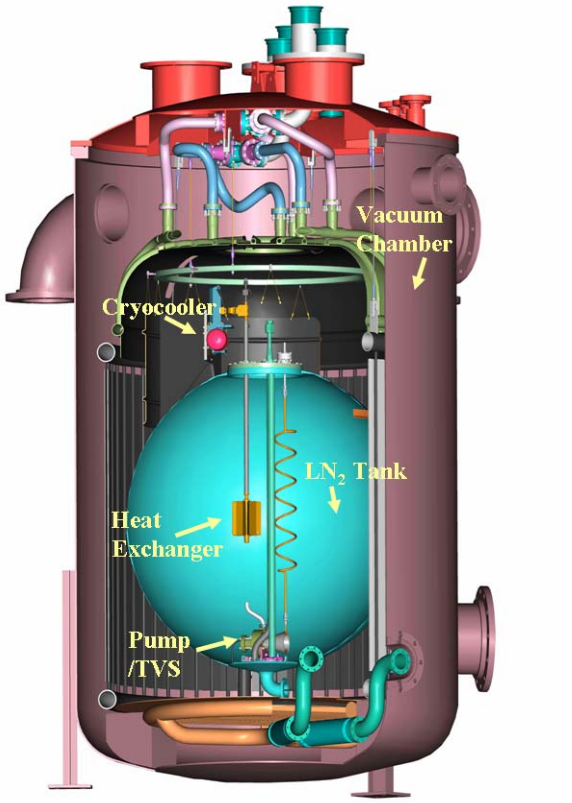

Figure 1. The TVS Tank Pressure Control System

As shown in Table 1 and discussed in more detail in section 1.2, current technology baselines defined by the NASA Exploration Architecture Studies (NASA, 2005) requires option 1 for the Earth Departure Stage (EDS). The Lunar Lander Descent Module (LLDM) is base-lined with option 2. In this case, mixing will be primarily performed in conjunction with a Thermodynamic Vent System (TVS) similar to the system shown in Fig. 1. In a TVS heat exchange system, small amounts of the liquid are passed through a Joule-Thompson valve and the temperature drop associated with the expansion of the liquid to vapor will be used to cool the bulk liquid thus minimizing the overall amount of venting that is needed for pressure control.

The Lunar Lander Ascent Module (LLAM) storage tanks are base-lined for ventless storage with mixing of the bulk liquid (option 3) to enhance thermal destratification. Due to uncertainties with lunar climate, these tanks will also be equipped with a TVS system (option 2) to be used as needed during the envisioned 210 days of surface operation.

ZBO with active cooling (option 4) is under consideration as a contingency option for both the LLDM and LLAM. In this case, as shown in Fig. 2, active heat removal by a cryo-cooler is

Table 1. Exploration Architecture Cryogenic Storage Tank Pressure Control System Requirements

	Nominal Baseline	**210 Day Surface Contingency**	**33 Day LEO Contingency**
Earth Departure System	Option 1		
Lunar Lander Descent Module	Option 2 (with TVS)		Option 4
Lunar Lander Ascent Module	Option 3	Option 2 (with TVS)	Option 4
Mars	Option 4		
ISRU	Option 4		

combined with forced mixing of the bulk liquid to establish tank pressure control without venting (Plachta and Kittel, 2003). It is anticipated that ZBO with active cooling (option 4) will also serve as the baseline pressure control technology for all the ISRU propulsion elements.

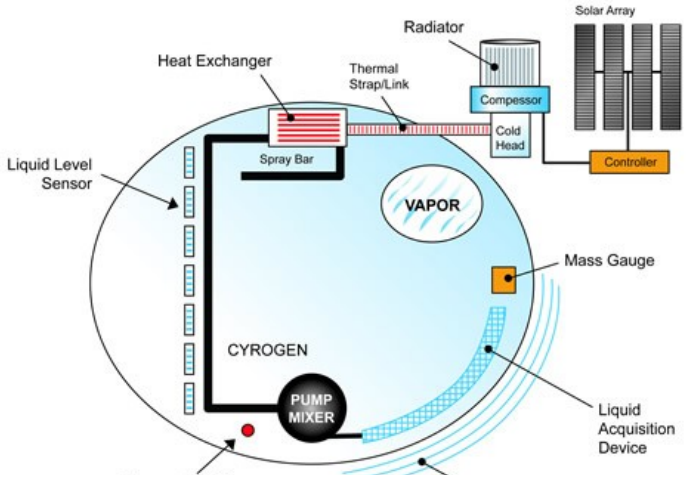

Figure 2. The ZBO Pressure Control System

It is clear that NASA's future exploration architecture will require dynamic pressure control in order to decrease the risks associated with propellant tank self- pressurization in space. Regardless of how the short-term Lunar and long-term Mars Architectures evolve, destratification through forced mixing with or without active cooling will be the centerpiece of the future cryogenic storage tank pressure control systems. Although, both mixing and destratification are strongly influenced by gravity-dependent transport processes in the tank, current time and budgetary constraints imposed on the Exploration Architecture allows only for 1g testing of the technology. Thus fundamental knowledge and understanding of the fluid flow and heat transport processes associated with microgravity mixing and destartification will be essential to reduce the risks and uncertainties associated with the ground-testing-only design approach. In this context, the main goal of the present research project and the associated ISS experiment is to acquire valuable microgravity knowledge and flow and heat transfer data for understanding and characterizing self-pressurization, mixing, and destratification of a two-phase fluid in a ventless Dewar with controlled heat flux inputs, fill levels, and mixing flow rates. The experimental data can be used to derive useful empirical engineering correlations for storage tank design. It will also serve to validate and verify a two-phase CFD storage tank code that will be developed during the course of this research. More importantly the high quality and controlled microgravity validation data will also be available to the CFM community at large and can be used to benchmark other in-house or commercially available storage tank CFD codes currently used in the storage tank design process. It is anticipated that the availability of relevant microgravity data and the development of the much-needed empirical correlations for

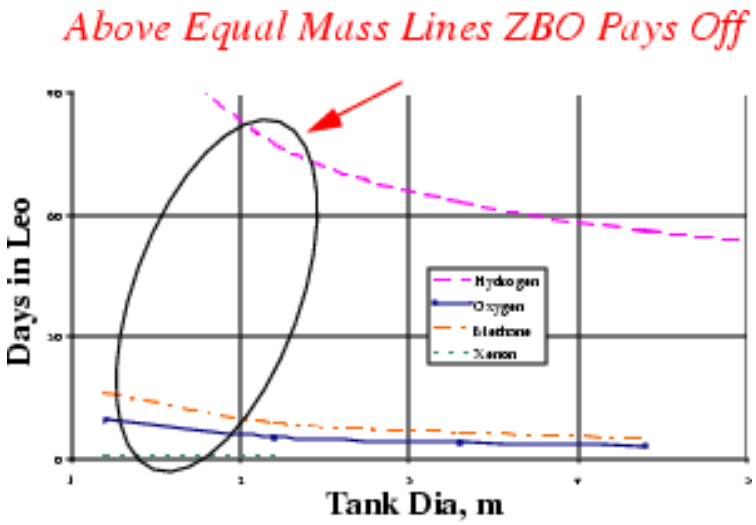

Figure 3. Equal Mass lines above which ZBO Design Strategy Provides Distinct Advantage.

mixing and destratification in space, together with verification and validation of the CFD codes used in the scale-up the design of the future storage tank prototype will all contribute significantly to reduce the risks and uncertainties associated with the ground-testing-only design process.

Ultimately, integration of a ZBO pressure control strategy into the cryogenic storage tank design has numerous mission enabling benefits:

1. Decreases the launchable propellant and storage tank mass. (See Fig. 3 for a comparison of ZBO and passive mass requirements for a 1.3 meter diameter tank in low earth orbit.
2. Increases system reliability through active-passive pressure control.
3. Promotes crew safety by allowing manned flight operations such as rendezvous and docking around the cryogenic tanks.
4. Enables new opportunities by building flexibility into both the mission planning and revision phases since manned flights encountering delays for whatever reason can be tolerated without major risk and/or cost increase considerations.

Naturally, these benefits will all lead to a significant reduction in cost and increase in safety and reliability for both short- and long-duration expeditions. However, before these benefits can be realized several key engineering and scientific issues with regard to multiphase fluid flow and heat transfer associated with storage tanks design must be resolved.

1.2 Relevance to the NASA Exploration Program: Lunar and Mars Architectures.

From a mission point of view, efficient and innovative cryogenic fluid management and storage is an enabling technology in the critical path of all human space expeditions pursued by NASA. A brief summary of the pressure control requirements for the Lunar and Mars Exploration Architectures was included in Table 1. A review of this table reveals the strong relevance of the present work in that:

1. All the base-lined designs associated with the main elements of Lunar Architecture include pressure control brought about by thermal destratification through forced mixing of the bulk liquid.
2. Ventless pressure control is envisioned for the Lunar Ascent Module.
3. Lunar Descent Module will use mixing and cooling by a TVS system as the baseline pressure control. The TVS system will also constitute as the contingency system for the Lunar Ascent Module to deal with the uncertain lunar thermal climate.
4. The long-duration storage requirements of Mars Architecture and its ISRU options will rely on ZBO pressure control brought about by active cooling and mixing.

1.3 Engineering Significance

From an engineering point-of-view, designing a highly reliable fluid storage system of limited cost for an environment with limited accessibility (for testing) is indeed a great challenge. The evolutionary engineering response to this challenge has been to avoid the problem all together by sacrificing costs in favor of reliability through over-design. The result has been larger than necessary static/passive (thermally insulated) systems. In the design of the static/passive storage tanks, thermodynamics and empiricism rule. Therefore, in a sense, these oversized storage systems are *g-independent* and *ground-testable*.

As the results of several NASA workshops including the *Workshop on Research Needs in Fluids Management for the Human Exploration of Space* (NCMR/NASA GRC, 2000,

Chiaramonte and Joshi, 2004) have suggested, the over-design strategy is not a viable option for future planetary missions due to its prohibitive costs. This is also reflected by the base-lined requirements for the Lunar Architecture (NASA: 2005) discussed in the previous section that envisions some kind of a dynamic pressure control based on forced mixing with or without active cooling as an integral part of the next generation space storage tanks. As is with all dynamic fluids and heat transfer systems, transport processes will play a dominant role in the design and implementation of dynamic storage tank pressure control. Judicious engineering decisions must be made, for example, with regard to:

1. How much natural mixing will takes place in a given tank during operation at various gravitational levels?
2. How much forced mixing is needed to thermally destratify the tanks without active cooling?
3. Under what conditions will it be necessary to augment the thermal destratification through active cooling?
4. How effectively do mixing-only and/or mixing-with-active-cooling decrease the pressure reduction times?

The information needed to answer these questions will be crucial in sizing of the pumps, determining forced mixing modes, possible placement of flow control structures, and sizing and implementation of the active cooling mechanisms (TVS, Cryocooler, etc.) for the different applications. In answering these questions, the present experiment will help develop reliable engineering correlations for mixing, destratification, and pressure reduction times as functions of relevant tank parameters such as heat leak rates, mixing flow rates, and fill levels to help the tank engineering design processes. The two phase flow storage tank CFD model that will be developed, validated, and verified as part of this project will also serve as a powerful tool to aid the engineering design of the future storage tanks.

1.4 Scientific Significance

From a scientific point of view, the thermophysical processes that occur in a cryogenic storage tank are one of the most complicated and compelling two-phase fluid flow problems encountered in both ground and space-based technologies. Pressure change and mass loss in the cryogenic storage tank are governed by an intricate interplay among heat transfer in the liquid and vapor, mass transfer due to evaporation/condensation processes that may occur in the presence of non-condensable gases, and complicated fluid flow in the liquid brought about by forced jet mixing and by natural and/or thermocapillary convective flows. The fluid flows may span both laminar and turbulent regimes depending on the specific application. Moreover, due to thermal stratification and significant superheats in microgravity, there is a large possibility for sudden nucleation and rapid bubble growth resulting in alarming pressure spikes. Through hand-in-hand experimentation, theoretical analysis, and computational modeling this research will strive to:

1. Gain a broader understanding and clearer picture of the above-mentioned phase change and transport phenomena associated with tank pressurization and pressure control
2. Analyze the time constants associated with the various interacting mechanisms that occur in the cryogenic storage tank for different gravitational environments.
3. Validate and verify a state-of-the-art two-phase CFD model for cryogenic storage.

If the results of this research are brought to fruition, they will contribute significantly to our state-of-art scientific knowledge of two-phase fluid behavior in 1g, microgravity and variable-gravity environments with significant benefits not only for the cryogenic storage tank design but for a multitude of other two-phase flow operations and processes in space.

1.5 Microgravity Relevance

NASA's microgravity fluid storage challenges are more acute than partial-g or macro-g challenges due to the absence of a solid empirical foundation in microgravity and thus the need to rely heavily on assumption-based analyses and computational models. Three past microgravity workshops (NCMR/NASA GRC: 2000a, 2000b, 2003) predicted that due to scarcity of microgravity data and lack of opportunities for large technology validation experiments in the real operational environments there will be an unusually heavy reliance on theory for the design of future space-based cryogenic storage facilities demanding powerful and comprehensive computational models. Current budgetary and timeline constraints placed on the Lunar Architecture design and development proves the merit of these prior predictions. The CFM community is, however, still hesitant to trust current theoretical/numerical models due to lack of microgravity validation and verification.

While drop tower tests can be effectively used to obtain useful data with regard to phase distributions, interface behavior, and jet penetration of the ullage, the time constants for stratification, pressurization, mixing, destratification, and pressure reduction during storage do not lend themselves well to short-duration microgravity testing in drop towers and/or parabolic flights (see sections 2 & 3). Long-duration microgravity provided by the ISS is needed to obtain high quality data in both transient and stationary phases of tank pressurization, mixing and destratification. The long duration microgravity data can then be used to develop appropriate engineering correlations and to validate the two-phase CFD models.

Long-duration microgravity is also necessary for studying the possibility of closed tank nucleation and bubble growth caused by superheats that are very specific to the space environment. On the ground, any significant superheat is greatly diminished by the strong mixing effects of natural convection. However, significantly larger superheats are possible in microgravity and, as a result, the probability of nucleation and sudden bubble growth is greatly increased. If such sudden microgravity nucleation and bubble growth occur in a large tank, the resulting pressure spikes may possibly lead to structural failure with disastrous consequences.

1.6 Research Scope and Objectives

As stressed before, the aerospace engineering community is uneasy to solely rely on theoretical or computational models to develop the next generation space cryogenic storage tank because the existing models have not been properly validated and verified, especially with regard to the fidelity of their predictions with regard to the microgravity two phase flow behavior. Therefore, there is a strong desire for large-scale in-space storage tank prototype technology validation tests. Unfortunately, past attempts to move directly to TRL 6-7 experiments in space (Schuster et al, 1990) have proved to be too costly and ultimately abandoned. In any case, before such costly endeavors become justifiable and warranted, it seems a series of small-scale microgravity experiments addressing different aspects of cryogenic fluid storage and management in space is appropriate.

In this context, the goal of this research is to develop a small-scale long-duration microgravity storage tank experiment with *simulant* fluids to be performed aboard the

International Space Station (ISS). The experiment will provide microgravity data to: (a) delineate the primary two-phase transport and phase change mechanisms that influence cryogen vaporization and condensation during 1g and microgravity storage; (b) expand the scientific and engineering foundation for space-based cryogenic fluid storage by obtaining valuable long duration two-phase transport and phase change microgravity data that can be effectively used in developing the much-needed empirical correlations for tank pressurization, destratification, and pressure control time constants; and (c) validate and verify a state-of-the-art variable gravity two-phase CFD model and computer codes developed as part of this project for tank pressurization and pressure control. The model can then serve as a valuable and cost-effective tool for the future storage tank scale-up designs.

Within the framework of these goals, the original ZBOT proposal, included in Appendix A, aimed at addressing a wide and comprehensive range of Cryogenic Fluid Management (CFM) issues such as tank self-pressurization, passive pressure control through jet mixing, active pressure control through various heat removal mechanisms such as cold-finger and broad-area cooling, effect of non-condensable gases on both pressurization and pressure control, the effect of microgravity super heats, and drop tower ullage penetration studies . Upon the review of the proposal, the NASA Review Panel was of the opinion that although all the above-mentioned CFM issues considered by the proposal were important, they can be best addressed not by one but by a series of ISS experiments prioritized based on the NASA Exploration Program's needs. In their report, included in Appendix B, it was recommended that the first experiment in this series be focused on pressurization and pressure control through jet mixing and on model validation.

In agreement with the Review Panel's view and judgment, the original scope of the proposal was modified according to the *Response to Review Panel Comments* included in Appendix C. As a result only the following elements of cryogenic storage will be considered by the present experiment, henceforth, called ZBOT-1:

1. Tank pressurization
2. Pressure control through forced jet mixing
3. CFD model validation and verification.

The remaining elements of the original proposal will be deferred to future ISS experiments. These elements are as follows:

1. Active cold finger cooling
2. Active intermittent mixing with cold finger cooling
3. Active broad area (wall) cooling
4. Active intermittent mixing with broad area (wall) cooling
5. Non-condensable pressurization studies
6. Non-condensable pressure control studies
7. Microgravity super heat studies
8. Drop-Tower jet-ullage penetration studies

At this point, it is hoped that a follow-on experiment ZBOT-2 will address the important elements and issues associated with the active cooling pressure control.

2. Technical Background

This research effort is focused on the storage of cryogenic liquids for propellant and life support, one of the most significant technological challenges in the path of NASA's Exploration Program. Cryogens are stored at very low temperatures and may be subjected to large heat loads while the storage tanks are loitering in LEO, in transit, or sitting on the surface of the Moon or Mars. The heat load can come from a variety of internal or external sources. The external sources can include incident solar radiation, planetary albedo, aerodynamic heating, or conduction loads from the tank's support structure and plumbing. Internally, the exothermic reaction of ortho/para conversion of LH2 and the kinetic energy associated with liquid sloshing, which eventually dissipates as heat (Meerbeke, 1968), can all be factors. When heat leaks into the tank, it will be carried to the liquid-vapor interface by conduction and natural convection. Once this thermal energy reaches the surface, the liquid may start vaporizing. Since vaporization is occurs in a closed tank, the tank pressure will increase. Design constraints regarding the tank's maximum operating pressure and requirements regarding tolerable liquid losses make controlling both the phase change process and the tank pressure a necessity.

Traditionally, pressure control in microgravity has been achieved by first firing thrusters to settle the liquid and then venting the vapor. In passive pressure control, efficient thermal insulation technology is used to minimize the heat leaks into the tank. In dynamic pressure control, in addition to the passive thermal insulation, forced mixing is used to destratify the tank and decrease the need for venting. In future, storage tanks may be equipped with Thermodynamic Vent Systems (TVS). In this case, in addition to the bulk mixing of the liquid a heat exchange system based on the operation of a Joule-Thompson valve is conveniently used to cool the liquid and the vapor during venting. This provides larger reductions in the tank pressure and minimizes the overall need for direct venting. Naturally, in this system, some liquid and/or vapor mass is still lost from the tank. Another promising tank pressure control scheme is based on the Zero Boil-Off concept. In this case, the required reduction in pressure is achieved in a ventless manner by active mixing and removing heat from the bulk liquid using efficient cryo-cooler technology. Regardless of what specific pressure control technology is employed, all dynamic pressure management systems will be strongly influenced by two phenomena:

1. The fluid dynamics and heat transfer mechanisms that control thermal stratification in the bulk liquid
2. The phase change phenomena and mass transfer that govern the evaporation/condensation processes at the liquid-vapor interface.

2.1 Problem Definition: Role of the Transport Phenomena

The extent of the heat leak responsible for self-pressurization of a cryogenic storage tank is directly dependant on the conductive, convective, and radiative heat transfer links between the tank wall and its surrounding environment. The heat transfer links are, in turn, functions of the thermal characteristics of the multilayer insulation (MLI) system, the conduction paths provided by the structural support systems, the levels of containment, and the environmental conditions associated with each application (i.e., earth laboratory, during launch, in-orbit, and on planetary surfaces). Transverse temperature gradients generated by the heat leaks will give rise to natural convective boundary layers along the wall as shown in Fig. 4a and b. If the natural convection current is not controlled, it will create thermal stratification in the liquid and lead to considerable evaporation at the interface causing a pressure rise. Thermal destratification can be promoted and enhanced by forced mixing of the bulk liquid. This can be accomplished, for example, by an

intermittent forced jet flow as shown in Fig. 4. The jet flow counteracts the effect of natural convection by carrying cooler liquid from the lower central regions of the tank thus promoting condensation at the interface. Because of the low viscosity of the cryogen fluids (e.g. hydrogen, oxygen, and methane) and the large dimensions of the storage tank, both the natural and forced convection will be in the turbulent regime for typical on-surface (partial-gravity) applications. Even in microgravity, the natural convective flow can be strong and may indeed be in a transitional regime while the forced jet is likely turbulent.

In general, while significant thermal stratification occurs in the bulk liquid, the interfacial temperature will be uniform for the most part as dictated by the ullage saturation temperature/pressure. However, there may be three notable exceptions: (a) variations in temperature may occur along the liquid-vapor interface near the wall contact line due to the thermal influence of the wall; (b) variations in the interfacial temperature may arise due to the presence of non-condensable gases in the vapor region that would result in the vapor saturation temperature at the interface be a function of the spatial distribution of the vapor partial pressure (c) deviation of interface temperature from saturation temperature may occur during any rapid and intensive heat or mass transport at the interface. All of the above three cases may give rise to surface tension driven thermocapillary flows in the liquid because the temperature of the interface will not be solely controlled by equilibrium thermodynamics but may be affected in one way or another by various transport processes in the tank.

The convective transport will be quite complicated in microgravity because natural convection is not only driven by the background g-level but also by the time-dependant g-jitter or impulse accelerations. Thus, the intensity and characteristics of the natural convective flow in the tank will depend on the direction, magnitude and frequency of the residual acceleration vector. In contrast, the surface tension driven thermocapillary flow is independent of the gravitational environment and as mentioned before under certain conditions may dominate the convective transport in microgravity applications. Moreover, in space, the position of the liquid-vapor interface is not well defined as indicated in Fig. 4b and will be also influenced by the direction and magnitude of the residual gravitational field that can vary with time. This can create a continuous ullage motion that may contribute significantly to mixing and destratification in the tank. In any case, the multiple time scales associated with the various convective and transport mechanisms have to be all characterized and analyzed in order to properly predict the tank pressure reduction time constants.

In the ZBO system with active cooling, pressure is controlled by cooling and forced mixing of the bulk liquid. The temperature field and stratification in the tank is therefore affected by the dynamic competition between the intermittent forced flow at

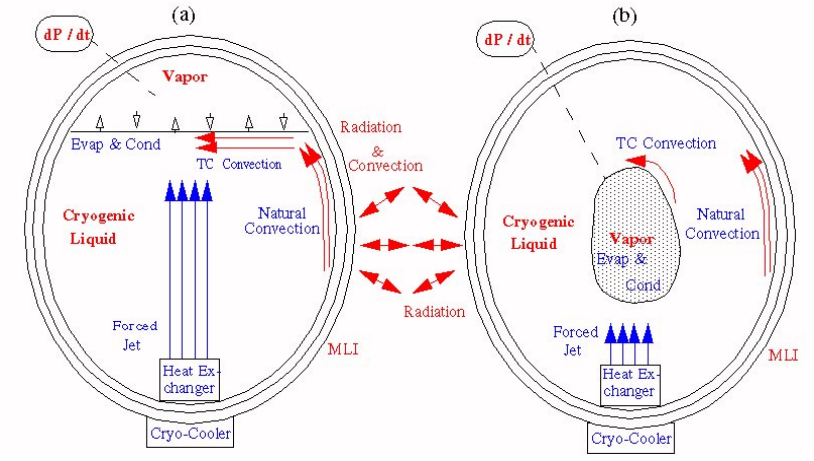

Figure 4. Cryogenic Storage Tank: (a) On-Surface 1g, 1/6g, and 3/8g Applications and (b) In-Orbit Microgravity Applications

the center of the tank and the natural and thermocapillary convective flows originating from the regions near the wall and near the liquid-vapor interface. The complicated convective flow that ensues ultimately determines the evaporation (condensation) rate at the liquid-vapor interface and the extent of pressure rise (fall) in the tank. In a ZBO system, the cooling and the mixing can be done separately through use of a cold finger and a mixer (axial jet or spray-bar) or simultaneously by means of a sub-cooled forced flow. Therefore from an engineering point of view, the cold finger location and configurations and the jet or spray-bar flow parameters become important design variables.

Another important issue that needs to be understood is the possibility of nucleate boiling at the wall or within the liquid due to the unusually large superheats that may arise in the absence of significant natural or forced convection in microgravity. The probability of either homogenous or heterogeneous nucleation increases as the superheat increases, and if such nucleation and bubble growth occur, they may lead to sudden undesirable pressure spikes similar to those observed in the brief TPCE microgravity experiment (Bentz et al, 1993; Hasan et al, 1996). Such pressure spikes may possibly compromise the structural integrity of the storage tank. Therefore, conditions that promote this phenomenon in microgravity must be properly investigated.

2.2 Evolution of Various Strategies for Tank Pressure Control

Various strategies have been identified as possible mechanisms to control tank pressure. The simplest strategy involves periodically venting the vapor overboard to reduce the pressure. Venting is a straightforward operation in a normal or partial gravity environment where the lighter vapor sits atop the heavier liquid. In a reduced gravitational environment, where the position of the vapor is less certain, venting only vapor becomes more challenging. While venting does reduce tank pressure, it does nothing to mitigate boil-off losses. That is, venting over time will still lead to considerable propellant losses.

Other strategies involve storing the liquid as a bulk sub-cooled phase (Motil and Meyer, 2007) or using combinations of MLI blankets to insulate the tank and sunshades to shield the tank from solar and infra-red radiation, or planetary albedo (Motil and Meyer, 2007; DeWitt and Boyle, 1977; Plachta et al., 2006; Guernsey et al., 2005). Bulk liquid sub-cooling can increase the amount of energy the liquid can hold before vaporization and boiling takes hold thus delaying the tank's pressure rise. Sunshades serve to reduce the heat load on the storage tank. While both of these strategies offer some benefits, both lack the robustness of an active pressure control system.

When heat leaks into the tank from the surroundings, the temperature field inside stratifies. Mixing the fluid inside the tank can destratify the thermal field; reducing temperature gradients near the liquid-vapor interface and bringing the cooler fluid that had settled out closer to the surface -both of which promote condensation and a reduction in tank pressure. Mixing strategies alone have been the subject of much research. Passive mixing has been shown to have a significant effect on fluid behavior in low gravity environments. Gebhart (1963) showed that random disturbances can result in transport rates much greater than would be expected in the absence of all disturbances. Grodzka and Bannister (1974) report that experiments conducted during Apollo 14 and 17 and data taken from the oxygen tanks aboard Apollo 15 have all revealed that natural convection caused by g-jitter can be significant. Passive mixing however lacks the robustness necessary for active pressure control. Active mixers such as axial or radial liquid jets or spray bars have also been studied. Axial jets exhibit considerable gravity dependence. Often times, the liquid jet flows opposite the direction of buoyancy which tends to

reduce its effectiveness. Spray bars, on the other hand, are typically gravity independent since liquid is ejected radially into both phases from a bar running the entire length of the tank. As will be discussed shortly though, which active mixing strategy is more effective remains uncertain. Regardless, active mixing alone offers only a temporary reduction in tank pressure. Because the mixing device itself adds energy to the system, the net heat load post-destratification can be larger than if no mixer were present.

Consequently, active mixers are often coupled to a refrigeration system. One of the earliest refrigeration concepts considered for cryogenic storage systems was a Thermodynamic Vent System (TVS) (Mitchell et al., 1967). In a TVS, some sacrificial liquid passes through a throttling device to reduce its temperature. The colder two-phase fluid then passes through a heat exchanger which can be attached to the outer surface of the tank to intercept the incident heat load (Hofmann, 2004; Cunnington, 1984; Hill and Salvinski, 1967; Warren and Anderson, 1967; Liggett, 1993). Due to heat transfer into the two-phase fluid, vaporization occurs and the resulting vapor is eventually vented overboard. Alternatively, after passing through the throttling valve, the fluid can enter a heat exchanger which can be used to sub-cool a liquid jet or be placed internal to the tank to remove energy from the bulk liquid and vapor. A spray bar/heat exchanger TVS system designed by Rockwell Aerospace (Lak and Wood, 1994) and extensively tested at the Marshall Space Flight Center has demonstrated the ability to control tank pressure within a very tight control band for a variety of cryogens and mission scenarios. (Flachbart et al., 1999; Flachbart et al., 2005; Hedayat et al., 2005; Hastings et al., 2003) Although it is less common, a TVS system consisting of an axial jet mixer and a heat exchanger (Stark and Blatt, 1967; Sterbentz, 1968) has also been tested (Overbeke, 2004). In a recent review, Hastings et al (2005) reported TVS performance comparisons between an axial jet mixer and a spray bar. Although tank pressure decayed more rapidly during the spray bar operation, the axial liquid jet resulted in better bulk mixing. The comparisons appear to be inconclusive especially since the liquid flow rates were different in the two test cases. Regardless of the combination of mixer or heat exchanger employed, a TVS is designed to sacrifice some liquid to reduce the bulk energy of the system. Hence, operation over extensive periods of time will lead to loss of usable propellant.

Recent advances in zero boil-off (ZBO) technologies have improved the prospects of a truly zero loss storage system (Hastings et al., 2002). The main refrigeration system used in a ZBO system is a cryocooler. The cooler can be mounted outside of the tank and mated to heat exchangers, internal condensing surfaces, heat pipes, or wall-mounted thermally conducting sheets (Plachta, 2004; Plachta, 1999). Plachta (1999) was able to achieve ZBO conditions during ground testing of a LN2 tank using only passive mixing. But since conduction and natural convection time scales are much slower in low gravity, a ZBO cryocooler must often be combined with an active mixer to enhance condensation and pressure control in space. Thus preliminary ground-based testing has been also performed with both axial jet mixers (Plachta, 2004) and spray bars (Hedayat et al, 2001) with favorable outcomes.

The proof-of-concept tests mentioned above are quite promising. As shown by Salerno and Kittel (1999), even a modest reduction in boil-off losses (and thus launch mass) can translate into significant mass savings. Plachta and Kittel (2003) compared a ZBO system with a passive storage system with insulation and showed that for short duration missions a ZBO system is not as attractive as a passive storage tank due to the increased launch mass of the mixer and cryocooler. However, after a relatively short time (1 week for LOX, 2 weeks for LCH4, and 2 months for LH2) the mass and cost benefits of a ZBO system are quickly realized. Besides the

cost and mass savings, ZBO adds to mission flexibility as delays in rendezvous or docking would no longer jeopardize propellant mass margins (Hastings et al., 2002). While the benefits of a ZBO system may be substantial, more work is required before its full potential is realized. From a power consumption and reliability standpoint, it may not be practical to continuously operate an active mixer. Optimization is necessary to tune the system to maximize performance. Optimizing a ZBO system requires a better understanding of the complicated and coupled transport phenomena inside the tank which can affect thermal stratification, self-pressurization, and pressure control. These same issues were identified in past reviews (Clark, 1965) as critical to cryogenic storage and remain as relevant today.

Due in part to these reviews, extensive research dating back to the Apollo program has been performed but unanswered questions still remain. To answer some of these questions, large-scale flight demonstrations are generally preferred. Large-scale flight experiments, however, can be costly and time consuming. As pointed out by Chato (2006), computational tools can offer development cost savings and improved designs but these tools must be quantitatively validated and verified. As such, the design approach currently converged upon by the cryogenic fluid management community is to develop numerical models of the cryogenic storage tank, validate the models against small-scale experiments in both normal and reduced gravity, and then use both the sub-scale experimental data and the computational models to extrapolate the design to an actual flight system. Indeed, this is the approach adopted in this project.

2.3 Flight Experiments

NASA has a rich heritage of flight testing and flight qualifying cryogenic fluid management technologies in support of past exploration programs. Beginning in the early 1960s, and continuing for several years, several experiments were conducted aboard Aerobee sounding rockets which provided for approximately 4.5 minutes of low gravity. Knoll et al. (1962) performed LH2 experiments in a 9” diameter partially full Dewar subjected to radiant heating. The measured self-pressurization rate was larger than a simple thermodynamic analysis predicted. Thermal measurements indicated that during the experiment an initially wetted-wall eventually formed dry spots during the flight. The experiment sat on a de-spin platform to counter the effects of the spin-stabilized rocket. Misalignment of the de-spin platform resulted in accelerations of ±0.02g. In a subsequent flight, McArdle et al. (1962) performed a similar experiment and, this time, nucleate boiling was observed. Unfortunately for this flight, the de-spin platform malfunctioned. In a similar experiment reported by Nunamaker et al. (1963), temperature measurements indicated wall dry out conditions and fluid sloshing in the tank. Once again, the self-pressurization rate was under-predicted by thermodynamics.

Later in the Aerobee program, Aydelott (1965) conducted similar experiments but with a higher liquid fill level. He reported that: (a) the measured self-pressurization rate was approximately twice the rate predicted by thermodynamics; (b) ullage motion during the flight resulted in some fluid mixing: and (c) it took approximately two minutes for the radiant heaters to reach their set point temperature. Thus for a significant portion of the experiment, the incident heat load was not relatively constant. Abdalla et al. (1965) reported on the pressurization experiments conducted on an Atlas rocket which provided for 21 minutes of low gravity. During the flight, the experimental pod began tumbling and resulted in an acceleration of 0.001g. Consequently, the pressure rise characteristics were similar to testing done in 1g and temperature measurements exhibited cyclic behavior in phase with the external perturbations. During the

Atlas/Centaur AC-8 flight, Lacovic et al. (1968) studied propellant behavior during an orbital coast and temperature measurements indicated significant thermal stratification in the ullage. Bradshaw (1970) and Navickas et al. (1968) described the self-pressurization results on the Saturn IVB-AS203 flight. Continuous venting of the O2 tanks during most of the flight provided a settling acceleration to the instrumented LH2 tank. Data was taken during an orbital coast. However, half of the data was lost due to a loss of signal during the middle of the test. Allgeier (1968) reported on a small-scale LN2 experiment conducted on the AS-203 flight. During this experiment, the tank was allowed to self-pressurize after which a small amount of liquid was withdrawn from the tank and passed through a heat exchanger brazed to the outer wall of the test cell. This system exhibited good pressure control.

Several relevant experiments (Yanke, 1977) were also conducted on the LOX/LH2 Titan/Centaur upper stage. While these experiments were primarily investigating liquid orientation and engine restart capability after an orbital coast, temperature and pressure measurements were also made to study stratification and pressurization. From temperature measurements taken during these flights, Lacovic (1977) inferred that sections of the tank's wall dried out during the coast. While many of these proof-of-concept flight experiments yielded important data, unknown or uncontrolled boundary or initial conditions rendered them less useful for the purposes of validating numerical models. In a recent review, Chato (2006) noted that while piggy-backing on the Saturn and Centaur upper stages made many of these experiments cost effective, it unfortunately also prevented them from carrying more extensive instrumentation to produce more detailed and unambiguous data for future model validation.

Besides these orbital and sounding rocket tests, cryogenic fluid management experiments have also been performed aboard aircraft. Ordin et al. (1960) mounted a 450 gal LH2 tank to the wing tip of a jet aircraft to investigate the effects of atmospheric turbulence on thermal stratification. As a result of significant agitation during the flight, the degree of stratification in the tank was diminished when compared to similar ground tests. Bentz (1993) conducted a small-scale Freon 113 self-pressurization/axial jet mixing experiment aboard a Lear jet flying parabolic profiles. As pointed out by Eberhardt et al. (1982), the value of these particular parabolic flight experiments was limited due to their short duration exposure to low gravity (± 0.01g). Bentz (1993) reported that there was insufficient time between parabolas for the liquid to reach a quiescent state in the experiment.

To obtain more long duration periods of low gravity, Bentz and colleagues (Bentz, 1993; Hasan et al., 1996; Bentz et al., 1997) performed the Tank Pressure Control Experiments (TPCE) on three shuttle flights in the early 1990s. During the first flight, a small tank partially filled with Freon 113 was self-pressurized using submerged heaters in the liquid. Heating was initiated and maintained for several minutes after which the heaters were turned off and the liquid was withdrawn and pumped back into the tank via an axial liquid jet. The pressure collapse as a result of axial jet mixing was studied. On the second flight, during heating, higher local superheats were observed that apparently resulted in liquid flashing causing a pressure spike in the tank. The third experiment was similar to the first two, except now the test was performed at a lower fill level. The TPCE experiments provided some useful microgravity results but unfortunately the data obtained is not suitable for proper numerical model validation. First, the liquid jet was not thermally controlled and unfortunately no jet temperature measurements were recorded. It's uncertain how much heat leaked from the liquid jet to the surroundings. Any sub-cooling of the jet would have had a profound effect on the pressure collapse times. Second, no thermal controls existed between the tank and the ambient environment. Yet no attempts were made to quantify

the amount of heat lost from the tank. Third, there was only a 20 minute wait period between the experimental runs. It's unclear whether 20 minutes provided sufficient time for each test to be started from the same thermal and dynamic initial conditions. Finally, for all three TPCE experiments, contaminant species leaked into the test cell. The amount of non-condensable species was estimated from the overpressure above saturation. During the three experiments, the partial pressure of the non-condensable gases ranged between 1 kPa and 6.2 kPa. While the investigators claimed the non-condensable contaminants had no effect on the results, other theoretical and experimental studies as exemplified by Rose (1969), Minkowycz and Sparrow (1966), and Hastings et al. (2003)) suggest otherwise.

2. 4 Ground-Based Experiments

In addition to the flight experiments, there have been also been a wealth of ground tests both in support of and independent of the flight projects. While investigating thermal stratification in a ground liquid nitrogen experiment, Fan et al. (1969) observed a thin thermal boundary layer near the tank walls and noted that convection heat transfer was significant. Beduz et al. (1984) performed wall heating stratification studies of LOX and LN2 in small Dewars. Using temperature measurements in the liquid, they were able to map the morphology of the temperature fields. Below the interface, they observed a thin thermally conducting layer, a few hundred microns thick, exhibiting a steep temperature gradient and residing on top of a convective layer with a shallow temperature gradient. Both layers sat atop a liquid region of near uniform bulk tempertaure. Swim (1960) conducted stratification studies using Dewars partially full of liquid helium. He also observed steep temperature gradients on either side of the interface in line with Beduz's (1984) morphology studies. Tatom and colleagues (1964), performing stratification experiments in a 500 gal LH2 tank, noted that a considerable amount of thermal energy went into raising the temperature of the bulk fluid which suggests an absence of a well-defined boundary layer. Neff and Chiang (1967) reported on stratification experiments using both water and cryogenic fluids. They noted that an increase in the bulk liquid temperature indicated quasi-steady flow and temperature conditions in the tank. Moreover, they attempted to describe the stratification process semi-empirically by approximating the temperature profile in the liquid as a polynomial. These stratification tests were not limited to only recording temperature. Lovrich et al., (1974) using a Schlieren system, performed flow visualization experiments using Freon and water with local side wall heating. They found that most of the heat remained above the heater with a sharp drop off in the temperature profile below. Anderson and Kolar (1963) also used a Schlieren setup to compare side wall heating temperature fields with bottom heating ones. For side wall heating, they observed a stable temperature gradient below the interface. The bottom heating configuration led to better mixing of the bulk liquid which resulted in a more uniform temperature profile. More recently, Das et al. (2004) used a dye injection system to map out the temperature field in a side heated cavity containing water.

Nearly all of these stratification experiments were primarily concerned with thermal behavior and not the coupling between the temperature field and the vapor pressure. Ji et al. (1992), studied stratification and pressure rise, and based on scaling analysis identified three dimensionless parameters in an attempt to describe and characterize the underlying physics. Several small-scale tests were performed to verify the validity of these dimensionless groups. Results indicated that the vapor pressure histories agreed reasonably well between the scaled pairs of tests but point-to-point temperature matches were not possible indicating that the three proposed dimensionless parameters were not sufficient for characterizing the entire system

behavior. Manson (1965) also identified dimensionless parameters to achieve geometric, dynamic, and thermal similitude. However, in practice, matching all the parameters simultaneously is difficult. Neff (1960) performed scaling experiments with LOX and LN2 to verify that the dimensionless parameters he had identified were able to completely characterize the underlying physics. Comparing scaled pairs of tests, he observed similar temperature profiles although agreement between the temperature values was again lacking. Bourgarel et al. (1967) performed a scaling analysis without considering conduction and interfacial phenomena. They also chose not to match Grashof numbers. While the similarity between their scaled pairs of tests was initially fair, deviations developed with time.

Blatt (1968) came up with a self-pressurization rate equation in terms of the heat input, tank volume, and fill fraction. He used available data from ground and flight LOX/LH2 self-pressurization experiments to fit the constants in his function. The correlation, however, was based on only a limited number of data points and still exhibited discrepancies as high as 89%. Scott et al. (1960) investigated stratification and pressurization in a partially full LHe Dewar. They initially observed a thermally stratified liquid but after placing thermally conducting copper rods in the Dewar, the temperature gradients were reduced and the recorded a pressure rise that agreed better with thermodynamic analysis.

In the early 1990's, a series of self-pressurization experiments were performed with a 4.95 m^3 partially full LH2 tank at NASA Glenn's Plum Brook Station. In these tests, as with many experiments involving cryogens, the incident heat load was not an independent parameter but was rather computed from measured boil-off rates. A detailed description of this calculation, as well, as the tank's thermal boundary conditions are outlined in Stochl and Knoll (1991). It is always uncertain whether the heat load determined from a boil-off test is applicable throughout the entire experiment i.e. at all the test points. Regardless, Hasan et al. (1991) still found that the self-pressurization rate increased with increasing heat load. For the lower heat flux cases, there was less deviation between the measured and thermodynamically predicted pressurization rates than for the higher heat flux cases. Van Dresar et al. (1992) re-ran these experiments at lower fill levels. In all cases, thermodynamics under-predicted the self-pressurization rate. The effect of fill level on the pressurization rate was difficult to discern from the experimental data. Moreover, the expected trend for the effect of fill level on pressurization was not reflected by the experimental results.

In support of the Aerobee sounding rocket tests, Aydelott (1967b, 1967a) performed a series of ground self-pressurization tests in a 9" diameter spherical tank partially filled with LH2. He found the pressurization rate was affected mostly by the heating configuration (top, bottom, or uniform heating) with only a slight effect from varying the fill levels. Comparisons were also made with a homogeneous thermodynamic model that assumes a well-mixed fluid and a surface evaporation model that assumes all the incident energy is used to vaporize the liquid and keep the vapor in a saturated state. The experimental data was found to be bounded by predictions of the two models with the homogeneous thermodynamic model under-predicting the pressurization rate. Several tests were performed while shaking the tank. In these cases the pressurization rates approached the homogeneous predictions. Aydelott and Spuckler (1969) also investigated the effects of tank size by comparing the previous 9" tank tests with tests in a 22" diameter spherical tank. They found similar pressure rises for equal values of the heating rate to volume ratio. Summarizing his results from both the ground and flight 9" diameter tank experiments, Aydelott (1986) noted a reduced pressurization rate in low gravity. He attributed this reduction to the

increased wetted-wall area of the tank in microgravity and the fact that direct heating of the vapor usually will result in a larger pressure rise rate.

While most of the ground self-pressurization experiments were conducted using small-scale tanks, Liebenberg and Edeskuty (1965) performed tests in a 55,000 gal LH2 Dewar with a 94.7% fill level. The observed pressure rise rate was almost 10 times greater than the predictions of a homogeneous model.

Ground testing was not limited to self-pressurization studies. Several pressure control tests were also performed. Huntley (1960) experimented with a closed LN2 Dewar and found that after mechanically stirring the liquid, the pressure temporarily decayed. Interestingly, he also found that mixing the ullage resulted in an increase in the pressurization rate.

In evaluating TVS designs, Bullard (1972) noted that a bottom-mounted axial jet was more effective at collapsing the pressure than a side-mounted horizontal jet. In his mixing-only tests, the pressure reduction was temporary and as noted that the minimum pressure was reached after only 20-30% of the liquid circulated through the jet nozzle. He also observed that introducing a non-condensable gas into the system significantly increased the pressure collapse time. Dominick (1984) also examined the effects of jet orientation on the condensation rate in a small-scale tank partially filled with Freon. He observed higher rates of condensation and liquid destratification when the jet nozzle was oriented perpendicular to the liquid vapor interface. In Dominick's experiment however, the pressure in the tank was constant since vapor was supplied to the ullage at the same rate mass was condensing at the surface. Moreover, there were no thermal controls between the tank and the surroundings and it's uncertain how much heat was being lost to the outside environment.

Lin et al. (1994) conducted a series of axial jet mixing experiments in a partially full LH2 tank. However, it is unclear whether the same level of stratification was attained between the different test cases. Nonetheless, they found the pressure to collapse faster for faster jet flow rates. For the lowest flow rate considered, the pressure continued to increase during mixing as the jet flow was not strong enough to counter the effects of buoyancy. Later, Lin et al. (1993) also showed that buoyancy effects could be neglected for Richardson numbers less than 0.5. Here also, two mixing times were identified; one to describe how fast the liquid destratified and the second to describe how fast the pressure collapsed.

Finally, Jones and colleagues (Jones et al, 1994; Meserole et al., 1987) conducted several ground-based pressure control tests in a small-scale tank partially filled with Freon 11. Self-pressurization was initiated by activating a heating coil submerged slightly below the surface. After an initial pressurization, the heater was deactivated and an axial liquid jet was used to destratify the liquid. They found buoyancy dominated the flow for jet Reynolds numbers (Re) below 2000. The data did not correlate well with steady-state condensation or dye-mixing correlations. Later, Jones et al. (1991) developed a closed form pressure collapse equation by assuming that the pressure drop was due to condensation and not vapor cooling. Here, it was also noted that the dimensionless mixing time correlated with Re for low jet Reynolds numbers. For larger values, the dimensionless mixing time was constant.

While most of the ground and flight experiments described thus far were applied in nature, there have been several investigations that focused on more fundamental aspects of the problem. McNaughton and Sinclair (1966) studied the stability of liquid jets in terms of Re. Four flow regimes were characterized: dissipated laminar, fully laminar, semi-turbulent, and fully turbulent. Mollendorf and Gebhart (1973a, 1973b) performed stability and perturbation analyses investigating how buoyancy affects the liquid jet behavior. Though primarily concerned with

positive buoyancy, they noted that the effect on the temperature and velocity fields could be particularly strong if buoyancy opposed the jet motion.

Symons and Labus (1971) and Labus and Symons (1972) performed a series of ground tests to characterize the jet flow behavior for a GHe jet into a GHe medium. Later, Symons and Staskus (1971) studied the interaction of a liquid jet and a free surface and developed a critical Weber number (We) criterion that described the stability of the surface. The stability of the interface is important since a jet geysering into the ullage increases the interfacial area through which mass transfer occurs.

Berenyi et al. (1968) performed drop tower tests on a spherical tank with a radial jet and tried to characterize the different flow patterns using the jet velocity. Aydelott performed similar tests with an axial jet in both cylindrical (Aydelott, 1979) and spherical (Aydelott, 1976) containers. Several flow patterns, including jet geysering ones, were observed. Correlations were developed to describe the flow patterns in terms of Weber and Bond numbers. In Aydelott's tests, only 70% of the incoming liquid was being withdrawn from the tank. It's unclear what effect the accumulation of liquid in the tanks had on his results and conclusions.

In addition to these circulation and flow characterization tests, numerous experiments were also conducted to better understand jet mixing. Fox and Gex (1956) used an acid/base neutralization technique to develop mixing time correlations in both laminar and turbulent jet regimes. Both correlations exhibited a dependence on Re and included a gravitational effect. Fossett and Prosser (1949) were able to correlate their jet mixing data independently of Re. Okita and Oyama (1963) used their data, obtained through a density-matched dye technique, together with the Fox and Gex data to develop a mixing time correlation that was dependant on Re for low Reynolds numbers but independent of it for higher Re values. The mixing tests by Lane and Rice (1982) also observed a stronger Re number dependence for laminar jets than for turbulent ones. Poth et al. (1972, 1968) evaluated several mixing devices and found jet mixers to be superior. It was observed that the time required for the jet to reach the interface was approximately twice as long as a simple kinematic analysis would predict which highlights the retarding effects of negative buoyancy.

Aydelott (1979, 1976) used his drop tower experiments to develop a mixing time correlation in terms of We and Bo numbers. Lehrer (1981) attempted to derive a correlation independent of any empirical data but his results were inconclusive. That is, when compared to the Fox & Gex (1956) and Fossett & Prosser (1949) data, his correlation sometimes under-predicted and sometimes over-predicted the measurements. Grenville and Tilton (1996) postulated that liquid jet entrainment controlled the mixing in the entire vessel. They, therefore, included the path length of the jet as one of the characteristic length scales in their mixing time correlation. Patwardhan and Gaikwad (2003) performed several mixing tests and found that their data agreed best with the Grenville and Tilton correlation. In a detailed review, Revill (1992) notes that mixing is highly dependant on a number of factors including the relative size of the tank and the jet, the protrusion of the jet into the tank, the fill level, and the shape of the tank. It seems unlikely though that any one correlation can fit the entire range of data given the extent of the parametric space. Comparisons between the different correlations are also complicated by the fact that many of the investigators define mixing time differently from each other.

Most of the above mentioned studies were concerned with jet mixing alone and not with the effect of a jet interacting with a condensing interface. Helmick et al. (1986) performed a set of steady-state steam-on-water condensation experiments that employed an axial liquid jet. They noted that a turbulent liquid enhances condensation and that the condensation rate can be

quantified in terms of fluid properties and the liquid-side turbulence. Thomas and Morse (1963) conducted similar experiments and observed that as the liquid jet penetrated the interface, the condensation rate, which he characterized in terms of a heat transfer coefficient, increased. Chun et al. (1986) observed that if the jet subcooling was significant (30-80 K) mass transport can become unstable resulting in condensation bursts with rapid pressure decays. Sonin et al. (1986) developed a turbulent condensation correlation assuming steady state mass transfer, isotropic turbulence, small surface waviness, and negligible buoyancy. His correlation required the R.M.S. value of the turbulent velocity at the free surface that he estimated from a simple k-ε analysis. Brown et al. (1990) extended this work by including buoyancy effects through a Richardson number dependency. Brown (1991) also extended the Sonin correlation by developing another expression for the R.M.S. turbulent velocity at the free surface which was valid for smaller jet submergence depths. It remains to be seen however whether these steady state condensation correlations are applicable to the transient situation that prevails during the pressure control of cryogenic storage tanks.

This comprehensive experimental review covering various thermal stratification, self-pressurization, and pressure control studies underscores the degree of uncertainty in many of these experimental investigations. The lack of agreement between data and simple thermodynamic analyses is also unsettling. Moreover, the experiments do not provide sufficiently detailed and controlled data that is suitable for a comprehensive and rigorous model validation and verification effort. Detailed measurements of the flow field are not provided by any of the experiments. In most cases, as pointed out by Chato et al. (2005) the bulk of the experimental data is compressed into a simple engineering correlation. Unfortunately the level of uncertainty and lack of detailed data can cloud the comparisons between model and experiment and make undertaking of systematic validation efforts extremely difficult.

2.5 Theoretical Research and Numerical Modeling

In parallel to the experimental efforts described above, numerous theoretical, modeling and computational studies with varying degrees of sophistication have been undertaken to both interpret and predict the experimental behavior. Historically, a homogeneous thermodynamic model was one of the earliest analytical means for predicting the self-pressurization rate in a cryogenic tank partially filled with a liquid. Here, a First Law energy balance is performed over the entire liquid-vapor system. To close the problem, the homogeneity assumption is invoked. That is, the temperature of both the liquid and vapor phases are equal and at saturation. There have been many versions of the homogeneous thermodynamic model over the years. If the functional form of the internal energy of the two-phase fluid is known, then the energy derivative appearing in the energy balance can be computed explicitly and the vapor pressure can be evolved in time (Lin et al., 2004; Forester, 1967; Riemer, 1986). Assuming constant specific heats, others, notably, Panzarella and Kassemi (2003), Cha et al. (1993), and Rotenberg (1986) have represented the time derivative of energy as the product of specific heat and the time derivative of temperature. Still others such as Aydelott, 1967 and Li et al. (2004) have avoided using the rate form of the First Law by resorting to a thermodynamic balance to determine the final thermodynamic state of the two phase system knowing the net energy input. Naturally, the thermodynamic analysis assumes that the average energy of the liquid and vapor phases changes at the same rate as the energy of the two phase mixture defined at the saturation temperature. Since this condition is not met during the initial phases of self-pressurization experiments, when thermal boundary layers are developing and temperature gradients in the liquid and vapor are not

stationary, the agreement between thermodynamics and experiment has generally been poor, especially, in predicting the level of pressure rise. Moreover, because the homogeneous thermodynamic model forces the energy of each phase to change at the same rate, and the thermal inertia of the liquid is typically the largest contribution to the energy balance, thermodynamics usually under-predicts measured self-pressurization rates. Recognizing this, Aydelot (1967a) developed a surface evaporation model which assumed that the sensible energy of the liquid is constant and all of the incident energy is used for evaporation or maintaining the ullage at a saturation state. Since this model neglects the contribution of the liquid's sensible energy to the net energy balance altogether, it generally over-predicts the measured self-pressurization rates.

In order to obtain better agreement with experimental data, transport effects must be considered. A number of investigators have developed models which include energy and mass transport. These models are most easily classified as zonal methods whereby the liquid-vapor system is divided into zones at constant temperature and engineering correlations are used to model the energy and mass transport between the zones. The number of zones is completely arbitrary. Riemer (1986) developed a two zone model, one for each phase. Estey et al. (1983) included a separate zone bounding the interface. Epstein and Georgius (1965) divided the tank wall, liquid phase, and vapor phase into many axial zones. Schallhorn et al. (Schallhorn et al., 2006) partitioned the liquid into annular boundary layer zones and axial zones in the bulk. In comparing his two-zone model to the homogeneous thermodynamic model, Riemer (1986) noted that the zonal model did a better job of reproducing experimental data. Hedayat, et al (2003), compared the zonal model of Nguyen (1994) against a self-pressurization experiment and found that the model over-predicted the self-pressurization rate. The results of these models are unfortunately not unique and can vary depending on the correlations that are used to model heat and mass transport between the different zones.

Many investigators have tried to explicitly account for transport effects in their models instead of relying on correlations. In an early stratification analysis, Knuth (1959) modeled only the liquid phase and treated it as a semi-infinite solid. For changes in the interfacial temperature, he was determining the response of the temperature field in the liquid. Knuth (Knuth, 1962) and Thomas and Morse (1963) extended this analysis by modeling the liquid and vapor phases as two semi-infinite media coupled at the interface. Schmidt et al. (1960) performed a subcooled stratification experiment and compared his results with the semi-infinite conduction solution. He found initially there was some agreement, but it deteriorated as time progressed. Segel (1965) performed his own pressurized stratification tests and found for low heat fluxes, there was good agreement between the measured temperature profiles in the liquid and the semi-infinite conduction solution. For higher heat fluxes, however, deviations were observed and attributed to the increased convection in the liquid.

To represent natural convection effects in the liquid, a number of approximate integral methods have been developed. Bailey et al. (1963) developed a model to study stratification in the liquid. He assumed that all of the incident energy appears as sensible heat in the free convection boundary layer and that this energy is carried to an upper stratum layer where it remains without any mixing between the upper stratum and the bulk liquid. With these severe restrictions and assumed boundary layer temperature and velocity profiles, he performed integral heat and mass balances. Not surprisingly, comparisons between the model's predictions and empirical stratification data were poor. In the stratification experiment, Bailey et al. (1963) observed mixing between the upper stratum and the bulk which was not accounted for in the

model. Later, Bailey and Fearn (1964) compared their approximate integral model to a 70 ft^3 LH2 stratification experiment but again were unable to accurately predict the temperature profiles in the liquid. Tellep and Harper (1963) performed a similar analysis but included an interfacial energy contribution in the integral balance and assumed a time-invariant temperature profile in the upper stratum. This resulted in a better agreement between the predicted and measured temperature profiles. Ruder (1964) and Robbins and Rogers (1966) developed similar models but noted that modifications were necessary to include the effects of bottom heating and phase change. Vliet (1966) extended the analysis by including the effects of bottom heating but neglected the interfacial energy contribution in the integral balance. Barnett et al. (1968) included a parameter that allowed for energy exchange with the bulk liquid but still obtained poor agreement between the measured and predicted surface temperature rise. More recently, Kirk et al. (2007) used these approximate methods to study a rotating upper stage. They assumed the liquid to be in solid-body rotation with a static paraboloid interface. They noted that the rotation had an effect on the heat transfer due to the increase in wetted-wall area, but no comparisons with experiments were made.

Eventually, these approximate integral methods grew into more sophisticated boundary layer type analyses. Barnett et al (1965) applied correlations for the boundary layer thickness, the growth of the upper stratum, and the natural convection speed at the edge of the boundary layer. He obtained reasonable agreement with measured temperature profiles after including a term that accounted for the heat of compression in the liquid. Arnett and Millhiser (1965) included both the liquid and vapor phases in their analysis and accounted for inter-phase energy and mass transport. They assumed turbulent free convection boundary layer profiles for velocity and temperature but assumed the functional form of the boundary layer thickness and velocity at the edge of the boundary layer. Arnett and Voth (1972) used integral balances to compute these parameters at every location along the boundary layer. In comparing their results with Atlas/Centaur pressurization data (Lacovic et al., 1968), they observed poor agreement between measured and predicted temperature profiles and under-predicted the pressurization rate by as much as 15%. Venkat and Sherif (2004) extended the Arnett and Voth model by including variable fluid properties, bottom heating, and an ortho/para conversion routine. Most of these changes resulted in only marginal differences with Arnett and Voth's predictions. For the ortho/para concentrations analyzed, there was no discernable effect on the results. Gursu et al. (1993a, 1993b) tested several free convection boundary layer profiles and found no significant effect on the results. Their ortho/para conversion routine showed clearly, and quite intuitively, that the boil-off rate increases with increasing ortho concentration.

Most of the above mentioned boundary layer analyses assume a stationary and well-developed free convection boundary layer and a relatively simple tank geometry both of which may not be plausible in a real storage tank setting. To obtain more meaningful predictions, these approximate techniques have given way to more sophisticated computational models. Initially, several numerical studies were conducted to investigate thermal stratification in the liquid phase due to some external heating without accounting for the complicated interfacial heat and mass transfer. Nikitin and Polezhaev (1976) considered a partially filled sphere in microgravity. Assuming a static, insulated, and spherically shaped free surface, they studied the interaction between buoyancy and Marangoni convection for different ullage locations inside the tank. Cherkasov (1984) assumed a static, flat, and shear-free surface and computed the time evolution of the temperature field for different wall and interface heating configurations. Lin and Hasan (1990a) numerically studied the steady-state flow and temperature fields that developed as a

result of buoyancy in a tank with a flat shear-free interface. They tried to characterize the thermal behavior of the tank in terms of the liquid subcooling. They fixed the interfacial temperature to its saturation value and the temperature at the bottom of the tank was kept at some subcooled level. Sengupta (2001) performed similar numerical stratification studies by enforcing an adiabatic temperature condition along the interface. His computed temperature profiles below the interface deviated from the experimental data but the deviations decreased in the bulk liquid. Tanyun et al. (1996) also forced the interface to be adiabatic and noted that the computed interface temperature was higher than experimental measurements. Barakat and Clark (1965) set the interfacial temperature equal to the saturation temperature and were able to obtain some agreement with experimental temperature profiles. Navickas (1988) numerically studied the effect of baffles on the thermal stratification in a partially filled rectangular cavity with a flat interface. His results indicated that through judicious placement of baffles, thermal stratification can be suppressed.

All of the preceding computational studies ignored the vapor phase and treated the interface as a static surface. Grayson et al. (Grayson, 1995; Grayson and Navickas, 1993) removed the second limitation by allowing the interface to freely evolve and deform. They studied how the interface and the thermal field respond to different gravitational accelerations while still neglecting the vapor phase transport and assuming an adiabatic interface.

In addition to the numerical stratification studies, a number of computational studies have been reported on jet mixing. Hasan and Lin (1989) performed isothermal steady-state computations of axial jet mixing and its interaction with a flat interface. They compared the computed turbulent R.M.S. velocity profile with Sonin's expression (Sonin et al., 1986) and noted an increased deviation close to the interface. They attributed the discrepancy to the Neumann boundary conditions imposed on the turbulent kinetic energy and dissipation rate at the free surface. Later, Lin and Hasan (1992a) performed a similar computational analysis and obtained good agreement with Brown's expression (Brown, 1991) for the turbulent R.M.S. velocity profile at low jet submergences.

Hochstein et al (1984) also investigated isothermal jet mixing. Instead of Neumann conditions on the turbulent kinetic energy, they prescribed it to be zero at the interface. Unfortunately, no comparisons to experiments were made. Later, Hochstein, et al (1987) used a k-ε turbulence model again while neglecting buoyancy and allowing for free surface deformation of the interface. They were not able to obtain a solution for high jet flow rates. But for lower jet speeds, modeling the interface justifiably as a solid boundary produced more successful results. Wendl, et al (1991) were able to predict the flow patterns including the geysering effects that Aydelott observed in his drop tower experiments (Aydelott, 1979), but their predictions were only in qualitative agreement with the experimental results. In order to predict the geyser height better, Thornton and Hochstein (2000) performed a sensitivity study to determine how various parameters affect the computational solution. But they found that the CFD results were relatively insensitive to the parametric variations. Simmons et al. (2005) critically reviewed Aydelott's experiment (Aydelott, 1979) and inferred different boundary conditions and fluid properties than the ones used in previous simulation studies. But even with these modifications the deviations between measured and predicted geyser heights persisted. Marchetta et al. (2006) tried to improve the geysering simulations by using a k-ω turbulence model but the results indicated the original k-ε formulation yielded better agreement with the experiment. Marchetta and Bendetti (2007) performed 3D geysering simulations and tested a suite of two equation turbulence models. They noted that while the k-ε model predicted the geyser height more accurately when

geysering occurred, Menter's SST k-ω formulation (Menter, 1993) was far superior at predicting the different flow regimes that Aydelott had observed.

The previously mentioned deformable free surface simulations employed the Volume-of-Fluid (VOF) method. Chato and Jacqmin (2001) used a phase field model (Jacqmin, 1999) to simulate interfacial deformation during geysering. Their simulations overpredicted the geyser height at faster jet flow rates. They attributed this discrepancy to a lack of a turbulence model in their analysis. Chato (2002) later added a simple turbulence model based on a constant turbulent viscosity. This modification resulted in under-predicting the geyser height. Chato (2003) also performed a parametric study investigating the effects of contact angle, geometry, and surface tension on the predicted geyser height. He found that the geyser height increased by increasing the contact angle.

Mukka and Rahman (2004a) conducted a steady-state finite element analysis of a liquid jet entering a completely filled tank. They evaluated the effectiveness of mixing by comparing the recirculation patterns produced by different jet configurations. Later, Mukka and Rahman (2004b) extended their work by including both the liquid and vapor phases. However, given the predicted magnitudes of temperature in the liquid phase and velocity in the vapor phase, the results seem to be incorrect. Ho and Rahman (2005) performed 3D steady-state finite element simulations of a horizontal liquid jet impinging on a heat pipe in a full cryogenic storage vessel. They primarily studied the different circulation patterns for varying jet speeds and did not include any two-phase analysis or thermodynamic effects.

A number of investigators have built on this body of computational work involving thermal stratification and jet mixing by including the effects of self-pressurization. Lin and Hasan (1992b) developed a simple conduction model in the liquid and coupled it to a thermodynamic model developed by Brown (Brown, 1991). They neglected gas-phase transport but allowed the interface to expand and contract radially. They included a lumped compressibility term in their energy balance in the liquid and found that for increasing fill levels the pressurization rate was initially higher because of liquid expansion. But after some time had elapsed, the final trend suggested that the pressurization rate was indeed higher for lower fill levels as expected due to the thermal inertia of the liquid. Hochstein et al. (1986, 1990) again neglecting the gas-phase transport, employed an effective conductivity model to account for transport in the liquid. They performed a cell-by-cell mass balance along the interface to account for evaporation. Comparisons of their numerical predictions with experiments by Aydelott (1967a) and Abdalla et al. (1965) yielded reasonable agreement for the bottom heating and uniform heating cases in 1g. Unfortunately, noticeable discrepancies were noted for both the top heating test case in 1g and for the uniform heating case in low g. Although, Hochstein (1986) concluded that more work was required to improve the heat transport modeling in the tank, they still used the above model to study the effects of bulk liquid subcooling and found that the self-pressurization rate decreased with increased subcooling.

Grayson et al. (2006), included transport in the ullage and using a pressurization model provided by the CFD code Flow3D (Hirt, 2001) simulated the AS-203 flight experiment (Bradshaw, 1970; Navickas and Madsen, 1968). In an attempt to validate the model, he reported an apparent 3.5-4% deviation between the average measured and predicted pressurization rates. However, the validation was only based on the initial and final pressures. Half way through the experiment, Grayson's model predicted a prominent change in the pressurization rate that could not be corroborated by the experiment because the data was missing.

Merte et al. (1968) also developed a pressurization model which included the effects of gas-phase transport. The interface was assumed flat and the pressure for the incompressible/incompressible system was updated using a First Law energy balance. Merte et al. (1970) later compared their predictions to the data from the AS-203 flight but the agreement was not good. They attributed the errors to an inadequate representation of the tank geometry that, in turn, could result in an inaccurate representation of the heat distribution along the wall. Val'tsiferov and Polezhaev (1975) included the effects of transport in the ullage and used an integrated form of the ideal gas law to update the pressure but were not able to obtain agreement with Aydelott's self-pressurization experiments (Aydelott, 1967a). Tunc et al. (2001) also developed a gas-phase model to study thermal stratification and pressure behavior when a LOX tank is pressurized with GHe. While no experimental comparisons were provided, the computational results were judged unreliable as the non-condensable gas contribution to the ullage pressure appears to be incorrectly modeled.

Barsi et al. (2007) developed a self-pressurization model that included gas phase transport. Numerically, the liquid and vapor phases were modeled as an incompressible-incompressible system. Ullage compressibility, as well as interfacial heat and mass exchange, were modeled in a lumped fashion and then coupled to the bulk transport equations. While no experimental comparisons were performed, the numerical results agreed favorably with the prior self-pressurization results of Panzarella and Kassemi (2003).

There are many difficulties associated with including transport effects in the ullage. Therefore, it's no surprise that several investigators continued to couple lumped thermodynamic balances in the ullage to solution of the transport equations in the liquid. This approach is not without its own merit since the total pressure in the ullage is for the most part uniform as dictated by thermodynamics and the transport timescales in the vapor are much faster than in the liquid. Thus it makes sense to lump the vapor region and couple it to a detailed transport analysis of the liquid region. The accuracy and validity of these models of course depend on the fidelity of using global mass and energy balances at the interface to account for the phase change.

Amirkhanyan and Cherkasov (2001) coupled an effective conduction analysis in the liquid to a lumped model of the ullage. Their results appear to be inconclusive when compared to experimental data. In some cases they over-predict the measured pressurization rates, in other cases they under-predict the rates, and in no case their results agree with the predictions provided by a homogeneous thermodynamic analysis. Panzarella and Kassemi (2003) rigorously coupled a lumped energy and lumped mass model of the ullage to the detailed solution of the incompressible Navier Stokes and energy equations in the liquid. While experimental comparisons were not made, their simulations for a given heat load and fill level in the tank showed that the long-term self-pressurization rate is independent of the heating configuration. Additionally, the computed pressurization rates agreed with a lumped thermodynamic analysis of the system.

The Panzarella and Kassemi model was recently validated by Barsi and Kassemi (2008) based on experimental data extracted from a self-pressurization ground experiment in a flight weight liquid hydrogen tank. (Van Dresar et al., 1992, Hasan et al., 1991) The predicted ullage pressure history agreed well with the lowest and highest fill levels tested in the experiment while some deviation, most likely due to a non-uniform heat load, was noted for the median fill level. The numerical results of Barsi and Kassemi (2008) also suggest that one should exercise caution when interpreting experimental data. It is interesting to note that the expected and intuitive trend that lower fill levels should produce higher pressurization rates was not observed in the

experimental data. However this trend was recovered by the numerical model by marching the solution farther in time (beyond the experimental run times) until a stationary state was reached. This suggests that the tank had not yet reached a stationary state during the self-pressurization experiments and further highlights the need for long duration pressurization test runs.

Extending their model to larger LH2 tanks in microgravity, Panzarella et al. (2003) showed that the thermal stratification in a reduced gravity field can be significant even in a 10^{-6} g field. Their results also revealed that ullage migration from the center to the top of the tank occurs on a much faster time scale than heat or mass transport development inside the tank. Later, Panzarella and Kassemi (2005) computed the effect of fill level on the pressurization of a large LH2 spherical tank in microgravity. These results again indicated the considerable effect of natural convection in a large tank even in microgravity. They also pointed out the importance of ullage location on the thermal stratification and local superheats developed in the liquid.

Numerical investigations have not only been limited to thermal stratification, jet mixing, and self-pressurization but have also included pressure control with a subcooled axial mixing jet. Albayyari (2002) developed a simple analytic pressure control model and claimed the model to be validated. The validation claim is surprising as the nearly identical and previously published model of Bentz (1993) yielded better agreement with experimental data. The major difference between the two models is that different correlations were used to account for the heat transfer between the impinging jet and the free surface.

More sophisticated computational models have been developed in a strive to obtain better agreement with experimental data. Lin (1989) numerically studied the effects of jet Reynolds number (Re) and Prandtl number (Pr) on the condensation rate which he quantified in terms of an average Stanton number. His steady-state computations in a rectangular domain with a flat free surface at saturation temperature revealed that for the range of parameters considered, the average Stanton number is independent of Re and only weakly dependant on Pr. Lin and Hasan (1990b) continued this analysis and showed how geometry, heat load, and jet subcooling can affect the condensation rate. In all the aforementioned numerical studies by Lin and colleagues, buoyancy was neglected. Hasan and Lin (1990) included the effects of buoyancy and showed that natural convection can reduce the condensation rate noticeably.

Panzarella et al. (2004) performed a numerical study of subcooled axial jet mixing in microgravity. Their lumped vapor active liquid model showed that for most jet speeds, subcooled jet mixing was quite effective at reducing the tank pressure. For the lowest jet speed, however, buoyancy due to residual acceleration prevented the jet from reaching the interface and no pressure reduction was observed.

Van Overbeke (2004) developed a 1g pressure control model that neglected gas-phase transport. In this two-point vapor model, he used the temperature at the upper bulk head and the saturation temperature at the interface to approximate the temperature gradient on the vapor-side of the interface. He compared his results to experiments by Lin et al. (1994, 1993). However, the plausibility of such comparison seems to be questionable. In the Lin experiments, the vapor was superheated and it's unlikely that the global energy transfer can be accurately represented by the two-point approximation of the local temperature gradient on the vapor-side of the interface as in Van Overbeke's analysis. Not surprisingly, the validation results were inconclusive. In some cases the pressure collapse was overpredicted while in other cases it was under-predicted.

Finally, the explosive boiling event observed in the microgravity Tank Pressure Control Experiment (TPCE) described in Hasan et al. (1996) suggests that some type of rapid nucleation and vapor generation event is occurring when the liquid superheat gets too large. The process of

vapor bubble growth in a superheated liquid has been subject of extensive scholarly research, such as the ones by Plesset and Zwick (1954), Birkoff, Margulies and Horning (1958), Scriven (1959), Zwick (1960), Bankoff (1964), Mikic, Rohsenow and Griffith (1970), Dalle Donne and Ferranti (1975), and Prosperetti (1978). All of these studies have seemingly been limited to situations where the vapor bubble is free to expand without influencing the surrounding ambient liquid pressure far from the bubble. This is not the case if the bubble growth occurs in a closed container like a cryogenic tank since the total volume inside the tank is fixed. In a closed tank, the additional vapor volume of the growing bubble would necessarily lead to a compression of all the other preexisting vapor regions resulting in a rapid increase in the bulk liquid pressure. This could be the explanation for the rapid pressure spikes observed in the TPCE as previously mentioned. However, there seems to be little or no previous theoretical investigations of this phenomenon.

2.6 Closing Remarks

This rather comprehensive review of previously published experimental and numerical research work associated with the cryogenic storage tank pressurization and pressure control as presented above paints a clear picture of the state-of-the-art in the scientific and engineering treatment of the subject. The survey highlights several important shortcomings, limitations, and gaps that still persist in the theoretical and experimental treatment of the problem and clearly underscores the elusive nature of success in the model validation and verification efforts. On the experimental front, the high degree of uncertainty in the experiments, lack of detailed flow and thermal measurements, and absence of proper initial condition and boundary condition controls makes the use of the experimental results as benchmarks to validate and verify self-pressurization and pressure control models extremely difficult. On the theoretical/computational front, there are still substantial capability gaps, especially, in detailed and rigorous representation of phase change, interfacial dynamics, and ullage transport. In short it is clear that for proper benchmarking and systematic validation and verification of storage tank models, improvements in both the capability of the numerical models and in the nature of the experimental efforts are needed. The ZBOT project is a step towards this goal.

3. Preliminary Ground-Based Research

Our preliminary ground-based experimental and modeling research activities are described briefly in this section. The 1g and microgravity case studies presented here will not only provide good physical insight into the effect of transport processes on storage tank pressurization/pressure control, but will also examine the feasibility of using the ZBO strategy as an effective means of variable gravity tank pressure control.

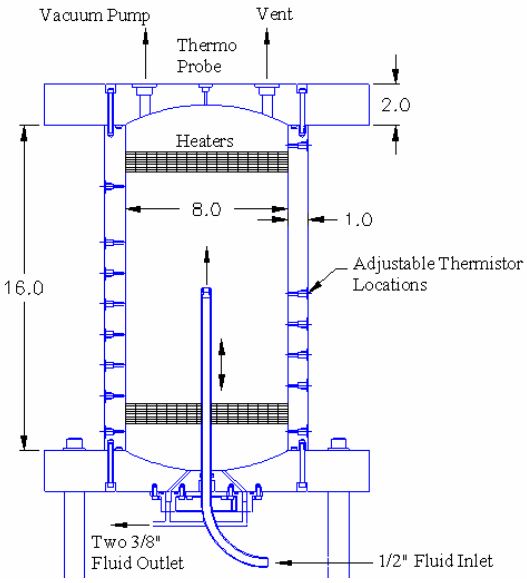

Figure 5. Test Cell Apparatus

3.1 Preliminary Ground-Based Experiment

A schematic of the preliminary ground-based experimental apparatus is shown in Fig. 5. The test cell consists of a cylindrical tank of dimensions 4" x 18" x 1" (r x h x wall thickness). Hemispherical ends with a radius of curvature of 8.5" cap the top and bottom ends of the test cell. The transparent test cell is made out of high quality optical acrylic and sits on a stand atop a vibration isolation optical bench.

Strip heaters (1 W $\pm$ 0.01 W) are affixed via adhesive to the inside surface of the test cell. Two strip heaters are employed to simulate heat leak in both the liquid and vapor regions. The time evolution of the pressure inside the test cell is measured by a highly accurate pressure transducer ($\pm$ 0.01 psi) located on the top end cap in the vapor region.

The time evolution of the temperature field is captured by 15 thermistors ($\pm$ 0.03 ^{o}C) placed inside the tank. One thermistor enters the tank through the top end cap to measure the temperature at the interface. The other 14 thermistors enter the tank through the sidewall to provide a matrix of local temperature measurements inside the liquid and vapor regions. In addition, 10 RTD elements ($\pm$ 0.1 ^{o}C) are cemented onto the outside wall of the test cell to monitor wall temperature profiles. Implementation of the ZBO strategy requires removal of liquid from the bottom of the tank. This is accomplished via twelve ports located in circumferential symmetry around the jet orifice (1/4" ID). The withdrawn fluid collects in a common manifold and passes through a micro-pump into a heat exchanger loop (see Fig. 6). The heat exchange fluid is distilled water and is pumped through the heat exchanger by a Haake heating / refrigeration circulating bath. The Haake circulator bath controls the temperature of the water so that the temperature of the test fluid, HFE-7000, measured downstream of the pump by an in-line temperature probe, is maintained at some preset value. There is a flow meter downstream of the heat exchanger to monitor the low flow rates encountered during the experiments. After passing through the flow meter, the test fluid reenters the test cell through an orifice aligned with the central axis at the bottom of the tank.

The duration of a typical experiment is approximately three hours. Temperature measurements are recorded continuously using a data logger. HFE-7000 is transparent, environmentally non-hazardous (it can be vented) and has a normal boiling temperature of 34 ^{o}C – making it ideal for studying evaporation/condensation processes at around laboratory

temperatures. It is electrically inert, non-flammable, non-corrosive and has good material compatibility. Its only disadvantage is its affinity for dissolved gases.

The gas solubility in HFE-7000 requires degassing of the fluid before an experimental run. Degassing proceeds as follows: Initially all fluid is kept in the storage tank, shown in Fig. 6 and all valves are closed. Temperature and pressure measurements are made inside the storage tank and compared with the empirical pressure/temperature curve provided by 3M. It is assumed that any deviation from the empirically- obtained pure HFE values is due to the dissolved gasses in the fluid. The cold trap is filled with liquid nitrogen and the vacuum pumping system is primed. As the valves between the reservoir tank and the vacuum pump are opened pressure in the reservoir is reduced and bulk boiling occurs. The liberated gasses, along with some vapor, will pass through the cold trap where the vapor is condensed into liquid and stored for future use. The liberated gasses are expelled from the laboratory.

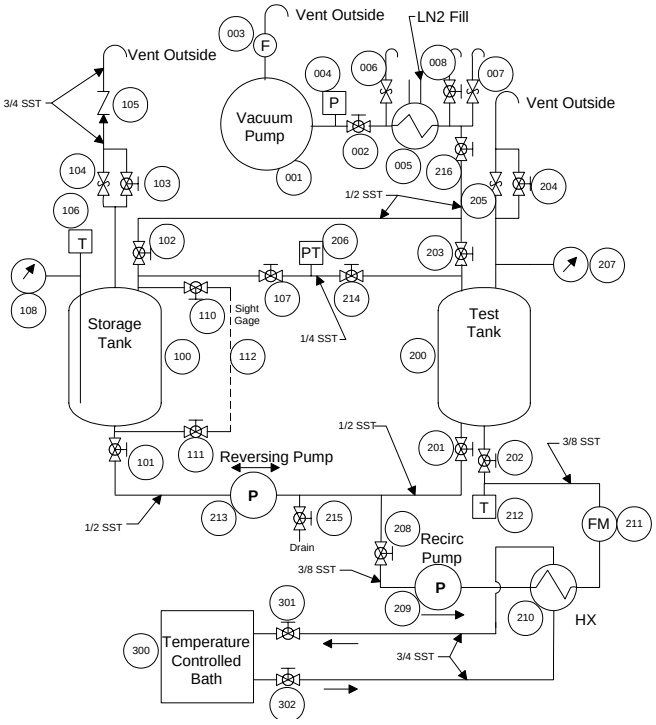

Figure 6. Experimental Set up and Fluid Loop

Once the HFE is purified and contained in the reservoir tank, the vacuum pumping system is used to vacuum purge the test cell to 500 milli-torr. Valves 101 and 201 are opened at a rate slow enough to accommodate and minimize the initial pressure spikes in the evacuated test cell. When the pressures in the two tanks equilibrate, pump 213 is started in the forward direction to transfer the fluid from the storage tank to the test cell. The test cell will be filled by maintaining a no-vent-fill condition largely in the same way that a commercial liquid propane tank is filled. If necessary, mixing via the subcooled liquid jet loop is used to enhance condensation inside the test cell.

A comprehensive set of parametric experimental test runs were undertaken whereupon the heater power, fill ratio, heat distribution, jet speed and jet temperature were varied.

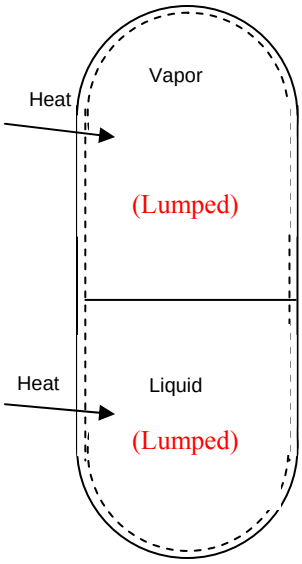

Figure7. Schematic for The TTP Model.

3.2 The Tank Pressurization/Pressure Control Numerical Models

Two preliminary models have already been developed for the storage tank. The first is the Thermodynamic Tank Pressurization (TTP) model. This model assumes homogeneous thermal equilibrium conditions in the

ullage, the liquid, and the wall and predicts the rate of pressure rise in the vapor based on the net heat flow into the tank. The second is the Active-Liquid Lumped-Vapor Tank (ALLVT) model that couples thermodynamic prediction of pressure in the ullage to transport of heat, mass, and momentum in the liquid and conduction in the tank wall. Under the conditions of a continuous constant heat leak into the tank, agreement between the long term predictions of the rate of pressure rise in the tank by the TTP and ALLVT models is essential.

3.2.1 The Thermodynamic Tank Pressurization Model

A schematic describing the essential features of the TTP model is included in Fig. 7. Several key assumptions are invoked in order to construct this thermodynamic model. The primary assumption is that the liquid and vapor are at the same temperature and pressure under saturation conditions. The secondary assumptions are: (a) the tank wall is in thermal equilibrium with the liquid and the vapor; (b) the liquid is incompressible; (c) all the thermal properties are constant; and (d) the tank is rigid. Based on these assumptions, the first law of thermodynamics for the tank can be written as:

$$\frac{d}{dt}\left(\rho_v e_v V_v + \rho_l e_l V_l + \rho_w e_w V_w\right) = \dot{Q} \tag{1}$$

Here, ρ ,. is the density, V, is the volume, e, is the internal energy, $\dot{Q}$, is the heat leak rate, and the subscripts v, l, and, w, respectively denote the vapor, liquid, and the wall..

Since the tank represents a closed system, mass conservation implies that,

$$\frac{d}{dt}\left(\rho_v V_v\right) + \frac{d}{dt}\left(\rho_l V_l\right) = 0 \tag{2}$$

and volume conservation requires that:

$$V_l = V_T - V_v \tag{3}$$

where V_T is the total internal volume of the tank. Substitution of Eq (3) into Equation (2) and integrating the resulting equation from an initial state denoted by subscript , o , provides an expression for the vapor volume in terms of the vapor density:

$$V_v(p_v) = V_0 \frac{\rho_l - \rho_{v,o}}{\rho_l - \rho_v} \tag{4}$$

The energy equation (1) can be expanded to yield:

$$e_v \frac{d\rho_v V_v}{dt} + \rho_v V_v \frac{de_v}{dt} + \rho_l V_l \frac{de_l}{dt} + \rho_l e_l \frac{dV_l}{dt} + \rho_w V_w \frac{de_w}{dt} = \dot{Q} \tag{5}$$

The internal energy is defined with respect to an arbitrary reference state and assuming constant specific heat:

$$e = c\left(T - T_o\right) + e_o \tag{6}$$

Using this definition together with Eq (2), the terms in Eq (5) can be rearranged to give:

$$\left[\rho_v V_v c_v + \rho_l V_l c_l + \rho_w V_w c_w\right]\frac{dT}{dt} + \frac{d\left(\rho_v V_v\right)}{dt}(e_v - e_l) = \dot{Q} \tag{7}$$

For convenience, the latent heat, expressed as,

$$L = \left(e + \frac{p}{\rho}\right)_v - \left(e + \frac{p}{\rho}\right)_l, \tag{8}$$

can be used to rewrite Eq (7) as:

$$\left[\rho_v V_v c_v + \rho_l V_l c_l + \rho_w V_w c_w\right]\frac{dT}{dt} + \frac{d\left(\rho_v V_v\right)}{dt}\left[L - p_v\left(\frac{1}{\rho_v} - \frac{1}{\rho_l}\right)\right] = \dot{Q} \tag{10}$$

Expressing the derivatives in terms of pressure, an evolution equation for the vapor pressure is derived:

$$\frac{dp}{dt}\left\{\left[\rho_v V_v c_v + \rho_l V_l c_l + \rho_w V_w c_w\right]\frac{dT}{dp} + \frac{d\left(\rho_v V_v\right)}{dp}\left[L - p_v\left(\frac{1}{\rho_v} - \frac{1}{\rho_l}\right)\right]\right\} = \dot{Q} \tag{11}$$

There are three important variables in Eq (11). These are the vapor density, the vapor temperature and the vapor volume. Fortunately, they can all be readily expressed in terms of the vapor pressure. Under saturation conditions, the vapor temperature is related to vapor pressure through the Clausius Clapeyron equation:

$$T(p_v) = \left[\frac{1}{T_B} - \frac{R}{L}\ln\left(\frac{p_v}{p_B}\right)\right]^{-1}; \tag{12}$$

Eq (4) from before can be used to provide a convenient expression for vapor volume in terms of vapor pressure as explicitly indicated below :

$$V_v(p_v) = V_0\frac{\rho_l - \rho_{v,o}}{\rho_l - \rho_v(p_v)} \tag{13}$$

And finally the ideal gas law can be invoked to provide a relationship between vapor density and vapor pressure:

$$\rho_v(p_v) = \frac{p_v}{RT(p_v)}. \tag{14}$$

Thus, the pressure evolution equation takes the following reduced and generalized form:

$$F(p_v)\frac{dp_v}{dt} = \dot{Q} \tag{15}$$

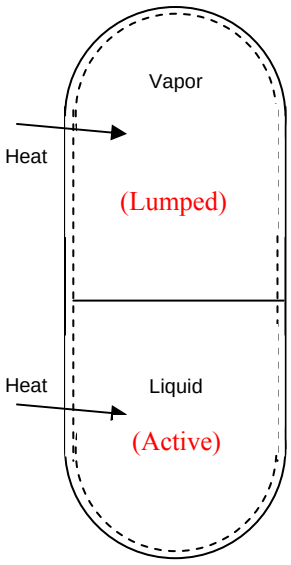

Figure 8. Schematic for the ALLVT model.

Eqs (11) – (14) constitute the TTP model. Provided the net heat flow rate to the tank is known, Eq (14) can be readily marched in time to predict the pressure change in the tank.

3.2.2 The Active-Liquid Lumped-Vapor Tank Model

The ALLVT model will be presented here in the context of a cryogenic storage tank in 1g where a saturated ullage resides above the liquid as shown in Fig 8. The tank is subject to a non-uniform heat leak, $\dot{Q}$, that may also be a function of time. This heat leak is the main cause of pressurization in the tank. Following a typical ZBO concept, the tank pressure is controlled (reduced and maintained) using a liquid jet that enters the tank along its central axis at a specified uniform sub-cooled temperature level. In the ALLVT model, the transport equations in the liquid are coupled to the lumped thermodynamic equations in the ullage. Thus, the liquid is treated as an incompressible Newtonian fluid with spatially nonuniform velocity and temperature fields while the vapor is assumed to behave as a compressible ideal gas with spatially uniform pressure, temperature and density.

The Liquid Equations:

The flow field in the liquid is described using the continuity equation and momentum balance as:

$$\nabla \cdot \vec{V} = 0 \tag{16}$$

$$\rho\left(\frac{\partial \vec{V}}{\partial t} + \vec{V} \cdot \nabla \vec{V}\right) = -\nabla p + \nabla \cdot \tau - \rho \vec{g} \beta \theta \tag{17}$$

The temperature field in the liquid is simply described by the conservation of energy equation as:

$$\rho c\left(\frac{\partial \theta}{\partial t} + \vec{V} \cdot \nabla \theta\right) = -\nabla \cdot (k \nabla \theta) + \nabla \tau : \vec{V} - \rho c \frac{dT_s}{dt} \tag{18}$$

Here the last term on the right hand side is due to a change of variable:

$$\theta(\vec{x}, t) = T(\vec{x}, t) - T_s(t) \tag{19}$$

This transformation is performed solely for increasing the ease and efficiency of generating the numerical solutions and implies that if the temperature field, T, achieves a transient but stationary state (due, for example, to continuous but constant heat leakage, Q), the transformed field, θ, approaches steady state conditions. The middle term on the right hand side is a heat source due to viscous dissipation that may have to be considered at high mixing jet velocities.

The momentum and energy equations are coupled due to the buoyancy term in the momentum equation that is a driver for the natural convection flow. Here, the Boussinesq approximation is invoked that retains the leading order density variation with temperature only in the body force (buoyancy) term. Moreover, as a result of the change in variable, the pressure appearing in the momentum equation includes an additional term in the hydrostatic contribution:

$$p = p_{static} - \rho \vec{g} \cdot \vec{r}\left(1 - \beta[T_s(t) - T_s(0)]\right) \tag{20}$$

The Lumped Vapor Equations:

Since the vapor is assumed to be an compressible ideal gas with spatially uniform temperature, pressure and density, its pressure and temperature can be evaluated as a function of time using a lumped approach based on near equilibrium thermodynamic considerations. This is valid as long as the heat flow into the vapor region and mass flux due to evaporation are relatively small (Panzarella and Kassemi, 2003). Under these conditions, even if there is some fluid flow and spatial temperature distribution in the ullage, pressure variations due to these spatial non-uniformities would be extremely small compared to the thermodynamic pressure. The thermodynamic pressure dictates the saturation temperature which under near-equilibrium conditions assumed here specifies the interfacial temperature, an important boundary condition for the liquid region. Even though pressure is spatially uniform it will change over time due net heat or mass transfer into the vapor region. If V_v is the volume of the vapor and J_v is the evaporation mass flux, then the rate at which the total vapor mass changes is given by:

$$\frac{d}{dt}(\rho_v V_v) = M_v \tag{21}$$

where

$$M_v = \iint_I J_v dS \tag{22}$$

Neglecting contributions from kinetic and potential energies, the total energy in the ullage due to the heat and mass transport is given by the following conservation equation:

$$\frac{d}{dt}(\rho_v V_v e_v) = M_v(e_v + \frac{p_v}{\rho_v}) - p_v \frac{dV_v}{dt} + \dot{Q}_{Iv} + \dot{Q}_{wv} \tag{23}$$

Here, the first two terms on the right hand side are respectively contributions to the ullage energy due to evaporation (mass transfer). The 3rd term is due to P-V work and the last two terms are respectively contributions to the ullage energy due to heat flow into the vapor from the vapor side of the liquid-vapor interface and from the tank wall.

The energy required by the evaporation process is provided by the difference between the integrated heat fluxes across the interface on the vapor and liquid sides, that is:

$$LM_v = \dot{Q}_{Il} - \dot{Q}_{Iv} \tag{24}$$

Where the liquid side integrated flux, Q_{Il}, can be evaluated from the solution of the temperature field on the liquid side as:

$$\dot{Q}_{Il} = \iint_I -k_l \nabla T\big|_l \cdot n_I dS \tag{25}$$

Using Eq (25) with together with Eq (21) for the rate of change of vapor mass, Eqs (2) and (3) for mass and volume conservation and Eq (6) for internal energy, Eq (23) can be cast into the following evolution equation for ullage pressure:

$$\frac{dp_v}{dt} = F(p_v) \cdot [\dot{Q}_{IW} + \dot{Q}_{Il}] \tag{26}$$

Where F(p) is given by

$$F(p_v) = \left[\left(\rho_v c_v V_v\right) \frac{dT}{dp} + \frac{\partial(\rho_v V_v)}{\partial p} \left\{ L - p\left(\frac{1}{\rho_v} - \frac{1}{\rho_l} \right) \right\} \right] \tag{27}$$

Again, the expression for, F, only depends on the ullage pressure, because the vapor temperature, volume, and density can all be defined in terms of pressure using respectively, the Clausius Clapeyron relationship [Eq (12)] , the global mass balance [Eq (13)], and the ideal gas law [Eq (14)].

The Interfacial Balance Equations:

Conservation of mass requires the interfacial mass flux, J_l, due to evaporation or condensation to be equal to the rate at which the liquid is flowing towards the interface, that is

$$J_v = J_l = \rho_l(\vec{V}_l - \vec{V}_I) \cdot n_I \tag{28}$$

Here, n_I , is the unit normal vector pointing towards the vapor region and, $\vec{V}_I$, is the interfacial velocity. Based on the convention used, J_v , is positive for evaporation and negative for condensation. If, $J_v = 0$, this equation reduces to the kinematic condition which states that the fluid must be moving with the same velocity as the interface. Moreover, the no-slip condition requires the tangential component of the liquid velocity to be equal to the tangential component of the interface velocity:

$$(\vec{V}_l - \vec{V}_I) \cdot \hat{t} = 0 \tag{29}$$

where $\hat{t}$ is the unit tangent vector at the interface.

A normal stress balance across the interface, neglecting viscous stresses in the vapor and the momentum jump due to evaporation reduces to:

$$p_v - p_l + 2\mu_l S_l \cdot n_I \cdot n_I = 2H\sigma \tag{30}$$

Here, σ, is the interfacial surface tension, H, is the mean curvature of the interface and, S_l , is the rate-of-strain tensor for the liquid defined as:

$$S_l = \frac{1}{2}[\nabla \vec{V}_l + (\nabla \vec{V}_l)^T] \tag{31}$$

Similarly, the tangential stress condition can be written as:

$$S_l \cdot n_I \cdot \hat{t} = \nabla \sigma \cdot \hat{t} \tag{32}$$

Since surface tension is assumed to be constant for this analysis (near-equilibrium, pure vapor, $T_I = T_s$ = constant), the shear–stress condition reduces to

$$S_l \cdot n_I \cdot \hat{t} = 0$$

Here, the viscous stress on the vapor side is justifiably neglected because the dynamic viscosity of the vapor is much smaller than that of the liquid.

At the interface, the temperature of the liquid is equal to the interfacial temperature. That is:

$$T_l = T_I . \tag{33}$$

If the liquid at the interface were in complete thermodynamic equilibrium with the adjacent vapor, then the interfacial temperature, T_I, would be equal to the saturation temperature, T_s. Of course, strictly speaking, the interface is not in complete equilibrium when there is evaporation or condensation and the interfacial temperature must be different from the saturation temperature. However, the difference between the interfacial and saturation temperatures is still quite small for near-equilibrium conditions, where the phase change proceeds at a relatively slow pace. Therefore, under near equilibrium condition we can still safely assume that:

$$T_I = T_s \tag{34}$$

For rapid and intense phase change where departure from equilibrium is drastic, the difference between the interfacial and saturation temperatures is described by a constitutive relationship derived from kinetic theory (Shrage, 1953) as will be discussed in Section 7.

The formulation of the ALLVT model is now complete. Note that there is a strong coupling between the energy equations in the vapor and liquid regions through two terms. First the interfacial temperature which is a thermal boundary condition for the energy equation on the liquid side is implicitly computed from the evolution of pressure on the ullage side described by Eqs (26) and (27) and the Clausius Clapeyron relationship (12). Second, the integrated interfacial liquid heat flux that is a source term in the ullage pressure evolution equation (26) is determined by integrating the normal interfacial temperature gradients computed from the solution of the energy equation on the liquid side according to Eq (25).

Finally, there are also cross-coupling between the energy and the Navier-Stokes equations on the liquid side due to the convective terms in the energy equation and the buoyancy term in the momentum equation. As a result of these nonlinear couplings, Eqs. (16)-(20) for the velocity and temperature field on the liquid side and Eqs (26) and (27) for evolution of pressure on the ullage side must be simultaneously marched in time while satisfying the complete set of interfacial balances and boundary conditions for a complete transient simulation of the problem.

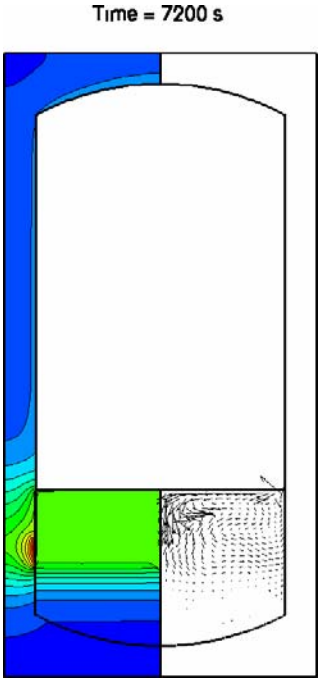

Figure 9. Temperature and Flow Fields in the Pressurized Experimental Tank in 1G.

3.3 Proof of Concept: Preliminary Pressurization and ZBO Pressure Control Simulations & Experiments

In this section we present results extracted from a series of parametric numerical simulations generated by the TTP and ALLVT models. We have basically three aims in mind:

1. Perform partial validation of the existing tank models against 1g pressurization data provided by the preliminary ground-based simulant fluid (HFE7000) experiment.
2. Underscore the main functional difference between the TTP (thermodynamic) and ALLVT (transport) models.
3. Demonstrate conceptually how the ZBO heat removal and jet-mixing mechanisms can be used to control the pressure in a spherical hydrogen storage tank on earth and in microgravity.

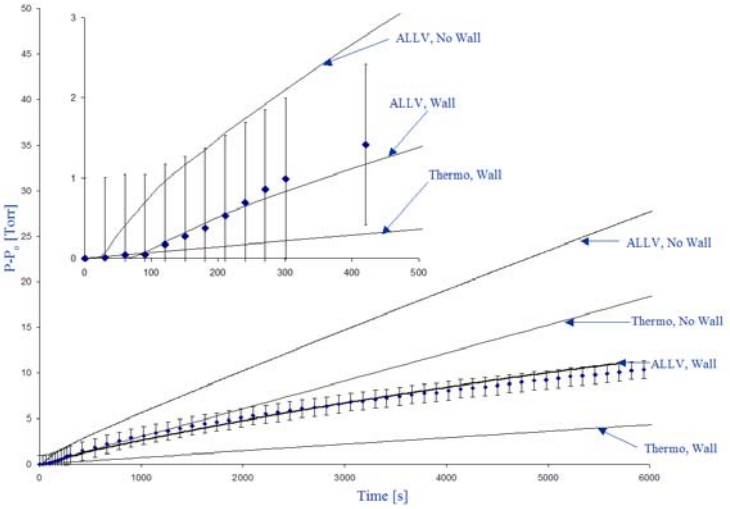

Figure 10. Comparison between the 1G Pressure Rise Predictions of Several Tank Models.

Detailed discussion of the mathematical models and the numerical results generated can be found in Panzarella and Kassemi, (2003, 2004, 2005) and Barsi and Kassemi (2005, 2006). To save space, in all the time sequences of flow and temperature fields presented in the remainder of this section, symmetry is exploited by showing the temperature contours on the left half and the streamline contours or velocity vectors on the right half of the tank diagrams.

3.3.1 Preliminary Validation of the Pressurization Model

In order to validate the tank models and to focus attention on the functional differences between the Thermodynamic (TTP) and the transport (ALLVT) models, they were benchmarked against pressurization data obtained in our preliminary ground-based experimental setup that was described in detail in section 3.1. The case considered is that of the 8''x18'' transparent acrylic tank, as shown in Fig. 5, containing the transparent simulant fluid, HFE7000, at a fill ratio of 25%.

At time zero, only the strip heater in the liquid region is activated and a total heat of 1W distributed uniformly in the strip is imposed on the inner tank wall. The near stationary natural convection flow and the resulting thermal stratification of the liquid in the tank at time = 7200s as predicted by the ALLVT model are shown in Fig. 9. At, Ra = 10^{11}, the natural convection flow is quite strong and is driven by extremely thin thermal and velocity boundary layers at the wall. After about 5 minutes, considerable thermal stratification occurs in the liquid and continues until a near stationary state is approached at around 2 hrs. The flow and temperature fields, however, are still strictly speaking transient and exhibit an oscillatory nature seemingly indicative of a flow regime transitioning between laminar and turbulent natural convection.

Evolution of tank pressure during the experiment is shown in Fig. 10 where the predictions of four different models are compared to the measured data. The experimental pressure evolution curve denoted by dots with error bars indicates an initial delay of about 1.5 minutes followed by a transient nonlinear pressure rise of approximately 10 minutes that eventually starts to asymptote to a linear slope (a constant pressure rise rate) at about 1 hour into the experiment.

Comparisons between the different tank model predictions and the experimental pressure evolution curve indicate that both the transport ALLVT model and the thermodynamic TTP model grossly misrepresent the actual pressure rise when the thermal inertia of the wall is not considered. When the effects of thermal inertia of the wall are included in the models, the comparisons become quite favorable. The TTP model, with wall thermal inertia included, predicts a constant pressure rise rate that agrees well with the slope of the experimental asymptote. However, the thermodynamic model still under-predicts the magnitude of the pressure rise. The conjugated ALLVT model that includes both wall thermal inertia and wall conduction along with transport of heat, mass, and momentum in the liquid follows the experimental pressure curve in both trend and magnitude with great fidelity. The expanded scale inset of Fig. 10 clearly shows that the thermodynamic TTP model is incapable of predicting the initial experimental pressure lag and the nonlinear pressure evolution during the transient interval. However, the conjugated ALLVT model predicts both the lag and the nonlinear transient pressure behavior with impressive accuracy.

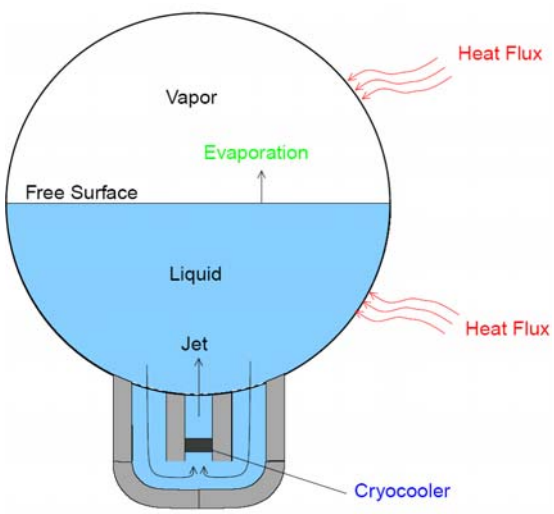

Figure 11. Schematic of the Spherical Storage Tank

Finally, there seems to be a small but widening discrepancy between the experimental data and the pressure predictions of the conjugated ALLVT model at larger times. We attribute this widening discrepancy to an increase in unaccounted heat loss from the tank as time goes on. Three important conclusions can be derived from this preliminary but important benchmarking case study:

1. The long duration pressure rise rate should be the primary standard for comparison between different models and experiment. Lack of agreement is symptomatic of inaccurate and inadequate knowledge of energy distributions within the tank system.
2. Thermodynamic models cannot predict the initial (or for that matter any) transient behavior. As a result they will have difficulty in predicting the magnitude of the tank pressure rise.
3. Proper and adequate book keeping of energy distributions within the tank system and how it changes with time is a prerequisite for any tank model and essential to the success of any pressurization/pressure control experiment.

3.3.2 Further Ground-Based Simulations of Pressurization and Pressure Control

The case studies presented in this section are concerned with pressurization and pressure control of storage tanks in 1g. Here, the goal is to:

1. Further delineate the functional differences between the thermodynamic and transport models
2. Show the effect of different wall heat leak distributions
3. Indicate the conceptual feasibility of ZBO pressure control

In the simulations presented here, the pressure rise is caused by a constant heat leak from the sidewall into the liquid region of a 10 cm diameter spherical cryogenic tank half filled with liquid hydrogen as shown in Fig. 11. Initially, the liquid is motionless. Heat is added through the tank walls at a rate of 0.6283 mW as if distributed by means of a 2 cm strip heater placed up against the tank wall in the liquid region at height of 2 cm from the bottom of the tank. The remainder of the tank wall is assumed to be insulated. Two basic case studies are presented here. In the first case, there is no jet mixing or cooling of the fluid. In the second case, a jet with an initial diameter of 1 cm, an average velocity of 1 cm/sec, and an inlet temperature of 20 K is used to mix and cool the liquid. Mass is conserved by the liquid leaving from an outlet at the bottom of the tank at the same rate at which it is supplied by the incoming jet flow. In this set up, it is inherently assumed that heat is continuously removed from the tank, since the jet inlet temperature is always equal to the initial (sub-cooled) liquid temperature of 20 K but the liquid, which leaves the tank, is at a slightly higher temperature. The simulations represent ground-based applications with the acceleration of gravity set to its normal value of 981 cm/sec^2.

The temperature and flow (streamlines) fields of the no-jet case are examined first as shown in Fig. 12T. At t=2.5 sec, a thermal boundary layer is just developing near the heated section of the tank, but it has not yet reached the interface. During this time, the pressure is not increasing since there is no significant heat transfer across the interface. The streamlines indicate that there is a counterclockwise circulation starting up near the heater due to natural convection. There is a slight spreading out of the temperature contours above the heater due to this convection. At t=50 sec, the thermal boundary layer has finally reached the liquid-vapor interface, and both the pressure in the vapor and the temperature at the interface begin to rise as depicted in Figs. 13T-a and 13T-b. After 2 hours, the spatial temperature distribution in the liquid reaches a quasi-steady or stationary state even though as shown in Fig. 13T, the temperature at the interface, the vapor pressure and the overall tank temperature levels all keep increasing because of the steady heat flux (leakage) at the wall. The final maximum convective velocity in the liquid is about 0.0932 cm/sec and is located on the interface above the heater, where the spacing between the streamlines is a minimum.

Fig. 13T-a displays a comparison between the pressure evolution predicted by the TTP and ALLVT models. It is clearly shown that when there is no jet, the vapor pressure keeps on rising at a rate that will eventually agree with a purely thermodynamic prediction. The results of the two other case studies pertaining to the uniform heating of the entire tank and uniform heating of only the vapor region are also included in Fig. 13T. Note that the TTP model cannot predict the effect of wall heat flux distribution on the magnitude of the pressure rise and therefore severely under-predicts the pressure rise in the uniform and vapor heating cases.

The temperature and flow (streamlines) fields for the jet-mixing case, as predicted by the ALLVT model, are shown in Fig. 12B. Here, at t=2.5 sec, the jet, which enters at an inlet in the bottom of the tank, has ascended halfway to the interface, and the thermal boundary layer is still very localized near the heater. At t=60 sec, the jet has already reached the interface, spread across it, and eventually runs up against the tank wall. Essentially, the cold jet flow isolates the hot region near the wall from the liquid-vapor interface. As time goes on, the jet flow turns around at the sidewall and continues downwards to the bottom of the tank where it exits through

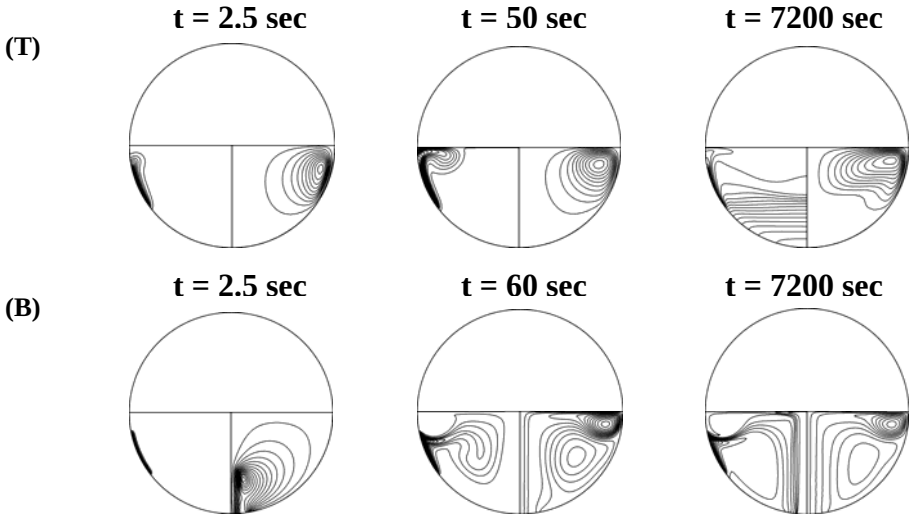

Figure 12. (T) Temperature contours and streamlines without a jet. The minimum and maximum temperature at t = 2.5 sec is 20 K and 20.002 K, respectively (10 contours). The minimum and maximum temperature at t = 50 sec is 20 K and 20.0021 K, respectively (20 contours). The minimum and maximum temperature at t = 7200 sec is 20.018 K and 20.024 K, respectively (20 contours). The final maximum convective velocity is 0.0932 cm/sec. (B) Temperature contours and streamlines when there is a jet. The minimum and maximum temperature at t = 2.5 sec is 20 K and 20.0006 K, respectively (10 contours). The minimum and maximum temperature at t = 60 sec is 20 K and 20.0028 K, respectively (20 contours). The minimum and maximum temperature at t = 7200 sec is 20 K and 20.0043 K, respectively (20 contours).

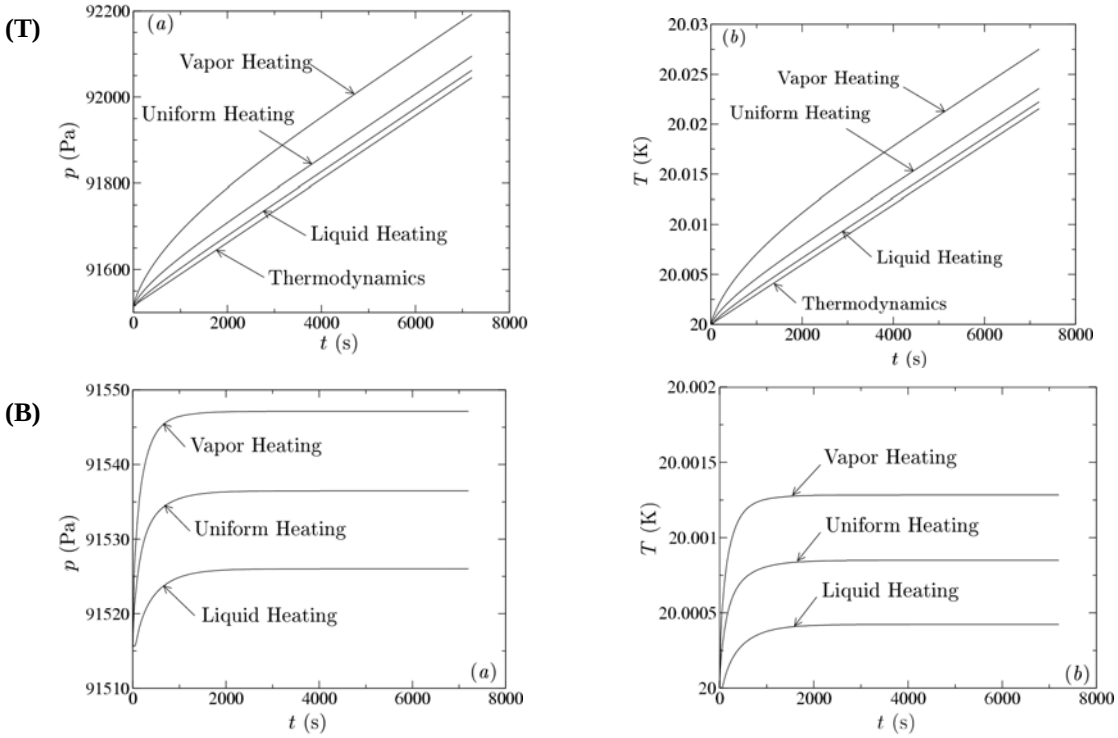

Figure 13. Pressure (a) and temperature (b) rise when there is no jet (T) and when there is a jet (B). The total heat power input is the same in all cases and is equal to 0.6283185 mW.

Figure 14. Final isotherms and streamlines after 150 days for jet speeds of (a) $\bar{w}_j = 0.005$ cm/s, (b) $\bar{w}_j = 0.05$ cm/s and (c) $\bar{w}_j = 0.5$ cm/s.

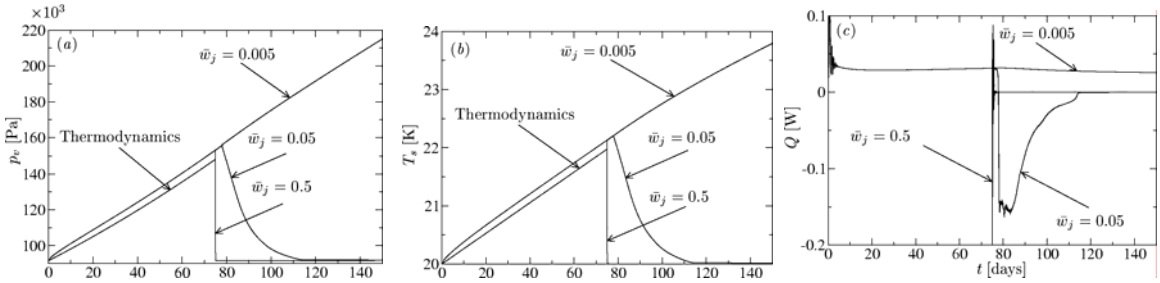

Figure 15. The long-term (a) pressure, (b) saturation temperature and (c) total heat flow both before and after the subcooled jet has been turned on.

the outlet. In this manner, the counter-clockwise recirculation of heated liquid is trapped near the sidewall instead of rising towards the liquid-vapor interface (as it did in the no-jet case where it caused significant vaporization).

The time histories of the vapor pressure and interfacial temperature for the jet-mixing case are respectively depicted in Figs. 13B-a and 13B-b. It's interesting to see that the pressure has initially a small rise but as soon as the jet flow reaches the liquid-vapor interface it isolates it from the warm fluid near the sidewall. As a result both the vapor pressure and the interfacial temperature level off at values slightly above their initial values. This happens because the cooling/isolating effect of the jet eventually balances the effects of the imposed wall heat flux and ZBO conditions are established and prevail at a true stationary state after about 2 hours.

Finally, it should be again emphasized that the TTP model is not capable of accurately computing the cooling time constants because they are so dependent on transient evolution of transport and spatial distributions of flow and temperature in the liquid region.

3.3.3 Simulation of Pressurization and Pressure Control of a Large Spherical Tank in Microgravity

Preliminary simulations of ZBO pressure control in a microgravity environment as generated by the ALLVT model are examined next for a large 3 m diameter tank. The tank is 95% full of liquid hydrogen and allowed to self-pressurize for 75 days before turning on the jet. The tank temperature and flow fields produced by three different jet speeds are included in Fig. 14 and the resulting pressure rises are shown in Fig. 15.

For the lowest jet speed of $\bar{w}_j = 0.005$ cm/s, pressure and temperature continue to rise at nearly the same rate as the no jet case since the forced flow is unable to penetrate far enough into the liquid region to reach the vapor. The temperature and flow fields surrounding the vapor region are nearly the same as those before the jet is turned on, as shown in Fig. 14a. Obviously, the

thermal stratification is hardly disrupted since the cooling effect of the jet is limited to the bottom of the tank and the net heat flow into the vapor is only slightly decreased as shown in Fig. 15c. This is insufficient to cause any noticeable change in the pressure rise. Therefore, at its lowest speed, the jet cannot effectively control the pressure over the time span considered here.

When the jet speed is increased by an order of magnitude to $\bar{w}_j = 0.05$ cm/s, it becomes more effective. Fig. 15 shows that it still takes about 2.8 days before there is any significant cooling effect since it takes that long for the jet to reach the interface. This is considerably slower than the timescale of about one hour that is predicted if a simple calculation based on the jet inlet velocity and the distance from the bottom of the tank to the interface is used. This discrepancy is due primarily to the counter-flow vortex generated by natural convection and the effect of buoyancy that tends to suppress the penetration of the cold jet into the warmer regions of the tank. Fig. 15 shows that once cooling begins, it takes about 45 days for the jet to bring the saturation temperature and vapor pressure back down to their initial values. This time, the cooler jet fluid penetrates into the liquid region and encapsulates the entire vapor region as indicated by the final isotherms in Fig. 13b. But, there is still some thermal stratification in the remainder of the liquid.

The cooling effect is further enhanced when the jet speed is increased by another order of magnitude to $\bar{w}_j = 0.5$ cm/s. In this case, the net heat flow into the vapor drops after only 6 min as shown in Fig. 15. This is in better agreement with the timescale derived from a simple calculation based solely on distance and jet speed because of the overwhelming jet speed. Once cooling begins, it only takes about 5 hours for the jet to bring the saturation (also interface) temperature and vapor pressure back down to their initial values. The final temperature profile of Fig. 13c also shows that the recirculation of the cooler fluid due to the jet flow now encompasses over half of the liquid volume, and the circulation cell due to natural convection is much weaker and only limited to a small region near the bottom of the tank. As a result, thermal stratification in the liquid is almost entirely disrupted by the stronger jet in this case.

In summary, the preliminary simulations presented in this section underscore the fact that a simple thermodynamic analysis is very informative and probably adequate for design of a passive storage tank. But, if active ZBO pressure control is desired the interaction among the intricate transport phenomena become quite important and affects tank pressurization and pressure control time constants profoundly. These effects can only be captured if the transient transport in the liquid is properly included as in the ALLVT model. It is also apparent that the microgravity experiment must provide temperature and pressure data in both the initial transient and the final stationary states of self-pressurization in as both are necessary for proper validation of the theory and the models across the regimes.

4. Research Approach & Objectives

From the discussions in the preceding sections, It is clear that reliable, affordable, and efficient active pressure control systems for future space cryogenic tanks cannot be built by brute force – that is through a design-build-fly-redesign-rebuild-refly-…-… trial-and-error engineering approach. We stress again, that the aerospace engineering community feels that there are no real alternatives to a large-scale in-space storage tank prototype technology validation test. However, as mentioned before, past attempts to move directly to TRL 6-7 experiments such as in the case of COLD-SAT (Schuster et al, 1990) have proved too costly and ultimately abandoned.

It seems before such costly endeavors become warranted, a series of small-scale microgravity experiments are needed to test and compare different aspects of CFM and storage design concepts including the main elements of the ZBO strategy. For example, have in mind that currently there are large knowledge gaps and serious engineering impediments in the path of developing and implementing the ZBO pressure control technology for space storage tanks:

1. The impact and nature of various interacting transport phenomena such as natural and forced convection are still not clear and need scientific clarification.
2. Microgravity data for deriving relevant empirically-based engineering correlations for pressurization, mixing, destratification, and pressure control time constants are scarce and insufficient and/or based on ill applied theory.
3. Comprehensive, customized and fully validated numerical models (in all the right environments) to aid the scale-up design and provide a virtual platform for assessing the performance of ground-tested-only storage tank design for extrapolation to microgravity and variable gravity space applications are not available.

In this light, the major goals of the present research can be restated as follows:

1. Build a science base for the future space storage tank engineering efforts by elucidating the roles of the various interacting transport and phase change phenomena that impact tank pressurization and pressure control in variable gravity through systematic 1g and microgravity investigation.
2. Develop a small-scale simulant-fluid experiment for both preliminary ground-based testing and subsequent ISS flight experiments in order to obtain valuable microgravity empirical data such as pressurization, mixing, destratification, and pressure control time constants as a function of important design variables for tank design
3. Develop a variable gravity two-phase model for storage tank pressure control that can be used to aid scale-up tank design.
4. Obtain archival microgravity science data for CFD model validation and verification.
5. Show the feasibility of ZBO pressure control scheme for microgravity applications.

To accomplish these objectives, a coordinated hand-in-hand experimental-theoretical-computational research approach is adopted. The theoretical/computational effort consists of comprehensive scaling analyses, development of in-depth zonal thermodynamic and two-phase CFD models for tank pressurization and pressure control, and a series of targeted parametric numerical simulations and sensitivity analyses. The experimental effort consists of a small scale ISS microgravity experiment using a transparent simulant fluid contained in a transparent tank test cell.

5. The ISS Microgravity Experiment

The ISS microgravity experiment will involve both pressurization and pressure reduction tests. The pressurization tests will be conducted by direct heating of the tank wall and the pressure reduction test will be accomplished through thermal destratification of the bulk liquid by forced liquid jet mixing. Parametric test runs will investigate the effect of the important system elements of a pressure control strategy on pressurization and pressure control. These include:

1. Wall heat flux
2. Jet flow rate
3. Jet Temperature
4. Tank fill level.

During each test, the ullage pressure and the liquid temperature are locally measured at several locations and the velocity field in the liquid is non-intrusively captured.

5.1 The Experimental Setup

The experimental apparatus and the diagnostic rig consist of eight main components that will be briefly described below.

The Test Cell: The schematic of a proposed test cell is shown in Fig. 16. It consists of a tank with a diameter to length aspect ratio of 1:2 with hemispherical end caps.. The test cell material is chosen to withstand the tank Maximum Operating Pressure (MOP) while providing optical quality transparency for ullage bubble position determination and field view velocimetry (PIV). It is anticipated that the tank shall be aligned with the residual gravity vector such that the ullage will stay at one end of the test cell away from the jet nozzle.

Test Fluid: The test fluid will be a transparent model fluid. The candidate test fluid is Perfluoro-N-Pentane (PNP). This fluid was chosen due to its low normal boiling point, its nominally nontoxic and environmentally friendly properties and its relatively steep saturation curve. It needs to be approved by NASA's stringent ISS safety review. All the constituent species in the test fluid and ullage will be accurately determined pre-mission. The limit of tolerable particulate level is set by the PIV particles and will be chosen to be sufficiently small to

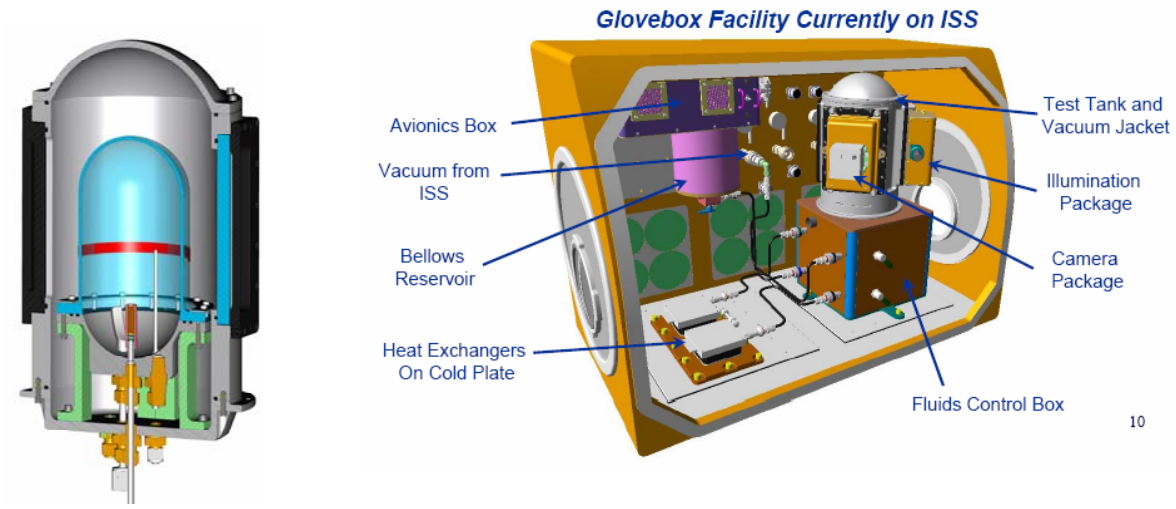

Figure 16. Schematic of The Transparent Test Cell and the ISS Glove Box

prevent bubble nucleation. The tests will be conducted at three different fluid fill levels.

Test Cell Thermal Isolation: Since self pressurization is primarily a function of total heat flow into the tank, there are stringent requirements for thermal isolation of the test cell from the general MSG surrounding environment. The test cell will be placed in a thermal isolation jacket as shown in Fig. 16. Vacuum will be drawn to minimize conductive heat loss between the test cell and the thermal isolation jacket. The inside walls of the jacket including the view ports will be coated with reflective coating and the temperature of the jacket will be controlled to minimize the radiation losses from the test cell.

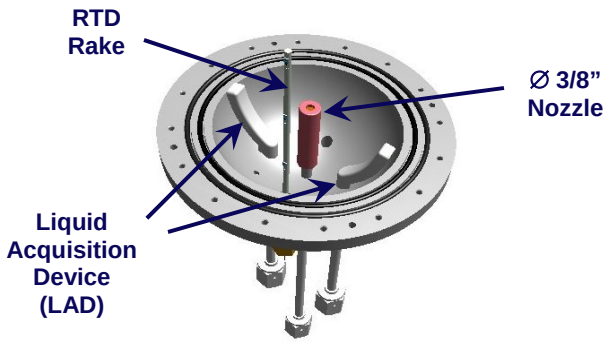

Figure 17. Schematic Displaying The Jet Flow Nozzle, and The LADs.

Test Cell Heating: The test cell will be heated with electrical strip-heaters placed circumferentially at the transverse mid-plane of the cylindrical test section. The strip heater will provide a constant heat power at pre-designated set levels throughout each experimental run.

Liquid Mixing Jet Operation: During the mixing, destratification, and pressure control studies, jet mixing will be accomplished by drawing the working fluid from the test cell, through a flow loop, and pumping it back into the tank via a jet flow nozzle as shown in Fig 17. The nozzle will be aligned along the longitudinal axis of the tank and made out of stainless steel to minimize any axial temperature drop along the its body. It is planned to keep the outlet of the jet nozzle projecting into the test cell. In this fashion, the jet flow and spread angle will be completely in the field of view (FOV) for flow visualization and PIV velocimetry.

Several different jet flow rates will be studied during the test runs as described in Section 5.4 spanning both laminar and turbulent regimes. During the test runs, the jet flow rate will be kept constant and its temperature will be maintained to the desired level. Since the position of the ullage in microgravity is unknown, a simple liquid acquisition device (LAD) will be designed and implemented at test cell outlet as indicated in Fig. 17 to prevent withdrawal of vapor from the tank into the fluid loop.

Sub-Cooled Jet Mixing: In the mixing and destratification studies, the temperature of the liquid jet must be maintained and controlled to set points close to either the average tank outlet temperature or to a pre-designated sub-cooled level. Therefore, when the liquid is pumped out of the tank, it will pass through a heat exchanger connected to the fluid loop.

Local Temperature & Pressure Measurements: Accurate and precise local temperature measurements will be taken in the range of 20 – 70 ^{o}C. The thermistors will be located on a specially designed mounting rake inserted into the test cell and on the interior and exterior of the test cell wall. The tank pressure will be measured at the one location.

Velocity Field Visualization/Measurement: Standard Particle Image Velocimetry (PIV) will be used to visualize the important flow structures that develop in the tank as shown Fig. 18. As a result of the ongoing competition that might occur between natural convection and the forced jet mixing, the flow structures may occupy the entire liquid region (i.e. locations near the walls, near the liquid-vapor interface, and in the central region of the tank). Therefore, we will ideally strive for a near full flow visualization. The PIV particles will be compatible and density-matched with

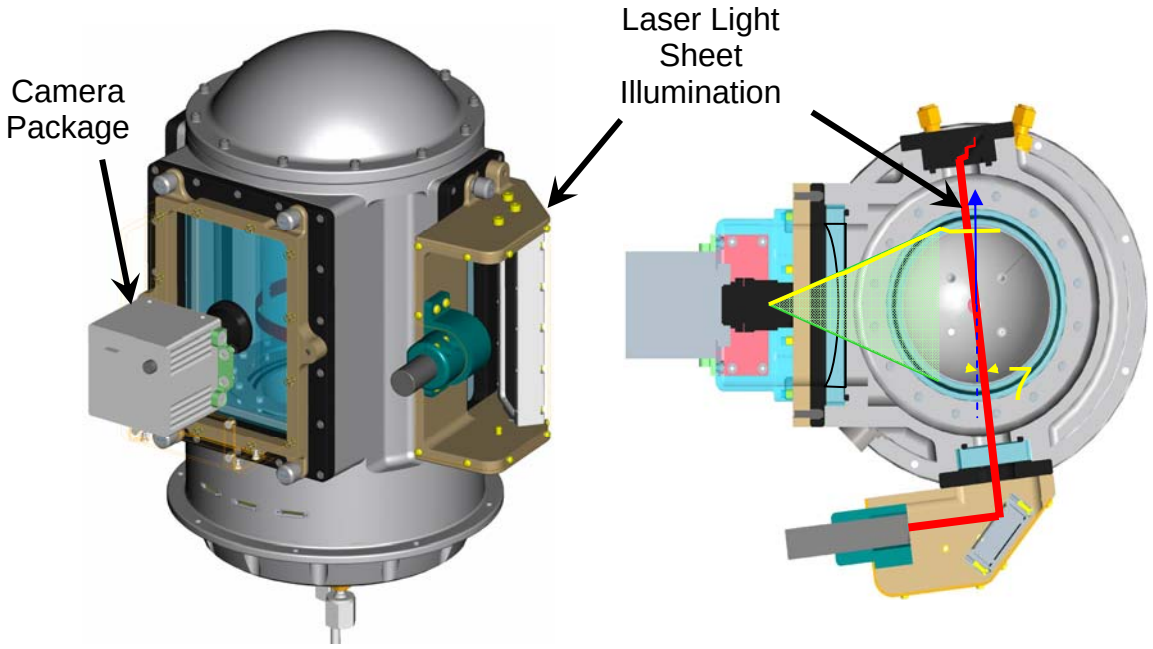

Figure 18. Particle Image Velocimery (PIV) System for Flow Visualization and Measurement.

the test fluid as much as possible. Spatial resolution and recording frequency of the PIV technique will be optimized to allow simultaneous measurement of multiple flow structures with different velocities.

Ullage Location Measurement: The position of the ullage will be captured in the field of view during the video imaging. This information is needed for the model validation and verification.

5.2 The ISS Microgravity Environment

The Zero Boil-Off Tank (ZBOT) experiment will be sensitive to the overall acceleration vector of the International Space Station (ISS), since during the experiment, the ullage will migrate in the direction of the residual acceleration vector. It is desirable to keep the ullage at the end of the ZBOT test tank opposite of the mixing nozzle. This is beneficial for both model validation and visualization purposes and jet mixing test runs.

5.2.1 Residual Acceleration on ISS: The residual acceleration on the ISS is comprised of the gravity gradient, rotational, and drag components. The gravity gradient and rotational components are location dependent within the ISS. The drag component is small compared to the other two components. The ISS operates in three primary attitudes, each producing a different acceleration:

1. LVLH (Local Vertical, Local Horizontal) – This is sometimes called XVV (X-axis Velocity Vector). This is when the ISS flies as if it were an airplane flying over the earth's surface: its x-axis is always pointed towards the direction of travel, and the ISS appears to always be level with the horizon. In reality, the ISS must constantly be pitched in order to maintain this same relative attitude as it orbits the earth. This attitude is currently used about 50% of the time.

2. YVV (Y-axis Velocity Vector) – This is the same as XVV except the ISS is yawed to fly in the direction of its y-axis. This attitude is rarely used.
3. XPOP (X-axis Perpendicular to Orbital Plane) – This is where the ISS flies with its x-axis pointed towards the sun. It keeps a constant orientation relative to the sun-earth system, but it appears to always be rotating with respect to the earth's surface. This attitude is currently used about 50% of the time.

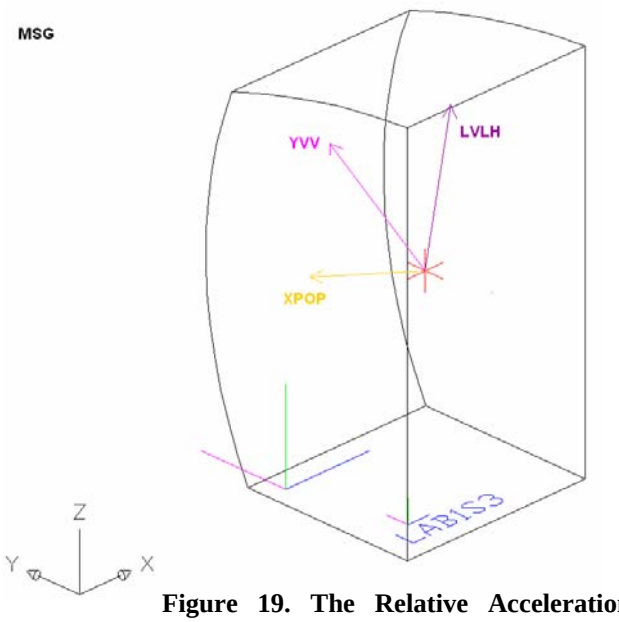

Figure 19. The Relative Acceleration Vectors For Each Attitude In The MSG Rack.

Table 2. MSG Acceleration Vectors (Micro-g)
(Rack Coordinates, Crew Sleep Period)

Attitude	Mean Accelerations			Magnitude (Micro-g)
	X	Y	Z	
LVLH	0.03	0.01	1.44	1.44
XPOP	-1.24	0.10	0.36	1.30
YVV	-1.36	-0.24	1.77	2.24

Table 2 summarizes the magnitudes and directions of the acceleration vectors as measured by the PIMS program using SAMS triaxial heads. The measurements were all obtained during May and July, 2004. Note the reported values were obtained during crew sleep periods. During waking periods the same trends can be seen but are superimposed with a great deal of random noise from crew movement and activities.

5.2.2 Orientation of the Experimental Tank in The MSG Rack

It is expected that ZBOT experiment will be housed in the MSG rack. Fig. 19 graphically shows the relative acceleration vectors for each attitude in the MSG rack. All the vectors tend to point upwards somewhat along the z-axis. The ZBOT test tank will be oriented in a manner that its top points in the +Z direction. This will allow all the vapor bubbles to collect at the top end, as desired.

It should be noted the XPOP attitude has a periodic behavior, which means its average vector is not a good representation of its actual direction. The real XPOP vector orbits around the average vector as demonstrated in Fig. 20 which may prove to be experimentally unacceptable for ZBOT. Therefore, test runs will be limited to LVLH.

Finally, it should be noted that the expected attitudes of the ISS may change over time. Both the frequency of occurrence of LVLH, YVV, and XPOP may change, and new modes may be introduced. Furthermore, the MSG is currently scheduled to be moved from its rack location in the U.S. Laboratory module to the European Columbus module sometime in the future after this the Columbus module is launched. A new rack location will change all acceleration vectors and necessitate a re-examination of the microgravity acceleration environment in the MSG and how ZBOT will be designed and oriented to accommodate it. The temporal variation of the magnitude and direction of the gravitational vector will be measured at a position as close as possible to the test rig.

5.3 The Microgravity Tests & Experimental Procedures

Three different testing categories are planned. These include; (1) self-pressurization tests; (2) jet mixing tests; (3) subcooled jet mixing tests. Before each test run the experimental tank must be prepared. Prior to tank preparation, it is assumed that the saturated liquid is in the test cell at the desired fill level. Before any of the experimental runs begin, the temperature of liquid inside the tank must be determined. All subsequent runs shall begin at the same initial temperature

5.3.1 Tank Preparation

The following general steps are taken to prepare the tank before each test run in order to ensure that the tests are all started from a common initial state:

1. Set the jet temperature to the desired initial fluid temperature.
2. Set jet flow rate so that fluid will be well mixed.
3. Continue to run the jet until:
4. All thermal gradients have sufficiently decayed (i.e. until all thermistor temperatures are within +/- 0.25 ^{o}C of each other).
5. All thermistors are within +/- 0.25 ^{o}C of the desired starting temperature.
6. Turn on the heater power supply and set desired heat input.
7. Configure the data acquisition system to record desired.

5.3.2 Microgravity Tests

Brief descriptions of the microgravity test categories are as follows:

1. <u>Self-Pressurization Tests:</u> Isolate test cell from mixing/cooling loop by valving off the jet inlet and the tank outlet. At time = 0, turn on the heater and record measurements. After a prescribed pressurization time, turn off the heaters and go back to step #1 to prep the tank for the next run. The pressurization time shall be approximately 12 hrs or until the maximum operating pressure and temperature criterion for the tank structural integrity is reached.

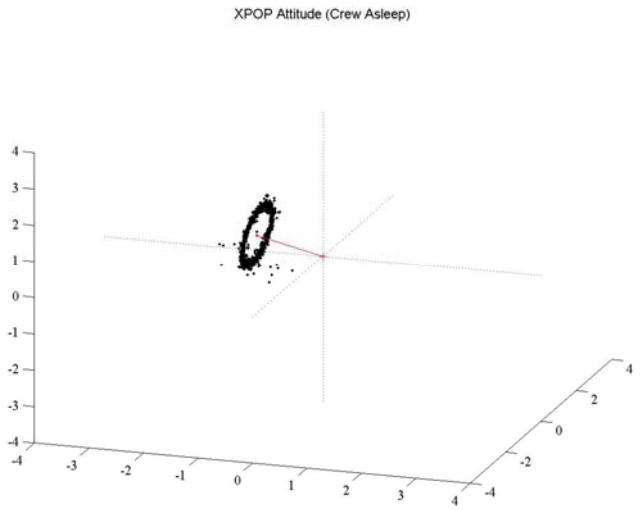

Figure 20. The Real XPOP Vector Orbiting around the Average Vector

2. Jet-Mixing Tests: Set desired jet speed. At time = 0, turn on the heaters allowing the tank to pressurize for a specified time period. After the pressurization time has elapsed, turn on the jet and continue to run until either the maximum allowable mixing time has elapsed or the tank pressure has returned to the initial pressure for this particular experimental run. Turn off the heaters and jet and go back to step #1 to prep the tank for the next run.
3. Subcooled Jet Mixing Tests: Specify heater power, jet inlet temperature and jet speed. At time = 0, turn on the heaters allowing the system to pressurize. After the pressurization time as elapsed turn on the jet. Continue until either the maximum allowable mixing time has elapsed or the tank pressure has decayed to the initial pressure. Turn off jet and heaters and return to step #1.

5.4 Microgravity Test Matrix

The ISS experiment test matrix associated with the three microgravity tests listed in section 5.3 is included Table 4.

Table 3. Microgravity Test Matrix

Test No.	Test Category	Fill %	Total Heat Input (W)	Average Jet Speed (cm/s)	Jet Temp (^oC)	Success Criteria (M)inimum (S)ubstantial (C)omplete
I-1	**Self-Pressurization Tests**	75	1	-	-	M
I-2		85	1	-	-	S
I-3		95	0.5	-	-	M
I-4		95	1	-	-	M
I-5		95	0.75	-	-	M
II-1	**Jet Mixing Tests**	75	1	1	T_{outlet}	M
II-2		75	1	2	T_{outlet}	M
II-3		75	1	5	T_{outlet}	M
II-4		95	0.50	1	T_{outlet}	S
II-5		95	0.50	2	T_{outlet}	S
II-6		95	0.50	5	T_{outlet}	S
II-7		95	0.75	1	T_{outlet}	M
II-8		95	0.75	2	T_{outlet}	M
II-9		95	0.75	5	T_{outlet}	M
II-10		95	1	1	T_{outlet}	M
II-11		95	1	2	T_{outlet}	M
II-12		95	1	5	T_{outlet}	M
II-13		95	1	10	T_{outlet}	S
II-14		95	1	20	T_{outlet}	C
II-15		95	1	25	T_{outlet}	C
III-1	**Sub-Cooled Jet Mixing Tests**	75	1	1	T_o	M
III-2		75	1	2	T_o	S
III-3		75	1	5	T_o	S
III-4		95	0.50	1	T_o	M
III-5		95	0.50	2	T_o	M
III-6		95	0.50	5	T_o	M
III-7		95	0.75	1	T_o	C
III-8		95	0.75	2	T_o	C
III-9		95	0.75	5	T_o	M
III-10		95	1	1	T_o	M
III-11		95	1	1	T_o-2	S
III-12		95	1	1	T_o-4	S
III-13		95	1	2	T_o	M
III-14		95	1	5	T_o	M
III-15		95	1	5	T_o-2	M
III-16		95	1	5	T_o-4	M

6. Experimental Requirements

6.1 Science Requirement Summary Table

Table 4. Science Requirement Summary

Item	Experiment Component	Science Requirement
1	**Section 6.1.1 Test Cell - Tank Prototype**	The test cell shall consist of a tank with a diameter to length aspect ratio of 1:2 with hemispherical end caps.
2		The internal tank volume shall be at least 80 in^3.
3		The tank shall either be transparent or provide optical quality transparent sections to meet the imagery requirements for ullage position determination and field view velocimetry.
4		The Maximum Operating Pressure (MOP) shall be 30 psia.
5		The tank shall be aligned with the residual gravity vector such that the ullage will stay within the half of the test cell away from the jet.
6	**Section 6.1.2 Test Fluid –Transparent *Model* Fluid**	The test fluid shall be a transparent *model* fluid. Perfluoro-n-pentane (PNP) is a viable candidate.
7		The test fluid shall be delivered and maintained in the test cell and the associated fluid support loops at 99.5% purity or better.
8		All the constituent species in the test fluid and ullage shall be accurately determined pre-mission.
9		The test fluid shall be filtered with a 1 μm filter prior to loading and the system shall be flushed with the test fluid.
10		The amount of non-condensable gas present in the ullage shall result in less than a 5 torr deviation from the saturation pressure.
11		The ullage fill levels shall be 75% +/- 3%, 85% +/- 3%, and 95% -3% and known to an accuracy of +/- 1%.
12	**Section 6.1.3 Test Cell Heating**	A constant heat power shall be maintained within 5 mW RMS of the set point throughout each test run.
13		The heat flow range shall be between 0.5 W - 1.0 W. The width of the heater should be 0.5” +/- .125”.
14		The heater strip shall be located circumferentially at the transverse mid-plane of the cylindrical test

		section offset towards the nozzle so that the top edge of the strip is on the transverse centerline of the test cell.
15		The heater power shall be recorded at a rate of 1/60 Hz.
16	**Section 6.1.4** **Test Cell Thermal Isolation**	The average jacket temperature shall be within 0.2 ^{o}C of the average outer wall temperature of the tank. The temperature of the jacket shall be uniform to within 0.2 ^{o}C. The average tank temperature shall be representative of the "true" average temperature. This is to be established a priori via an experimental temperature-grid convergence test.
17	**Section 6.1.5** **Jet Mixing**	The nozzle shall be aligned along the longitudinal axis of the tank and shall have an inner diameter between 0.125" and 0.20".
18		The jet velocity profile at the exit from the oulet shall be flat (plug flow).
19		The jet velocity shall be set as described in the test matrix between 1 cm/s - 25 cm/s with a tolerance of 10% reading and an accuracy of +/- 5% reading.
20		The jet flow rate shall be recorded at a rate of 1/60 Hz during jet operation.
21		In order to prevent withdrawal of vapor from the tank into the fluid loop, a simple liquid acquisition device (LAD) shall be designed and implemented at the tank outlet to the fluid loop.
22		For the subcooled jet cases, the jet temperature range shall be 20 - 30 °C with a tolerance of 0.25 °C and an accuracy of +/- 0.05 °C.
23		For the mixing only cases, the heat imbalance in the fluid between tank inlet and outlet shall be less than 150 mW for jet speeds up to 5 cm/s.
24		The jet temperature shall reach its designated set point within 5 to 30 seconds of being turned on for jet speeds from 1 to 25 cm/s.
25	**Section 6.1.6** **Temperature Measurements**	Accurate and precise local temperature measurements shall be taken in the range of 20 - 70 °C with a resolution of 0.02 °C and accuracy of +/- 0.1 °C.
26		The temperature measurements shall be taken at a rate of 1/60 Hz for all the wall and ambient locations and 1 Hz for the rest of the tank locations.

27		Temperature measurements can be made sequentially with respect to the other local measurements but the time of the measurement has to be known within 0.4 s.
28		The response time of the temperature measurement has to be less than 1 s.
29		The thermistor rake shall position the individual thermistors as specified in Fig. 21.
30		The thermistor rake shall be made as non-intrusive as possible with a maximum rake diameter not exceeding 1/8''.
31	**Section 6.1.7 Pressure Measurements**	Static pressure shall be measured either inside the test cell or as close as possible to the test cell but definitely within the thermal isolation jacket. For ground-based measurements effect of hydrostatic pressure must be determined.
32		The measurement shall cover a range between 0 psia and the Maximum Operating Pressure (30 psi) of the tank with a resolution of 0.006 psi, and an accuracy of 0.05 psi.
33		Pressure measurement shall be performed at the rate of 1 Hz.
34		Pressure measurements can be made sequentially with respect to the other local measurements but the time of the measurement has to be known within 0.4 s.
35		The response time of the pressure measurement has to be less than or equal to 0.4 s.
36	**Section 6.1.8 Velocity Field Visualization/Measurement**	Standard Particle Image Velocimetry (PIV) shall be used to visualize the important flow structures that develop in the tank.
37		The PIV Field of View (FOV) shall be the cylindrical region bounded by the hemispherical end caps and within 94% of the tank radius measured from the central axis. The heater strip can be within this region.
38		The PIV particles shall be compatible and density-matched with the test fluid as much as possible.
39		If the density matching is less than perfect, proper measures shall be implemented to mitigate the risks of particle sedimentation.
40		The particles shall be small enough to not affect the boiling/phase change process.

41		Spatial resolution and recording frequency of the PIV technique shall be optimized to allow simultaneous measurement of multiple flow structures with velocities ranging from 25 microns/s to 2.5 mm/s with a resolution of +/- 5-10%. Flow visualization shall be best effort over a velocity range of 2.5 mm/s to 25 cm/s.
42	**Section 6.1.9 Ullage Location Measurement**	The position of the ullage shall be captured by the camera.
43	**Section 6.1.10 Microgravity Acceleration Measurements**	The temporal variation of the magnitude and direction of the gravitational vector shall be measured at a position as close as possible to the test rig.
44		The acceleration measurement shall be made in the range of +/- 0.01 g, three times per second, with a resolution of 2.4 micro-g, a relative accuracy of 1.2 $(10)^{-5}$ g, and an absolute accuracy of 5 $(10)^{-4}$ g.
45	**Section 6.2 In-Flight Data Deliverables**	After the initial proof test and at the end of each class of experiments the following data shall be downloaded: all local/point measurements of the temperature, pressure, flow rates (jet loop), heater power, tank fill fraction and all digital field data corresponding to velocity and ullage location.
46		All local/point measurements of the temperature, pressure, flow rates (jet loop), heater power, average tank & jacket temperature, and tank fill fraction shall be stored in ASCII or binary format on the hard drive and recorded in ASCII Format on DVD media for final delivery.
47	**Section 6.2 Post-Flight Data Deliverables**	All digital field data corresponding to velocity and ullage location shall be stored on the hard-drive and recorded on DVD media for delivery.

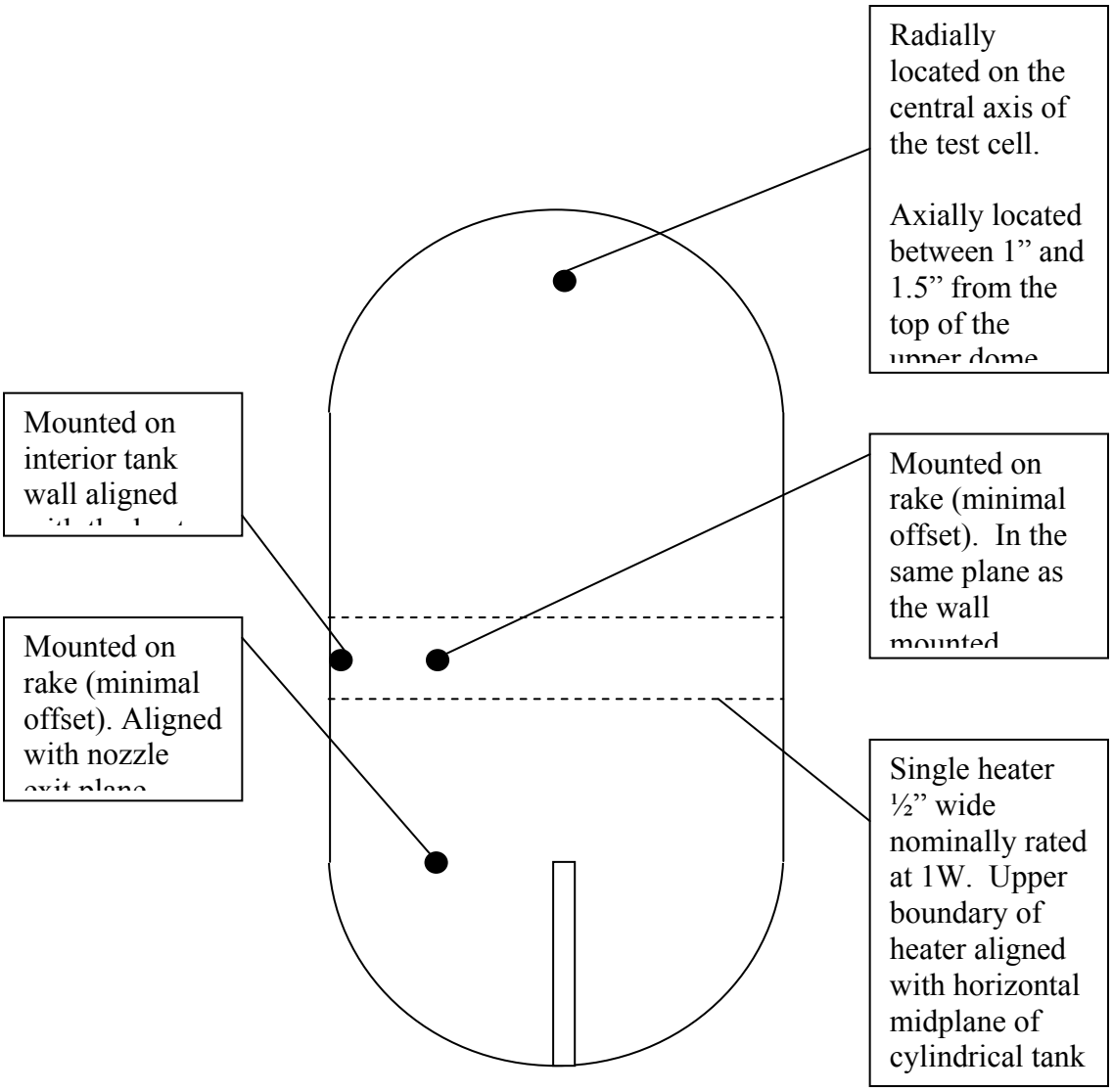

Figure 21. Schematic Displaying The Thermistor Locations in The Transparent Test Tank.

6.1.1 Test Cell

The schematic of a proposed test cell is shown in Fig. 16. It consists of a tank with a diameter to length aspect ratio of 1:2 with hemispherical end caps. The internal tank volume is at least 80 in^3. The test cell material must satisfy the following two important requirements:

1. Withstand the tank Maximum Operating Pressure (MOP) of 30 psia.
2. Provide optical quality transparent sections for ullage/bubble position determination and field view velocimetry (PIV).

The tank shall be aligned with the residual gravity vector such that the ullage will stay within the half of the test cell away from the jet.

6.1.2 Test Fluid

The test fluid will be a transparent simulant fluid with a low normal boiling point and nominally nontoxic and environmentally friendly properties. It must exhibit a relatively steep pressure-temperature saturation curve. A candidate test fluid that satisfies these requirements is Perfluoro-n-pentane (PNP). PNP needs to pass NASA's stringent ISS safety review. The test fluid is to be delivered and maintained in the test cell and the associated fluid support loops at 99.5% purity or better. All the constituent species in the test fluid and ullage must be accurately determined pre-mission. The test fluid shall be filtered with a 1 μm filter prior to loading and the system shall be flushed with the test fluid. The amount of non-condensable gas present in the ullage shall result in less than a 5 torr deviation from the saturation pressure. Tank fill levels will be set at 75%+/-3%, 85%+/-3%, and 95% -3% with an accuracy of +/- 1%.

6.1.3 Test Cell Heating

The electrical strip heater will be located circumferentially at the transverse mid-plane of the cylindrical test section offset towards the nozzle so that the top edge of the strip is on the transverse centerline of the test cell. Constant power must be maintained in the heater within 5 mW RMS of the set point through out each test run. The heat flow rates shall be between 0.5W – 1.0W. The width of the heater shall be between 0.5" +/- 0.125". The heater power shall be recorded at a rate of 1/60 Hz.

6.1.4 Test Cell Thermal Isolation

The test cell shall be insulated from the MSG environment by a Vacuum Thermal Isolation Jacket. Heat loss from the tank shall be less than 100 mW. The average jacket temperature shall be within 0.2 ^oC of the average outer wall temperature of the tank. The temperature of the jacket shall be uniform to within 0.2 ^oC. The average tank temperature shall be representative of the "true" average temperature. This is to be established a priori via an experimental temperature-grid convergence test.

6.1.5 Liquid Mixing Jet Operation

The nozzle shall be aligned along the longitudinal axis of the tank and shall have an inner diameter between 0.125" and 0.20". A nominal wall thickness is acceptable. The nozzle will be made out of aluminum to minimize the axial temperature drop along the its body.

The outlet of the jet nozzle will be projected one half diameter (equal with the hemisphere's end) into the test cell. In this fashion, the jet flow and spread angle will be completely in the field of view (FOV) for flow visualization and PIV velocimetry.

Several different jet flow rates will be used during the test runs as described in test matrix spanning both laminar and turbulent regimes. In all cases, the jet velocity profile at the outlet of the nozzle shall be flat as in a plug flow. The jet velocity shall be set to the prescribed levels stated in the test matrix (between 1 cm/s - 25 cm/s) with a tolerance of 10% of the set value and an accuracy of +/- 5% reading. The jet flow rate shall be recorded at a rate of 1/60 Hz during jet operation.

The position of the ullage in microgravity is unknown. Thus, in order to prevent withdrawal of vapor from the tank into the fluid loop, a simple liquid acquisition device (LAD) shall be designed and implemented at the tank outlet to the fluid loop.

For the subcooled jet cases, the jet temperature range shall be 20 - 30 °C with a tolerance of 0.25 °C and an accuracy of +/- 0.05 °C. For the mixing only cases, the heat imbalance in the fluid between tank inlet and outlet shall be less than 150 mW for jet speeds up to 5 cm/s. The jet temperature shall reach its designated set point with in 5 – 30 seconds of being turned on for jet speeds from 1 to 25 cm/s.

6.1.6 Temperature Measurements

There will be a total of four thermistors interior to the tank volume. Accurate and precise local temperature measurements must be taken in the range of 20 – 70 °C with a resolution of 0.02 °C and accuracy of +/- 0.1 °C. The envisioned sensor locations as shown in Fig. 21 are as follows:

- 10 uniformly distributed temperature measurements on the wall
- 1 each at jet inlet and outlet
- 1 in the ullage volume
- 3 in different locations in the cylindrical section and bottom dome

The temperature measurements shall be taken at a rate of 1/60 Hz for all the wall and ambient locations and 1 Hz for the rest of the tank locations. They can be made sequentially with respect to the other local measurements but the time of the measurement has to be known within 0.4 s. The response time of the temperature measurement has to be less than or equal to 1 s

The thermistor rake shall position the individual thermistors as specified in Fig. 21. The thermistor rake shall be made as non-intrusive as possible with a maximum rake diameter not exceeding 1/8’’. The sensors inside the tank should minimize the creation of pinning points for the ullage.

6.1.7 Pressure Measurements

Static pressure shall be measured either inside the test cell or as close as possible to the test cell but definitely within the thermal isolation jacket. For ground-based measurements, the effect of hydrostatic pressure must be determined. The measurement shall cover a range between 0 psia and the Maximum Operating Pressure of the tank with a resolution of 0.006 psi, and an accuracy of 0.05 psi.

Pressure measurement shall be performed at the rate of 1 Hz. Pressure measurements can be made sequentially with respect to the other local measurements but the time of the measurement has to be known within 0.4 s The response time of the pressure measurement has to be less than or equal to 0.4 s.

6.1.8 Velocity Field Visualization/Measurement

Standard Particle Image Velocimetry (PIV) as shown in Fig. 18 shall be used to visualize the important flow structures that develop in the tank. The PIV Field of View (FOV) shall be the cylindrical region bounded by the hemispherical end caps and within 94% of the tank radius measured from the central axis. The heater strip can be within this region.

The PIV particles shall be compatible and density-matched with the test fluid as much as possible. If the density matching is less than perfect, proper measures shall be implemented to mitigate the risks of particle sedimentation. The particles shall be small enough to not affect the boiling/phase change process.

Spatial resolution and recording frequency of the PIV technique must be optimized to allow simultaneous measurement of multiple flow structures with velocities ranging from 25 microns/s for natural convection to 2.5 mm/s for jet mixing with a resolution of +/- 5-10%. Flow visualization shall be best effort over a velocity range of 2.5 mm/s – 25 cm/s. The video data will be time-stamped to easily synch the data with each experimental run.

6.1.9 Ullage Location Capture

The position of the ullage shall be captured by the camera. This information is essential for the model validation and verification.

6.1.10 Microgravity Acceleration Measurement

The temporal variation of the magnitude and direction of the gravitational vector shall be measured at a position as close as possible to the test rig.The acceleration measurement shall be made in the range of +/- 0.01 g, at a frequency of 3 Hz, with a resolution of 2.4 micro-g, a relative accuracy of 1.2 $(10)^{-5}$ g, and an absolute accuracy of 5 $(10)^{-4}$ g.

6.2 Data Handling and Delivery

During Flight: The following data must be downloaded during flight after the initial proof test and at the end of each class of experiments: tank pressure; heat powers; fill ratio; temperature at all locations (inside and outside); ullage position; inlet jet temperature; tank outlet temperature; jet flow rate; gravitational acceleration data; velocity field visualization-PIV. The digital temperature, velocity, and bubble location data should be compressed, recorded and delivered on DVD-R media. The rest of the (point) data should be delivered in ASCII format and recorded on DVD-R media.

Post-Flight: All local/point measurements of the temperature, pressure, flow rates (cold finger loop, jet loop), heater power, and tank fill fraction shall be stored in ASCII or binary format on the on-orbit hard drive and recorded in ASCII Format on DVD media for fdelivery. All digital field data corresponding to velocity and ullage location will be stored on the hard-drive and recorded on DVD media for delivery.

6.3 Success Criteria

Project success criteria are presented here to rank the need and priority for the different elements of this research effort as grouped in the following three categories:

- Experimental capabilities.
- Microgravity test matrix.
- Model Development & Validation.

The individual items in each category are ranked according to their need for *Minimum Success*, *Substantial Success*, and *Complete Success* of the investigation. The success criteria for the experimental and modeling elements are presented in Tables 5 and 6, respectively. The success rankings for the microgravity test matrix were included in Table 3 of Section 5.4.

Table 5. Experimental Elements Success Criteria	
Capability	Success Criteria (M) Minimum Success (S) Substantial Success (C) Complete Success
Local Pressure Measurements	M
Local Temperature Measurements	M
Flow Visualization	S
Ullage Visualization (Phase Distribution)	S
PIV	S
Jet Mixing	M
Subcooled Jet Mixing	S

Table 6. Modeling Validation/Verification Success Criteria	
Capability	(M) Minimum Success (S) Substantial Success (C) Complete Success
Pressurization	M
Pressure Control	M
Non-Condensable Effects	S
Non-Equilibrium Effects	C
Level Set Interface Capturing Model	C

7. Two-Phase Tank CFD Model

As an integral part of the proposed research, comprehensive two-phase numerical models for tank pressurization and pressure control will be developed. These state-of-the-art models will address many of the scientific and engineering issues that were previously identified. Once validated and verified through this research effort, these models will also serve as powerful simulation tools to aid the scale-up of future cryogenic storage tanks for specific mission scenarios. The numerical model development will proceed in a stepwise fashion by building upon and extending the current capabilities of the ALLVT two-phase transport model.

While the ALLVT model has been successful in predicting tank pressurization behavior for a variety of cases, a current limitation in the implementation (but not formulation) is that the dynamic behavior of the interface must be weak or relatively well behaved. The existing ALLVT model either assumes a static interface or uses a front-tracking algorithm to resolve the free surface shape motion (Panzarella and Kassemi, 2003). Front-tracking methods can accommodate moderate interface deformation but at a cost of numerous remeshing of the domain as the computational grids drastically distort due to ullage movement (Panzarella and Kassemi, 2004, 2005). Unfortunately front tracking methods are not computationally efficient in handling extensive phase motion, fluid slosh, or topological changes associated with the coalescence or break-up of multiple vapor regions – all of which may be present in a space-based cryogenic tank. In general, it is more appropriate to use a front-capturing technique such as level set and follow multiple interfaces on a fixed computational grid. The level set method (Osher and Sethian, 1988), with the ghost fluid corrections (Fedkiw et al., 1999), was selected to capture interfacial motion because, as a sharp interface method, it is not prone to generating spurious solutions typically seen in smeared out diffuse interface methods such as the volume-of-fluid technique.

Following a tiered approach, we will develop the level set model in several stages. First, the existing lumped vapor model will be recast into a level set framework. In this stage, the ullage is still treated as a lumped system with the interface being modeled as a free surface. Incorporating the existing lumped vapor model into a level set scheme allows for more moderate interfacial motions to be captured without much of the computational overhead associated with a front tracking algorithm.

Once the lumped vapor level set model is validated against our previous results, the formulation will be modified to include transport effects in the vapor. Because a fully compressible formulation of the vapor may lead to fluctuations of the field variables on an acoustic scale, as a first step, we would treat the vapor as a weakly compressible system and, similar to our previous model, mass transfer across the interface would be accounted for using an integral mass balance. Here it is implicitly assumed that the mass flux due to phase change is weak enough that the effect on the overall flow field in the ullage is negligible.

For stronger evaporation or condensation, it will be necessary to include the effects of the mass flux on the flow fields. In these cases, the mass flux will be computed locally at each point along the interface and the fully compressible equations in the vapor must be solved. For a compressible liquid like hydrogen, a single equation of state can be applied in both phases of the compressible-compressible system. For stiffer fluids, the ghost fluid method as described by Caiden et al. (2001) will be used to couple the compressible vapor equations to the incompressible equations in the liquid.

Once these basic phase change models are fully developed, it is relatively straightforward to add additional capabilities to account for secondary effects.

7.1 Non-Condensable Effects

Because cryogenic tanks are typically pressurized with a non-condensable gas, the capability to model non-condensable gases would also be added to the formulations described above. A non-condensable gas can affect the phase change process in several ways. First, the saturation temperature along the interface is now a function of the partial vapor pressure. Partial pressure variations on the vapor-side of the interface can result in temperature non-uniformities along the interface, which can drive a Marangoni flow on the liquid-side of the surface. Furthermore, for condensation processes, the presence of a non-condensable gas is particularly acute since even trace amounts of an inert gas can accumulate in a thin Knudsen layer adjacent to the interface and significantly retard condensation. In this instance, we will follow the approach similar to Kryukov (2004) and couple a kinetic model of the Knudsen layer (Pong and Moses, 1986; Labunstov and Kryukov, 1979) to the hydrodynamic equations in the ullage.

7.2 Non-Equilibrium Effects

For most cases of practical interest, the assumption of local equilibrium at the interface is approximately valid owing to the weak evaporative and condensation mass fluxes across the surface. For these cases, as is done with most computational phase change studies, we will set the interfacial temperature to its saturation value. For cases where strong evaporation/condensation is present, non-equilibrium effects must be included and an additional constitutive relationship relating the fluxes at the interface to the jumps in intensive thermodynamic variables must be applied. The particular form of the constitutive model has been the subject of intense scientific debate since Hertz (1882) published his seminal work on phase change. The resulting constitutive model – "the Hertz-Knudsen formula has been casually extended to continuum flow, although little justification for such extension can be found." (Koffman et al., 1984) A popular variant – the Schrage (1953) equation – is often applied even though this constitutive model is not energy conserving (Barrett, 1992). Recently a survey of various non-equilibrium models was conducted (Bond, 2000) and the models that compared favorably to experiments were identified. Once again though, in the same vein of Kryukov, the particular constitutive model selected would be coupled to the hydrodynamic equations in the ullage.

7.3 Turbulence Modeling

For most microgravity applications, the natural convective flows in the liquid and vapor are laminar even for larger tanks. For on-surface applications, the convective flow will likely be turbulent. Additionally the mixing jet will most likely be turbulent even in microgravity. Reynolds Averaged Navier Stokes equations (with zeroeth order closure laws at the interface) are still the optimum means of modeling turbulence in the cryogenic storage tank. Our prior benchmarking has revealed that for natural convection flows, the k-ω model is superior at reproducing experimental results. For free jet flows, the realizable k-ε model yielded better agreement with data. Consequently, for the current cryogenic tank problem, where both natural convection and jet flows are present, we will employ Menter's SST k-ω model (Menter, 1993) which is essentially a blend of the k-ω and k-ε turbulence models.

8. Scaling Analysis

Scaling to an actual flight tank is an important aspect of ZBOT. It is generally well known that a complete geometric and dynamic similitude between a small simulant fluid experiment, such as ZBOT, and a large scale tank with cryogenic fluid is difficult. Unfortunately, the Microgravity Science Glovebox (MSG) facility aboard the International Space Station (ISS) does not allow for a larger test cell and the stringent ISS safety requirements makes flying even specially designed environmentally-friendly refrigerant fluids such as PNP (candidate ZBOT test fluid) extremely difficult. Thus, ISS experiments with actual cryogens are not in the realm of possibility. In this light, the approach ZBOT has taken to overcome this inherent shortcoming is to use the sub-scale and simulant fluid experiment to validate and verify the CFD model and then use the CFD model for scaling-up to the actual flight cryogenic storage system.

For the CFD tank model developed as part of this research effort to be truly validated and verified for the scale-up task, it must be benchmarked not only against the ground-based and microgravity data that are collected as part of this project, but also against considerable amount of ground-based and flight data that have been accumulated as a result of years of engineering prototyping and system validation experiments. In this regard, actual flight data are a rare and valuable commodity and it will be used for model validation as much as possible. Although we have to still be mindful that the existing flight test data, correspond to cases with much higher heat loads than required by current tank designs for the lunar architecture and where active mixers were not employed.

As mentioned, it is difficult for the proposed experiment to match the performance of the full scale hardware exactly, as is generally true with most subscale tests. This is the classical dilemma of model testing. Even a geometrically scaled model of actual flight hardware (which is impossible because the flight hardware has not been designed) may behave inaccurately, being laminar where the full scale flow is turbulent or being dominated by surface tension effects when the full scale system is not. Of course, the classical solution to this problem is dimensional analysis and use of non-dimensional numbers. Usually, it is more important to be in a similar regime than to match the magnitude of the dimensionless parameters exactly.

For stratification and natural convection, the important non-dimensional parameters are Grashof (Gr) and Rayleigh numbers (Ra). Table 7 shows a comparison between the ZBOT experiment and a 1m hydrogen tank with a heat load of about 1.5 watts (similar to proposed designs for the Crew Exploration Vehicle and Lunar Lander Ascent Module)

Table 7: Convection Comparison

G-Level (m/sec^2)	Gr, Hydrogen Tank (based on tank radius)	Gr, ZBOT (based on tank radius)	Ra, Hydrogen Tank (based on tank radius)	Ra, ZBOT (based on tank radius)
$9.81(10^{-4})$	$1.4x10^{8}$	$1.4x10^{6}$	$1.7x10^{8}$	$1.1\ x10^{7}$
$9.81(10^{-6})$	$1.4x10^{6}$	$1.4\ x10^{4}$	$1.7\ x10^{6}$	$1.1\ x10^{5}$

In any case, for Gr numbers which tend to be quite large, a variation of 1-2 orders of magnitude is not significant as both flows will be still in the same regime. The Ra numbers that represent the ratio of the natural convective to conductive heat transfer are even closer.

Bond number governs the shape of the free surface. For both ZBOT and a 1 m hydrogen tank, the Bond numbers are less than one leading to similar spherical equilibrium free surface shapes. The fact that the Bond number is less than one for both the ZBOT experiment and the 1m

hydrogen tank in microgravity, also suggests that the interfacial dynamics and ullage breakup is governed by a balance between inertia and surface tension forces as represented by the Weber number.

Thus, for studying jet spread and mixing and its interaction with the ullage, the key dimensionless quantities are jet Reynolds and Weber numbers, as many prior investigators have also pointed out. Since both of these parameters depend on velocity, they cannot be varied independently with the same test fluid. Nevertheless, the present experiment is capable of covering a broad range. Table 8 shows the Reynolds and Weber numbers achievable with the ZBOT experiment. (Note: Reynolds number is based on nozzle diameter and Weber number is based on jet diameter at the free surface). Of particular importance is the ability to cover the various low-g mixing flow regimes that will be present in a real tank configuration. Hasan et al. (1996) found at We < 1 there was little disturbance to the free surface, at We 3-5 a geyser formed on the free surface but was constrained, at We > 5 the geyser was unconstrained, resulted in ullage breakup and a re-circulating flow pattern developed. Similarly, as shown in Table 8, ZBOT will study the full range of Reynolds number regimes from laminar, through transitional, to full turbulent flow.

Table 8: ZBOT Flow Regimes

Fill Ratio		75% full	95% full
Average Jet Speed (cm/s)	Re	We	We
1	179	0.004	0.002
2	357	0.017	0.008
5	893	0.108	0.051
10	1786	0.430	0.204
20	3572	1.721	0.815
25	4465	2.690	1.274

9. Connection to the NASA Constellation and the Exploration Program.

The Cryogenic Fluid Management (CFM) Project has been formed by NASA to address key engineering and development issues associated with storage, transfer, and handling of cryogenic fluids in support of the Lunar and Mars architectures for Constellation. A central focus of the CFM program has been the development of efficient and safe tank pressure control systems. In this context, the anticipated contributions of the ZBOT ISS experiment to the CFM project will be significant.

9.1 Anticipated Contributions to NASA's Cryogenic Fluid Management Project

First, the ZBOT ISS experiment will provide microgravity data that will be used to develop new and/or extend and compliment existing empirical engineering correlations for the storage tank design including the time constant correlations for liquid mixing, thermal destratification, and pressure reduction.

Second, it is expected that the microgravity pressurization and pressure control data provided by the ZBOT experiment will be collected under precise, known, and controlled heat input, fill level, and mixing rate condition. Thus the data will be well-suited for validation and verification of the state-of-the-art two-phase CFD storage tank models and codes used in the CFM program. The microgravity validation data will also be made available to the CFM community at large to benchmark other in-house or commercially available CFD codes currently used in the storage tank design process by the different NASA centers and their prime contractors.

Third, the ZBOT project will demonstrate the feasibility of a Zero-Boil-Off tank pressure control scheme for microgravity applications by examining the effect of forced mixing of the bulk liquid on destratification and pressure reduction in a ventless Dewar. From a long-term perspective, integration of a ZBO pressure control strategy into the cryogenic storage tank design has numerous benefits such as: (a) decreasing the launchable propellant and storage tank mass; (b) increasing operational system reliability through active-passive pressure control; and (c) promoting crew safety by allowing manned flight operations such as rendezvous and docking around the cryogenic tanks.

9.2 Coordination with the NASA Cryo-Working Group

The results of this research will also be closely shared with key cryogenic engineering groups at NASA GRC, ARC, MSFC, KSC, JSC, GFSC as well as the Air Force and NIST. This will be done under the auspices of NASA's Cryogenic Technology Development Working Group. Through regular technical discussions and exchange among the Principle Investigator, Co-Investigator and Project Scientist and the rest of the Cryogenic Working Group members, this forum will ensure that the scientific directions of this project will remain relevant to the current and future needs of NASA and the Constellation Program and that its scientific and engineering developments and findings will be properly disseminated throughout the agency and the CFM community at large.

10. Closure

It is clear that NASA's future exploration architecture will require some form of dynamic pressure control in order to decrease the risks associated with propellant tank self- pressurization in space. Regardless of the details of how the short-term Lunar and/or long-term Mars Architectures evolve, destratification through forced mixing with or without active cooling will form an integral part of the future cryogenic storage tank pressure control systems for Constellation. Implementation and optimization of any dynamic pressure control strategy cannot be accomplished empirically alone because:

1. The dynamic impact of many interacting transport phenomena on pressure reduction times are still not clear and need scientific clarification.
2. Empirical data for mixing, destratification and pressure reduction in microgravity applications are scarce.
3. Comprehensive and customized numerical models for scale-up must be validated to ensure the fidelity of their microgravity predictions.

Thus fundamental knowledge and understanding of the fluid flow and heat transport processes associated with microgravity mixing and destratification will be essential to reduce the risks and uncertainties associated with the engineering analyses that guide the design process. In this context, the major goals of the ZBOT project are as follows:

1. Develop a small-scale simulant fluid experiment for both preliminary ground-based testing and subsequent flight experiments to obtain valuable microgravity empirical data.
2. Develop, validate, and verify a two-phase CFD models for the cryo-storage tank pressurization and pressure control.
3. Build a science base for the future space storage tank design by elucidating the roles of the various interacting transport and phase change phenomena through systematic scientific investigation.
4. Build an engineering base by deriving empirical engineering correlations for stratification, mixing, and pressure reduction in microgravity from the controlled microgravity experimental data.

These objectives will be accomplished through a coordinated hand-in-hand experimental-theoretical-numerical research program that involve both ground-based and microgravity experiments. The theoretical effort will consist of comprehensive scaling analyses, development of state-of-the-art two-phase CFD models for tank pressurization/pressure control, and a series of targeted parametric numerical simulations and sensitivity analyses. The experimental effort will consist of experimental prototype development for microgravity gravity testing, and measurement and flow visualization experiments with a simulant fluid.

The results of this research will provide an expanded scientific and engineering knowledge base for efficient cryogenic fluid storage in space that will ultimately lower the cost and decrease the risks of the future space expeditions.

References

Abdalla, K., Frysinger, T., and Androcchio, C. (1965). Pressure-rise characteristics for a liquid hydrogen Dewar for homogeneous, normal gravity, quiescent, and zero-gravity tests. NASA TM X-1134.

Albayyari, J. (2002). Cryogenic fuel tanks pressure reduction: A low-g fluid mixing experiment. Int. J. Fluid Mechanics Research, 29(v2):135–145.

Allgeier, R. (1968). Subcritical cryogenic storage development and flight test. NASA TN D-4293.

Amirkhanyan, N. and Cherkasov, S. (2001). Theoretical analysis and procedure for the calculation of thermophysical processes occurring in a cryogenic vessel under conditions of non-vented storage. High Temperature, 39(6):905–911.

Anderson, B. and Kolar, M. (1963). Experimental investigation of the behavior of a confined fluid subjected to non uniform source and wall heating. NASA TM D-2079.

Arnett, R. and Millhiser, D. (1965). A theoretical model for predicting thermal stratification and self pressurization of a fluid container. In Proc. of the Conference on Propellant Tank Pressurization and Stratification, NASA Marshall Space Flight Center.

Arnett, R. and Voth, R. (1972). A computer program for the calculation of thermal statification and self-pressurization in a liquid hydrogen tank. NASA CR 2026.

Aydelott, J. (1967a). Normal gravity self-pressurization of 9-inch (23cm) diameter spherical liquid hydrogen tankage. NASA TN D-4171.

Aydelott, J. (1967b). Self-pressurization of liquid hydrogen tankage. Master's thesis, Cornell U.

Aydelott, J. (1976). Axial jet mixing of ethanol in spherical containers during weightlessness. NASA TM X-3380.

Aydelott, J. (1979). Axial jet mixing of ethanol in cylindrical containers during weightlessness. NASA TP 1487.

Aydelott, J. (1986). Effect of gravity on self-pressurization of spherical liquid hydrogen tankage. NASA TN D-4286.

Aydelott, J., Corpus, E., and Gruber, R. (1965). Comparison of pressure rise in a hydrogen Dewar for homogeneous, normal-gravity, quiescent, andzero gravity conditions -flight 9. NASA TM X-1052.

Aydelott, J. and Spuckler, C. (1969). Effect of size on normal-gravity self-pressurization of spherical liquid hydrogen tankage. NASA TN D-5196.

Bailey, T. and Fearn, R. (1964). Analytical and Experimental Determination of Liquid-Hydrogen Temperature Stratification, volume 9 of Advances in Cryogenic Engineering, pages 254–264. Plenum Press.

Bailey, T., Vandekoppel, R., Skartvedt, G., and Jefferson, T. (1963). Cryogenic propellant stratification analysis andtest data correlation. AIAAJ., 1:1657– 1659.

Bankoff, S.G.; "Asymptotic growth of a bubble in a liquid with uniform initial superheat," *Appl. Sci. Res. A*, **12**, pp. 267-281, 1964.

Barakat, H. and Clark, J. (1965). Transient natural convection in closed containers. Technical report, Heat Transfer Laboratory, U. of Michigan. Tech Report No.
2.

Barnett, D. (1968). Liquid Nitrogen Stratification Analysis and Experiments in a
Partially Filled Spherical Container, Volume 13 of Advances in Cryogenic Engineering, pages 174–187. Plenum Press.

Barnett, D., Winstead, T., and McReynolds, L. (1965). An Investigation of Liquid Hydrogen Stratification in a Large Cylindrical Tank of the Saturn Configuration, pages 314–324. Int. Advances in Cryogenic Engineering. Plenum Press.

Barrett, J., Clement, C.; "Kinetic Evaporation and Condensation Rates and Their Coefficients" *J. Colloid Interface Sci.* **150** [2] (1992) 352-364.

Barsi, S, and Kassemi, M.,"A Tank Self-Pressurization Experiment Using a Model Fluid in Normal Gravity", AIAA-2005-1143, The 43rd AIAA Aerospace Meeting, January 2005.

Barsi, S, and Kassemi, M.,"A Numerical Study of Tank Pressure Control in Reduced Gravity", AIAA-2006-0936, The 44th AIAA Aerospace Meeting, January 2006.

Barsi, S., Panzarella, C.H. , and Kassemi, M. "An Active Vapor Approach to Modeling Pressurization in Cryogenic Tanks," AIAA 2007-5553 (2007).

Barsi, S. and Kassemi, M. "Numerical and Experimental Comparisons of the Self-Pressurization Behavior of an LH2 Tank in Normal Gravity", Cryogenics (In Press) 2008.

Beduz, C., Rebiai, R., and Scurlock, R. (1984). Thermal Overfill and the Surface Vaporisation of Cryogenic Liquids Under Storage Conditions, volume 29 of Advancesin Cryogenic Engineering, pages 795–804. Plenum Press.

Bentz, M.D., et al. "Tank Pressure Control Experiment - A Low-g Mixing Investigation," AIAA 90-2376

Bentz, M. D; Knoll, R. H; Hasan, M. M; Lin, C. S.; “Low-g fluid mixing - Further results from the Tank Pressure Control Experiment” AIAA PAPER 93-2423, Jun. 1993

Bentz, M. (1993). Tank pressure control in low gravity by jet mixing. NASA CR 191012.

Bentz, M., Albayyari, J., Knoll, R., Hasan, M., and Lin, C. (1997).Tank Pressure Control Experiment: Results of three space flights. AIAA 1997-2816.

Berenyi, S., Nussle, R., and Abdalla, K. (1968). An experimental investigation of the effect of gravity on a forced circulation pattern in spherical tanks. NASA TN D-4409.

Birkhoff, G.; Margulies, R.S; Horning, W.A.; “Spherical bubble growth,” *Phys. Fluids*, **1**, pp. 201-204, 1958.

Blatt, M. (1968). Empirical correlations for pressure rise in closed cryogenic containers. J. Spacecraft and Rockets, 5(6):733–735.

Bond. M. “Non-Equilibrium Evaporation and Condensation”. M.S. Thesis. University of Victoria (2000).

Bourgarel, M., Segel, M., and Huffenus, J. (1967).Study of Stratification Similtude Laws in Liquid Hydrogen, volume 12 of Advances in Cryogenic Engineering, pages 103–111. Plenum Press.

Bradshaw, R. (1970). Evaluation and application of data from low gravity orbital experiment phase I -final report. NASA CR-109847.

Brown, J. (1991). Vapor Condensation on Turbulent Liquid. PhD thesis, MIT.

Brown, J., Khoo, B., and Sonin, A. (1990). Rate correlation for condensation of pure vapor on turbulent, subcooled liquid. Int. J. Heat and Mass Transfer, 33(9):2001–2018.

Bullard, B. (1972). Liquid propellant thermal conditioning system test program final report. NASA CR-72971.

Bush, G. W.,``A Renewed Spirit of Discovery: The Presidents Vision for
U. S. Space Exploration", January 2004.

Caiden, R., Fedkiw, R., Anderson, C., A Numerical Method for Two-Phase Flow Consisting of Separate Compressible and Incompressible Regions; **J. Comp. Phys.**, 166, 1-27 (2001).

Cha, Y., Niemann, R., and Hull, J. (1993). Thermodynamic analysis of helium boil-off experiments with pressure variations. Cryogenics, 33:675–679.

Chato, D. (2002). Influence ofturbulence on the restraint of liquid jets bysurface. AIAA 2002-0758.

Chato, D. (2003). Parametric investigation of liquid jets in low gravity. AIAA 2003-997.

Chato, D. (2005). Low gravity issues of deep space refueling. AIAA 2005-1148.

Chato, D. (2006). The role of flight experiments in the development of cryogenic fluid management technologies. NASA TM 2006-214261.

Chato, D. and Jacqmin, D. (2001).Modeling the restraint of liquid jets by surface tension in microgravity. AIAA 2001-0931.

Cherkasov, S. (1984). Natural convection in a vertical cylindrical vessel with heat supplied to its side and free surfaces. Izv. Akad. Navk SSSR, Mekh. Ahidk.

Chiaramonte, F. and Joshi, J. (2004). Workshop on critical issues in microgravity fluids, transport, and reaction processes in advanced human support technology. NASA TM 2004-212940.

Chun, J.-H., Shimko, M., and Sonin, A. (1986). Vapor condensation onto a turbulent liquid II: Condensation burst instability at high turbulence intensities. International Journal of Heat and Mass Transfer, 29(9):1333–1338.

Clark, J. (1965). A Review of Pressurization, Statification, and Intefacial Phenomena, pages 259–283. Int. Advances in Cryogenic Engineering. Plenum Press.

Cunnington, R. (1984). Reducing Boil Off Losses in Cryogenic Storage Systems to the Minimum, volume 29 of Advances in Cryogenic Engineering, pages 767–776. Plenum Press.

Dalle Donne, M.; Ferranti, M.P.; "The growth of vapor bubbles in superheated sodium," *Int. J. Heat Mass Transfer*, **18**, pp. 477-493, 1975.

Das, S., Chakraborty, S., and Dutta, P. (2004). Studies on thermal stratification phenomenn in LH2 storage vessel. Heat Transfer Engineering, 25(4):54–66.

DeWitt, R. and Boyle, R. (1977). Thermal performance of an integrated thermal protection system for long-term storage of cryogenic propellants in space. NASA TN D-8320.

Dominick, S. (1984). Mixing induced condensation inside propellant tanks. AIAA 84-0514.

Dresar, N. V., Lin, C., and Hasan, M. (1992). Self-pressurization of a flightweight liquid hydrogen tank: Effects of fill level at low wall heat flux. NASA TM 105411.

Eberhardt, R., Fester, D., Johns, W., and Marino, J. (1982). An Experiment to Evaluate Liquid Hydrogen Storage in Space, volume 27 of Advances in Cryogenic Engineering, pages 1107–1116. Plenum Press.

Epstein, M. and Georgius, H. (1965). A Generalized Propellant Tank-Pressurization Analysis, pages 290–302. Int. Advances in Cryogenic Engineering. Plenum Press.

Estey, P., Lewis, D., and Connor, M. (1983).Prediction of a propellant tank pressure history using state space methods. J. Spacecraft and Rockets, 20(1):49– 54.

Fan, S., Chu, J., and Scott, L. (1969). Thermal Statification in Closed Cryogenic Containers, volume 14ofAdvancesinCryogenicEngineering, pages 249–257. Plenum Press.

Fedkiw, R., Aslam, T., Xu, S.; *A Non-Oscillatory Eulerian Approach to Interfaces in Multimaterial Flows (The Ghost Fluid Method)*; **J. Comp. Phys**., 152 457-492 (1999).

Flachbart, R., Hastings, L., Hedayat, A., Nelson, S., and Tucker, S. (2005). Testing of a spray-bar thermodynamic vent system in liquid nitrogen. In Proceedings of the 2005 Cryogenic Engineering Conference, Keystone, CO.

Flachbart, R., Hastings, L., and Martin, J. (1999). Testing of a spray bar zero gravity cryogenic vent system for upper stages. AIAA 99-2175.

Forester, C. (1967). Non-equilibrium Storage and Expulsion of Single-Phase Cryogens, volume 12 of Advances in Cryogenic Engineering, pages 82–91. Plenum Press.

Fossett, H. and Prosser, L. (1949). The application of free jets to the mixing of fluids in bulk. Proc. Inst. of Mech. Engineers, 160(2):224–232.

Fox, E. and Gex, V. (1956).Single phase blending of liquids.AIChEJ., 2(4):539– 544.

Gebhart, B. (1963). Random convection under conditions ofweightlessness.AIAA J., 1(2):380–383.

Grayson, G. (1995). Coupled thermodynamic-fluid-dynamic solution for a liquid-hydrogen tank. J. Spacecraft and Rockets, 32(5):918–921.

Grayson, G., Lopez, A., Chandler, F., Hastings, L., and Tucker, S. (2006). Cryogenic tank modeling for the Saturn AS-203 experiment. AIAA 2006-5258.

Grayson, G. and Navickas, J. (1993). Interaction betweeen fluid-dynamic and thermodynamic phenomena in a cryogenic upper stage. AIAA 93-2753.

Grenville, R. and Tilton, J. (1996). Anew theory improves the correlation of blend time data from turbulent jet mixed vessels. Trans. IChemE Part A: Chem. Eng.Res.Design, 74:390–396.

Grodzka, P. and Bannister, T. (1974). Natural convection in low-g environments. AIAA 74-156.

Guernsey, C., Baker, R., Plachta, D., and Kittel, P. (2005). Cryogenic propulsion with zero boil-off storage applied to outer planetary exploration. AIAA 20053559.

Gursu, S., Sherif, S., Veziroglu, T., and Sheffield, J. (1993a). Analysis and optimization of thermal statification and self-pressurization effects in liquid hydrogen storage systems part I: Model development. J. Energy Resources Technology, 115:221–227.

Gursu, S., Sherif, S., Veziroglu, T., and Sheffield, J. (1993b). Analysis and optimization of thermal stratification and self-pressurization effects in liquid hydrogen storage systems part II: Model results and conclusions. J. Energy ResourcesTechnology, 115:228–231.

Hasan, M. and Lin, C. (1989). Axisymmetric confined turbulent jet directed towards the liquid surface from below. NASA TM 101409.

Hasan, M. and Lin, C. (1990). Buoyancy effects on the vapor condensation rate on a horizontal liquid surface. NASA TM 102437.

Hasan, M., Lin, C., and Dresar, N. V. (1991). Self-pressurization of a flightweight liquid hydrogen storage tank subjected to low heat flux. NASA TM 103804.

Hasan, M., Lin, C., Knoll, R., and Bentz, M. (1996). Tank Pressure Control Experiment: Thermal phenomena in microgravity. NASA TP 3564.

Hastings, L., Flachbart, R., Martin, J., Hedayat, A., Fazah, M., Lak, T., Nguyen, H., and Bailey, J. (2003). Spray bar zero-gravity vent system for on-orbit liquid hydrogen storage. NASA TM 2003-212926.

Hastings, L., Plachta, D., Salerno, L., and Kittel, P. (2002). An overview of NASA efforts on zero boil off storage of cryogenic propellants. Cryogenics, 41:833– 839.

Hastings, L., Tucker, S., Flachbart, R., Hedayat, A., and Nelson, S. (2005). Marshall space flight center in-space cryogenic fluid management program overview. AIAA 2005-3561.

Hedayat, A., Hastings, L., Bailey, J., Flachbart, R., and Holt, K. (2003).Thermo-dynamic venting system modeling and comparison with liquid hydrogen test data. AIAA 2003-4450.

Hedayat, A., Hastings, L., Bryant, C., and Plachta, D. (2001). Cryogenic propellant long-term storage with zero boil off. In Proceedings of the2001Cryogenic EngineeringConference, Madison, WI.

Hedayat, A., Nelson, S., Flachbart, R., and Tucker, S. (2005). Liquid nitrogen (oxygen simulant)thermodynamic vent system test data analysis. In Proceedings of the 2005CryogenicEngineeringConference, Keystone, CO.

Helmick, M., Khoo, B., and Sonin, A. (1986). Vapor condensation on a turbulent liquid interface. In Cryogenic Fluid Management Technology Workshop Vol. I: Presentation Material andDiscussion, NASA CP-10001, pages 301–315.

Hertz, H.; “Ueber die verdunstung der flussigkeiten, insbesondere des quecksilbers, im luftleeren raume” *Annalen der Physik and Chemie* **17** (1882) 177-200.

Hill, D. and Salvinski, R. (1967). A thermodynamic system for zero-g venting, storage, and transfer of cryogenic propellants. J. Spacecraft and Rockets, 4(7):955–957.

Hirt, C. (2001). Modeling phase change and homogeneous bubbles. FSI-01-TN57, Flow Science Inc.

Ho, S. and Rahman, M. (2005). Three-dimensional analysis of liquid hydrogen cryogenic storage tank. AIAA 2005-5712.

Hochstein, J. (1986). Numerical modelling of cryogenic propellant behavior in low g. In Microgravity Fluid Management Symposium, NASA CP-2465, pages 85–100.

Hochstein, J., Gerhart, P., and Aydelott, J. (1984). Computational modeling of jet induced mixing of cryogenic propellants in low g. NASA TM 83703.

Hochstein, J., Ji, H.-C., and Aydelott, J. (1986). Effect of subcooling on the on-orbit pressurization rate of cryogenic propellant tankage. AIAA 86-1253.

Hochstein, J., Ji, H.-C., and Aydelott, J. (1987). Temperature fields due to jet induced mixing in a typical OTV tank. AIAA 87-2017.

Hochstein, J., Ji, H.-C., and Aydelott, J. (1990). Prediction of self-pressurization rate of cryogenic propellant tankage. J. Propulsion and Power, 6(1):11–17.

Hofmann, A. (2004). Theory to boil-off gas cooled shields for cryogenic storage vessels. Cryogenics, 44:159–165.

Howell, J., Mankins, J., and Fikes, J. (2006). In-space cryogenic propellant depot stepping stone. Acta Astronautica, 59:230–235.

Huntley, S. (1960). Temperature-Pressure-Time Relationships in a Closed Cryogenic Container, volume 3 of Advances in Cryogenic Engineering, pages 342–352. Plenum Press.

Jacqmin, D. (1999). Calculation oftwo-phase Navier Stokes flows using phase-field modeling. J. Computational Physics, 155:96–127.

Ji, H.-C., Schwartz, S., Lovrich, T., Hochstein, J., and Holmes, L. (1992). Experimental verification of scaling parameters for thermal stratification. J. Thermophysics and Heat Transfer, 6(3):522–530.

Jones, O., Meserole, J., and Bentz, M. (1991), Correlation of ullage condensation rate with mixing intensity in propellant tanks. AIAA 1991-2543.

Jones, O., Meserole, J., and Fortini, A. (1994). Measurements of jet-induced pressure decay in a thermally stratified tank. J. Spacecraft and Rockets, 31(2):290–296.

Kirk, D., Oliveira, J., and Schallhorn, P. (2007). Cryogenic propellant stratification in a rotating and reduced gravity environment. AIAA 2007-954.

Kittel, P.; Plachta, D.W.; Propellant Preservation for Mars Missions, Advances in Cryogenic Engineering, **45** Ed. Shu et al.; Plenum Publishers, p. 443, 2000.

Knoll, R., Smolak, G., and Nunamaker, R. (1962). Weightlessness experiments with liquid hydrogen in aerobee sounding rockets; uniform radiant heat addition -flight 1. NASA TM X-484.

Knuth, E. (1959). Non stationary phase changes involving a condensed phase and a saturated vapor. Physics of Fluids, 2(1):84–86.

Knuth, E. (1962). Evaporation and condensations in one-component systems. ARS Journal, 32:1424–1426.

Koffman, L.D., Plesset, M.S., Lees, L.; "Theory of Evaporation and Condensation" *Phys. Fluids* **27** [4] (1984) 876-880.

Kryukov, A.P., Levashov, V.Yu., Sazhin, S.S.; "Evaporation of diesel fuel droplets: kinetic versus hydrodynamic models" *Int. J. Heat and Mass Transfer* **47** (2004) 2541-2549

Labuntsov, D.A, and Kryukov, A.P, "Analysis of Intensive Evaporation and Condensation", Int J. Heat Mass Transfer, **22**, pp. 989-1022, 1979.

Labus, T. and Symons, E. (1972). Experimental investigation of an axisymmetric free jet with an initially uniform velocity profile. NASA TN D-6783.

Lacovic, R. (1977). Propellant management report for the Titan/Centaur TC-5 extended mission. NASA TM-73749.

Lacovic, R., Yeh, F., S.V. Szabo, J., Brun, R., Stofan, A., and Berns, J. (1968). Management of cryogenic propellants in a full scale orbiting space vehicle. NASA TN D-4571.

Lak, T. and Wood, C. (1994). Zero g thermodynamic vent system final report. Report no. SSD 94M0038, Rockwell Aerospace.

Landis, G. and Linne, D. (2001). Mars rocket vehicle using in situ propellants. J. Spacecraft and Rockets, 38(5):730–735.

Lane, A. and Rice, P. (1982). An investigation of liquid jet mixing employing an inclined side entry mixer. Trans. IChemE, 60:171–176.

Lehrer, I. (1981). A new model for free turbulent jets of miscible fluids of different density and jet mixing time criterion. Trans. IChemE, 59:247–252.

Li, Z., Xu, L., Sun, H., Xiao, Y., and Zhang, J. (2004). Investigation on performances ofnon-loss storage for cryogenic liquefied gas.Cryogenics, 44:357–362.

Liebenberg, D. and Edeskuty, F. (1965). Pressurization Analysis of a Large-Scale Liquid Hydrogen Dewar, pages 284–289. Int. Advances in Cryogenic Engineering. Plenum Press.

Liggett, M. (1993). Space-based LH2 propellant storage system: Subscale ground testing results. Cryogenics, 33(4):438–442.

Lin, C. (1989). Numerical studies of the effects of jet-induced mixing on liquid-vapor interface condensation. NASA TM 182285.

Lin, C., Dresar, N. V., and Hasan, M. (2004). Pressure controlanalysis ofcryogenic storage systems. J. Propulsion and Power, 20(3):480–485.

Lin, C. and Hasan, M. (1990a). Numerical investigation ofthe thermalstatification in cryogenic tanks subjectedto wall heat flux.NASA TM 103194.

Lin, C. and Hasan, M. (1990b). Vapor condensation on liquid surface due to laminar jet-induced mixing: The effects of system parameters. NASA TM 102433.

Lin, C. and Hasan, M. (1992a). Effect of Liquid Surface Turbulent Motion on the Vapor Condensation in a Mixing Tank, pages 1526–1537. Transport Phenomena in Heat and Mass Transfer. Elsevier.

Lin, C. and Hasan, M. (1992b). Self-pressurization of a spherical liquid hydrogen storage tank in a microgravity environment. NASA TM 105372.

Lin, C., Hasan, M., and Dresar, N. V. (1994). Experimental investigation of jet-induced mixing of a large hydrogen storage tank. NASA TM 106629.

Lin, C., Hasan, M., and Nyland, T. (1993). Mixing and transient interface condensation of a liquid hydrogen tank. NASA TM 106201.

Lovrich, T., Schwartz, S., and Holmes, L. (1974). Flow visualization of thermal stratification with localized heat sources. J. Spacecraft and Rockets, 11(9):664–669.

Manson, L. (1965).A Technique for the Simulation of Thermal Behavior of Fluids in a Low Gravity Field, volume 10 of Advances in Cryogenic Engineering, pages 297–304. Plenum Press.

Marchetta, J. and Benedetti, R. (2007). Three dimensional modeling of jet-induced geysers in low gravity. AIAA 2007-955.

Marchetta, J., Kain, C., Simmons, B., and Benedetti, R. (2006). Simulation and prediction of jet induced geyser formation in microgravity propellant tanks. AIAA 2006-937.

McArdle, J., Billon, R., and Altmos, D. (1962). Weightlessness experiments with liquid hydrogen in aerobee sounding rockets; uniform radiant heat addition flight 2. NASA TM X-718.

McNaughton, K. and Sinclair, C. (1966). Submerged jets in short cylindrical flow vessels. J. Fluid Mechanics, 25(2):367–375.

Meerbeke, R. V. (1968). Thermal Stratification and Sloshing in Liquid Helium Trailers, volume 13 of Advances in Cryogenic Engineering, pages 199–206. Plenum Press.

Menter, F. (1993). Zonal two-equation k-w turbulence models for aerodynamic flows. AIAA 93-2906.

Merte H. et al. et (1970). Transient pressure rise of a liquid-vapor system in a closed container under variable gravity. 4th Int. Heat Transfer Conference, Paris, France.

Merte, H., Clark, J., and Barakat, H. (1968). Finite difference solution of stratification and pressure rise in containers. Technical report, Heat Transfer Laboratory, U. of Michigan. Tech Report No. 4.

Meserole, J., Jones, O., and Fortini, A. (1987). Mixing-induced fluid destratification and ullage condensation. AIAA 1987-2018.

Mikic, B.B.; Rohsenow, W.M.; Griffith, P.; "On bubble growth rates," *Int J. Heat Mass Transfer*, **13**, pp. 657-666, 1970.

Minkowycz, W. and Sparrow, E. (1966). Condensation heat transfer in the presence of noncondensable, interfacial resistance, superheating, variable properties, and diffusion.Int.J.Heat andMassTransfer, 9:1125–1144.

Mitchell, R., Stark, J., and White, R. (1967). Zero-g Hydrogen Tank Venting Systems, volume 12 of Advances in Cryogenic Engineering, pages 72–81. Plenum Press.

Mollendorf, J. and Gebhart, B. (1973a). An experimental and numerical study of the viscous stability of a round laminar vertical jet with and without thermal buoyancy for symmetric and asymmetric disturbances. J. Fluid Mechanics, 61(2):367–399.

Mollendorf, J. and Gebhart, B. (1973b). Thermal buoyancy in round laminar vertical jets. Int.J.Heat andMassTransfer, 16:735–745.

Motil, S. and Meyer, M. (2007). Cryogenic fluid management technologies for advanced green propulsion systems. AIAA 2007-343.

Mukka, S. and Rahman, M. (2004a). Analysis of fluid flow and heat transfer in a liquid hydrogen storage vessel for space applications. In El-Genk, M., editor, Space Technology and Applications International Forum -STAIF2004, volume 699, pages 37–44, Albuquerque, NM. AIP Conference Proceedings.

Mukka, S. and Rahman, M. (2004b). Computation of fluid circulation in a cryogenic storage vessel. AIAA 2004-5728.

NASA (2005). NASA Exploration Systems Architecture Study. NASA TM-2005-214062.

Navickas, J. (1988). Prediction of a liquid tank thermal stratification by a finite difference computing method. AIAA 88-2917.

Navickas, J. and Madsen, R. (1968). Propellant Behavior During Venting in an Orbiting Saturn S-IVB Stage, volume 13 of Advances in Cryogenic Engineering, pages 188–198. Plenum Press.

NCMR/GRC; Multiphase Flow in Space Power and Propulsion Workshop and Fluid Stability and Dynamics Workshop, (http://www.ncmr.org/events/multiphase) National Center for Microgravity Research, NASA Glenn Research Center, Cleveland, Ohio, May, 2003.

NCMR/GRC; Workshop on Research Needs In Fluids Management for the Human Exploration of Space, (http://www.ncmr.org/events/fluidsmgmt) National Center for Microgravity Research, NASA Glenn Research Center, Cleveland, Ohio, September 2000.

NCMR/GRC; Workshop on Research Needs in Space Thermal Systems and Processes for Human Exploration of Space, (http://microgravity.grc.nasa.gov/6712/thermal/workshop.html),National Center for Microgravity Research, NASA Glenn Research Center, Cleveland, Ohio, July 2000.

Neff, B. and Chiang, C. (1967).FreeConvectioninaContainer ofCryogenicFluid, volume 12 of Advances in Cryogenic Engineering, pages 112–124. Plenum Press.

Neff, R. (1960). A Survey of Statification in a Cryogenic Liquid, volume 5 of AdvancesinCryogenicEngineering, pages 460–466. Plenum Press.

Nguyen, H. (1994). Zero-g thermodynamic venting system (TVS) performance prediction program. Technical report, Rockwell Aerospace.

Nikitin, S. and Polezhaev, V. (1976). Convection and heat transfer in a spherical vessel, partly filledwith liquid, under low-gravity conditions.Izv.Akad.Navk SSSR,Mekh.Zhidk.Gaza, 2:154–159.

Nunamaker, R., Corpas, E., and McArdle, J. (1963). Weightlessness experiments with liquid hydrogen in aerobee sounding rockets; uniform radiant heat addition -flight 3. NASA TM X-872.

Okita, N. and Oyama, Y. (1963). Mixingcharacteristics in jetmixing.Jap.Chem.

Ordin, P., Weiss, S., and Christenson, H. (1960). Pressure-Temperature Histories ofLiquidHydrogenUnderPressurization andVenting, volume 5ofAdvances inCryogenicEngineering, pages 481–486. Plenum Press.

Osher, S.; Sethian, J.A.; "Fronts Propagating with Curvature Dependent Speed: Algorithms based on Hamilton-Jacobi Formulations", *J. Comp. Physics*, **79** pp. 12-49, 1988.

Overbeke, T. V. (2004). Thermodynamic vent system test in a low earth orbit simulation. AIAA 2004-3838.

Panzarella, C. and Kassemi, M. (2003). On the validity of purely thermodynamic descriptions of two-phase cryogenic fluid storage. J. Fluid Mechanics, 484:41– 68.

Panzarella, C. and Kassemi, M. (2005).Self-pressurization of large sphericalcryogenic tanks in space. J. Spacecraft and Rockets, 42:299–308.

Panzarella, C., Plachta, D., and Kassemi, M. (2004). Pressure control of large cryogenic tanks in microgravity. Cryogenics, 44:475–483.

Patwardhan, A. and Gaikwad, S. (2003). Mixing in tanks agitated by jets. Trans. I Chem E Part A: Chem. Eng. Res. Design, 81:211–220.

Plachta, D. (1999). Hybrid thermal control testing of a cryogenic propellant tank. NASA TM 1999-209389.

Plachta, D. (2004). Results of an advanced development zero boil-off cryogenic propellant storage test. AIAA 2004-3837.

Plachta, D., Christie, R., Jurns, J., and Kittel, P. (2006). Passive ZBO storage of liquid hydrogen and liquid oxygen applied to space science mission concepts. Cryogenics, 46:89–97.

Plachta, D. and Kittel, P. (2003). An updated zero boil-off cryogenic propellant storage analysis applied to upper stages or depots in an leo environment. NASA TM 2003-211691.

Plesset, M.S.; Zwick, S.A.; "The growth of vapor bubbles in superheated liquids," *J. Appl. Phys.*, **25**, pp. 493-500, 1954.

Pong, L. and Moses, G.A., "Vapor Condensation in the Presence of a Noncondensable Gas", Phys. Fluids, **29,** (6), pp1796-1804, 1986.

Poth, L. and Hook, J. V. (1972). Control of the thermodynamic state of space-stored cryogens by jet mixing. J. Spacecraft and Rockets, 9(5):332–336.

Poth, L., Hook, J. V., Wheeler, D., and Kee, C. (1968). A study of cryogenic propellant mixing techniques final report vol. I: Mixer design and experimental investigations. NASA CR 73908.

Prosperetti, A.; Plesset, M.S.; “Vapour-bubble growth in a superheated liquid,” *J. Fluid Mech.*, **85,** pp. 349-368, 1978.

Revill, B. (1992). Jet mixing. In Harnby, N., Edwards, M., and Nienow, A., editors, Mixing in the Process Industries. Butterworth Heinemann, 2nd edition.

Riemer, D. H. (1986). Cryogenic Tank Stratification: A Simpler Approach, volume 31 ofAdvancesinCryogenicEngineering, pages 957–962.Plenum Press.

Robbins, J. and A.C. Rogers, J. (1966). An analysis on predicting thermal stratification in liquid hydrogen. J. Spacecraft and Rockets, 3:40–45.

Rose, J.(1969). Condensation of a vapour in the presence of a non-condensing gas. Int.J.Heat andMassTransfer, 12:233–237.

Rotenberg, Y. (1986). Numerical Simulation of Self-Pressurization in a Small Cryogenic Tank, volume 31 of Advances in Cryogenic Engineering, pages 963–972. Plenum Press.

Ruder, J. (1964). Stratification in a pressurized container with side wall heating. AIAAJ., 2:135–137.

Salerno, L. and Kittel, P. (1999). Cryogenics and the human exploration of mars. Cryogenics, 39:381–388.

Schallhorn, P., Campbell, D., Chase, S., Piquero, J., Fortenberry, C., Li, X., and Grob, L. (2006). Upper stage tank thermodynamic modeling using SINDA/FLUINT. AIAA 2006-5051.

Schmidt, A., Purcell, J., Wilson, W., and Smith, R. (1960). An Experimental Study Concerning the Pressurization and Stratification of Liquid Hydrogen, volume 5 of Advances in Cryogenic Engineering, pages 487–497. Plenum Press.

Schrage, R.W., “Interphase Mass Transfer”, Columbia University Press, New York, 1953.

Scriven, L.E.; “On the dynamics of phase growth,” *Chem. Eng. Sci.*, **10**, pp. 1-13, 1959.

Schuster, J. (1986). Long term cryogenic facility systems study. In Microgravity Fluid Management Symposium, NASA CP-2465, pages 17–30.

Schuster, J. R., Russ, E. J. and Wachter, J. P., “Cryogenic On-Orbit Liquid Depot Storage, and Transfer Satellite (COLD-SAT)” General Dynamics Space systems Division and Ford Aerospace Space Systems Division, NASA CR-185249, July 1990.

Scott, L., Robbins, R., Mann, D., and Birmingham, B. (1960). Temperature stratification in a non venting liquid helium Dewar.J.ResearchNBS, 64C(1):19–23.

Segel, M. (1965). Experimental Study of the Phenomena of Stratification and Pressurization of Liquid Hydrogen, pages 308–313. Int. Advances in Cryogenic Engineering. Plenum Press.

Sengupta, A. (2001). Comparison ofcomputedto measured liquid hydrogen stratification. In Proc. of the 2001 ASME Fluids Engineering Division Summer Meeting, pages 629–636.

Simmons, B., Marchetta, J., and Hochstein, J. (2005). Reduced gravity cryogenic propellant tankre-supplysimulation and geyser prediction. AIAA 2005-1150.

Sonin, A., Shimko, M., and Chun, J.-H. (1986). Vapor condensation onto a turbulent liquid I: The steady condensation rate as a function of liquid-side turbulence. Int.J.Heat andMassTransfer, 29(9):1319–1332.

Stark, J. and Blatt, M. (1967). Cryogenic zero-gravity prototype vent system. NASA CR 98079.

Sterbentz, W. (1968). Liquid propellant thermal conditioning system final report. NASA CR-72365.

Stochl, R. and Knoll, R. (1991). Thermal performance of a liquid hydrogen tank multilayer insulation system at warm boundary temperatures of 630, 530, and 152 R. NASA TM 104476.

Swim, R. (1960).TemperatureDistributioninLiquidandVaporPhases ofHelium inCylindricalDewars, volume 5ofAdvancesinCryogenicEngineering, pages 498–504. Plenum Press.

Symons, E. and Labus, T. (1971). Experimental investigation of an axisymmetric fully developed laminar free jet. NASA TN D-6304.

Symons, E. and Staskus, J. (1971). Interface stability during liquid inflow to partially full, hemispherical ended cylinders during weightlessness. NASA TM X-2348.

Tanyun, Z., Zhongping, H., and Li, S. (1996). Numerical Simulation of Thermal Statification in Liquid Hydrogen, volume 41 of Advances in Cryogenic Engineering, pages 155–161. Plenum Press.

Tatom, J., Brown, W., Knight, L., and Coxe, E. (1964). Analysis of Thermal Stratification of Liquid Hydrogen in Rocket Propellant Tanks, volume 9 of AdvancesinCryogenicEngineering, pages 265–272. Plenum Press.

Tellep, D. and Harper, E. (1963). Approximate analysis of propellantstratification. AIAAJ., 1(8):1954–1956.

Thomas, P. and Morse, F. (1963). Analytic Solution for the Phase Change in a Suddenly Pressurized Liquid-Vapor System, volume 8 of Advances in Cryogenic Engineering, pages 550–562. Plenum Press.

Thornton, R. and Hochstein, J. (2000). Microgravity geyser and flow field prediction. AIAA 2000-0858.

Tunc, G., Wagner, H., and Bayazitoglu, Y. (2001). Space shuttle upgrade liquid oxygen tank thermal stratification. AIAA 2001-3082.

Val'tsiferov, Y. and Polezhaev, V. (1975). Convective heat transfer in a closed axisymmetric vessel with curvilinear generatrix in the presence of phase boundaries and phase transitions. Izv. Akad. Navk SSSR, Mekh. Ahidk. Gaza, 6:126–134.

Venkat, S. and Sherif, S. (2004). Self-pressurization and thermal stratification in a liquid hydrogen tank under varying gravity conditions. AIAA 2004-1341.

Vliet, G. (1966). Stratification with bottom heating. J. Spacecraft and Rockets, 3(7):1142–1144.

Warren, R. and Anderson, J. (1967). A System for Venting a Propellant Tank in the Absense of Gravity, volume 12 of Advances in Cryogenic Engineering, pages 63–71. Plenum Press.

Wendl, M., Hochstein, J., and Sasmal, G. (1991). Modeling of jet-induced geyser formation in a reduced gravity environment. AIAA 91-0803.

Yanke, A. (1977). Titan/Centaur flightevaluation TC-5. Technical Report Report CASD/LVP-76-066, General Dynamics Convair.

Zwick, S.A.; "The growth of vapor bubbles in a rapidly heated liquid," *Phys. Fluids*, **3**, pp. 685-692, 1960.

Appendix A

The Original ZBOT Proposal

NASA Advanced Capabilities Division
Office of Human Systems Research and Technology

The Zero Boil-Off Tank (ZBOT) Experiment

Principle Investigator:
Dr. Mohammad Kassemi
National Center for Space Exploration Research (NCSER)
NASA Glenn Research Center, 21000 Brookpark Rd., Mail Stop 110-3
Cleveland, Ohio 44135
(216) 433-5031 (phone)
(216) 433-5033 (fax)
Email: Mohammad.Kassemi@grc.nasa.gov

Co-Investigators:
Dr. David Chato,
NASA Glenn Research Center,
Cleveland, Ohio 44135
Email: David.J.Chato@nasa.gov

Research Collaborator:
Stephen Barsi
National Center for Space Exploration Research (NCSER)
Case Western Reserve University
Cleveland, Ohio 44106

July 21, 2006

Summary

NASA's projected exploration program includes a series of human and robotic expeditions to low and high earth orbit, Moon, Mars, and possibly the asteroids and moons of other planets. Integral to all phases of these space and planetary expeditions is *affordable* and *reliable* cryogenic fluid storage for use in the propellant or life support systems. Without safe, efficient, and flexible cryogen storage, economically justified human missions may not be possible.

Cryogen vaporization is one of the main causes of mass loss and self-pressurization in the storage tanks. This has led to the development of the Zero-Boil-Off (ZBO) concept as an innovative ventless means of controlling tank pressure through a synergetic application of active heat removal and forced liquid jet mixing. Unfortunately, both tank pressurization and pressure control are governed by intricate and complicated gravity-dependant dynamic interactions among the forced-jet mixing, the various transport mechanisms in the vapor and liquid phases, and the condensation/evaporation process at the interface. As a result, effective implementation and optimization of a variable-gravity ZBO pressure control system cannot be accomplished empirically, especially, since there is a serious scarcity of relevant microgravity data.

The aerospace engineering community feels that a large-scale in-space technology validation test of the cryogenic storage tank prototype will be ultimately necessary. But, in the absence of any comprehensive prior research, this might turnout to be both a costly and risky endeavor. Before such an ambitious undertaking becomes warranted, small-scale targeted ground-based and microgravity simulant fluid experiments and state-of-the-art verified and validated two-phase flow CFD models of the storage tank are needed to first understand the underlying physical phenomena influencing tank pressurization and then to optimize and scale-up the pressure control mechanism for microgravity and/or on-surface storage. In this light, the objectives of this proposal are threefold:

- Develop a small-scale simulant-fluid experiment for both preliminary ground-based testing and subsequent ISS flight experiments in order to obtain valuable microgravity empirical data for a ZBO tank design and archival science data for model validation.
- Build a science base for the future space storage tank engineering efforts by elucidating the roles of the various interacting transport and phase change phenomena that impact tank pressurization and pressure control in variable gravity through systematic 1g and microgravity scientific investigation.
- Develop, validate, and verify variable gravity two-phase CFD models for ventless ZBO storage tank pressure control that can be used to aid scale-up tank design.
- Show the feasibility of ZBO pressure control scheme for microgravity and variable gravity applications.

These step-wise accomplishments are essential before a large-scale microgravity engineering prototype experiment can be justifiably undertaken.

The products of this research will be: a small-scale simulant-fluid tank pressurization flight experiment; validated and verified two-phase CFD models for ZBO cryogenic storage tanks; a science document containing valuable 1g and microgravity theoretical and experimental science data expanding the two-phase flow foundation for the development of future space storage technologies; and an engineering document for future ZBO storage tank design.

If the results of this research are brought to fruition they will ultimately contribute to lowering the cost and increasing the safety of future space expeditions in line with the needs of the NASA Exploration Initiative in preserving and sustaining human life and human habitats in space.

Table of Contents

1.0 Introduction

The extension of human space exploration from low earth orbit into the solar system is currently one of NASA's biggest challenges for the next millennium. The projected exploration programs include a series of human and robotics expeditions to low and high earth orbit, Moon, Mars, and possibly the asteroids and other planetary moons. Integral to all phases of these space expeditions is *affordable* and *reliable* cryogenic fluid storage for use in the propellant or life support systems. This is true for both manned and unmanned mission scenarios with either traditional chemically fueled rockets or innovative (chemically-augmented) nuclear-electric and/or nuclear-thermal propulsion systems (Anderson, 2000; Borowski, 2003). Efficient storage technology is also crucial for all the In-Situ Resource Utilization (ISRU) options that are currently being considered for both propellant and life support fluids in various planetary surface-launch concepts. As a result, large volume cryogenic liquid storage and handling is among NASA's top enabling technologies in need of targeted strategic research (Wieslogel, 2003).

An important problem that the space storage technologies must address is vaporization of the cryogenic liquids. Cryogen vaporization is one of the main causes of mass loss and self-pressurization in the storage tanks (Salerno and Kittel, 1999; Kittel and Plachta, 2000) and occurs when heat leaks through the thermal protection system cause vaporization of the liquid. Ordinarily, direct venting to the outside surrounding can relieve the excess pressure. Unfortunately, in the microgravity environment, the position of the vapor-liquid interface is not well defined and direct venting is precluded due to the possibility of expelling the liquid along with the vapor. In-space venting is also undesirable because it prohibits manned flight operations around the storage tanks. Moreover, even in on-surface applications, where the position of the vapor is better defined, continuous venting over a significant length of time results in considerable loss of the propellant or life support fluids. If conventional storage technologies are used, larger tanks are required to account for these losses. For long-term missions, the added mass needed to compensate for the cryogen boil-off and the weight of the oversized tanks that will be required to accommodate the extra mass can render the use of cryogenic propellants prohibitive, causing mission planners to consider propellants with much lower specific impulses.

Table 1: ZBO and Passive Mass Requirements

	ZBO* (MLI: 15 Layers)	Passive** (MLI: 30 Layers)	Difference	* Includes the weight of Propellant, Tank, Insulation, CryoCooler, Solar Array, Radiator ** Includes Propellant, Tank, Insulation, Boil-Off, Tank & Insulation Growth Due to Boil-Off
50 Days	2824 kg	2934 kg	110 kg	
100 Days	2824 kg	3178 kg	354 kg	
1000 Days	2824 kg	6302 kg	6286 kg	

1.1 Ventless Cryogenic Fluid Management

Realization of these problems has made ventless storage technology highly desirable. The *Zero-Boil-Off* (ZBO) design concept has emerged as one of the most promising and innovative pressure control strategies. As shown in Fig. 1, ZBO design combines both passive (thermal insulation) and active (cryo-cooler) thermal control technologies together with forced mixing of the liquid cryogen to control evaporation at the liquid-vapor interface (Plachta and Kittel, 2002). While utilizing passive storage technology exclusively will not realize the maximum mass saving, relying on active technologies alone always raises concern over reliability and power

consumption. Therefore, the ZBO design strategy of integrating active and passive technologies in the form of a hybrid pressure control system seems to be the only effective means of minimizing mass and power requirements while retaining significant protection in case of a cooler failure or unanticipated power restrictions. The integration of the Zero Boil-Off pressure control strategy into the storage tank design has many mission enabling benefits because it:

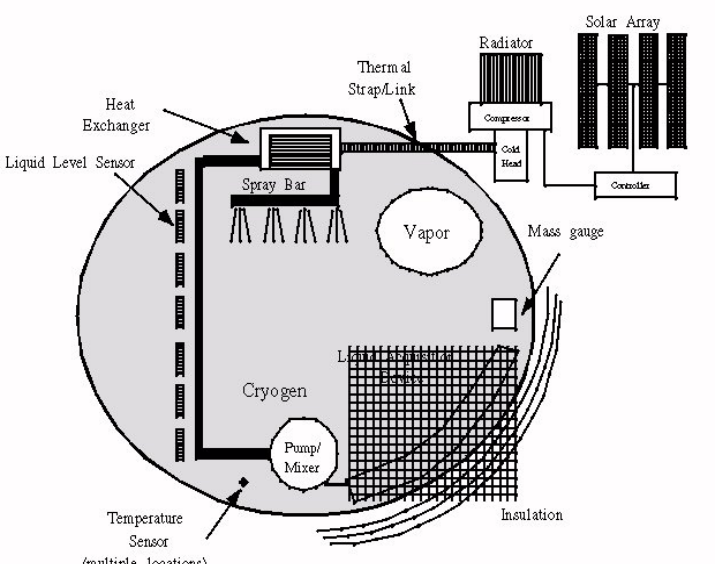

Figure 1. The ZBO Pressure Control System

1. Decreases the launchable propellant and storage tank mass. (See Table 1 and Fig. 2 for a comparison of ZBO and passive mass requirements for a 1.3 meter diameter tank in low earth orbit.
2. Increases system reliability through active-passive pressure control.
3. Promotes crew safety by allowing manned flight operations such as rendezvous and docking around the cryogenic tanks.
4. Enables new opportunities by building flexibility into both the mission planning and revision phases since manned flights encountering delays for whatever reason can be tolerated without major risk and/or cost increase considerations.

Naturally, these will all lead to a significant reduction in cost and an increase in safety and reliability for both short and long duration expeditions. However, before these benefits can be realized several key engineering and scientific issues associated with multiphase fluid flow and heat transfer in cryogenic storage tanks must be resolved.

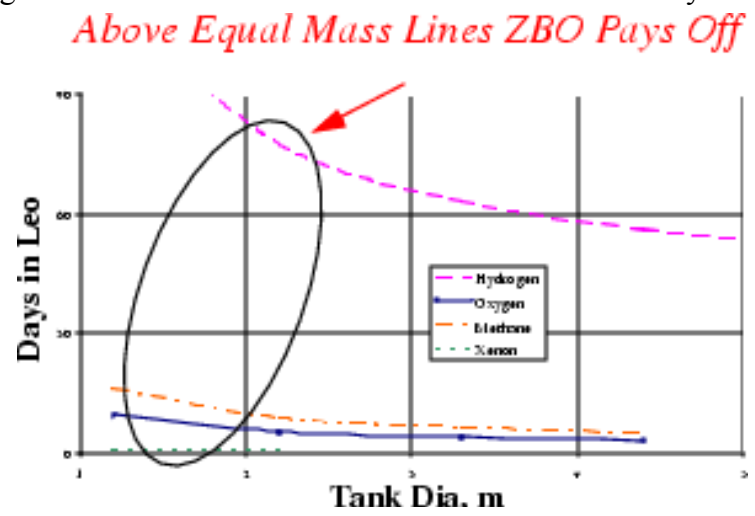

Figure 2. Equal Mass Lines above which ZBO Design Strategy Provides a Distinct Advantage

1.2 Objectives and Approach

This research has two broad and two specific objectives. The broad research objectives are: (a) to delineate the primary two-phase transport and phase change mechanisms that influence cryogen vaporization and condensation during 1g and microgravity storage; and (b) to expand the scientific and engineering foundation for space-based cryogenic fluid storage by

obtaining valuable long duration two-phase flow and phase change microgravity data that can be ultimately used to derive the much-needed empirical correlations for tank pressurization, destratification, and pressure control.

The specific objectives of the research are: (a) to assess the effectiveness of the Zero Boil-Off (ZBO) strategy as an innovative means of eliminating thermal stratification, self-pressurization, and mass loss in space cryogenic storage tanks based on an optimized and synergetic application of active heat removal and forced-mixing; and (b) to develop, validate and verify a state-of-the-art variable gravity two-phase CFD model and computer code for tank pressurization and ZBO pressure control to serve as a valuable tool for the storage tank scale-up design.

These objectives will be accomplished through a three-pronged scientific approach comprised of coordinated theoretical and scaling analyses, numerical modeling and simulations, and experimental prototype testing and measurement.

1.3 Engineering Significance

From an engineering point-of-view, designing a highly reliable fluid storage system of limited cost for an environment with limited accessibility (for testing) is indeed a great challenge. Unfortunately to date, the evolutionary engineering response to this challenge has been to avoid the problem all together by sacrificing costs in favor of reliability through overdesign. The result has been larger than necessary passive (insulated) systems. In the design of the passive storage tank, thermodynamics and empiricism rule. Therefore, in a sense, these oversized *passive* storage systems are *g-independent* and *ground-testable*.

As the results of the recently held *Workshop on Research Needs In Fluids Management for the Human Exploration of Space* (NCMR/NASA GRC, 2000) have suggested, the overdesign strategy is not a viable option for future planetary missions due to its prohibitive costs. On the other hand, the ZBO storage strategy provides a highly reliable and affordable alternative for future missions because it is based on dynamic pressure control. As is with all dynamic fluids and heat transfer systems, transport processes will play a dominant role in the implementation of the ZBO pressure control strategy. Rigorous transient multi-phase thermal and fluid flow analyses together with experimental prototyping, testing and measurement are required to first understand the dynamics of the underlying transport processes and then to optimize the design of the tank and the ZBO pressure control system for target applications and their associated environmental conditions.

1.4 Scientific Significance

From a scientific point of view, the thermophysical processes that occur in the cryogenic storage tank are one of the most complicated and compelling two-phase fluid flow problems encountered in both ground and space-based technologies. Pressure change and mass loss in the cryogenic storage tank are governed by an intricate interplay among heat transfer in the liquid and vapor, mass transfer due to evaporation/condensation processes that may occur in the presence of non-condensable gases, and complicated fluid flow in the liquid brought about by forced jet mixing and by natural and thermocapillary convective flows. The fluid flows may span both laminar and turbulent regimes depending on the specific application. Moreover, due to thermal stratification and significant superheats in microgravity, there is a large propensity for sudden nucleation and rapid bubble growth causing alarming pressure spikes.

Free surface turbulence, condensation in presence of noncondensables, thermocapillary flow driven by partial pressures on the gaseous side, and sudden nucleation and bubble growth in closed containers due to local superheats are all fundamental scientific two-phase flow issues that are encountered during the engineering design of a ZBO tank system and will be studied and addressed during the course of this research effort. Resolving these fundamental issues and analyzing the transport mechanisms, the fluid flow behavior, and the associated time constants of the various interacting phenomena that occur in the cryogenic storage tank for different gravitational environments is crucial for the optimum design of a the ZBO pressure control system. It will also contribute significantly to our state-of-art scientific knowledge of two-phase fluid behavior in variable-gravity (2, 1, 1/6, and micro-g) environments with significant benefits for a multitude of other two-phase flow operations and processes in space.

1.5 Microgravity Relevance

NASA's microgravity fluid storage challenges are more acute than partial-g or macro-g challenges due to the absence of a solid empirical foundation in micro-g and the need to rely heavily on assumption-based analyses. Consequently, as indicated by three recent microgravity workshops (NCMR/NASA GRC: 2000a, 2000b, 2003), there will be an unusually heavy reliance on theory during the design phase for future space-based cryogenic storage facilities demanding powerful and comprehensive computational models. But the community is hesitant to trust current and proposed theoretical/numerical models due to lack of validation and verification. As a result, it is difficult to imagine low-g systems flying without low-g demonstrations.

While drop tower tests can be effectively used to obtain useful data with regard to phase distributions, interface behavior, mixing times, and jet penetration of the ullage, the time constants of the pressurization and pressure control problem do not lend themselves well to short-duration microgravity testing in drop towers and/or parabolic flights (see sections 2 & 3). Thus the impetus has been for NASA to focus on small-scale long-duration microgravity investigations with *simulant* fluids that can nevertheless provide relevant microgravity data for both tank design and validation/verification of the CFD models before a large-scale technology validation prototype test in space is warranted.

Long-duration microgravity is also necessary for studying closed tank nucleation and bubble growth caused by superheats that are very specific to the space environment. On the ground, any significant superheat is greatly diminished by the strong mixing effects of natural convection. But, significantly larger superheats are possible in microgravity and as a result the probability of creation of active nucleation sites and sudden bubble growth is greatly increased. If such sudden microgravity nucleation and bubble growth occur in a large tank, the resulting pressure spikes may lead to imminent structural failure with disastrous consequences. Finally due to the diminished role of natural convection, the microgravity environment will provide a better means of unmasking the presence of any thermocapillary convection induced by the presence of the noncondensable pressurant gases in the ullage.

1.6 Relevance to NASA Missions

From a mission point of view, efficient and innovative cryogenic fluid management and storage is an enabling technology in the critical path of all human space expeditions pursued by NASA. The designated mission options include manned flights to Mars, Moon, Callisto, and Europa, as well as large planetary-return robotics missions, earth-orbiting depots, and large probes. All of the propulsion concepts (including nuclear-electric and nuclear-thermal) for these

options have elements that include cryogenic propulsion and storage, whether they are in the return mission leg fueled by in-situ propellants produced at the destination or as part of the main vehicle propulsion system or both. In a recent assessment of prioritized technologies for NASA missions by *The National Space Propulsion Synergy Team,* cryogenic fluid management was second in technical and programmatic priorities for both human exploration and commercial development of space. A NASA-commissioned survey just completed by Weislogel (2003) involving detailed interviews of more than 40 mission planners, scientists, and system and component engineers from NASA and the aerospace industries specializing in space fluids/transport phenomena has placed cryogenic storage systems first in NASA's top priorities in need of focused strategic research. Finally, the recently released "Exploration Systems Architecture Study" (NASA, 2006) underscores the need for long term storage data to support technology development activities of the Earth Departure Stage, Lunar Surface Ascent Module, and In-situ Resource Utilization Constellation elements.

In this context, this proposal serves as a means of involving scientists, from early on, on the problem of long-duration variable gravity storage of cryogenic propellants and life support fluids with the ultimate goal of reducing costs while expanding the operational robustness of future exploration and commercial space activities.

2.0 Technical Background

Traditionally, pressure control in microgravity has been achieved by first firing thrusters to settle the liquid and then venting vapor. In tanks that will be equipped, in the future, with a Thermodynamic Vent System (TVS), a Joule-Thompson valve and the accompanying heat transfer are conveniently used to cool the bulk liquid and the vapor during venting in order to get further reduction in the tank pressure. Nonetheless, liquid and/or vapor mass are lost in either case. The ZBO concept, however, achieves the required reduction in pressure, in an innovative approach, by removing heat form the bulk liquid without any need for venting. Consequently, both the design and performance of the ZBO pressure management system are strongly influenced by the fluid dynamics and heat transfer mechanisms that control thermal stratification in the bulk liquid and the phase change phenomena and mass transfer that govern the evaporation/condensation processes at the liquid-vapor interface.

2.1 Problem Definition: Role of the Transport Phenomena

Self-pressurization in the cryogenic storage tank is mainly due to heat leaks from the surrounding environment. The extent of the heat leak depends on the conductive, convective, and radiative heat transfer links between the tank wall and its immediate surroundings. The heat transfer links are, in turn, functions of the thermal characteristics of the multilayer insulation (MLI) system, the conduction paths provided by the structural support systems, the levels of containment, and the environmental conditions associated with each application (ie, earth laboratory, during launch, in-orbit, and on planetary surfaces). Transverse temperature gradients generated by the heat leaks will give rise to natural convective boundary layers along the wall as shown in Fig. 3a and b. If the natural convection current is not controlled, it will create thermal stratification in the liquid and lead to considerable evaporation at the interface causing a pressure rise. An intermittent forced jet flow as shown in Fig. 3 can be used to destratify the liquid by promoting mixing. The jet counteracts the effect of natural convection by carrying cooler liquid from the lower central regions of the tank thus promoting condensation at the interface. Because of the low viscosity of the cryogen fluids (e.g. hydrogen) and the large dimensions of the storage

tank, both the natural and forced convection will be in the turbulent regime for typical on-surface (partial-gravity) applications. Even in microgravity, the natural convective flow can be strong and may indeed be in a transitional regime while the forced jet is probably turbulent.

While significant thermal stratification occurs in the bulk liquid, the interfacial temperature will be uniform for the most part as dictated by the ullage saturation temperature/pressure. However, there may be three notable exceptions: (a) variations in temperature may occur along the liquid-vapor interface near the wall contact line due to the thermal influence of the wall; (b) variations in the interfacial temperature may arise due to the presence of non-condensable gases in the vapor region that would result in the vapor saturation temperature at the interface be a function of the spatial distribution of the vapor partial pressure in the ullage region; (c) deviation of interface temperature from saturation temperature may occur during any rapid and intensive (nonequilibrium) heat or mass transport at the interface. All of the above three cases may give rise to surface tension driven thermocapillary flows in the liquid because the temperature of the interface will no longer be solely controlled by equilibrium thermodynamics but may be affected in one way or another by various transport processes in the tank.

The convective transport will be quite complicated in microgravity because natural convection is not only driven by the background g-level but also by the time-dependant g-jitter or impulse accelerations. Thus, the intensity and characteristics of the natural convective flow in the tank will depend on the direction, magnitude and frequency of the residual acceleration vector. In contrast, the surface tension driven thermocapillary flow is independent of the gravitational environment and may dominate the convective transport in microgravity applications. Moreover, in space, the position of the liquid-vapor interface is not well defined as indicated in Fig. 3b and will be also influenced by the direction and magnitude of the residual gravitational field that can vary with time. This can create a continuous ullage motion that may contribute significantly to mixing and destratification in the tank. In any case, the multiple time scales associated with the various convective and transport mechanisms have to be all considered and analyzed in order to properly predict the tank pressure reduction time constants.

In the ZBO system, pressure is controlled by cooling and forced jet mixing of the bulk liquid. The temperature field and stratification in the tank is therefore affected by the dynamic competition between the intermittent forced jet flow at the center of the tank and the natural and thermocapillary convective flows originating from the regions near the wall and near the liquid-vapor interface. The complicated convective flow that ensues ultimately determines the evaporation (condensation) rate at the liquid-vapor interface and the extent of pressure rise (fall) in the tank. In a ZBO system, the cooling and the mixing can be done separately through use of a cold finger and a mixing jet or simultaneously by means of a subcooled forced jet.

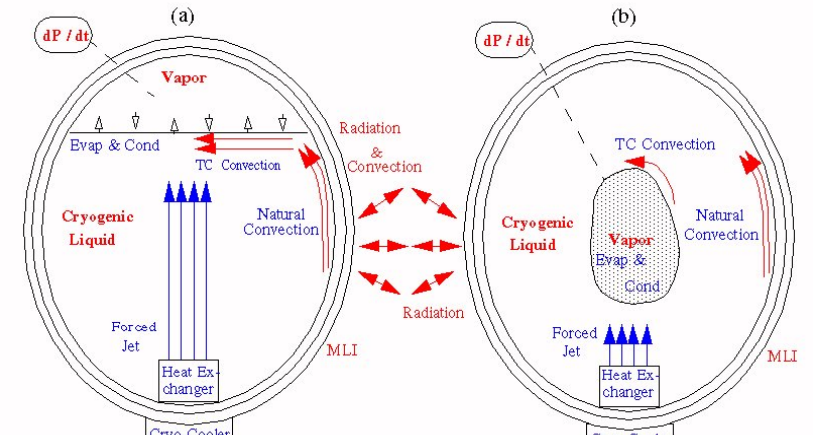

Figure 3. Cryogenic Storage Tank: (a) On-Surface 1g, 1/6g, and 3/8g Applications and (b) In-Orbit Microgravity Applications

Therefore from an engineering point of view, the cold finger location and surface configurations and the jet flow parameters become important design variables.

Another important issue that needs to be understood is the possibility of nucleate boiling at the wall or within the liquid due to the unusually large superheats that may arise in the absence of significant natural or forced convection in microgravity. The probability of either homogenous or heterogeneous nucleation increases as the superheat increases, and if such nucleation and bubble growth occur, they can lead to sudden undesirable pressure spikes similar to those observed in the brief TPCE microgravity experiment (Bentz et al, 1993; Hasan et al, 1996). Such pressure spikes can lead to mechanical failure of the storage tank. Therefore, conditions that promote this phenomenon in microgravity must be properly investigated.

2.2 Previous Research and Related Work

Propellant tank pressurization has been the subject of extensive theoretical and experimental studies. Self-pressurization of a flight-weight liquid hydrogen tank was studied by Van Dresar et al. (1992) where they showed that heat fluxes in the range representative of future space applications might create a considerable pressure rise in the tank. The mode of heat transfer was found to be complex and influenced by natural convection. The rate of pressure rise proved to be a complicated function of fill ratio, liquid-vapor interfacial area and mode of wall heating. Application of jet-induced mixing to control the tank pressure rise was investigated experimentally by Lin et al. (1994). They showed that the effects of natural convection boundary layers, formed at the wall due to external heating, could be effectively countered by a subcooled jet flow emerging from the center of the tank. They also concluded that a thermal equilibrium state is hard to achieve and that the existing correlations for mixing time and vapor condensation rates based on small-scale tanks may not be applicable to large scale liquid hydrogen systems. The correct extrapolation can only be determined when the interaction between the forced and natural convective flows is properly understood. Experimental determination of scaling parameters for thermal stratification in the cryogenic propellant tank was carried out by Ji et al. (1992). They identified three dimensionless parameters for scaling tank pressure and liquid surface temperature. Unfortunately, there were deviations in the detailed temperature and pressure profiles between the scaled pairs of tests indicating that the three dimensionless scaling parameters are not adequate to represent the physical phenomena completely. Hasan et al. (1996) undertook an interesting tank pressurization experiment in microgravity. The tests used Freon 113 as the test liquid. The experiments demonstrated the sustainability of liquid superheats for long periods and occurrences of explosive boiling for low wall heat fluxes. The results also underscored the inherent differences between 1-g and low-g vapor-liquid interactions with serious implications for forced mixing scenarios. Finally the effects of hybrid thermal control on pressurization of a cryogenic propellant tank were investigated by Plachta (1999) where it was shown experimentally that through effective use of passive insulation and active cryo-cooler technology it is possible to control tank pressurization by establishing zero boil-off conditions at Earth's normal gravity environment.

The theoretical/numerical treatments of propellant storage tanks can be divided into three main categories. The first category consists of tank self-pressurization studies that compute the pressure rise in the vapor mainly in terms of thermodynamic considerations (Lin and Hasan, 1992). The second category consists of investigations that examine the cryogen fluid flow. These investigations focus on the liquid phase alone and model the fluid flow in the liquid in terms of either pure natural convection (Grayson et al., 1997; Lin et al., 1990) or pure forced jet

flow (Lin et al, 1990; Hochstein, 1984). Moreover, in these representations the transport processes in the vapor phase is typically ignored, and the temperature of the liquid-vapor interface is assumed uniform and equal to its saturation value. Finally, in the third category are the investigations that examine the behavior and evolution of the liquid-vapor interface in both 1-g and microgravity applications using mainly the Volume of Fluid (VOF) approach as embodied by the Los Alamos code Ripple and its derivatives (Kothe et al., 1991). Investigations in this category have focused on: the evolution of the free surface as influenced by the microgravity environment (Liu, 1992); on the reorienting of the vapor subject to spacecraft thrust (Hung and Shyu, 1992); and on the free surface deformation as affected by the jet flow (Kothe et al., 1991) or by a magnetic field (Marchetta and Hochstein, 2000). The studies in this category are all limited to isothermal models and, therefore, divulge no information with regard to tank pressurization.

The explosive boiling event observed in the microgravity Tank Pressure Control Experiment (TPCE) described in Hasan et al. (1996) suggests that some type of rapid nucleation and vapor generation event is occurring when the liquid superheat gets too large. The process of vapor bubble growth in a superheated liquid has been subject of extensive scholarly research, such as the ones by Plesset and Zwick (1954), Birkoff, Margulies and Horning (1958), Scriven (1959), Zwick (1960), Bankoff (1964), Mikic, Rohsenow and Griffith (1970), Dalle Donne and Ferranti (1975), and Prosperetti (1978). All of these studies have seemingly been limited to situations where the vapor bubble is free to expand without influencing the surrounding ambient liquid pressure far from the bubble. This is not the case if the bubble growth occurs in a closed container like a cryogenic tank since the total volume inside the tank is fixed. In a closed tank, the additional vapor volume of the growing bubble would necessarily lead to a compression of all the other preexisting vapor regions resulting in a rapid increase in the bulk liquid pressure. This could be the explanation for the rapid pressure spikes observed in the TPCE as previously mentioned. However, there seems to be little or no previous theoretical investigations of this phenomenon.

The Multipurpose Hydrogen Test Bed (MHTB) facility (Martin and Hastings, 2001) has been established at the NASA Marshall Space and Flight Center for testing various cryogenic fluid management concepts and issues including different pressurization and pressure control strategies for space storage. MHTB has been recently used to develop a spray bar vent system for on orbit liquid hydrogen storage (Hastings et al, 2003). The result has been an impressive array of pressurization and pressure control tests and data that have been used to benchmark a customized two-phase tank model based on the commercial CFD code Flow3D (Grayson and Lopez, 2006).

NASA Drop Tower facilities have been used extensively to provide data for fluid flow behavior and interfacial dynamics in reduced gravity. Symons (1968, 1969, 1970, 1971) and Spuckler (1972) studied the liquid inflow via axial jet into a broad range of tank shapes both empty and partially full. Symons work established an empirical limit for jets of Weber number equal to 1.3-1.5 depending on jet velocity profile. Staskus (1972) extended this work by placing baffles in front of the jet. However, no attempt was made to analyze the resulting complex flows. Instead results were reported in the form of an improved performance as reflected by the ratio of baffled to unbaffled jet Weber numbers. Labus (1972) also studies the effect of baffles including the ones that break the central jet into several small jets. Aydelott (1976, 1979, 1983) considered the performance of a recirculating jet while the tank liquid level is kept constant. He classified his results in terms of four flow patterns characterized by dissipation, geyser formation, aft

collection, and circulation. Aydelott concluded the geyser formation/aft collection transition is accompanied by a decrease in mixing. Finally, Labus (1977) studied both stagnation flow and free surface shape during reduced gravity drops by concentrating on the free surface on the back side of a liquid jet that stagnates against a flat plate.

Shuttle-based experiments have provided more useful and extensive low gravity data. Shuttle experiments provide several improvements over drop tower tests; including increasing the scale from 4" tanks to 12" tanks and extending the duration of the tests from 2 to 5 seconds to half-an-hour. The previously mentioned, Tank Pressure Control Experiment (TPCE), has flown three times. The first flight experiment by Bentz (1990) focused on mixing studies that were similar to Aydelott's but performed actual heat transfer measurements using a condensing fluid (refrigerant 113). Bentz (1990, 1993a, 1993b) was able to confirm the geysering and circulating regimes of Aydelott, but encountered an asymmetric regime between these two regimes that had even a lower mixing rate and heat transfer performance than the aft collection regime, that provided the lowest mixing rate among Aydelott' four mixing regimes. The second flight of TPCE focused mostly on rapid boiling phenomena (Hasan et al, 1996) and pressure spikes were observed that were attributed to the local superheats occurring in the liquid due to reduced mixing in microgravity. Finally, the third flight experiment (Bentz et al, 1997) was done at a lower fill level and basically confirmed the results of the other two microgravity studies.

The Tank Pressure Control Experiments (TPCE)s are probably the most relevant microgravity experiment to date. However, the data collected is mostly qualitative in nature and unfortumately not entirely suitable for validation and verification of comprehensive tank models. In this context some of the short comings of these experiments are as follows:

1. Heaters were submerged in the fluid to raise the tank pressure, therefore, the thin thermal boundary layers on the tank wall that are characteristic of large storage tanks were not developed.
2. There was no flow visualization/measurement and the thermal measurements were limited.
3. Although, the thermal conductivity of tank wall was greater than thermal conductivity of test fluid, yet thermal losses to the wall and to the surrounding were not accounted for.
4. Test durations were 10-40 minutes. Our current analysis indicates that this is with in the initial transient regime. Hence, no information is provided on the long term stationary state of the tank and comparisons even to thermodynamics predictions are not possible.
5. Contaminant species leaked into the tank during the experiment (Contaminant mass fraction ~2%). An overpressure tends to suppress nucleation that raises questions as to the origins of the observed onset of pressure spikes. The noncondensables may have affected the evaporation and condensation process.
6. Settling time was only 30 minutes between runs. This is may be insufficient to return to a common and identical initial state before each test. Unfortunately, pressurization results are sensitive to the initial conditions because different test runs could correspond to different location on the pressure-temperature saturation curve yielding different results. This creates substantial difficulty for using the data for model validation.

3.0 Preliminary Ground-Based Research

In this section, we will first describe our preliminary ground-based experimental and modeling research activities. Then we will present and briefly discuss several 1g and microgravity simulation case studies of tank pressurization and pressure control. The results of these computational case studies will not only provide good physical insight into the effect of transport processes on storage tank pressurization/pressure control, but will in effect serve as good proofs of concept for the main premise of this proposal – i.e. the feasibility of using the ZBO strategy as an effective variable gravity tank pressure control strategy.

3.1 Preliminary Ground-Based Experiment

A schematic of the preliminary ground-based experimental apparatus is shown in Fig. 4. The test cell consists of a cylindrical tank of dimensions 4" x 18" x 1" (r x h x wall thickness). Hemispherical ends with a radius of curvature of 8.5" cap the top and bottom ends of the test cell. The transparent test cell is made out of high quality optical acrylic and sits on a stand atop a vibration isolation optical bench.

Strip heaters (1 W $\pm$ 0.01 W) are affixed via pressure-sensitive adhesive to the inside surface of the test cell. Two strip heaters are employed to simulate heat leak in both the liquid and vapor regions. The time evolution of the pressure inside the test cell is measured by a highly accurate pressure transducer ($\pm$ 0.01 psi) located on the top end cap in the vapor region.

The time evolution of the temperature field is captured by 15 highly accurate thermistors ($\pm$ 0.03 ^{o}C) placed inside the tank. One thermistor enters the tank through the top end cap to measure the temperature at the interface. The other 14 thermistors enter the tank through the sidewall to provide a matrix of local temperature measurements inside the liquid and vapor regions. In addition, 10 RTD elements ($\pm$ 0.1 ^{o}C) are cemented onto the outside wall of the test cell to monitor wall temperature profiles. Implementation of the ZBO strategy requires removal of liquid from the bottom of the tank. This is accomplished via twelve ports located in circumferential symmetry around the jet orifice (1/4" ID). The withdrawn fluid collects in a common manifold and passes through a micro-pump into a heat exchanger loop (see Fig. 5). The heat exchange fluid is distilled water and is pumped through the heat exchanger by a Haake heating / refrigeration circulating bath. The Haake circulator bath controls the temperature of the water so that the temperature of the test fluid, HFE-7000, measured downstream of the pump by an in-line temperature probe, is maintained at some preset value. There is a flow meter downstream of the heat exchanger to monitor the low flow rates encountered during the experiments. After passing through the flow meter, the test fluid reenters the test cell through an orifice aligned with the central axis at the bottom of the tank.

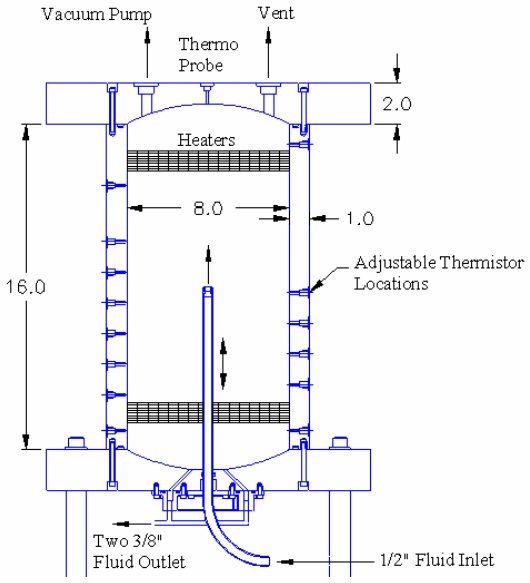

Figure 4. Test Cell Apparatus

The duration of a typical experiment is approximately three hours. Temperature measurements are recorded continuously using a data logger. The ullage pressure is monitored using LabView. HFE-7000 is transparent, environmentally non-hazardous (it can be vented) and has a normal boiling temperature of 34 ^{o}C – making it ideal for studying evaporation/condensation processes at around laboratory temperatures. It is electrically inert, non-flammable, non-corrosive and has good material compatibility. Its only disadvantage is its affinity for dissolved gases.

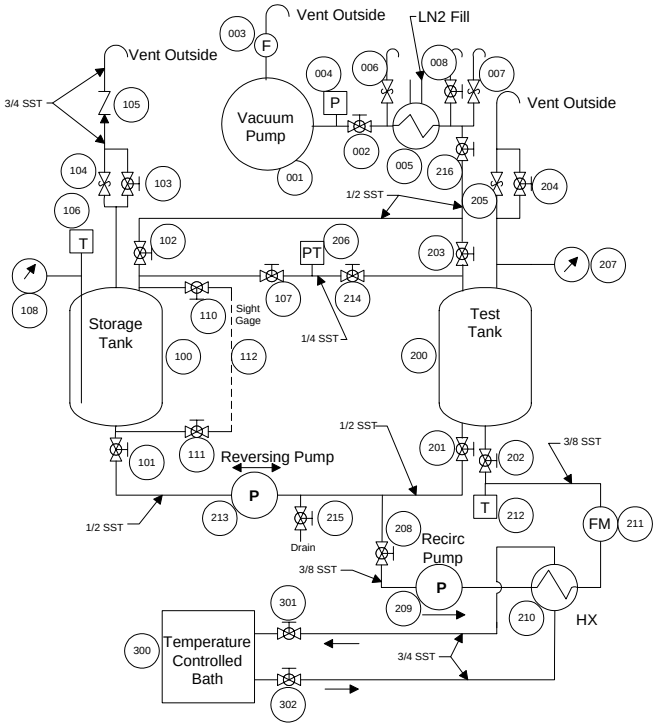

Figure 5. Experimental Set up and Fluid Loop

The gas solubility in HFE-7000 requires degassing of the fluid before an experimental run. Degassing proceeds as follows: Initially all fluid is kept in the storage tank, shown in Fig. 5 and all valves are closed. Temperature and pressure measurements are made inside the storage tank and compared with the empirical pressure/temperature curve provided by 3M. It is assumed that any deviation from the empirically- obtained pure HFE values is due to the dissolved gasses in the fluid. The cold trap is filled with liquid nitrogen and the vacuum pumping system is primed. With valves 002 and 216 open, valve 102 will be gradually opened – reducing the pressure in the storage tank. As the pressure is reduced, bulk boiling occurs. The liberated gasses, along with some vapor, will pass through the cold trap where the vapor is condensed into liquid and stored for future use. The liberated gasses are expelled from the laboratory.

Once the HFE is purified and contained in the storage tank, the vacuum pumping system is used to vacuum purge the test cell to 500 milli-torr. Valves 101 and 201 are opened at a rate slow enough to accommodate and minimize the initial pressure spikes in the evacuated test cell. When the pressures in the two tanks equilibrate, pump 213 is started in the forward direction to transfer the fluid from the storage tank to the test cell. The test cell will be filled by maintaining a no-vent-fill condition largely in the same way that a commercial liquid propane tank is filled. If necessary, mixing via the subcooled liquid jet loop is used to enhance condensation inside the test cell.

A comprehensive set of parametric experimental test runs were undertaken whereupon the heater power, fill ratio, heat distribution, jet speed and jet temperature were varied.

3.2 The Tank Pressurization/Pressure Control Numerical Models

Two preliminary models have already been developed for the storage tank. The first is the Thermodynamic Tank Pressurization (TTP) model. This model assumes homogeneous thermal equilibrium conditions in the ullage, the liquid, and the wall and predicts the rate of pressure rise

in the vapor based on the net heat flow into the tank. The second is the Active-Liquid Lumped-Vapor Tank (ALLVT) model that couples thermodynamic prediction of pressure in the ullage to transport of heat, mass, and momentum in the liquid and conduction in the tank wall. Under the conditions of a continuous constant heat leak into the tank, agreement between the long term predictions of the rate of pressure rise in the tank by the TTP and ALLVT models is essential.

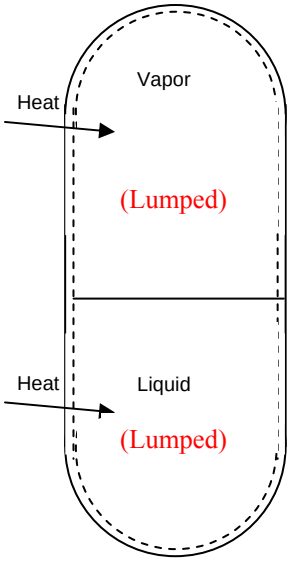

Figure 6. Schematic for The TTP Model.

3.2.1 The Thermodynamic Tank Pressurization Model

A schematic describing the essential features of the TTP model is included in Fig. 6. Several key assumptions are invoked in order to construct this thermodynamic model. The primary assumption is that the liquid and vapor are at the same temperature and pressure under saturation conditions. The secondary assumptions are: (a) the tank wall is in thermal equilibrium with the liquid and the vapor; (b) the liquid is incompressible; (c) all the thermal properties are constant; and (d) the tank is rigid. Based on these assumptions, the first law of thermodynamics for the tank can be written as:

$$\frac{d}{dt}\left(\rho_v e_v V_v + \rho_l e_l V_l + \rho_w e_w V_w\right) = \dot{Q} \tag{1}$$

Here, ρ ,. is the density, V, is the volume, e, is the internal energy, $\dot{Q}$, is the heat leak rate, and the subscripts v, l, and, w, respectively denote the vapor, liquid, and the wall..

Since the tank represents a closed system, mass conservation implies that,

$$\frac{d}{dt}\left(\rho_v V_v\right) + \frac{d}{dt}\left(\rho_l V_l\right) = 0 \tag{2}$$

and volume conservation requires that:

$$V_l = V_T - V_v \tag{3}$$

where, V_T, is the total internal volume of the tank. Substitution of Eq (3) into Equation (2) and integrating the resulting equation from an initial state denoted by subscript , o , provides an expression for the vapor volume in terms of the vapor density:

$$V_v(p_v) = V_0 \frac{\rho_l - \rho_{v,o}}{\rho_l - \rho_v} \tag{4}$$

The energy equation (1) can be expanded to yield:

$$e_v \frac{d\rho_v V_v}{dt} + \rho_v V_v \frac{de_v}{dt} + \rho_l V_l \frac{de_l}{dt} + \rho_l e_l \frac{dV_l}{dt} + \rho_w V_w \frac{de_w}{dt} = \dot{Q} \tag{5}$$

The internal energy is defined with respect to an arbitrary reference state and assuming constant specific heat:

$$e = c\left(T - T_o\right) + e_o \tag{6}$$

Using this definition together with Eq (2), the terms in Eq (5) can be rearranged to give:

$$\left[\rho_v V_v c_v + \rho_l V_l c_l + \rho_w V_w c_w\right]\frac{dT}{dt} + \frac{d\left(\rho_v V_v\right)}{dt}(e_v - e_l) = \dot{Q} \tag{7}$$

For convenience, the latent heat, expressed as:

$$L = \left(e + \frac{p}{\rho}\right)_v - \left(e + \frac{p}{\rho}\right)_l, \tag{8}$$

can be used to rewrite Eq (7) as:

$$\left[\rho_v V_v c_v + \rho_l V_l c_l + \rho_w V_w c_w\right]\frac{dT}{dt} + \frac{d\left(\rho_v V_v\right)}{dt}\left[L - p_v\left(\frac{1}{\rho_v} - \frac{1}{\rho_l}\right)\right] = \dot{Q} \tag{10}$$

Expressing the derivatives in terms of pressure, an evolution equation for the vapor pressure is derived:

$$\frac{dp}{dt}\left\{\left[\rho_v V_v c_v + \rho_l V_l c_l + \rho_w V_w c_w\right]\frac{dT}{dp} + \frac{d\left(\rho_v V_v\right)}{dp}\left[L - p_v\left(\frac{1}{\rho_v} - \frac{1}{\rho_l}\right)\right]\right\} = \dot{Q} \tag{11}$$

There are three important variables in Eq (11). These are the vapor density, the vapor temperature and the vapor volume. Fortunately, they can all be readily expressed in terms of the vapor pressure. Under saturation conditions, the vapor temperature is related to vapor pressure through the Clausius Clapeyron equation:

$$T(p_v) = \left[\frac{1}{T_B} - \frac{R}{L}\ln\left(\frac{p_v}{p_B}\right)\right]^{-1}; \tag{12}$$

From before, the global mass conservation given by Eq (2) can be integrated to yield an expression for the vapor volume:

$$V_v(p_v) = V_0\frac{\rho_l - \rho_{v,o}}{\rho_l - \rho_v(p_v)} \tag{13}$$

And the ideal gas law can be invoked to provide a relationship between vapor density and vapor pressure:

$$\rho_v(p_v) = \frac{p_v}{RT(p_v)}. \tag{14}$$

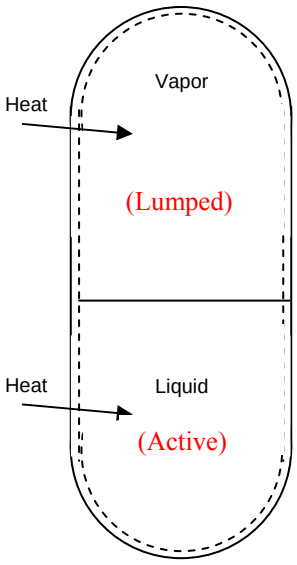

Figure 7. Schematic for The ALLVT Model.

Thus, the pressure evolution equation takes the following reduced and generalized form:

$$F(p_v)\frac{dp_v}{dt} = \dot{Q} \tag{15}$$

Eqs (11) – (14) constitute the TTP model. Provided the net heat flow rate to the tank is known, Eq (14) can be readily marched in time to predict the pressure change in the tank.

3.2.2 The Active-Liquid Lumped-Vapor Tank Model

The ALLVT model will be presented here in the context of a cryogenic storage tank in 1g where the ullage resides above the liquid at equilibrium as shown in Fig 7. The tank is subject to a non-uniform heat leak Q that may also be a function of time. This heat leak is the main cause of pressurization in the tank. Following a typical ZBO concept, the tank pressure is controlled (reduced and maintained) using a liquid jet that enters the tank along its central axis at a specified uniform sub-cooled temperature level. In the ALLVT model the transport equations in the liquid are coupled to the

lumped thermodynamic equations in the ullage. Thus, the liquid is treated as an incompressible Newtonian fluid with spatially nonuniform velocity and temperature fields while the vapor is assumed to behave as an inviscid, compressible ideal gas with spatially uniform pressure, temperature and density.

The Liquid Equations:

The flow field in the liquid is described using the continuity equation and momentum balance as:

$$\nabla \cdot \vec{V} = 0 \tag{16}$$

$$\rho\left(\frac{\partial \vec{V}}{\partial t} + \vec{V} \cdot \nabla \vec{V}\right) = -\nabla p + \nabla \cdot \tau - \rho \vec{g} \beta \theta \tag{17}$$

The temperature field in the liquid is simply described by the conservation of energy equation as:

$$\rho c\left(\frac{\partial \theta}{\partial t} + \vec{V} \cdot \nabla \theta\right) = -\nabla \cdot (k \nabla \theta) + \nabla \tau : \vec{V} - \rho c \frac{dT_s}{dt} \tag{19}$$

Here the last term on the right hand side is due to the variable decomposition:

$$\theta(\vec{x}, t) = T(\vec{x}, t) - T_s(t) \tag{20}$$

This transformation is performed solely for increasing the ease and efficiency of generating the numerical solutions and implies that if the temperature field, T, achieves a transient but stationary state (due, for example, to continuous but constant heat leakage, Q), the transformed field, θ, approaches steady state conditions. The middle term on the right hand side is a heat source due to viscous dissipation that may have to be considered at high mixing jet velocities.

The momentum and energy equations are coupled due to the buoyancy term in the momentum equation that is a driver for the natural convection flow. Here, the Boussinesq approximation is invoked that retains the leading order density variation with temperature only in the body force (buoyancy) term. Moreover, as a result of the temperature decomposition, the pressure appearing in the momentum equation includes an additional term in the hydrostatic contribution:

$$p = p_{static} - \rho \vec{g} \cdot \vec{r}\left(1 - \beta[T_s(t) - T_s(0)]\right) \tag{18}$$

The Lumped Vapor Equations:

Since the vapor is assumed to be an inviscid compressible ideal gas with spatially uniform temperature, pressure and density, its pressure and temperature can be evaluated as a function of time using a lumped approach based on near equilibrium thermodynamic considerations. This is valid as long as the heat flow into the vapor region and mass flux due to evaporation are relatively small (Panzarella and Kassemi, 2003). Under these conditions, even if there is some fluid flow and spatial temperature distribution in the ullage, pressure variations due to these spatial non-uniformities would be extremely small compared to the thermodynamic pressure. This thermodynamic pressure dictates the saturation temperature which under near-equilibrium conditions, specifies the interfacial temperature, that is an important boundary condition for the liquid region. Even though pressure is spatially uniform it will change over time due net heat or mass transfer into the vapor region. If V_v is the volume of the vapor and J_v is the evaporation mass flux, then the rate at which the total vapor mass changes is given by:

$$\frac{d}{dt}(\rho_v V_v) = M_v \tag{21}$$

where

$$M_v = \iint_I J_v dS \tag{22}$$

Neglecting contributions from kinetic and potential energies, the total energy in the ullage due to the heat and mass transport is given by the following conservation equation:

$$\frac{d}{dt}(\rho_v V_v e_v) = M_v(e_v + \frac{p_v}{\rho_v}) - p_v \frac{dV_v}{dt} + \dot{Q}_{Iv} + \dot{Q}_{wv} \tag{23}$$

Here, the first two terms on the right hand side are respectively contributions to the ullage energy due to evaporation (mass transfer). The 3rd term is due to P-V work and the last two terms are respectively contributions to the ullage energy due to heat flow into the vapor from the vapor side of the liquid-vapor interface and from the tank wall.

The energy required by the evaporation process is provided by the difference between the integrated heat fluxes across the interface on the vapor and liquid sides, that is:

$$LM_v = \dot{Q}_{Il} - \dot{Q}_{Iv} \tag{24}$$

Where the liquid side integrated flux, Q_{Il}, can be evaluated from the solution of the temperature field on the liquid side as:

$$\dot{Q}_{Il} = \iint_I -k_l \nabla T\big|_l \cdot n_I dS \tag{25}$$

Using Eq (25) with together with Eq (21) for the rate of change of vapor mass, Eqs (2) and (3) for mass and volume conservation and Eq (6) for internal energy, Eq (23) can be cast into the following evolution equation for ullage pressure:

$$\frac{dp_v}{dt} = F(p_v) \cdot [\dot{Q}_{IW} + \dot{Q}_{Il}] \tag{26}$$

Where F(p) is given by

$$F(p_v) = \left[(\rho_v c_v V_v) \frac{\partial T}{\partial p} + \frac{\partial(\rho_v V_v)}{\partial p} \left\{ L - p\left(\frac{1}{\rho_v} - \frac{1}{\rho_l} \right) \right\} \right] \tag{27}$$

Again, the expression for, F, only depends on the ullage pressure, because the vapor temperature, volume, and density can all be defined in terms of pressure using respectively, the Clausius Clapeyron relationship [Eq (12)] , the global mass balance [Eq (13)], and the ideal gas law [Eq (14)].

The Interfacial Balance Equations:

Conservation of mass requires the interfacial mass flux, J_l, due to evaporation or condensation to be equal to the rate at which the liquid is flowing towards the interface, that is

$$J_v = J_l = \rho_l(\vec{V}_l - \vec{V}_I) \cdot n_I \tag{28}$$

Here, n_I , is the unit normal vector pointing towards the vapor region and, $\vec{V}_I$, is the interfacial velocity. Based on the convention used, J_v , is positive for evaporation and negative for condensation. If, $J_v = 0$, this equation reduces to the kinematic condition which states that the fluid must be moving with the same velocity as the interface. Moreover, the no-slip condition requires the tangential component of the liquid velocity to be equal to the tangential component of the interface velocity:

$$(\vec{V}_l - \vec{V}_I) \cdot \hat{t} = 0 \tag{29}$$

Where, $\hat{t}$, is the unit tangent vector at the interface.

A normal stress balance across the interface, neglecting viscous stresses in the vapor and the momentum jump due to evaporation reduces to:

$$p_v - p_l + 2\mu_l S_l \cdot n_I \cdot n_I = 2H\sigma \tag{30}$$

Here, σ, is the interfacial surface tension, H, is the mean curvature of the interface and, S_l , is the rate-of-strain tensor for the liquid defined as:

$$S_l = \frac{1}{2}[\nabla \vec{V}_l + (\nabla \vec{V}_l)^T] \tag{31}$$

Similarly, the tangential stress condition can be written as:

$$S_l \cdot n_I \cdot \hat{t} = \nabla \sigma \cdot \hat{t} \tag{32}$$

Since surface tension is assumed to be constant for this analysis (near-equilibrium, pure vapor, $T_I = T_s = constant$), the shear–stress condition reduces to

$$S_l \cdot n_I \cdot \hat{t} = 0$$

Here, the viscous stress on the vapor side is justifiably neglected because the dynamic viscosity of the vapor is much smaller than that of the liquid.

At the interface the temperature of the liquid is always equal to the interfacial temperature. That is:

$$T_l = T_I \tag{33}$$

If the liquid at the interface were in complete thermodynamic equilibrium with the adjacent vapor, then the interfacial temperature, T_I, would be equal to the saturation temperature, T_s. Of course, strictly speaking, the interface is not in complete equilibrium when there is evaporation or condensation and the interfacial temperature must be different from the saturation temperature. However, the difference between the interfacial and saturation temperatures is still quite small for near-equilibrium conditions, where the phase change proceeds at a relatively slow pace. Therefore, under near equilibrium condition we can still safely assume that:

$$T_I = T_s \tag{34}$$

For rapid and intense phase change where departure from equilibrium is drastic, the difference between the interfacial and saturation temperatures is described by a constitutive relationship derived from kinetic theory (Shrage, 1953) as will be discussed in Section 4.

The formulation of the ALLVT model is now complete. Note that there is a strong coupling between the energy equations in the vapor and liquid regions through two terms. First the interfacial temperature that is also a thermal boundary condition for the energy equation on the liquid side is implicitly computed from the evolution of pressure on the ullage side described by Eqs (26) and (27) and the Clausius Clapeyron relationship (12). Second, the integrated interfacial liquid heat flux that is a source term in the ullage pressure evolution equation (26) is determined by integrating the normal interfacial temperature gradients computed from the solution of the energy equation on the liquid side according to Eq (25).

Finally, there are also cross-coupling between the energy and the Navier-Stokes equations on the liquid side due to the convective terms in the energy equation and the buoyancy term in the momentum equation. As a result of these nonlinear couplings, Eqs (16)-(20) for the velocity and temperature field on the liquid side and Eqs (26) and (27) for evolution of pressure on the ullage side must be simultaneously marched in time while satisfying the complete set of interfacial balances and boundary conditions for a complete transient simulation of the problem.

3.3 Proof of Concept: Preliminary Pressurization and ZBO Pressure Control Simulations

In this section we present results extracted from a series of parametric numerical simulations generated by the TTP and ALLVT models. We have basically three aims in mind:

1. Perform partial validation of the existing tank models against 1g pressurization data provided by the preliminary ground-based simulant fluid (HFE7000) experiment.

2. Underscore the main functional difference between the TTP (thermodynamic) and ALLVT (transport) models.
3. Demonstrate conceptually how the ZBO heat removal and jet-mixing mechanisms can be used to control the pressure in a spherical hydrogen storage tank on earth and in microgravity.

Detailed discussion of the mathematical models and the numerical results generated can be found in Panzarella and Kassemi, (2003, 2004, 2005) and Barsi and Kassemi (2005, 2006). To save space, in all the time sequences of flow and temperature fields presented in the remainder of this section, symmetry is exploited by showing the temperature contours on the left half and the streamline contours or velocity vectors on the right half of the tank diagrams.

3.3.1 Preliminary Validation of the Pressurization Model

In order to validate the tank models and to focus attention on the functional differences between the Thermodynamic (TTP) and the Transport (ALLVT) models, they were benchmarked against pressurization data obtained in our preliminary ground-based experimental set up that was described in detail in section 3.1. The case considered is that of the 8''x18'' transparent acrylic tank, as shown in Fig. 4, containing the transparent simulant fluid, HFE7000, at a fill ratio of 25%.

At time zero, only the strip heater in the liquid region is activated and a total heat of 1W distributed uniformly in the strip is imposed on the inner tank wall. The near stationary natural convection flow and the resulting thermal stratification of the liquid in the tank at time = 7200s as predicted by the ALLVT model are shown in Fig. 8. At, Ra = 10^{11}, the natural convection flow is quite strong and is driven by extremely thin thermal and velocity boundary layers at the wall. After about 5 minutes, consideable thermal stratification occurs in the liquid and continues until a near stationary state is approached at around 2 hrs. The flow and temperature fields, however, are still strictly speaking transient and exhibit an oscillatory nature seemingly indicative of a flow regime transitioning between laminar and turbulent natural convection.

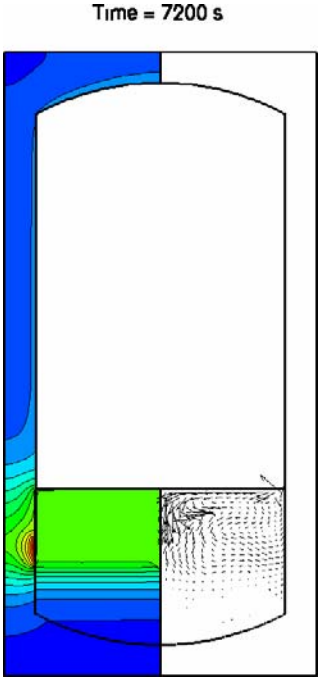

Figure 8. Temperature and Flow Fields in the Pressurized Experimental Tank in 1G.

Evolution of tank pressure during the experiment is shown in Fig. 9 where the predictions of four different models are compared to the measured data. The experimental pressure evolution curve denoted by dots with error bars indicates an initial delay of about 1.5 minutes followed by a transient nonlinear pressure rise of approximately 10 minutes that eventually starts to asymptote to a linear slope (a constant pressure rise rate) at about 1 hour into the experiment.

Comparisons between the different tank model predictions and the experimental pressure evolution curve indicate that both the transport ALLVT model and the thermodynamic TTP model grossly misrepresent the actual pressure rise when the thermal inertia of the wall is not considered. When the effects of thermal inertia of the wall are included in the models, the comparisons become quite favorable. The TTP model, with wall thermal inertia included, predicts a constant pressure rise rate that agrees well with the slope of the experimental asymptote. However,

the thermodynamic model still under predicts the magnitude of the pressure rise. The conjugated ALLVT model that includes both wall thermal inertia and wall conduction along with transport of heat, mass, and momentum in the liquid follows the experimental pressure curve in both trend and magnitude with great fidelity. The expanded scale inset of Fig. 9 clearly shows that the thermodynamic TTP model is incapable of predicting the initial experimental pressure lag and the nonlinear pressure evolution during the transient interval. However, the conjugated ALLVT model predicts both the lag and the nonlinear transient pressure behavior with impressive accuracy.

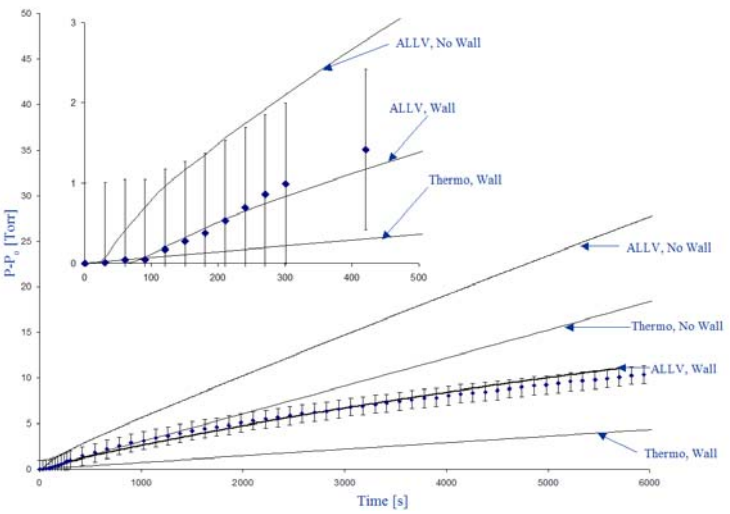

Figure 9. Comparison between the 1G Pressure Rise Predictions of Several Tank Models.

Finally, there seems to be a small but widening discrepancy between the experimental data and the pressure predictions of the conjugated ALLVT model at larger times. We attribute this widening discrepancy to an increase in unaccounted heat loss from the tank as time goes on. Three important conclusions can be derived from this preliminary but important benchmarking case study:

1. The long duration pressure rise rate should be the primary standard for comparison between different models and experiment. Lack of agreement is symptomatic of inaccurate and inadequate knowledge of energy distributions within the tank system.
2. Thermodynamic models cannot predict the initial (or for that matter any) transient behavior. As a result they will have difficulty in predicting the magnitude of the tank pressure rise.
3. Proper and adequate book keeping of energy distributions within the tank system and how it changes with time is a prerequisite for any tank model and essential to the success of any pressurization/pressure control experiment.

3.3.2 Ground-Based Simulations of Pressurization and Pressure Control

The case studies presented in this section are concerned with pressurization and pressure control of storage tanks in 1g. Here, the goal is to:

1. Further delineate the functional differences between the thermodynamic and transport models
2. Show the effect of different wall heat leak distributions
3. Indicate the conceptual feasibility of ZBO pressure control

In the simulations presented here, the pressure rise is caused by a constant heat leak from the sidewall into the liquid region of a 10 cm diameter spherical cryogenic tank half filled with liquid hydrogen as shown in Fig. 10. Initially, the liquid is motionless. Heat is added through the tank walls at a rate of 0.6283 mW as if distributed by means of a 2 cm strip heater placed up against the tank wall in the liquid region at height of 2 cm from the bottom of the tank. The

remainder of the tank wall is assumed to be insulated. Two basic case studies are presented here. In the first case, there is no jet mixing or cooling of the fluid. In the second case, a jet with an initial diameter of 1 cm, an average velocity of 1 cm/sec, and an inlet temperature of 20 K is used to mix and cool the liquid. Mass is conserved by the liquid leaving from an outlet at the bottom of the tank at the same rate at which it is supplied by the incoming jet flow. In this set up, it is inherently assumed that heat is continuously removed from the tank, since the jet inlet temperature is always equal to the initial (subcooled) liquid temperature of 20 K but the liquid, which leaves the tank, is at a slightly higher temperature. The simulations represent ground-based applications with the acceleration of gravity set to its normal value of 981 cm/sec^2.

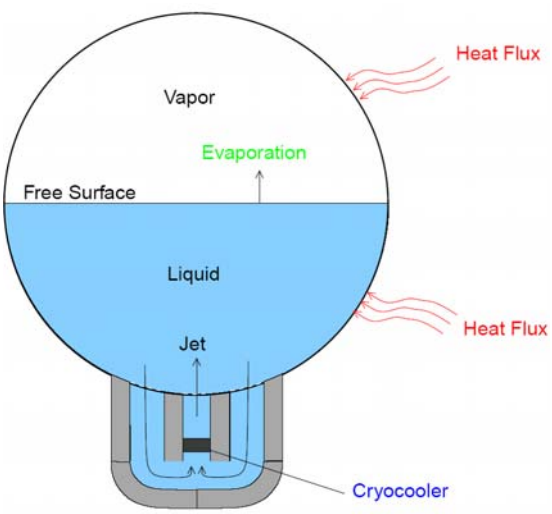

Figure 10. Schematic of the Spherical Storage Tank

The temperature and flow (streamlines) fields of the no-jet case are examined first as shown in Fig. 11T. At t=2.5 sec, a thermal boundary layer is just developing near the heated section of the tank, but it has not yet reached the interface. During this time, the pressure is not increasing since there is no significant heat transfer across the interface. The streamlines indicate that there is a counterclockwise circulation starting up near the heater due to natural convection. There is a slight spreading out of the temperature contours above the heater due to this convection. At t=50 sec, the thermal boundary layer has finally reached the liquid-vapor interface, and both the pressure in the vapor and the temperature at the interface begin to rise as depicted in Figs. 12T-a and 12T-b. After 2 hours, the spatial temperature distribution in the liquid reaches a quasi-steady or stationary state even though as shown in Fig. 12T, the temperature at the interface, the vapor pressure and the overall tank temperature levels all keep increasing because of the steady heat flux (leakage) at the wall. The final maximum convective velocity in the liquid is about 0.0932 cm/sec and is located on the interface above the heater, where the spacing between the streamlines is a minimum.

Fig. 12T-a displays a comparison between the pressure evolution predicted by the TTP and ALLVT models. It is clearly shown that when there is no jet, the vapor pressure keeps on rising at a rate that will eventually agree with a purely thermodynamic prediction. The results of the two other case studies pertaining to the uniform heating of the entire tank and uniform heating of only the vapor region are also included in Fig. 12T. Note that the TTP model cannot predict the effect of wall heat flux distribution on the magnitude of the pressure rise and therefore severely under-predicts the pressure rise in the uniform and vapor heating cases.

The temperature and flow (streamlines) fields for the jet-mixing case as predicted by the ALLVT model are shown in Fig. 11B. Here, at t=2.5 sec, the jet, which enters at an inlet in the bottom of the tank, has ascended halfway to the interface, and the thermal boundary layer is still very localized near the heater. At t=60 sec, the jet has already reached the interface, spread across it, and eventually runs up against the tank wall. Essentially, the cold jet flow isolates the hot region near the wall from the liquid-vapor interface. As time goes on, the jet flow turns around at the sidewall and continues downwards to the bottom of the tank where it exits through

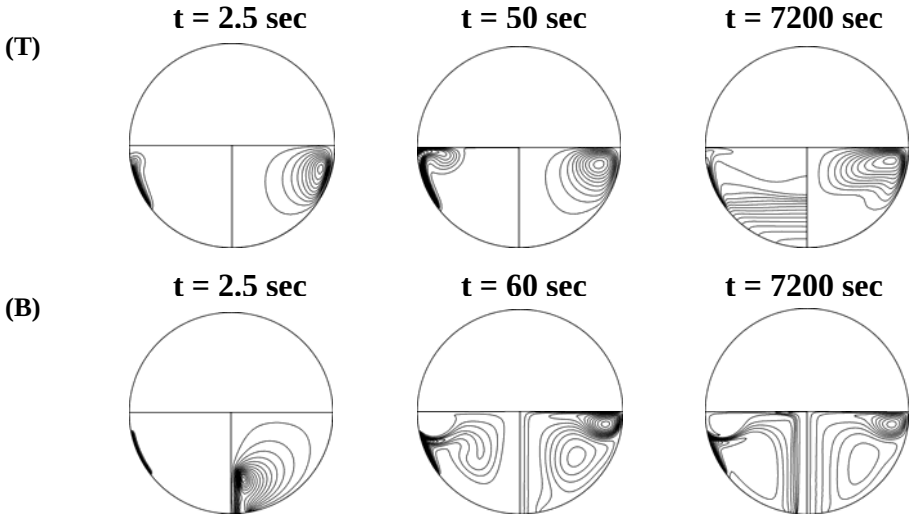

Figure 11. (T) Temperature contours and streamlines without a jet. The minimum and maximum temperature at t = 2.5 sec is 20 K and 20.002 K, respectively (10 contours). The minimum and maximum temperature at t = 50 sec is 20 K and 20.0021 K, respectively (20 contours). The minimum and maximum temperature at t = 7200 sec is 20.018 K and 20.024 K, respectively (20 contours). The final maximum convective velocity is 0.0932 cm/sec. (B) Temperature contours and streamlines when there is a jet. The minimum and maximum temperature at t = 2.5 sec is 20 K and 20.0006 K, respectively (10 contours). The minimum and maximum temperature at t = 60 sec is 20 K and 20.0028 K, respectively (20 contours). The minimum and maximum temperature at t = 7200 sec is 20 K and 20.0043 K, respectively (20 contours).

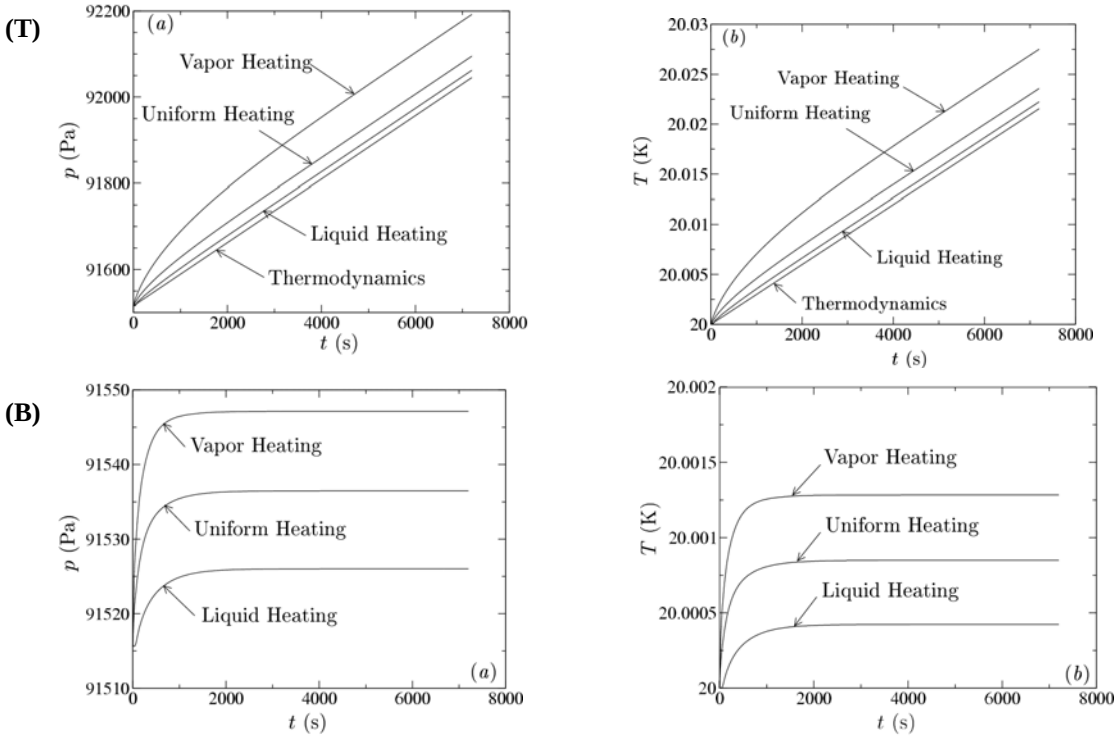

Figure 12. Pressure (a) and temperature (b) rise when there is no jet (T) and when there is a jet (B). The total heat power input is the same in all cases and is equal to 0.6283185 mW.

Figure 13. Final isotherms and streamlines after 150 days for jet speeds of (a) $\bar{w}_j = 0.005$ cm/s, (b) $\bar{w}_j = 0.05$ cm/s and (c) $\bar{w}_j = 0.5$ cm/s.

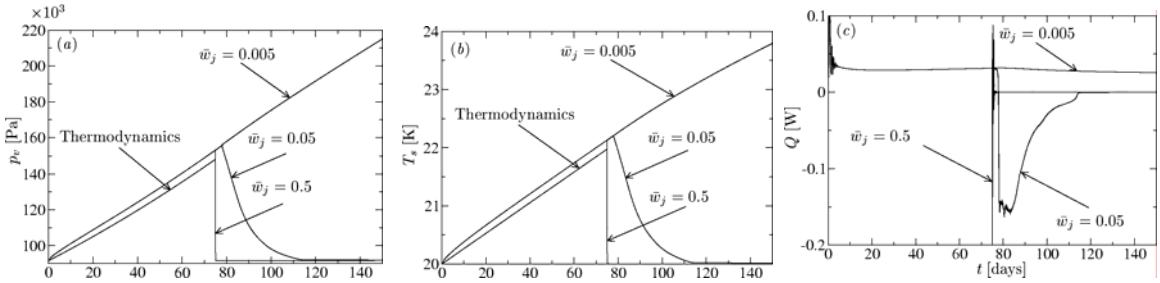

Figure 14. The long-term (a) pressure, (b) saturation temperature and (c) total heat flow both before and after the subcooled jet has been turned on.

the outlet. In this manner, the counter-clockwise recirculation of heated liquid is trapped near the sidewall instead of rising towards the liquid-vapor interface (as it did in the no-jet case where it caused significant vaporization).

The time histories of the vapor pressure and interfacial temperature for the jet-mixing case are respectively depicted in Figs. 12B-a and 12B-b. It's interesting to see that the pressure has initially a small rise but as soon as the jet flow reaches the liquid-vapor interface it isolates it from the warm fluid near the sidewall. As a result both the vapor pressure and the interfacial temperature level off at values slightly above their initial values. This happens because the cooling/isolating effect of the jet eventually balances the effects of the imposed wall heat flux and ZBO conditions are established and prevail at a true stationary state after about 2 hours.

Finally, it should be again emphasized that the TTP model is not capable of accurately computing the cooling time constants because they are so dependent on transient evolution of transport and spatial distributions of flow and temperature in the liquid region.

3.3.3 Simulation of Tank Pressurization and Pressure Control in Microgravity

Preliminary simulations of ZBO pressure control in a microgravity environment as generated by the ALLVT model are examined next for a large 3 m diameter tank. The tank is 95% full of liquid hydrogen and allowed to self-pressurize for 75 days before turning on the jet. The tank temperature and flow fields produced by three different jet speeds are included in Fig. 13 and the resulting pressure rises are shown in Fig. 14.

For the lowest jet speed of $\bar{w}_j = 0.005$ cm/s, pressure and temperature continue to rise at nearly the same rate as the no jet case since the forced flow is unable to penetrate far enough into the liquid region to reach the vapor. The temperature and flow fields surrounding the vapor region are nearly the same as those before the jet is turned on, as shown in Fig. 13a. Obviously, the

thermal stratification is hardly disrupted since the cooling effect of the jet is limited to the bottom of the tank and the net heat flow into the vapor is only slightly decreased as shown in Fig. 14c. This is insufficient to cause any noticeable change in the pressure rise. Therefore, at its lowest speed, the jet cannot effectively control the pressure over the time span considered here.

When the jet speed is increased by an order of magnitude to $\bar{w}_j = 0.05$ cm/s, it becomes more effective. Fig. 14 shows that it still takes about 2.8 days before there is any significant cooling effect since it takes that long for the jet to reach the interface. This is considerably slower than the timescale of about one hour that is predicted if a simple calculation based on the jet inlet velocity and the distance from the bottom of the tank to the interface is used. This discrepancy is due primarily to the counterflow vortex generated by natural convection and the effect of buoyancy that tends to suppress the penetration of the cold jet into the warmer regions of the tank. Fig. 14 shows that once cooling begins, it takes about 45 days for the jet to bring the saturation temperature and vapor pressure back down to their initial values. This time, the cooler jet fluid penetrates into the liquid region and encapsulates the entire vapor region as indicated by the final isotherms in Fig. 13b. But, there is still some thermal stratification in the remainder of the liquid.

The cooling effect is further enhanced when the jet speed is increased by another order of magnitude to $\bar{w}_j = 0.5$ cm/s. In this case, the net heat flow into the vapor drops after only 6 min as shown in Fig. 14. This is in better agreement with the timescale derived from a simple calculation based solely on distance and jet speed because of the overwhelming jet speed.. Once cooling begins, it only takes about 5 hours for the jet to bring the saturation (also interface) temperature and vapor pressure back down to their initial values. The final temperature profile of Fig. 13c also shows that the recirculation of the cooler fluid due to the jet flow now encompasses over half of the liquid volume, and the circulation cell due to natural convection is much weaker and only limited to a small region near the bottom of the tank. As a result, thermal stratification in the liquid is almost entirely disrupted by the stronger jet in this case.

In summary, the preliminary simulations presented in this section underscore the fact that a simple thermodynamic analysis is very informative and probably adequate for design of a passive storage tank. But, if active ZBO pressure control is desired the interaction among the intricate transport phenomena become quite important and affects tank pressurization and pressure control time constants profoundly. These effects can only be captured if the transient transport in the liquid is properly included as in the ALLVT model.

4.0 Proposed Work

It is clear that reliable, affordable, and efficient ventless cryogenic tanks for NASA's future space expeditions cannot be built by brute force – that is through a design-build-fly-redesign-rebuild-refly-…-… trial-and-error engineering approach. The aerospace engineering community feels that there are no alternatives to a large-scale in-space storage tank prototype technology validation test. However, past attempts to move directly to TRL 6-7 experiments such as in the case of COLD-SAT (Schuster et al, 1990) have proved too costly and ultimately abandoned.

In any case, before such costly endeavors become warranted, a series of small-scale microgravity experiments are needed to test and compare different vent-less design concepts including the ZBO strategy.

In this context, a small-scale microgravity experiment that examines the feasibility and details of the ZBO strategy for microgravity applications is imperative. For example, have in mind, that currently there are large knowledge gaps and serious engineering impediments in the

path of readily developing and implementing the ZBO pressure control technology for space storage tanks:

1. The impacts of various interacting transport phenomena are still not clear and need scientific clarification.
2. Microgravity data for deriving relevant empirically-based engineering correlations are scarce and insufficient.
3. Comprehensive, customized and fully validated numerical models to aid the scale-up design and provide a virtual platform for assessing the performance of ground-tested-only storage tank design for microgravity and variable gravity space applications are not available.

In this light, the major goals of the present proposed research can be restated as follows:

- Build a science base for the future space storage tank engineering efforts by elucidating the roles of the various interacting transport and phase change phenomena that impact tank pressurization and pressure control in variable gravity through systematic 1g and microgravity scientific investigation.
- Develop a small-scale simulant-fluid experiment for both preliminary ground-based testing and subsequent ISS flight experiments in order to obtain valuable microgravity empirical data for a ZBO tank design and archival science data for model validation.
- Develop, validate, and verify variable gravity two-phase CFD models for ventless ZBO storage tank pressure control that can be used to aid scale-up tank design.
- Show the feasibility of ZBO pressure control scheme for microgravity and variable gravity applications.

Step-wise achievement of these objectives will set the stage and provide the necessary tools and correlations for a ground-based scale-up design of future ZBO storage tanks in accordance with existing and upcoming NASA mission requirements. It is also imperative before any costly large-scale real-fluid technology validation space experiment can be properly designed and/or justifiably undertaken.

4.1 The Combined Numerical-Experimental Approach

To accomplish the goals of the proposed work, a coordinated hand-in-hand experimental-theoretical-computational research project is proposed. The theoretical/computational effort will consist of comprehensive scaling analyses, development of in-depth two-phase CFD models for tank pressurization and ZBO pressure control, and a series of targeted parametric numerical simulations and sensitivity analyses. The experimental effort will consist of prototype development for the initial 1g and the future ISS microgravity experiments using a transparent simulant fluid contained in a transparent tank test cell. The experiments will involve direct ullage pressure measurements and non-intrusive visualization of flow and thermal fields in the liquid. The experiments will also provide the needed data for design and optimization of all of the important elements of a variable gravity ZBO pressure control strategy.

In what follows, first, the important scientific and engineering pressurization and pressure control issues that will be addressed by the proposed combined experimental-computational research activity will be covered in section 4.2. Next, the two main components of the proposed research, namely, the experimental set-up and the two-phase CFD tank models will be discussed in detail in sections 4.3 and 4.4, respectively. Then, the details of the proposed ground-based and microgravity ISS experiments will be presented in sections 4.5 and 4.6. Finally, since both the proposed ground-based and microgravity experiments are quite broad and comprehensive a

project success criteria will be included in section 5.0 that will rank the need and priority of the different elements of this research effort in order to achieve *Minimum Success*, *Substantial Success*, and *Complete Success* for the investigation. The elements that will be considered and ranked are partitioned into three categories; individual experimental studies, experimental capabilities; and the microgravity experimental test matrix.

4.2 Important Scientific and Engineering Issues to Be Addressed

The following important scientific and engineering design issues will be addressed through hand-in-hand modeling and simulation and 1g and microgravity experiments.

4.2.1 Scientific Elucidation of Important Variable-Gravity Transport Phenomena

Parametric numerical simulations will be used in conjunction with the simulant fluid pressurization and pressure control experiments to isolate the effects of the various interacting transport and phase change processes in 1g and microgravity. A number of important phenomenological issues that will be examined through both ground-based and microgravity investigation are as follows:

1. The dynamic interaction between the intermittent forced jet flow and the natural/thermocapillary convection in 1g and microgravity.
2. The effect of the combined flow on the interfacial mass transfer.
3. Determination of the relevant transport time constants for pressurization, destratification and pressure reduction in both the 1g and microgravity environments.
4. The existence and extent of thermocapillary convection in 1g and microgravity due to wall contact or due to presence of the non-condensable gas in the vapor.
5. The effect of a non-condensable gas in the vapor region on the evaporation/condensation process.
6. The parametric range that natural convection and jet turbulences become an important factor affecting interfacial transport and tank pressurization in 1g.
7. The impact of boil-off due to sudden heterogeneous or homogeneous nucleation and bubble growth.
8. The dynamic interaction among an intermittent forced jet flow, a weakened natural convection and a pronounced thermocapillary convection in microgravity.
9. The effect of phase distribution (vapor location) on tank pressurization and pressure control.
10. The dynamic impact of g-jitter and impulse acceleration (frequency, magnitude, and direction) on vapor location and tank pressurization.

A great deal of attention will be devoted to items 1-5, because of their fundamental value not only to the present problem but to a multitude of ground-based and microgravity multiphase transport problems in general. Theoretical aspects of these issues are further discussed in the section 4.4.

4.2.2 Engineering Implementation and Optimization of ZBO Pressure Control

Parametric numerical simulations, sensitivity analyses, and 1g and microgravity simulant fluid experiments will be performed to study the impact of important system variables on the ZBO pressure control and to optimize the design. These include:

1. Heat removal parameters (location, power, cold surface configuration).
2. Jet flow parameters (location, flow rate, intermittency).

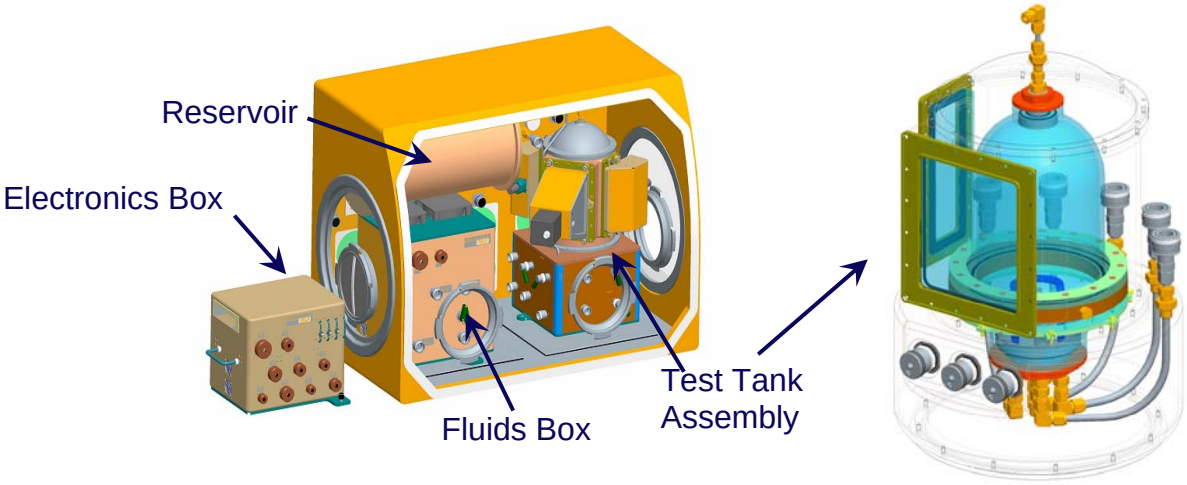

Figure 15. Proposed Glovebox Experimental Set up and Test Cell

3. Wall heat flux magnitude and distributions (vapor, liquid, vapor and liquid regions)
4. Tank fill levels.

Furthermore, numerical case studies will also be performed to optimize ZBO pressure reduction times based on the least power usage for different gravity environments and cryogenic fluids.

4.3 The Experimental Setup

The experimental apparatus and the diagnostic rig consist of eight main components that will be briefly described below. The reader is referred to sections (4.6.2) and (4.6.3) for the descriptions of the different tests.

4.3.1 Test Cell

The schematic of a proposed test cell is shown in Fig. 15. It consists of a tank with a diameter to length aspect ratio of 1:2 with hemispherical end caps. The internal tank volume is at least 80 in^3. The test cell material will be chosen as an optimized compromise among two important requirements:

1. Withstand the tank Maximum Operating Pressure (MOP). The MOP shall be 40 psia.
2. Provide optical quality transparency for ullage bubble positioning determination, field view velocimetry (PIV), and thermal imaging (LCT).

It is anticipated that the tank shall be aligned with the residual gravity vector such that the ullage will stay within the half of the test cell away from the jet.

4.3.2 Test Fluid

The test fluid will be a transparent model fluid. The candidate test fluid is HFE-7000 (3M). This fluid was chosen due to its low normal boiling point, its nominally nontoxic and environmentally friendly properties and its relatively steep saturation curve. It needs to be approved by NASA's stringent ISS safety review. The test fluid is to be delivered and maintained in the test cell and the associated fluid support loops at 99.5% purity or better. All the constituent species in the test fluid and ullage will be accurately determined pre-mission. The limit of tolerable particulate level is set by the PIV particles and will be chosen to be sufficiently small to prevent bubble nucleation. The limit of dissolved gas in the test liquid has to be below 10^{-3} mole/mole. Fill levels will be at 50%, 75%, and 95% to +/- 3% but known to within +/- 1%.

4.3.3 Test Cell Heating

There are stringent requirements on total heat flow and heat flux for the pressurization tests. The heaters are rated between 0.125W - 0.5W per heater (0.25W - 1W of total heat entering the system). The applied heat flux is to be less than 100 $W/m^{2.}$ The net thermal loss from the system (including drift from the set point) must be less than 100 mW but must be known to within +/-5mW. The system is defined as the total volume bounded by the exterior test cell wall. The heater power will be recorded at a rate of 1/60 Hz. The heaters' placement/attachment within the experiment must satisfy the following considerations:

1. If the heaters are located interior to the tank, there has to be a smooth transition between heater surface and tank wall surface as to minimize creation of pinning points for the ullage.
2. To maximize the field of view (FOV), in the current design, the heaters will be axially located where the hemispherical caps mate with the test cell body. For the heater closest to the jet, placement will be biased towards the end cap to allow visualization of the nozzle exit.

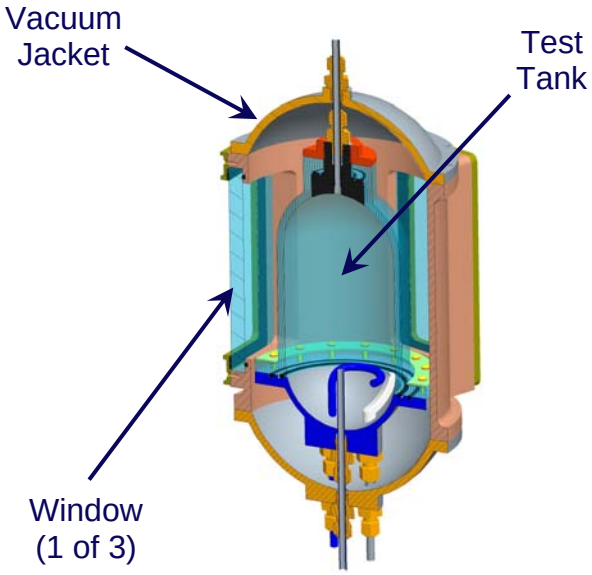

Figure 16. Microgravity Test Cell Showing The Jet Flow Nozzle, The Cold Finger, and The Vacuum Isolation Jacket

4.3.4 Liquid Mixing Jet Operation

During the destratification and pressure control studies, liquid mixing will be accomplished by drawing the working fluid from the test cell, through the flow loop, and pumping it back into the tank via a jet flow nozzle as shown in Fig 16. The nozzle has a circular ID between 7%-10% of the tank ID and will be aligned along the longitudinal axis of the tank. Nominal wall thickness is acceptable and the nozzle will be made out of aluminum to minimize the axial temperature drop along the its body.

It is planned to keep the outlet of the jet nozzle projecting one half diameter (equal with the hemisphere's end) into the test cell. In this fashion, the jet flow and spread angle will be completely in the field of view (FOV) for flow visualization and PIV velocimetry.

Several different jet flow rates will be used during the test runs as described in Section 4.11 in order to span both laminar and turbulent regimes. The jet speeds listed in the test matrix correspond to the average jet speed over the nozzle cross-section and will be within +/-2 cm/s of the set point. The flow profile at the nozzle exit should be parabolic. The jet flow rate will be recorded at a rate of 1/60 Hz during jet operation. The ability of the jet to counter the effects of thermal stratification and natural convection driven by residual gravity will be quantified. The temperature of the jet will be controlled as described in Section 4.3.5.

During most of the test runs, the jet flow rate will be kept constant. However, a set of intermittent jet flow studies are also planned. The flow rate will be controlled as described in the test matrix (Section 4.6.5). These test runs are undertaken in order to mimic the actual future scaled-up cryogenic storage tank operation in space where the pump is cycled on and off to save power consumption and also minimize the undesirable heat generated by the pump that may end up leaking into the tank.

The position of the ullage in microgravity is unknown. In order to prevent withdrawal of vapor from the tank into the fluid loop, a simple liquid acquisition device (LAD) will be designed and implemented at test cell outlet as indicated in Fig. 17. During the mixing-only cases, the jet temperature must be within 0.25 K of the tank outlet temperature within the first L/U seconds of mixing operation and remain within 0.25 K. L is the length of the nozzle interior to the tank and U is the average jet speed.

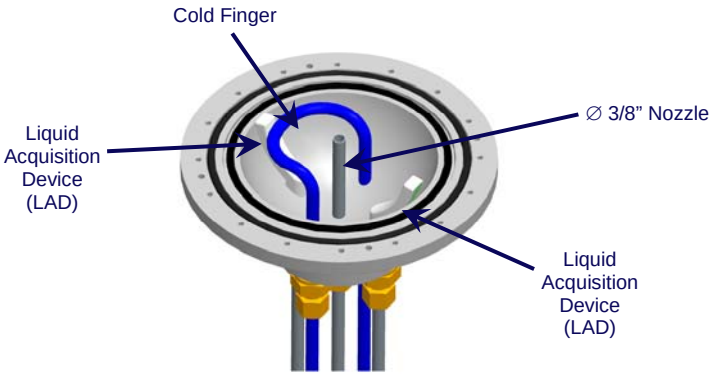

Figure 17. Schematic Displaying The Jet Flow Nozzle, The Cold Finger, and The LADs.

4.3.5 Heat Removal

Three independent mechanisms are proposed for heat removal from the tank during the pressure control studies. These are sub-cooled jet cooling, cold finger cooling, and uniform wall cooling.

4.3.5.1 Sub-Cooled Jet Cooling

During the jet cooling test runs, heat removal from the tank will be accomplished via the mixing jet. That is, when the liquid is pumped out of the tank, it will pass through a heat exchanger connected to the fluid loop. The temperature range of the jet will be T_o *+/- 2 C* with a resolution of 0.1 C where T_o is the initial temperature of the fluid in the tank during the first experimental run as established on orbit. Several jet cooling case studies are planned. In the first set of cases, pressure in the tank will be controlled by keeping the temperature of the jet at a prescribed subcooled set point equal to the initial tank fluid temperature. In these cases, the flow rate of the jet is varied. In the second set of cases the jet will have a fixed flow rate and the temperature of the liquid entering the tank will vary. In both cases the temperature of the nozzle's outlet must be within +/- 0.25 deg C of the desired outlet temperature within L/U seconds after the nozzle has been activated where L is the length of the nozzle interior to the test cell and U is the average jet speed.

4.3.5.2 Cold Finger Cooling

The efficacy of using a cold finger with or without liquid mixing to control tank pressure is also examined. Unlike the jet cooling cases, where cooling and mixing are accomplished simultaneously via the liquid jet loop, in the cold finger test runs, heat removal will be accomplished by a cold finger that is totally independent of the mixing provided by the liquid jet loop. The cold finger will be located entirely in the fluid, as shown in Fig. 17, and consists of a material with a high thermal conductivity. The temperature range will be (T_o-5) to T_o C with a resolution of 0.2 C. The surface area of the cold finger will be between 0.15 and 0.2 m^3. The exact shape of the cold finger will be determined during the ground-based bread boarding. But it is envisioned that it will be most likely configured as several closed coiled circular rings mounted on a longitudinal stem. The ID at the base of the ring will be between 15%-28% of the tank ID. The tubing used to form the ring will have an OD no larger than 0.5". The stem will be inserted into the domed section of the tank close to the central axis at the same end as the jet nozzle. The central axis of the ring will be located 1" +/- 1/8" downstream of the nozzle exit.

The flow through the cold-finger is chosen such that the temperature drop of the fluid circulating in the cold-finger loop is less than 0.25 C.

4.3.5.3 Wall Cooling

It is also interesting to study the effect of using the whole tank wall as a cold finger. It is envisioned that wall cooling will be accomplished in an innovative manner by injecting a gas such as helium into the vacuum maintained between the tank wall and the outer containment jacket (see Fig. 18) thus providing a conductive path between the two walls. Then, the tank wall will be maintained at a desired temperature level by controlling the temperature of the outer containment jacket to within the similar specifications as outlined for the cold finger.

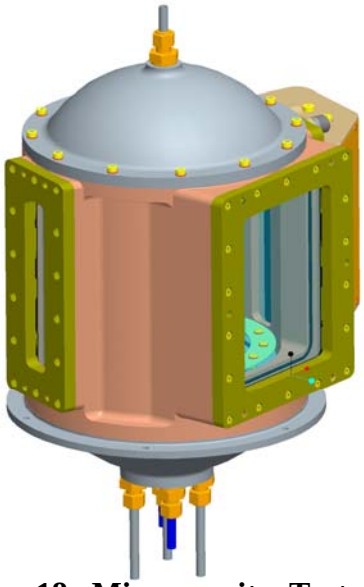

Figure 18. Microgravity Test Cell Inside the Containment/Isolation Jacket.

4.3.6 Non-Condensable Gas Injection

Gas injection studies will be performed to determine the effect of a non-condensable gas on the evaporation/condensation process and the overall tank pressurization and pressure control characteristics. It is envisioned that nitrogen will be used as the pressurant gas. The injection of gas will be directly into the existing ullage volume to provide the following mole fractions: 15%, 30%, 45%, 60% +/- 2% (moles of gas / moles of vapor). To minimize heat transfer in the ullage during injection the inert gas must be injected at a temperature of T_o +/- 0.25 C. Pressurization tests with the non-condensable will be terminated whenever the tank MOP is reached.

4.3.7 Local Measurements

Accurate temperature and pressure measurements are needed at different locations in the tank as described in the next two subsections.

4.3.7.1 Temperature Measurements

Accurate and precise local temperature measurements must be taken in the range of 20 – 50 C with a resolution of 0.01 deg and an accuracy 0.05 deg. The envisioned sensor locations are as follows:

- 10 temperature measurements on the wall
- 2 at jet inlet and outlet
- 1 in the cold finger
- 2 transversely located in the ullage volume
- 3 in different locations in the cylindrical section and bottom dome

There will be a total of five thermistors interior to the tank volume. Temperature measurements will be taken at a rate of 1/60 Hz for all the wall and ambient locations and 1 Hz for the rest of the tank locations. The sensors inside the tank should minimize the creation of pinning points for the ullage.

4.3.7.2 Pressure Measurements

Pressure measurement shall be performed at the rate of 1 Hz at one location on the assumed ullage end of the tank. The measurement will cover a range between 0 psia and the MOP of the tank with a resolution of 0.006 psi, and an accuracy of 0.05 psi.

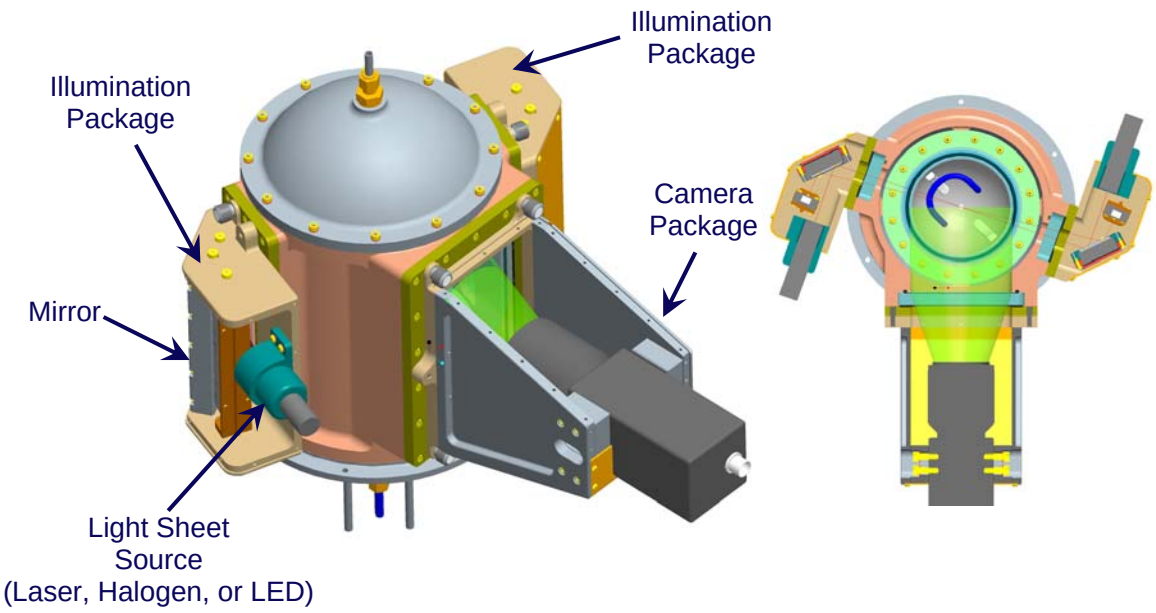

Figure 19. Microgravity Test Rig Showing The PIV Flow Visualization/Measurement Set-Up.

4.3.8 Field Visualization

Quantitative and qualitative data provided by field visualizations/measurements of the flow and temperature fields and bubble location are essential for code validation & verification. The video data will be time-stamped to easily synch the data with each experimental run.

4.3.8.1 Velocity Field Visualization/Measurement

Standard Particle Image Velocimetry (PIV) will be used to visualize the important flow structures that develop in the tank as shown Fig. 19. As a result of the ongoing competition that might occur between natural and thermocapillary convections in microgravity on one hand and the forced jet mixing on the other, the flow structures will encompass the entire liquid region (i.e. locations near the walls, near the liquid-vapor interface, and in the central region of the tank). Therefore, we will ideally strive for full flow visualization. If this is not possible, the Field of View (FOV) will consist of the cylindrical region in the tank that is bounded at top and bottom by the tank's hemispherical caps and extends in the radial direction to within 98% of the tank radius as measured from the central axis. The PIV particles will be compatible and density-matched with the fluid (HFE-7000) as much as possible. Spatial resolution and recording frequency of the PIV technique will be optimized to allow simultaneous measurement of multiple flow structures with velocities ranging from 0.3 microns/sec for natural convection to 25 cm/sec for jet mixing with a resolution of +/- 5-10%.

4.3.8.2 Temperature Field Measurement

The temperature field shall be captured and visualized using Liquid Crystal Thermometry (LCT). The FOV will be the same as PIV although we will strive to ideally encompass the whole tank. The temperature resolution will be +/- 0.5 C with a range of 20 C - 42 C. The LCT particles are subject to the same compatibility and density matching criteria as the PIV particles.

4.3.8.3 Ullage Location Measurement

The position of the ullage will be determined with in an accuracy of +/- 5 mm. This information is essential for the model validation and verification.

4.4 The Two-Phase Tank CFD Model Development

As an integral part of the proposed research, comprehensive, two-phase numerical models for tank pressurization and pressure control will be developed. These state-of-the-art models will address many of the scientific and engineering issues that were previously identified in Section 4.2. Once validated and verified through this research effort, these models will also serve as powerful simulation tools to aid the scale-up engineering design of future cryogenic storage tanks for specific application and mission scenarios. The numerical model development will proceed in a stepwise fashion by building upon and extending the current capabilities of the ALLVT two-phase transport model described in Section 3.2. The extensions that will be implemented are as follows:

1. Modeling the transport of momentum, energy, and species in the vapor
2. Incorporating the effect of non-condensable gases in a rigorous framework
3. Incorporating the effect of non-equilibrium phase change in a rigorous framework
4. Casting the formulation into the mathematical framework of the Level-Set interface capturing scheme that is extremely suitable for microgravity simulations.

Extensions 1, 2 and 3 to the existing ALLVT model are needed in order to account for: (a) contributions to pressure rise due to the direct heating of the ullage by the wall; (b) effect of noncondensable gases on the evaporation and condensation rates; and (c) sudden pressure rise due to rapid nonequilibrium phase change. The resulting new formulation will be embodied in the Active-Liquid Active-Vapor Lumped-Mass Tank (ALAV-LMT) model.

The existing ALLVT or the future ALAV-LMT models use a front-tracking numerical methodology to resolve the free surface shape and motion (Panzarella and Kassemi, 2004). The front tracking method is quite adequate and appropriate for any ground-based or on-surface simulation where interface movements are small and essentially only the static interface shape has to be computed and tracked. They can also accommodate moderate interface deformation but at a cost of numerous remeshing of the domain as the computational grids drastically distort due to ullage movement (Panzarella and Kassemi, 2004, 2005).

Unfortunately, the front tracking methods are not computationally efficient in handling extensive phase motions, fluid slosh, or topological changes associated with the merging or splitting of multiple vapor regions. Since, such conditions will arise in a space-based cryogenic tanks operating under microgravity conditions where there is no preferred location or orientation for the vapor region, a more versatile computational technique for handling the interface movement is needed. In general, it is more appropriate and more feasible to use a front-capturing computational technique such as the Level-Set method to capture and follow multiple interfaces with complex shapes and drastic movements because the methodology works on a fixed computational grid. Therefore, in order to provide a robust and accurate computational capability for microgravity simulations, the mathematical formulation of the ALAV-LMT model will be recast into a computational framework based on the Level-Set methodology for capturing the ullage shape and distribution. The resulting formulation will be embodied in the Active-Liquid Active-Vapor-Level-Set Tank (ALAV-LST) model.

4.4.1 Active-Liquid Active-Vapor Lumped-Mass Tank (ALAV-LMT) Model

The ALAV-LM model will be developed to resolve two main issues: (a) The pressure rise/fall due to direct heat transfer from the wall to the ullage; and (b) The impact of a non-condensable pressurant on the evaporation and condensation mass transfers at the interface. Currently, it is not possible to address these two issues in the context of the existing ALLVT

model due to its lumped treatment of the vapor phase Therefore, in the ALAV-LMT model, transport of mass, momentum, energy and species in the gaseous phase will be considered in addition to their counterparts in the liquid phase. This is accomplished by solving the compressible continuity and Navier Stokes equations for the ullage flow field, the incompressible continuity and Navier Stokes equations for the liquid flow field, the conservation of energy equations for the ullage and liquid temperature fields, and the conservation of species equation for the noncondensable and vapor mass fractions (i.e. the partial pressures of the non-condensable gas and vapor) in the ullage. In this model, the net evaporative and condensing mass transfer across the interface and its contribution to evolution of ullage (tank) pressure will be considered in a lumped or integrated fashion.

4.4.1.1 The Lumped Mass Approach

To describe the mathematical framework for the lumped mass approach, consider an ullage represented by a binary system that is composed of the vapor and a noncondensable gas. Assuming ideal gas behavior for both components, the tank pressure is given by:

$$p = p_v + p_a \tag{35}$$

Where, p_v , is the partial pressure of the vapor and, p_a , is the partial pressure of the noncondensable gas. We can define an average tank pressure, $\overline{p}$, given by

$$\overline{p} = \frac{1}{V}\iiint_V p dV \tag{36}$$

such that,

$$p = \overline{p} + p' \tag{37}$$

Here, V, is the entire ullage volume and, p', is the residual pressure that represents the combined contributions of hydrostatic, inertial, and viscous forces. It can be shown that generally, p', is several order of magnitudes smaller than the average background pressure, $\overline{p}$. Therefore, in our analysis, without any major loss in generality, we will assume that the total pressure is simply equal to the average pressure. That is, $p = \overline{p}$, except when computing the flow fields in the vapor and in the liquid that are driven by the pressure gradients, where, $\nabla p = \nabla p'$, and the absolute background pressure level is not relevant. Moreover, since the ullage contains a binary mixture, it is assumed that they both satisfy their respective ideal gas equations of state:

$$p_v = \frac{\rho_v RT}{m_v} \tag{38}$$

$$p_a = \frac{\rho_a RT}{m_a} \tag{39}$$

Where, m_v , and, m_a , are respectively the molar masses of the vapor and noncondensable, R, is ideal gas constant, and, T , is the local temperature in the ullage.

Substitution of Eqs. (38) and (39) into Eq. (35) results in the following equation for the ullage pressure:

$$\overline{p} = \frac{R}{\overline{T^{-1}}}\left(\frac{\overline{\rho}_v}{m_v} + \frac{\overline{\rho}_a}{m_a}\right) \tag{40}$$

This equation depends on the average vapor and average gas densities and on the average (integrated) reciprocal temperature that are respectively defined as:

(41)

$$\overline{\rho}_v = V^{-1}\iiint_V \rho_v dV$$

$$\overline{\rho}_a = V^{-1}\iiint_V \rho_a dV \tag{42}$$

$$\overline{T^{-1}} = V^{-1}\iiint_V T^{-1} dV \tag{43}$$

Thus to solve for the average ullage pressure, two additional evolution equations for the average vapor and average noncondensable densities are needed. The evolution equation for the average vapor density can be derived by the global conservation of mass and ullage volume expression derived in section 3.2 that is recast in terms of the average vapor density. The result is an expression for the evolution of average vapor density:

$$\frac{d\overline{\rho}_v}{dt} = \frac{M_v}{V}\left(1 - \frac{\overline{\rho}_v}{\rho_l}\right) \tag{44}$$

Similarly, an evolution equation for the non-condensable can be derived that, assuming the solubility of gas in the liquid is negligible, takes the following simple form:

$$\frac{d\overline{\rho}_a}{dt} = \frac{M_v}{V}\left(\frac{\overline{\rho}_a}{\rho_l}\right) \tag{45}$$

The total mass flow rate of the vapor into the ullage region across the ullage-liquid interface was previously given by Eq (22) as

$$M_v = \iint_I J_v dS \tag{46}$$

Once the evaporation mass flux, J_v, is known, Eq (46) together with Eqs. (40), (44) and (45) constitute a set of four equations in four unknowns that can be solved for the average pressure in the ullage. This is the essence of the lumped mass transfer analysis. A salient feature of this approach is that it inherently filters out contributions to pressure and density variations on the acoustic timescales. It thus renders a numerical methodology that can resolve the tank pressurization behavior on the time and spatial scales pertinent to the problem at hand.

4.4.1.2 The Interfacial Balance Equations

As mentioned, in order to predict the evolution of pressure in the ullage using Eqs (40), and (44)-(46) of the lumped mass approach, the interfacial vapor mass flux, J_v, is needed. This quantity can be evaluated from a set of intricately coupled energy, species, and momentum balance conditions at the ullage-liquid interface that, in turn, require a simultaneous solution of the highly coupled and nonlinear continuity, Navier Stokes, energy, and species equations for the two phases.

The thermal boundary conditions and the energy balances at the interface are of prime importance. Following the work of Tryggvesan (1998), it will be assumed that the temperature across the interface is continuous- that is:

$$T = T_I = T_l \tag{47}$$

As suggested by Schrage (1953), a simple constitutive relationship between the interfacial temperature, T_I , the saturation temperature at the interface, T_s , and the interfacial mass flux can be written in general terms as:

$$J_v = K_{pc}(T_I - T_s) \tag{48}$$

In this equation, K_{pc}, is a phase change coefficient that is determined by the nature of the phase change process: that is, existence of near-equilibrium or non-equilibrium conditions and presence or absence of noncondensable gases, as will be discussed later. The saturation temperature, T_s, is

dictated by the pressure of the vapor that may be, in turn, a function of the mass fraction of the noncondensable on the ullage side.

In order to solve for, J_v , and T_I , another equation is needed. In the ALAV-LMT model, this equation is provided by the interfacial energy balance that involves mainly the heat of fusion contribution due to evaporation/condensation phase change and the conductive fluxes at both sides of the interface.

It is interesting to note that in the ALAV-LMT model, the relationship between, T_s , and, T_I , will be determined by the relative magnitudes of, J_v , and, K_{pc} , in equation (48). If J_v is small and K_{pc} moderate to large, $T_s = T_I$. This is equivalent to the near-equilibrium assumption that was the cornerstone of the ALLVT model. If both, J_v , and, K_{pc} , are zero, then there is no relationship between the interfacial and saturation temperatures and the interface temperature is solely determined by the conductive energy balance at the interface and, therefore, greatly influenced by the conditions on the liquid side. Finally, if both, K_{pc} , and, J_v , are moderate to large then a condition arises that, T_I , is allowed to deviate from, T_s , to an extent determined by the magnitudes of the vapor mass flux and the thermal gradients on both sides of the interface.

In the ALAV-LMT model, once, J_v , is computed, it will also be fed into a Stefan wind type interfacial balance equation for the species equation. The ullage and liquid momentum equations will be also subject to continuity of velocity in the tangential direction across the interface. In addition, a normal stress balance will provide the means of tracking and updating the interface shape and a tangential stress balance will be used to account for any Marangoni convection that may develop as result of the presence of the noncondensable gas and/or nonequilibrium effects. Finally, when J_v is determined, the lumped mass average pressure and density equations (40) and (44-46) can be solved for to update the ullage pressure and average densities. These, in turn, will dictate a new saturation temperature.

4.4.1.3 Non-Condensable Gas Effects

When there is no other gas besides the vapor in the ullage region, the saturation temperature is nearly constant along the liquid-vapor interface and the transport in the vapor region is of only secondary importance because the saturation temperature depends on the absolute vapor pressure which is much larger than any pressure difference due to flow or temperature variation. The presence of a noncondensable gas in the ullage can complicate tank pressurization and pressure control in three ways:

1. It can affect the saturation pressure-temperature relationship.
2. It can suppress condensation and, therefore, cause a situation where the ZBO tank pressure control can become ineffective or dysfunctional.
3. It can lead to generation of Marangoni convection that can act as a natural mixing mechanism in microgravity aiding destratification and pressure control in on-orbit applications.

The first noncondensable gas effect changes the relationship $T_s = F\ (p_v\ ,\ p)$ and will be accounted for in ALAV-LMT model along the line described by Sears and Salinger (1975). The second effect is due to formation of a Knudsen layer next to the liquid (a few mean free paths from the interface) consisting of the noncondensable gas molecules. This layer creates resistance to the vapor molecules that want to go into the liquid but it does not significantly impede the liquid molecules that intend to go into the vapor. This implies that different K_{pc} expressions must be used in Eq (48) for evaporation and condensation. In the ALAV-LMT model, a rigorous relationship for condensation in presence of a noncondensible will be developed based on the non-equilibrium kinetics relationships developed by Pong and Moses (1986).

Finally, the third effect implies that the transport of the gas in the ullage is quite important when there is a non-condensable gas present. In this case, the partial pressure of the vapor can vary considerably along the interface depending on the local concentration (partial pressure) of the noncondensable as governed by the overall transport conditions in the ullage. Since the saturation temperature is related to the partial pressure of the vapor according to Clausius Clapeyron relationship (12), the saturation temperature and by consequence of Eq (34) the interfacial temperature will no longer be uniform even under near equilibrium conditions. This may lead to thermocapillary convection driven by the dependence of surface tension on the interfacial temperature that will be accounted for in the ALAV-LMT model through a shear stress balance at the interface similar to Eq (32) described in section 3.2.

Thus, a very curious and interesting situation might arise in which thermocapillary convection is driven by interfacial temperature gradients due to the partial pressure distributions on the vapor side and not by the heat transfer mechanisms on the liquid region. Under these circumstances, strikingly different convection profiles in the liquid and interfacial mass transfer rates are attained as compared to the pure vapor case. This is especially true in microgravity where the effects of natural convection are mitigated and the impact of any thermocapillary convection will be more pronounced.

4.4.1.4 The Non-Equilibrium Effects

There are several sources for nonequilibrium contributions to the ullage-liquid interfacial conditions as discussed by Juric and Tryggvason (1998). The most important contribution in the context of the present storage tank problem is due to large evaporation and/or condensation fluxes during rapid and intensive phase change. To account for these situations, special expressions for the accommodation coefficient, K_{pc}, in Eq (48) must be used for both evaporation and condensation even when noncondensable gases are not present. We will implement a rigorous formulation for, K_{pc} , based on nonequilibrium kinetics (Labuntsov and Kryukov, 1979). Again, it is emphasized that according to Eq (48), under nonequilibrium phase change, when J_v is large, the interfacial temperature can deviate from the saturation temperature. Since in this situation, the temperature of the interface is controlled by both mass transport and thermal gradients on the two sides of the interface, it can be highly nonuniform giving rise again to Marangoni convection. This time however the Marangoni convection will be present even for a pure vapor ullage and will be mostly influenced by transport of energy on the liquid side of the interface in contradiction to the case for the noncondensable gas effects when it was controlled by the vapor partial pressure on the ullage side.

4.4.1.5 The Turbulence Model

For most microgravity applications the natural convection flow in the liquid and vapor are laminar even for the larger tanks. In on-surface applications, the convective flow in both the liquid and vapor will be likely turbulent. In addition, the mixing jet will most likely be turbulent even in microgravity, especially, at higher flow rates required for larger tank. Reynolds Averaged Navier Stokes (RANS) equations are still the optimum means of modeling turbulence in the cryogenic storage tank. Among the different RANS methods the two equation k-ω turbulence seems to be the most promising model for the low Reynolds number turbulence associated with bounded natural convection and jet flows encountered in the tank problem. The fidelity of this method will be assessed by comparing the numerical results of the present modeling effort to benchmark solutions and existing experimental data (Aydelott, 1967 and 1979; Lin et al. 1992; Sonin et al., 1986; Chun et al., 1986; and Brown and Sonin, 1990) that are available in the literature.

It should be emphasized that the gray area in applying any of these turbulence models to the storage tank problem is the correct choice of boundary conditions at the free surface. The problem with any of the two equation RANS formulations is that the eddy viscosity models fail to capture the turbulent anisotropy at the liquid-ullage interface. The anisotropy can be captured by the more sophisticated and more computationally intensive Reynolds Stress models. However, proper free surface boundary conditions for the Reynolds Stress models are also not readily available.

From a practical engineering point of view, in most free surface problems isotropic turbulence is assumed and either Dirichlet or Neumann conditions are applied to the k and ε or ω variables. In his work on open channel flows, Rodi (1980) suggested prescribing the value of k and ε (and thus ω) in order to account for gradual dampening of the turbulent eddies as the freesurface isapproached from below. Alternatively, a Neumann boundary condition (zero flux) for the turbulent kinetic energy can be imposed at the free surface. This appears to have produced reasonable results for both stationary sharp interfaces (Hasan and Lin, 1989) and moving diffuse fronts (Gatson et al., 2000; Illinca and Hetu, 2000). However, it should be clear that in reality a free surface will deform under stress, and capillary waves will be excited at the expense of some of the turbulent kinetic energy. This would imply a nonzero flux of turbulent kinetic energy at the free surface. In fact, Hasselmann (1971) has shown for a smooth, non-overlapping interface that, indeed, there are flows of mass and momentum that need to be accounted for in the averaged free-surface boundary conditions when turbulence is present.

For situations involving strong turbulence, as discussed by Brocchini and Peregrine (2001a), the interface can become even more complex as droplets and bubbles develop and are ejected from the free surface as when splashing occurs. The most general treatment of the boundary conditions in this case has been developed with full mathematical rigor in Brocchini and Peregrine (2001b). They use an integral formulation with ensemble averaging to account for the complex two-phase nature of the interfacial region. They find that there are many new terms that appear in the averaged free-surface boundary conditions.

Unfortunately, extra information is required in order to close these equations and boundary conditions, and this can only come from experimental data, which is thus far lacking in the open literature. In the course of our numerical/experimental effort we will identify to what extent, if any, tank pressurization is affected by free surface turbulence and we will determine under what conditions a more rigorous treatment of the free surface turbulent boundary conditions is warranted. However it should be emphasized that an in-depth analysis of free surface turbulence is outside the scope of the present work.

4.4.1.6 The Micro-Nucleation Model

As mentioned before, the large superheats in microgravity might lead to sudden pressure spikes with serious implications. In the context of the present research, the nucleation and subsequent bubble growth phenomena will be investigated by coupling an analytical model of the micro-scale bubble growth process to the ALAV-LMT model. This model will be similar to the one used by Prosperetti and Plesset (1979) but modified to account for the total volume constraint imposed by our closed container. The micro-model will be capable of describing the bubble growth in both the inertia-controlled regime immediately after nucleation as well as the heat-transfer limited regime that develops later. The bubble growth rate will depend on the local superheat and the surrounding liquid pressure, both of which are determined by the solution of the large-scale transport equations in the liquid and vapor regions.

There will be a two-way coupling between the ALAV-LMT model and the bubble growth micro-model. The CFD module in the ALAV-LMT model will be used to predict the superheat (and the corresponding probability of nucleation) at every point inside the liquid. At the point of highest probability, a nucleation event will be initiated by assuming a vapor bubble with some initial radius. The bubble will, at least initially, be so small as to not be explicitly meshed in the large-scale tank model, but its effect on the overall tank pressure will be included. That is, tank pressure will increase as the bubble grows due to the total volume constraint. Of course, the extent to which the tank pressure is affected depends on the initial liquid volume (fill level) as well as on how fast the vapor in the other regions condenses due to the resultant pressure increase. But, as the overall tank pressure increases, it also tends to suppress further bubble growth. In this fashion, the bubble growth micro-model is intimately coupled to the two-phase tank pressurization model. Due to the multiplicity of the competing and coupled factors affecting bubble growth and tank pressurization, the overall dynamic pressure response of the whole systems is not obvious *a priori*. Therefore, the whole system of the coupled differential equations for the three regions must be solved simultaneously in order to properly determine the over all tank pressure dynamics.

This approach will be used to investigate the early behavior of a nucleation event with the specific goal of predicting under what conditions pressure spikes similar to those observed in the previously mentioned microgravity boiling experiment can occur.

4.4.1.7 The Thermal Link to the Environment

The driving force for tank pressurization is heat leaks from the surrounding environment. Therefore, the necessary formulations for the tank wall conduction, the insulation layers, and the spectral radiative and natural convective heat exchange with the surrounding environments (orbit, on-surface, laboratory) will be incorporated into the ALAV-LMT model and will be activated selectively depending on the nature of the cases studied.

4.4.2 Active-Liquid Active-Vapor Level Set Tank (ALAV-LST) Model

To capture topologically complex interfacial motions, which are likely to be present in reduced gravity environments, a number of computational techniques are available. Among them, the level set method (Osher and Sethian, 1988) has developed into a robust computational tool to capture complicated 2D or 3D interfacial dynamics. Therefore, in order to capture the microgravity liquid and ullage distributions and behavior the formulation developed and implemented in the ALAV-LMT model will be recast into the framework of a Level-Set phase capturing computational methodology to produce the ALAV-LST model. Thus in the ALAV-LST model a single field formulation represented by a level set function, ϕ, is used to implicitly capture the location of the interface. Typically the distance function is used as the level set variable:

$$\phi(\vec{x}) = \min\left(\left|\vec{x} - \vec{x}_I\right|\right) \tag{49}$$

for all $\vec{x}_I$ on an interface. Using this definition, as shown in Fig. 20, for any point on the interface, the level set function is zero. For points within a volume bounded by the interface, the level set function is negative and for points outside of this bounded region, the level set function is positive.

Interfacial motion is governed by a simple advection equation for the level set function:

$$\frac{\partial \phi}{\partial t} + \vec{V} \cdot \nabla \phi = -\frac{\dot{m}_e |\nabla \phi|}{\rho} \tag{50}$$

where $\dot{m}_e$ is the evaporative mass flux and can be computed from the local interfacial energy jump condition. The source term in the above equation ensures that the interface moves at the correct speed and accounts for interfacial motion due to evaporation and condensation.

As originally formulated, the level set method was notoriously dissipative and required higher order ENO/WENO discretization schemes to obtain meaningful results. Unfortunately, implementing a 2D/3D ENO or WENO discretization scheme on complicated unstructured finite volume meshes can be cumbersome and computationally expensive. Recently however, a number of techniques have been developed to correct for these dissipation errors while at the same time allow for a lower order implementation of the level set scheme. To enforce global mass conservation, the following PDE can be solved to steady state in fictitious time, τ :

$$\frac{\partial \phi}{\partial \tau} + \left[V_o(t) - V(\tau) \right] |\nabla \phi| f(\kappa) = 0 \tag{51}$$

Here, V is the volume bounded by the interface and is computed from the level set function: $\int (1 - H(\phi)) dV$ where $H(\phi)$ is the Heavyside function and integral is computed over the entire computational domain. V_o is what the vapor volume should be if no numerical dissipation were present. It can be calculated from a total mass balance and is a function of time to allow for vapor volume changes due to evaporation and condensation. The correction is also a function of interfacial curvature, κ, since dissipation losses are expected to be largest in regions of high curvature. This global mass conservation approach was successfully employed by Zhang et al. (1998) to reduce dissipation errors while simulating solidification processes.

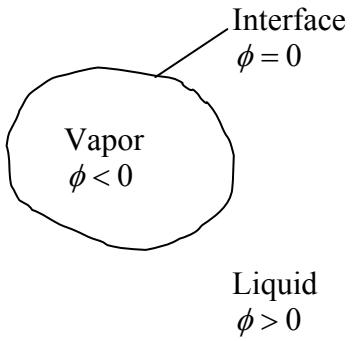

Figure 20: Level Set Function

To accurately compute the local interfacial curvature, the gradient of the level set function near the interface must be known with a high degree of precision. Forcing ϕ to be a distance function for all time generally leads to a more accurate computation of the level set gradient. Enforcing the distance function property, $|\nabla \phi| = 1$, requires solving the following equation to steady state:

$$\frac{\partial \phi}{\partial \tau} + S(\phi)\left(|\nabla \phi| - 1 \right) = 0 \tag{52}$$

where $S(\phi)$ is the local sign of the level set function.

To apply the additional jump boundary conditions at the interface, to couple a compressible vapor phase to an incompressible liquid phase and to prescribe a temperature boundary condition at the interface, the novel Ghost Fluid Method (GFM) (Fedkiw et al., 1999) will be used. While the GFM was originally developed using the level set technique, the method itself can be used with any interface capturing scheme to implicitly account for the jump conditions at the interface.

The strength of the GFM is that interfacial jump conditions are implicitly accounted for by defining a set of ghost nodes on either side of the interface. The ghost nodes and the nodes in the

parent continuous phase are then used to define the flux at the face of a cell cut by the interface. As an example, consider applying an energy jump condition at the interface shown in Fig. 21. The energy jump can be expressed in terms of a latent heat source at the interface and is due to any phase change that might be occurring. The purpose of the latent heat source is to enforce some condition on interfacial temperature. As suggested by Morgan (2005), instead applying the latent heat source directly, a prescribed temperature boundary condition could be applied at the interface. A saturation condition along with a gradient extrapolation in the normal direction can be used to construct the ghost values:

$$T_{GHOST} = T_{sat} + \phi \hat{n} \cdot \nabla T$$

The heat flux on face i of the cut cell shown in Fig. 21, can be easily approximated as:

$$q'' = -k \frac{T_{GHOST} - T_I}{x_{GHOST} - x_I} \tag{54}$$

This modified flux is used when discretizing the energy equation for a cell cut by the interface. In this way, the numerical scheme never interpolates across the interface. Since the jump conditions are implicitly taken into account, the need for any smeared out Dirac function sources in the field equations become unnecessary which results in greater numerical stability and robustness.

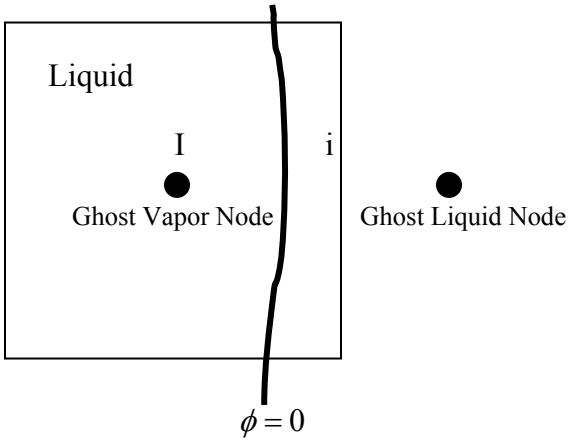

Figure 21: Ghost Fluid Method

To solve the present two-phase active liquid active vapor problem, the solution approach will be similar to the isothermal compressible-incompressible problems studied by Caiden et al. (2001). First the compressible flow equations in the vapor will be solved. The GFM, the mass flux balance, and the tangential momentum balance are used to obtain a boundary condition for velocity on the vapor side of the interface. With the newly solved field equations in the vapor, the normal momentum balance and the GFM will be used to prescribe a pressure on the liquid side of the interface. Now the incompressible field equations will be solved in the liquid. The prescribed temperature boundary condition at the interface is used to construct new ghost temperature nodes using gradient extrapolation. With the ghost nodes defined from the saturation condition, the energy equation can be solved in both phases and the level set function can be advected in time.

Since the vapor solution is coupled to the liquid solution through the interface, iteration will be necessary to obtain a solution. To speed up the solution process, since only the zeroth iso-contour of the level set function has any physical meaning, the narrow band formulation (Chopp, 1993) of the level set technique will be used. In this formulation, the level set equation is only solved in a computational domain consisting of a few grid cells on either side of the interface.

4.5 Ground-Based Research

The proposed ground-based research activity is designed with three aims in mind. First, is to support the design and development of the proposed ISS experiment by resolving key technical and engineering issues that must be addressed in order to satisfy the stringent science requirements for the microgravity tests. Second, is to acquire additional 1g data, especially, in the turbulent regimes necessary for variable gravity tank design and model validation and verification. Third, is to reduce the burden of the ISS experiment by moving some of the parametric tests that are needed but can also be performed in 1g, such as the noncondensable gas tests, to ground laboratory. As such the ground-based research is divided into three parts that will be briefly discussed as follows.

4.5.1 The Experimental Bread Board Studies

The bread board studies have three main components all geared towards optimizing the design of the experimental test rig and the associated diagnostics to meet the science requirements of the ISS experiment.

4.5.1.1 The Gas Leakage Studies

The ISS microgravity experiment requires pressurization tests at different fill levels (refer to the test matrix in section 4.6.3). This can be accomplished in two ways: (a) through a bellowed storage compartment and fluid loop that can empty and fill the tank on orbit; or (b) by performing the experiments with sealed tanks filled on the ground to the desired fill levels.

Option (a) provides a great deal of experimental flexibility but is complex and can provide additional highly undesirable heat loss paths from the tank to the surrounding. Option (b) is simple and will provide the best thermal isolation conditions but is only viable if leakage of foreign surrounding gases into the tank during the long storage interval (on ground and in space) is minimal and does not affect the experiment. The goal of the gas leakage tests is, therefore, to examine the viability of option (b) by demonstrating that typical amounts of expected air leakage from the surrounding will not affect the results of the pressurization and pressure control experiments both qualitatively and quantitatively.

The procedure for these tests is briefly described as follows. First, start the test with only pure liquid and vapor and bring the tank into thermal equilibrium within the accuracy of the instrumentation. Turn on the heaters to self-pressurize the tank. Then, activate the cooling jet to instigate condensation and a subsequent drop in the tank pressure. Repeat the test for different amount of air leaked into the system. The mole fraction of the leaked air can be computed from the measured total pressure and the vapor saturation pressure that can be deduced from the temperature measurements. Finally, compare the results of the pure vapor and leaked air cases to determine at what level of contamination test results will be affected.

4.5.1.2 The PIV Particle Nucleation Studies

Flow visualization as afforded by Particle Imaging Velocimetry (PIV) is an integral part of the proposed research and is indispensable to the model validation and verification goals of the project. Unfortunately, it is possible that the PIV particles introduced into the system can promote premature boiling by providing nucleation sites for vapor bubble growth in the bulk liquid. The motivation behind these tests are to assess whether boiling at the particle sites in the bulk liquid will occur at typical superheats that are expected to prevail in microgravity. The ALLVT model will be used to predict the typical microgravity superheats.

The tests will be performed in a small transparent container partially filled with particle laden test fluid (HFE7000). Pressure in the vapor and temperature at three locations (in the vapor, at

the interface, and in the bulk liquid) will be closely monitored. The system is first equilibrated to within the accuracy of the measurements. Then, the pressure in the ullage is rapidly dropped by drawing a vacuum until a desired superheat level in the bulk liquid is achieved where upon:

$$\Delta T_{microgravity} \le T_{bulk} - T_I \le 2\Delta T_{microgravity} \tag{55}$$

Here, ΔT, is a typical microgravity superheat as predicted by the ALLVT model. During this time, the bulk liquid will be optically monitored to observe at what superheat levels vapor bubbles will appear and disappear in the liquid.

4.5.1.3 The Test Chamber Thermal Insulation Assessment

To a large extent, the success of this experiment and proper validation and verification of the pressurization and pressure control models developed during the course of this research activity depend directly on highly accurate determination of energy/heat distributions in the experimental test chamber. The experimental design will strive to accommodate the stringent thermal isolation requirements for the microgravity experiment through a thermally controlled vacuum isolation jacket similar to the one shown in Fig. 18. But due to the optical windows, thermocouple leads, and fluid loop fittings, there will inevitably be numerous potential heat loss paths. The goal of this set of breadboard tests will be to: (a) strive for elimination or substantial reduction of heat leak paths from the test chamber through innovative thermal design and experimentation; and (b) estimate the extent of heat loss through the paths that cannot be entirely eliminated so that they can be accounted for in the models.

4.5.2 The 1G Experimental Studies

These experiments are needed to; (a) aid the design of the microgravity test setup; (b) fine tune the microgravity experimental test procedures and test matrix (c) reduce microgravity test matrix for noncondensable gas and mixing effects; and (d) obtain valuable 1g tank pressurization and pressure control data.

4.5.2.1 The 1G Pure Vapor Pressurization/Pressure Control Studies

A comprehensive set of tank pressurization and subcooled jet pressure control tests will be performed in 1g. The procedure and matrix for these tests will be similar to the ones described in sections (4.6.2) and (4.6.5) for the ISS microgravity experiment and hence will not be duplicated here. The 1g tests will be important because they will involve turbulent natural convection and turbulent jet and hence indispensable for variable gravity validation and verification of the tank models.

4.5.2.2 The 1G Noncondensable Studies

Relatively little data is available on the effect of noncondensable gases on tank pressurization and pressure control at any gravity level. It is conceivable that certain effects such as Marangoni convection driven by partial pressures in the vapor can be better captured and observed in microgravity where the natural convection flow is mitigated. But, by and large, the possible effect of the noncondensable on ZBO pressure control through, for example, suppression of condensation rates should be equally observable on earth. Therefore, a comprehensive set of noncondensable tests will be performed in 1g. Again, the description of the basic procedure for these tests will be similar to the ones included in sections (4.6.2) and (4.6.5) for the ISS microgravity experiment and hence will not be duplicated here. Since the ground-based effort can also accommodate a larger parametric test matrix compared to the ISS experiment it can result in a smaller test matrix for the ISS experiment by moving a major portion of the noncondensable tests to the ground laboratory.

4.5.3 The Reduced Gravity (Drop-Tower) Ullage Penetration Studies

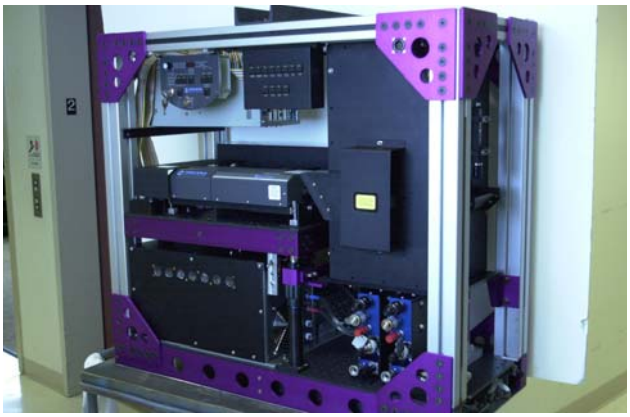

Figure 22. The Existing Drop Tower PIV Test Rig to Be Modified for The Proposed Ullage Penetration Studies.

Computational modeling of the free surface in microgravity has advanced tremendously in the last decade. But validation data has been limited to drop tower tests conducted in the 1970's. Most of the film of these tests has been lost. Recorded data from these tests is limited to a single number: geyser height. Other key parameters such as geyser width and the intensity of turbulence are unrecorded. Free surface shape is observed but through thick plastic cylinders, and hence subject to a great deal of optical distortion. Recent work has shown the importance of these parameters for proper validation and verification of free surface CFD models (Chato et al, 2004).

In this context, the objective of this set of ground-based studies is to accurately measure the deformation of the free surface caused through impingement by a submerged liquid jet in the reduced gravity environment provided by the 2.2 s drop tower at NASA GRC and to accurately measure the changes in velocity induced by this free surface deformation. The test will therefore provide valuable reduced gravity data for verification and validation of the ALAV-LST code in predicting reduced gravity ullage free surface behavior.

The experiment will use an existing PIV test rig for the 2.2-second drop tower (Wernet 2000) as shown in Fig. 22. Although designed for flame studies, the PIV system has enough flexibly to accommodate a liquid system as well. Removal of the flame chamber will allow a 53 cm tall by 25 cm diameter space for installation of a liquid test volume similar to that used by Symons (1968). Like Symons (1968) the liquid will be stored in a pressurized accumulator and released during the drop into a clear plastic tank (The piston pump system used by Aydelott (1979) has some advantages but its length make use in the 2.2 second drop tower difficult). A sheet lighting system similar to the approach used on the Surface Tension Driven Convection experiment (Ostrach and Kamotani 1996) will be used for visualization. The clear plastic tank will be illuminated along its centerline with a sheet of laser light. A dual pulse laser system allows for bursts of light at closely space time intervals allowing for accurate measurement of particle motion and calculation of fluid velocity. High-speed video will be taken of the clear plastic tank as it is dropped in free fall. At the start of the test, the tank will be partially filled with liquid. Tracer particles will be included in the liquid (probably in the initial fill, but locating tracers in the incoming jet will also be considered during design). Expected parameters to investigate will include inflow rate and fill level, and liquid properties.

The key measurements to characterize the fluid flow and free surface behavior will include:

- The undistorted geyser height and shape through laser sheet lighting
- Fluid velocity via PIV.
- Estimate of turbulence parameters from PIV

The mean jet flow rate will be measured by a flow meter in the transfer line. Local pressure and temperature measurements will be also performed to account for variation in the fluid conditions.

Different references suggest different time scales for the jet problem. Symons, working with 2 to 4 cm. tanks and looking at free surface shape, was able to see static free surfaces after 1.35 seconds. The time required for the motion in the liquid to reach steady state can be estimated by looking at the secondary eddies induced in the liquid. Aydelott (1979) measured the time to circulate the fluid completely around a 10-cm test tank obtaining values ranging from 1.4 to 5 seconds. His circulation results are shown in Fig. 23. Of course, the exact temporal behavior is a function of tank size, test fluid, and inlet flow, but there is every indication that the test can be designed to approach steady state within 2.2 seconds.

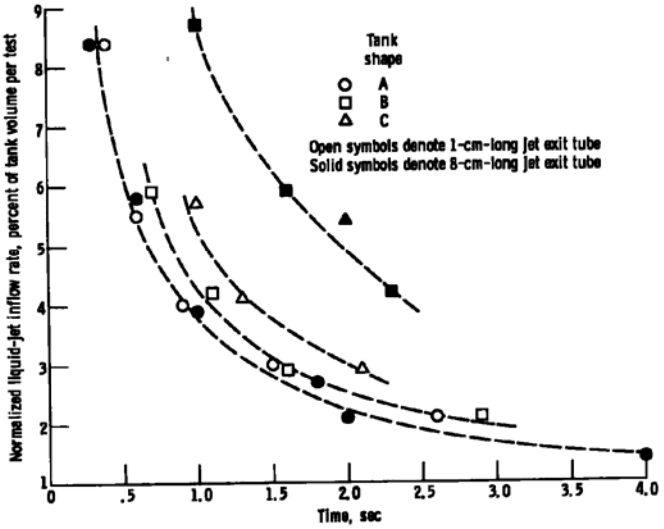

Figure 23. Drop Tower Circulation Time Constants for a 10 cm Test Cell.

4.6 The ISS Microgravity Experiment

The Zero Boil-Off Tank (ZBOT) experiment will be sensitive to the overall acceleration vector of the International Space Station (ISS), since during the experiment, the ullage will migrate in the direction of the residual acceleration vector. It is desirable to keep the ullage at one end of the ZBOT test tank opposite of the mixing nozzle. This is beneficial for both model validation and visualization purposes and jet cooling/mixing test runs.

4.6.1 The ISS Microgravity Environment

4.6.1.1 Residual Acceleration on ISS

The residual acceleration on the ISS is comprised of the gravity gradient, rotational, and drag components. The gravity gradient and rotational components are location dependent within the ISS. The drag component is small compared to the other two components. The ISS operates in three primary attitudes, each producing a different acceleration:

1. LVLH (Local Vertical, Local Horizontal) – This is sometimes called XVV (X-axis Velocity Vector). This is when the ISS flies as if it were an airplane flying over the earth's surface: its x-axis is always pointed towards the direction of travel, and the ISS appears to always be level with the horizon. In reality, the ISS must constantly be pitched in order to maintain this same relative attitude as it orbits the earth. This attitude is currently used about 50% of the time.
2. YVV (Y-axis Velocity Vector) – This is the same as XVV except the ISS is yawed to fly in the direction of its y-axis. This attitude is rarely used.
3. XPOP (X-axis Perpendicular to Orbital Plane) – This is where the ISS flies with its x-axis pointed towards the sun. It keeps a constant orientation relative to the sun-earth system, but it appears to always be rotating with respect to the earth's surface. This attitude is currently used about 50% of the time.

Table 2. MSG Acceleration Vectors (Micro-g)
(Rack Coordinates, Crew Sleep Period)

Attitude	Mean Accelerations			Magnitude (Micro-g)
	X	Y	Z	
LVLH	0.03	0.01	1.44	1.44
XPOP	-1.24	0.10	0.36	1.30
YVV	-1.36	-0.24	1.77	2.24

Table 2. summarizes the magnitudes and directions of the acceleration vectors as measured by the PIMS program using SAMS triaxial heads. The measurements were all obtained during May and July, 2004. Note the reported values were obtained during crew sleep periods. During waking periods the same trends can be seen but are superimposed with a great deal of random noise from crew movement and activities.

4.6.1.2 Orientation of The Experimental Tank in The MSG Rack

It is expected that ZBOT experiment will be housed in the MSG rack. Fig (24) graphically shows the relative acceleration vectors for each attitude in the MSG rack. All the vectors tend to point upwards somewhat along the z-axis. The ZBOT test tank will be oriented in a manner that its top points in the +Z direction. This will allow all the vapor bubbles to collect at the top end, as desired, regardless of the attitude of the ISS. The bubbles might move slightly to one side or the other depending on the ISS attitude, but this is not a significant problem.

It should be noted the XPOP attitude has a periodic behavior, which means its average vector is not a good representation of its actual direction. The real XPOP vector orbits around the average vector as demonstrated in Fig. (25). This may prove to be experimentally unacceptable for ZBOT. Therefore, test runs will be limited to LVLH and/or YVV modes, both of which have better vector directions along the test tank anyway.

Finally, it should be noted that the expected attitudes of the ISS may change over time. Both the frequency of occurrence of LVLH, YVV, and XPOP may change, and new modes may be introduced. Furthermore, the MSG is currently scheduled to be moved from its rack location in the U.S. Laboratory module to the European Columbus module sometime in the future after this the Columbus module is launched. A new rack location will change all acceleration vectors and necessitate a completely new examination of the microgravity acceleration environment in the MSG and how ZBOT will be designed and oriented to accommodate it.

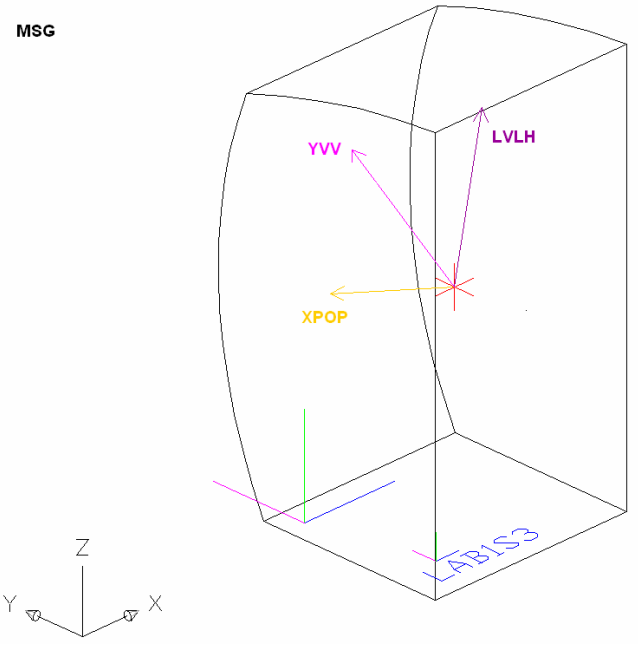

Figure 24. The Relative Acceleration Vectors For Each Attitude In The MSG Rack.

4.6.1.3 Microgravity Acceleration Measurement

The temporal variation of the magnitude and direction of the gravitational vector will be measured at a position as close as possible to the test rig. The acceleration measurement shall be made in the range of +/- 0.01 g, at a frequency of 3 Hz, with a resolution of 2.4 micro-g, a relative accuracy of 1.2 $(10)^{-5}$g, and an absolute accuracy of 5 $(10)^{-4}$ g.

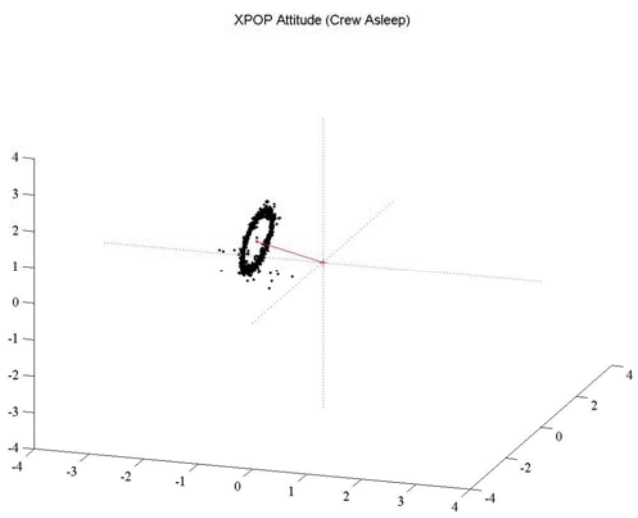

Figure 25. The Real XPOP Vector Orbiting around The Average Vector

4.6.2 The Microgravity Experiment: Tests & Procedures

Eight different testing categories are planned. These include; (1) self-pressurization tests; (2) mixing only tests; (3) subcooled jet tests; (4) cold finger cooling tests; (5) cold finger cooling with mixing tests; (6) cold wall tests; (7) cold wall with mixing tests; and (8) non-condensable gas tests. Before each test run the experimental tank must be prepared. Prior to tank preparation, it is assumed that the saturated liquid is in the test cell at the desired fill level. Before any of the experimental runs begin, the temperature of liquid inside the tank must be determined. All subsequent runs shall begin at this initial temperature to within +/- 0.25 C.

4.6.2.1 Tank Preparation

The following general steps are taken to prepare the tank before each test run in order to ensure that the tests are all started from a common initial state:

1. Set the jet temperature to the desired initial fluid temperature.
2. Set jet flow rate so that fluid will be well mixed.
3. Continue to run the jet until:
4. All thermal gradients have sufficiently decayed (i.e. until all thermistor temperatures are within +/- 0.25 ^{o}C of each other).
5. All thermistors are within +/- 0.25 ^{o}C of the desired starting temperature.
6. Turn on the heater power supply and set desired heat input.
7. Configure the data acquisition system to record desired.

4.6.2.2 Microgravity Tests

Brief descriptions of the microgravity test categories are as follows:

1. Self-Pressurization Tests: Isolate test cell from mixing/cooling loop by valving off the jet inlet and the tank outlet. At time = 0, turn on the heater and record measurements. After a prescribed pressurization time, turn off the heaters and go back to step #1 to prep the tank for the next run.
2. Mixing Tests: Set desired jet speed. At time = 0, turn on the heaters allowing the tank to pressurize for a specified time period. After the pressurization time has elapsed, turn on the jet and continue to run until either the maximum allowable mixing time has elapsed or the tank pressure has returned to the initial pressure for this particular

experimental run. Turn off the heaters and jet and go back to step #1 to prep the tank for the next run.

3. Subcooled Jet Cooling/Mixing Tests: Specify heater power, jet inlet temperature and jet speed. Specify whether jet will be active during the entire run or whether an initial pressurization will occur. For mixing throughout, at time = 0, turn on the jet and heaters. After a specified elapsed time, turn off the jet and the heaters and return to step #1. For an initial pressurization, at time = 0, turn on the heaters allowing the system to pressurize. After the pressurization time as elapsed turn on the jet. Continue until either the maximum allowable mixing time has elapsed or the tank pressure has decayed to the initial pressure. Turn off jet and heaters and return to step #1.
4. Cold Finger Tests: Specify the desired cold finger temperature. Specify whether the cold finger will be active during the entire run or whether an initial pressurization will occur. For cooling throughout, at time = 0, activate the cold finger and heater. After a prescribed time, turn off the heaters and cold finger and go back to step #1 to prep the tank for the next run. For a run where an initial pressurization occurs, at time = 0 turn on the heaters to pressurize the tank. After the pressurization time has elapsed, turn on the cold finger. Continue until either the maximum allowable cooling time has elapsed or tank pressure has returned to the initial pressure. Turn off the heaters and cold finger and return to step #1.
5. Cold Finger Cooling with Mixing Tests: Specify heater power and the duty cycle for the mixer. At time = 0, activate the heaters, allowing the system to self-pressurize. After an elapsed pressurization time, activate the cold finger. Run the jet mixer at the specified duty cycle.
6. Cold wall Tests: Same as IV but performed with a cooled wall.
7. Cold Wall Cooling with Mixing: Same as V but performed with a cooled wall.
8. Non-Condensable Gas Effects: Open the feed line from the non-condensable gas source to the test cell and inject the non-condensable gas into ullage until desired mole fraction is reached (determined by monitoring the pressure). Close feed line and proceed to 1 or 3, depending on which test is being run.

4.6.3 Microgravity Test Matrix

The ISS experiment test matrix associated with the eight microgravity tests listed in section 4.6.2.2 is included in Appendix A.

4.6.4 Data Handling and Delivery

During Flight: The following data must be downloaded during flight after the initial proof test and at the end of each class of experiments:

1. Tank Pressure
2. Heat Powers
3. Fill Ratio
4. Temperature at all locations (inside and outside)
5. Ullage position
6. Inlet Jet Temperature
7. Tank Outlet Temperature
8. Jet Flow Rate
9. Cold Finger Temperature

10. Cold wall Temperature
11. Flow rate, Temperature, and Pressure of the Non-Condensable at Injection
12. Gravitational Acceleration Data
13. Temperature Field Visualization - LCT
14. Velocity Field Visualization-PIV

The digital temperature, velocity, and bubble location data should be compressed, recorded and delivered on DVD-R media. The rest of the (point) data should be delivered in ASCII format and recorded on DVD-R media.

Post-Flight: All local/point measurements of the temperature, pressure, flow rates (cold finger loop, jet loop), heater power, heat removal rate, tank fill fraction, and non-condensable mole fraction shall be stored in ASCII or binary format on the on-orbit hard drive and recorded in ASCII Format on DVD media for final delivery. All digital field data corresponding to velocity, temperature and ullage location will be stored on the hard-drive and recorded on DVD media for delivery.

4.6.5 Project Deliverables

The deliverables of this research are listed as follows:

- A small-scale stimulant fluid tank pressurization flight experiment.
- Validated and verified two-phase thermodynamic and CFD models for ZBO cryogenic storage tank to aid engineering design of future storage tanks.
    1. TTP model
    2. ALLVT model
    3. ALAV-LMT model
    4. ALAV-LST model
- Information with regard to 1g and microgravity time constants associated with pressurization, destratification, and pressure reduction through different mixing/cooling strategies. This allows the development of a simple but robust and optimized mixing/cooling mechanism and control scheme for dynamic pressure control.
- A science document containing valuable microgravity science data and CFD simulations expanding the two-phase flow, transport phenomena, and phase change knowledge and data base for the development of future space fluid storage technologies.
- An engineering document for future ZBO storage tank design showing the effects of**:**
    1. Pressure control through mixing alone.
    2. Pressure control through cooling alone.
    3. Pressure control through cooling and mixing.
    4. Heat removal/mixing strategies: subcooled jet; cold finger, cold wall
    5. Jet flow parameters (flow rate, temperature, intermittency).
    6. Heat input parameters (power).
    7. Tank fill levels.
    8. Non-condensable gas effects.

5. Success Criteria

Since both the proposed ground-based and microgravity experiments are quite broad and comprehensive a project success criteria is presented here in order to rank the need and priority

for all the different elements of this research effort. The elements that are considered and ranked are partitioned into four categories:

- Individual experimental studies
- Experimental capabilities
- Microgravity test matrix.
- Model validation

The elements in each category are ranked as to their necessity in order to achieve *Minimum Success*, *Success*, and *Complete Success* for the entire investigation. The success criteria for the individual experimental studies, the experimental capabilities, and model validation are presented in Tables 3, 4 and 5, respectively. The success rankings for the microgravity test matrix are included in the last column of the tables in Appendix A.

Table 3. Experimental Studies Success Criteria

Tests	Success Criteria (M) Minimum Success (S) Substantial Success (C) Complete Success
Bread Boarding	M
Ground Based Pressurization/Pressure Control	M
Ground Based Non-Condensable Tests	S
Drop Tower Tests	C
ISS Experiment	M

Table 4. Experimental Capabilities Success Criteria

Capability	Success Criteria (M) Minimum Success (S) Substantial Success (C) Complete Success
Local Pressure Measurements	M
Local Temperature Measurements	M
Flow Visualization	S
Visualization (Phase Distribution)	S
PIV	S
LCT	C
Subcooled Jet Mixing	M
Cold-Finger Cooling	C
Cold-Wall Cooling	S

Table 5. Modeling Validation/Verification Success Criteria	
Capability	Success Criteria (M) Minimum Success (S) Substantial Success (C) Complete Success
Pressurization	M
Pressure Control	M
Non-Condensable Effects	S
Non-Equilibrium Effects	M
Micro-Nucleation Model	C
Level Set Interface Capturing Model	C

6. Coordination with The NASA Cryo Working Group

The proposed research will be closely coordinated with key cryogenic engineering groups at NASA ARC, MSFC, KSC, and JSC as well as the Air Force and NIST. This will be done under the auspices of NASA's Cryogenic Technology Development Working Group. Through regular technical discussions and exchange, this forum will ensure that the scientific direction, developments, and findings of the present work remain relevant to the engineering aspects and strategic requirements of the current and future NASA space cryogenic storage tank facilities.

7. Management & Primary Personnel

The Principle Investigator, Dr. M. Kassemi, is the Deputy Chief Scientist for fluids at the National Center for Exploration Research (NCSER) with extensive background in theoretical and experimental investigation of transport phenomena in multi-phase processes and microgravity sciences. He has been PI on six previous NASA-NRA microgravity projects. In the proposed work, he will lead the development of the numerical models and the design of the experimental matrix and test procedures. He will coordinate the theoretical, experimental and visualization parts of the research. He will also be responsible for the overall supervision of the project in terms of reporting and budgeting.

Co-Investigator, Dr. David Chato, is one NASA GRC's lead researchers in the areas of cryogenic rocket fuel and low gravity fluid management. He currently leads the development of space based experimentation for the Exploration Systems Research and Technology strategic technical challenge of Deep Space Refueling in support of NASA's exploration initiative. He also acted as principal investigator for the recently flown Sloshsat experiment. In the current research effort, he will aid in the development of ZBOT's experimental design and procedures. He will also undertake the design and performance of the reduced gravity ullage penetration drop tower tests.

Research Collaborator, Stephen Barsi is a PhD candidate at Case Western Reserve University and a research associate at NCSER. He will help in extending and developing the capabilities of the numerical models to include two active fluid phases in the context of the Level-Set method. He will also perform the parametric numerical simulations needed for optimizing the experimental test design and procedures and for validating and verifying the numerical models.

Project Scientist, David Plachta, is a Senior Research Engineer, in the Propellant Systems Technology Branch at GRC where he leads the research, development, and testing of the cryogenic thermal control system and hardware design. As the chairman of the NASA Cryogenic Technology Development Working Group, he will play an important role to ensure that the

activities and findings of this research effort meet or exceeds the customer-defined transport and exploration requirements for cryogenic storage. He will also coordinate the activities and findings of this research effort with representatives from each of the other NASA centers as well as the Air Force and NIST.

8.0 Closure

Integral to all phases of human space and planetary expeditions is efficient, affordable and reliable cryogenic fluid management for use in propellant or life support systems. Tank pressurization presents a serious engineering problem for future space expeditions. The ZBO concept has evolved as a promising no-vent engineering strategy for controlling self-pressurization of the storage tanks. Implementation and optimization of the ZBO pressure control strategy cannot be accomplished empirically because:

1. The dynamic impact of many interacting transport phenomena on pressure reduction times are still not clear and need scientific clarification.
2. Empirical data for microgravity applications are scarce.
3. Comprehensive and customized numerical models for scale-up and microgravity predictions are not available.

These shortcomings must be addressed, before a costly large-scale microgravity technology validation prototype test can be properly designed and justifiably undertaken.

In this context, the major goals of the proposed research are as follows:

- Develop a small-scale simulant fluid experiment for both preliminary ground-based testing and subsequent flight experiments to obtain valuable microgravity empirical data.
- Develop, validate, and verify a two-phase CFD models for the ZBO cryo-storage tank.
- Build a science base for the future space storage tank engineering efforts by elucidating the roles of the various interacting transport and phase change phenomena through systematic scientific investigation.
- Show the feasibility of ZBO pressure control scheme for variable gravity applications.

These objectives will be accomplished through a coordinated hand-in-hand experimental-theoretical-numerical research program that involve both ground-based and microgravity experiments. The theoretical effort will consist of comprehensive scaling analyses, development of state-of-the-art two-phase CFD models for tank pressurization/pressure control, and a series of targeted parametric numerical simulations and sensitivity analyses. The experimental effort will consist of experimental prototype development for initial 1g and subsequent reduced gravity testing, and measurement and flow visualization experiments with a simulant fluid.

This comprehensive undertaking is greatly facilitated by the computational, experimental, and diagnostic capabilities that are provided by NASA GRC. The results of this research will provide an expanded scientific and engineering knowledge base for efficient cryogenic fluid storage in space that will ultimately lower the cost and increase the safety of future space expeditions.

9.0 References

Anderson, J.E.; Fester, D.S.; Czysz, P.M.; “Evaluation of Long-term Cryogenic Storage System Requirements”, *Advances in Cryogenic Engineering*, **35**, pp. 1725-1731, 2000.

Aydelott, J.C.; “Effect of Gravity on Self-Pressurization of Spherical Liquid-Hydrogen Tank”, NASA TN-D-4286, pp. 1-18, 1967.

Aydelott, J.C. “Axial Jet Mixing of Ethanol in Spherical Containers During Weightlessness”: NASA TM X-3380: April 1976

Aydelott, J.C.; “Axial Jet Mixing of Ethanol in Cylindrical Containers during Weightlessness”, NASA TP-1487, 1979.

Aydelott, J.C.: “Modeling of Space Vehicle Propellant Mixing” NASA TP-2107: January 1983

Bankoff, S.G.; “Asymptotic growth of a bubble in a liquid with uniform initial superheat,” *Appl. Sci. Res. A*, **12**, pp. 267-281, 1964.

Barsi, S, and Kassemi, M.,“A Tank Self-Pressurization Experiment Using a Model Fluid in Normal Gravity“, AIAA-2005-1143, The 43rd AIAA Aerospace Meeting, January 2005.

Barsi, S, and Kassemi, M.,“A Numerical Study of Tank Pressure Control in Reduced Gravity“, AIAA-2006-0936, The 44th AIAA Aerospace Meeting, January 2006.

Bentz, M.D., et al. “Tank Pressure Control Experiment - A Low-g Mixing Investigation,” AIAA 90-2376

Bentz, Michael D., “Tank pressure control in low gravity by jet mixing”, NASA-CR-191012, March 1993

Bentz, M. D; Knoll, R. H; Hasan, M. M; Lin, C. S.; “Low-g fluid mixing - Further results from the Tank Pressure Control Experiment” AIAA PAPER 93-2423, Jun. 1993

Bentz, Michael D, et. al. “Tank Pressure Control Experiment - Results of three space flights”, AIAA Paper 97-2816, July 1997

Birkhoff, G.; Margulies, R.S; Horning, W.A.; “Spherical bubble growth,” *Phys. Fluids*, **1**, pp. 201-204, 1958.

Borowski, S.; Modular Bimodal Nuclear Thermal Rocket Transfer Vehicle Design, http://stop.grc.nasa.gov, 2003.

Brackbill, J.; Kothe, D.B.; Zemach, D.; A Continuum Method for Modeling Surface Tension, *J. Comput. Phys.,* **100**, pp. 335-354, 1992.

Brocchini, M.; Peregrine, D.H.; The Dynamics of Turbulent Free Surfaces. Part 1. Description, *J. Fluid Mech.*, **449**,pp. 225-254, 2001a.

Brocchini, M.; Peregrine, D.H.; The Dynamics of Strong Turbulence at Free Surfaces. Part 2. Free-Surface Boundary Conditions, *J. Fluid Mech.,* **449**, pp. 225-290, 2001b.

Brown, J.S.; Sonin, A.A.; "Rate Correlation for Condensation of Pure Vapor on Turbulent Subcooled Liquid", *Int. J. Heat Mass Trans.,* **33 [9]** pp. 2001-2018, 1990.

Caiden, R., Fedkiw, R., Anderson, C., *A Numerical Method for Two-Phase Flow Consisting of Separate Compressible and Incompressible Regions*; **J. Comp. Phys.**, 166, 1-27 (2001).

Chato, D. J.; Marchetta, J.; Hochstein, J. I.; and Kassemi, M.; "Approaches to Validation of Models for Low Gravity Fluid Behavior," AIAA-2004-1150, January 2004.

Chopp, D.; *Computing Minimal Surface via Level Set Curvature Flow;* **J. Comp. Phys.;** 106, 77-91 (1993).

Chun, J.H.; Shimko, M.A.; Sonin, A.A.; "Vapor Condensation onto a Turbulent Liquid –2 Condensation Burst Instability at High Turbulence Intensities", *Int. J. Heat Mass Trans*, **29 [9]** 1986.

Dalle Donne, M.; Ferranti, M.P.; "The growth of vapor bubbles in superheated sodium," *Int. J. Heat Mass Transfer*, **18**, pp. 477-493, 1975.

Fedkiw, R., Aslam, T., Xu, S.; *A Non-Oscillatory Eulerian Approach to Interfaces in Multimaterial Flows (The Ghost Fluid Method)*; **J. Comp. Phys**., 152 457-492 (1999).

Gaston, L.; Kamara, A.; Bellet, M.; "An Arbitrary Lagrangian-Eulerian Finite Element Approach to NonSteady State Turbulent Fluid Flow with Application to Mould Filling in Casting", *Int. J. Numer. Meth. Fluids,* **34**, pp. 341-369, 2000.

Grayson, G.D.; Watts, D.A.; Jurns, J.M.; "Thermo-Fluid-Dynamic Modeling of a Contained Liquid in Variable Heating and Accelerating Environments", ASME FEDSM97-3567, 1997.

Grayson, G. and Lopez A., "Pressure Control Data Correlation- Final Report", Boeing Report, 2006.

Hasan, M.M.; Lin, C.S.; "Axisymmetric Confined Turbulent Jet Directed Towards the Liquid Surface from Below", AIAA-89-0712, 1989.

Hasan, Mohammad M., Lin, Chin S., Knoll, Richard H., and Bentz, Michael D., "Tank Pressure Control Experiment: Thermal Phenomena", NASA TP 3564, March 1996.

Hasselmann, K.; "On the Mass and Momentum Transfer between Short Gravity Waves and Larger Scale Motions", *J. Fluid Mech.,* **50**, pp. 189-205, 1971.

Hastings, LJ, et al, Spray Bar Zero-Gravity Vent System for On-Orbit Liquid Hydrogen Storage", NASA/TM 2003-212926.

Hochstein, J.I.; "Computational Modeling of Jet Induced Mixing of Cryogenic Propellants in Low-G", AIAA 84-1344, 1984.

Hung, R.J.; Shyu, K.L.; "Constant Reverse Thrust Activated Reorientation of Liquid Hydrogen with Geyser Initiation", *J. Spacecraft and Rockets*, **29 [2]** pp. 279-285, 1992.

Illinca, F.; Hetu, J.F.; "Finite element Solution of 3D Turbulent Flows Applied to Mold-Filling Problems", *Int. J. Numer. Meth. Fluids*, **34**, pp. 729-750, 2000.

Ji, H.C.; Schwartz, S.H.; Lovrich, T.N.; Hochstein, J.I.; "Experimental Verification of Scaling Parameters for Thermal Stratification", *J. Thermophysics and Heat Transfer*, **6 [3]** pp. 522-530, 1992.

Juric, D., and Tryggvason, G, "Computations of Boiling", Int. J. Multiphase Flow, **24** (1) pp. 387-410, 1998.

Kittel, P.; Plachta, D.W.; Propellant Preservation for Mars Missions, Advances in Cryogenic Engineering, **45** Ed. Shu et al.; Plenum Publishers, p. 443, 2000.

Labuntsov, D.A, and Kryukov, A.P, "Analysis of Intensive Evaporation and Condensation", Int J. Heat Mass Transfer, **22**, pp. 989-1022, 1979.

Kothe, D.B.; Mjolsness, C.R.; Torrey, M.D.; "RIPPLE: A Computer Program for Incompressible Flows with Free Surfaces", Los Alamos National Laboratory, LA-12007-MS, 1991.

Labus, T.L., Aydelott, J.C., Andracchio, C.R., "Effect of Baffles on Inflow Patterns in Spherical Containers During Weightlessness", NASA TMX-2670, November 1972.

Labus, Thomas L., "Liquid Jet Impingement Normal to a Disk in Zero Gravity", NASA TP 1017, August 1977.

Lin, C.S.; Hasan, M.M.; "Self-Pressurization of a Spherical Liquid Hydrogen Storage Tank in a Microgravity Environment", AIAA-92-0363, 1992.

Lin, C.S.; Hasan, M.M.; "Vapor Condensation on a Liquid Surface Due to Laminar Jet-Induced Mixing: The Effects of System Parameters", AIAA-90-0354, 1990.

Lin, C.S.; Hasan, M.M.; "Numerical Investigation of the Thermal Stratification in Cryogenic Tanks Subjected to Wall Heat Flux", AIAA-90-2375, 1990.

Lin, C.S.; Hasan, M.M.; "Self-Pressurization of a Spherical Liquid Hydrogen Storage Tank in a Microgravity Environment", AIAA-92-0363, 1992.

Lin, C.S.; Hasan, M.M.; Van Dresar, N.T.; "Experimental Investigation of Jet-Induced Mixing of a Large Liquid Hydrogen Storage Tank", AIAA-94-2079, 1994.

Liu, Ch.-H; "A Numerical Calculation of Time Dependant Dynamical Behavior of Liquid Propellants in a Microgravity Environment", *Microgravity Sci. Tech.,* **VII/2**, pp. 169-172, 1992.

Marchetta, J.; Hochstein, J.I.; "Modeling Magnetic Propellant Reorientation", AIAA 2000-0700, 2000.

Martin, JJ, and Hastings, L., "Large-Scale Liquid Hydrogen Testing of a Variable Density Multilayer Insulation with a Foam Substrate", NASA/TM-2001-211089.

Mikic, B.B.; Rohsenow, W.M.; Griffith, P.; "On bubble growth rates," *Int J. Heat Mass Transfer*, **13**, pp. 657-666, 1970.

Morgan, N.R.; *A New Liquid-Vapor Phase Transition Technique for the Level Set Method*; PhD Dissertation, Georgia Inst. Tech. (2005).

NCMR/GRC; Multiphase Flow in Space Power and Propulsion Workshop and Fluid Stability and Dynamics Workshop, (http://www.ncmr.org/events/multiphase) National Center for Microgravity Research, NASA Glenn Research Center, Cleveland, Ohio, May, 2003.

NCMR/GRC; Workshop on Research Needs In Fluids Management for the Human Exploration of Space, (http://www.ncmr.org/events/fluidsmgmt) National Center for Microgravity Research, NASA Glenn Research Center, Cleveland, Ohio, September 2000.

NCMR/GRC; Workshop on Research Needs in Space Thermal Systems and Processes for Human Exploration of Space, (http://microgravity.grc.nasa.gov/6712/thermal/workshop.html),National Center for Microgravity Research, NASA Glenn Research Center, Cleveland, Ohio, July 2000.

Osher, S.; Sethian, J.A.; "Fronts Propagating with Curvature Dependent Speed: Algorithms based on Hamilton-Jacobi Formulations", *J. Comp. Physics*, **79** pp. 12-49, 1988.

Ostrach, S. and Kamotani, Y., "Surface Tension Driven Convection Experiment (STDCE)," NASA Contractor Report 198476, 1996.

Panzarella, C., Kassemi, M.; "On the Validity of Purely Thermodynamic Descriptions of Two-Phase Cryogenic Fluid Storage", *J. Fluid Mech.*, **484** pp. 41-68, (2003).

Panzarella C., Plachta D, Kassemi, M. "Pressure control of large cryogenic tanks in microgravity," 20th Space Cryogenics Workshop 2003, Girdwood, Alaska. Also *Cryogenics*, **44**, pp. 475-483, 2004.

Panzarella, C, Kassemi, M, "Pressurization of spherical cryogenic tanks in microgravity," *Journal of Spacecraft and Rockets*, **42** (2), pp.299-308, 2005

Plachta, D.W.; "Hybrid Thermal Control Testing of a Cryogenic Propellant Tank", NASA TM-209389, 1999.

Plachta, D.; Kittel, P.; "An Update to Zero Boil-Off Cryogenic Propellant Storage Analysis Applied to Upper Stages or Depots in a LEO Environment", 38th AIAA/ASME/SAE/ASEE Joint Propulsion Conference, AIAA 2002-3589 2002.

Plesset, M.S.; Zwick, S.A.; "The growth of vapor bubbles in superheated liquids," *J. Appl. Phys.*, **25**, pp. 493-500, 1954.

Pong, L. and Moses, G.A., "Vapor Condensation in the Presence of a Noncondensable Gas", Phys. Fluids, **29,** (6), pp1796-1804, 1986.

Prosperetti, A.; Plesset, M.S.; "Vapour-bubble growth in a superheated liquid," *J. Fluid Mech.*, **85,** pp. 349-368, 1978.

Rodi, W., "Turbulence models and their application in hydraulics: a state of the art review" Int. Assoc. for Hydraulic Research, The Netherlands, 1980.

Salerno, L.J.; Kittel, P.; "Cryogenics and Human Exploration of Mars", *Cryogenics*, **39**, pp. 381-388, 1999.

Schrage, R.W., "Interphase Mass Transfer", Columbia University Press, New York, 1953.

Scriven, L.E.; "On the dynamics of phase growth," *Chem. Eng. Sci.*, **10**, pp. 1-13, 1959.

Schuster, J. R., Russ, E. J. and Wachter, J. P., "Cryogenic On-Orbit Liquid Depot Storage, and Transfer Satellite (COLD-SAT)" General Dynamics Space systems Division and Ford Aerospace Space Systems Division, NASA CR-185249, July 1990.

Sonin, A.A.; Shimko, M.A.; Chun, J.H.; "Vapor Condensation onto a Turbulent Liquid-1 The Steady Condensation Rate as a Function of Liquid Side Turbulence", *Int. J. Heat Mass Transfer*, **29 [9]**, pp. 1319-1332, 1986.

Spuckler, Charles M. "Liquid Inflow to Initially Empty Cylindrical Tanks in Low Gravity", NASA TMX-2613, August 1972.

Staskus, John V, "Liquid Inflow into a Baffled Cylindrical Tank during Weightlessness", NASA TM X-2598, August 1972.

Symons, E.P.; Nussle, R.C. and Abdalla, K.L. "Liquid Inflow to Initially Empty, Hemispherical Ended Cylinders during Weightlessness": NASA TN D 4628: June 1968

Symons, Eugene P., Nussle, Ralph C., "Observations of Interface Behavior during Inflow to an Elliptical Ended Cylinder in Weightlessness", NASA TM X-1719, January 1969

Symons, Eugene P. "Interface Stability during Liquid Inflow to Initially Empty Hemispherical Ended Cylinders in Weightlessness", NASA TM X-2003, April 1970

Symons, Eugene P., Staskus, John V., "Interface Stability during Liquid Inflow to Partially Full, Hemispherical Ended Cylinders in Weightlessness", NASA TM X-2348, August 1971.

Van Dresar, N.T.; Lin, C.S.; Hasan, M.M.; "Self-Pressurization of a Flight-Weight Liquid Hydrogen Tank: Effects of Fill Level at Low Wall Heat Flux", AIAA-92-0818, 1992.

Weislogel, M.M; "Survey of Present and Future Challenges in Low-g Fluids Transport Processes", NASA Contract Report, C-74461-N, 2003.

Zhang, H., Zheng, L.L., Prasad, V., Hou, T.Y.; *A Curvilinear Level Set Formulation for Highly Deformable Free Surface Problems with Application to Solidification*; Numerical Heat Transfer, Part B, 34, 1-20 (1998).

Zwick, S.A.; "The growth of vapor bubbles in a rapidly heated liquid," *Phys. Fluids*, **3**, pp. 685-692, 1960.

Appendix A

The Microgravity Test Matrix

The following eight tables provide the test matrix for the microgravity experiment and their associated success criteria. The rows that are highlighted in yellow represent tests that could possibly be moved to ground-based.

1. Pressurization

Test No.	Fill %	Total Heat Input (W)	Average Jet Speed (cm/s)	Jet Temp	Cold Finger Temp	N.C.G. Mole Fraction	(S)imultaneous/ Initial Pressurization (IP)	Success Criteria (M)inimum (S)ubstantial (C)omplete
I-1	50	1	-	-	-	0	-	M
I-2	75	1	-	-	-	0	-	M
I-3	95	0.5	-	-	-	0	-	M
I-4	95	0.75	-	-	-	0	-	M
I-5	95	1	-	-	-	0	-	M

2. Axial Jet Mixing

Test No.	Fill %	Total Heat Input (W)	Average Jet Speed +/- 2 cm/s	Jet Temp	Cold Finger Temp	N.C.G. Mole Fraction	(S) / (IP)	Success Criteria (M)inimum (S)ubstantial (C)omplete
II-1	75	1	5 cm/s	-	-	0	IP	S
II-2	95	0.5	5 cm/s	-	-	0	IP	S
II-3	95	0.75	5 cm/s	-	-	0	IP	S
II-4	95	1	1 cm/s	-	-	0	IP	S
II-5	95	1	2 cm/s	-	-	0	IP	S
II-6	95	1	3 cm/s	-	-	0	IP	S
II-7	95	1	5 cm/s	-	-	0	IP	S
II-8	95	1	10 cm/s	-	-	0	IP	S
II-9	95	1	20 cm/s	-	-	0	IP	C
II-10	95	1	25 cm/s	-	-	0	IP	C

3. Subcooled-Jet Mixing

Test No.	Fill %	Total Heat Input (W)	Average Jet Speed (cm/s)	Jet Temp	N.C.G. Mole Fraction	(S)/(IP)	Success Criteria (M)inimum (S)ubstantial (C)omplete
III-1	75	1	1	T_o	0	IP	M
III-2	75	1	5	T_o	0	IP	M
III-3	75	1	10	T_o	0	IP	M
III-4	95	0.5	10	T_o	0	IP	M
III-5	95	0.75	1	T_o	0	IP	M
III-6	95	0.75	5	T_o	0	IP	M
III-7	95	0.75	10	T_o	0	IP	M
III-8	95	0.75	10	T_o-2K	0	IP	M
III-9	95	0.75	10	T_o+2K	0	IP	M
III-10	95	1	1	T_o	0	IP	M
III-11	95	1	5	T_o	0	IP	M
III-12	95	1	10	T_o	0	IP	M
III-13	95	1	10	T_o-2K	0	IP	M
III-14	95	1	10	T_o+2K	0	IP	M
III-15	95	1	1	T_o	0	S	M
III-16	95	1	5	T_o	0	S	M
III-17	95	1	10	T_o	0	S	M
III-18	95	1	10	T_o-2K	0	S	M
III-19	95	1	10	T_o+2K	0	S	M

4. Cold-Finger Cooling

Test No.	Fill %	Total Heat Input (W)	Jet Speed (cm/s)	Jet Temp	Cold Finger Temp	N.C.G. Mole Fraction	(S) / (IP)	Success Criteria (M)inimum (S)ubstantial (C)omplete
IV-1	75	1	-	-	T_1	0	IP	C
IV-2	95	0.5	-	-	T_1	0	IP	C
IV-3	95	0.75	-	-	T_1	0	IP	C
IV-4	95	1	-	-	T_1	0	IP	C
IV-5	95	1	-	-	T_1	0	S	C
IV-6	95	1	-	-	T_2	0	IP	C
IV-7	95	1	-	-	T_2	0	S	C
IV-8	95	1	-	-	T_3	0	IP	C
IV-9	95	1	-	-	T_3	0	S	C

5. Cold-Finger Cooling + Axial Jet Mixing

Test No.	Fill %	Total Heat Input (W)	Jet Speed (cm/s)	Jet Temp	Cold Finger Temp (K)	N.C.G. Mole Fraction	(S)/ (IP)	Jet Duty Cycle	Success Criteria (M)inimum (S)ubstantial (C)omplete
V-1	75	1	10	-	T_1	0	IP	Continuous	C
V-2	75	1	10	-	T_1	0	IP	10 s/min	C
V-3	75	1	10	-	T_1	0	IP	1 m/10m	C
V-4	75	1	10	-	T_1	0	IP	5 m/10m	C
V-5	95	0.5	10	-	T_1	0	IP	Continuous	C
V-6	95	0.5	10	-	T_1	0	IP	10 s/min	C
V-7	95	0.5	10	-	T_1	0	IP	1 m/10m	C
V-8	95	0.5	10	-	T_1	0	IP	5 m/10m	C
V-9	95	0.75	10	-	T_1	0	IP	Continuous	C
V-10	95	1	10	-	T_1	0	IP	Continuous	C
V-11	95	1	10	-	T_1	0	IP	10 s/min	C
V-12	95	1	10	-	T_1	0	IP	1 m/10m	C
V-13	95	1	10	-	T_1	0	IP	5 m/10m	C

6. Cold-Wall Cooling

Test No.	Fill %	Total Heat Input (W)	Jet Speed (cm/s)	Jet Temp	Cold Wall Temp	N.C.G. Mole Fraction	(S) / (IP)	Success Criteria (M)inimum (S)ubstantial (C)omplete
VI-1	75	1	-	-	T_1	0	IP	S
VI-2	95	0.5	-	-	T_1	0	IP	S
VI-3	95	0.75	-	-	T_1	0	IP	S
VI-4	95	1	-	-	T_1	0	IP	S
VI-5	95	1	-	-	T_1	0	S	S
VI-6	95	1	-	-	T_2	0	IP	S
VI-7	95	1	-	-	T_2	0	S	S
VI-8	95	1	-	-	T_3	0	IP	S
VI-9	95	1	-	-	T_3	0	S	S

7. Cold-Wall Cooling + Axial Jet Mixing

Test No.	Fill %	Total Heat Input (W)	Jet Speed (cm/s)	Jet Temp	Cold Wall Temp	N.C.G. Mole Fraction	(S)/ (IP)	Jet Duty Cycle	Success Criteria (M)inimum (S)ubstantial (C)omplete
VII-1	75	1	10	-	T_1	0	IP	Continuous	C
VII-2	75	1	10	-	T_1	0	IP	10 s/min	C
VII-3	75	1	10	-	T_1	0	IP	1 m/10m	C
VII-4	75	1	10	-	T_1	0	IP	5 m/10m	C
VII-5	95	0.5	10	-	T_1	0	IP	Continuous	C
VII-6	95	0.5	10	-	T_1	0	IP	10 s/min	C
VII-7	95	0.5	10	-	T_1	0	IP	1 m/10m	C
VII-8	95	0.5	10	-	T_1	0	IP	5 m/10m	C
VII-9	95	0.75	10	-	T_1	0	IP	Continuous	C
VII-10	95	1	10	-	T_1	0	IP	Continuous	C
VII-11	95	1	10	-	T_1	0	IP	10 s/min	C
VII-12	95	1	10	-	T_1	0	IP	1 m/10m	C
VII-13	95	1	10	-	T_1	0	IP	5 m/10m	C

8. Non-Condensable Tests

Test No.	Fill %	Total Heat Input (W)	Jet Speed (cm/s)	Jet Temp	Cold Finger Temp (K)	N.C.G. Mole Fraction	(S)/ (IP)	Success Criteria (M)inimum (S)ubstantial (C)omplete
VIII-1	50	1	-	-	-	0.15	-	S
VIII-2	50	1	-	-	-	0.30	-	S
VIII-3	50	1	-	-	-	0.45	-	S
VIII-4	50	1	-	-	-	0.60	-	S
VIII-5	95	1	10	T_o	-	0.45	S	C
VIII-6	95	1	10	T_o	-	0.60	S	C
VIII-7	95	1	10	T_o	-	0.45	IP	C
VIII-8	95	1	10	T_o	-	0.60	IP	C
VIII-9	95	1	-	-	T_1	0.45	S	C
VIII-10	95	1	-	-	T_1	0.60	S	C
VIII-11	95	1	-	-	T_1	0.45	IP	C
VIII-12	95	1	-	-	T_1	0.60	IP	C

Appendix B

Review Panels Comments

NASA HQ Review Panel Comments

The HQ Review Panel: Leon Hastings (NASA MSFC), John Hochstein (University of Memphis), Gary Grayson (Boeing), Bernard Kutter (Lockheed Martin)

NASA Goddard Comments

The Goddard Review Panel: Susan Breon, the Cryogenics and Fluids Branch Members (NASA Goddard)

The Zero Boil-Off Tank (ZBOT) Experiment
Review Panel Comments

Summary

The review panel agrees that a small-scale flight experiment could be used to significantly assist the cryogenic fluid management (CFM) engineering community. However, as the proposal stands, it is very broad-based and attempts to address a comprehensive range of CFM subjects and issues. Consequently, the proposed effort is diffuse, lacks incisive focus, and is inconsistent with reasonable funding and schedule constraints. Further, a stronger awareness of past and current engineering technology efforts in the arena of reduced gravity pressure control needs to be infused into the proposal to avoid duplication of effort, better leverage available data (both analytical and experimental), and to enable more rapid progress/timely inputs to the engineering community. It is suggested that: 1) the CFM community would be better served by a significantly simplified experiment with more selective objectives; 2) engineering data and objectives, , need to be strengthened in the proposal; 3) the experiment fidelity must be sufficient to support analytical code validation, but scaling to actual tank geometries and thermodynamic/fluid conditions need to be more carefully addressed, including definition of scaling limits inherent in experiments like that proposed; 4) CFD modeling activities should take full advantage of existing/proven analytical modeling capabilities and be designed for incorporation in already existing commercial CFD codes so that improvements can be made available as “Public Domain” information 5) rename the program to remove the emphasis on a single concept or aspect of CFM, i.e. zero boiloff 6) consider envisioning the experiment hardware as an orbital test facility that can be utilized for multiple flights that address a series of CFM issues, some of which are to be defined as CFM technology continues to mature; 7) focus the initial flight test on the issue of reduced gravity propellant mixing.

In summary, it is recommended that the Space Station flight experiment be continued, but with more focused, simplified objectives. It is strongly believed that such an approach will improve chances for experiment success and enable more timely data delivery. Further details on Review Panel observations and recommendations are listed below.

Review Panel Comments

Zero Boiloff: Section 1.1 ” Ventless Cryogenic Fluid Management”

Long duration cryogenic storage is enabled by four elements:

Modeling
Thermal isolation
Pressure control
Active cooling

Any use of cryogenic propulsion beyond current geosynchronous orbit type capability requires improvements to the first three elements. Application of the fourth element, active cooling, is more constrained

as it depends on many mission and vehicle design issues, and most likely has stronger application potential in the Mars missions. Since passive storage is inherent with any cryogenic mission, including active cooling concepts, it is suggested that passive storage be NASA's first priority.

Analytical Modeling: Section 3.2, "The Tank Pressurization/Pressure Control Numerical Models", Section 4.0, "Proposed Work"

• Historic experience has demonstrated that in-house, non-commercial CFD codes are not conducive to utilization by the CFM community. The use of such codes by other than the originator becomes impractical when the originator changes jobs and/or because resources cannot be made available to continually staff, maintain, and assist others with the use of the code. Development of a new full-featured CFD code, which is based on the proposed Active-Liquid Lumped-Vapor Tank (ALLVT) model, would require a substantial investment and duplicates already existing commercial code capabilities to a significant degree. It is recommenced that any CFD modeling activities should be designed for incorporation in already existing commercial codes so that improvements can be made available as "Public Domain" information (subject to normal export control measures). The primary commercial codes currently used by the CFM community are FLOW-3D (Flow Sciences Corp.) and CFX (ANSYS Inc.), however, other commercial codes should be considered as well.

• As an example, FLOW-3D already simulates 7 of the 10 phenomena listed in 4.2.1 "Scientific Elucidation of Important Variable-Gravity Transport Phenomena". Two of the remaining three involve thermocapillary flow and probably can be resolved. The third addresses bulk boiling due to pressure reductions below the liquid saturation pressure, the effects of which have already been amply demonstrated during the S-IVB AS-203 flight experiment. Further details regarding existing FLOW-3D models and activities related to the proposal are described in Appendix B-1.

• The pressure control simulation examples are oriented more toward a scientific experiment as opposed to acquiring engineering data. The example pressure reduction periods of 5 hours to 45 days indicate a level that is too marginal for actual applications. Thermodynamic venting and/or mixing for techniques for in-space vehicles must be conservatively designed to substantially overwhelm tank heat leak variations and any analyses uncertainties, and assure pressure reduction periods more on the order of minutes as opposed to hours or days.

• The problems involved with scaling to large scale data and actual flight vehicle applications are not adequately reflected in the proposal. Large-scale cryogenic ground test data and flight vehicle comparisons would be more appropriate. Example flight data sources are the Centaur and Saturn S-IVB AS-203 LH2 flight experiment. Available ground test data involving reduced gravity pressure control and fluid mixing is quite extensive and involves LH2, LN2, and LO2 with and without helium pressurization. The cited references do not reflect the magnitude of pressure control engineering data that already exists and are heavily slanted toward science as opposed to engineering. Appendix B offers some related avenues that NASA should consider for assisting the CFM community that are outside the scope of a Space Station flight experiment.

• It is recognized that geometric scaling is not always possible with a small scale experiment. However, it is believed that improved scaling could be reflected in the proposed experiment hardware selections. The proposed jet nozzle position of one-half the tank diameter would place it at an impractical height of 15 feet in a 30 ft diameter vessel. Similarly the proposed nozzle diameter of 7%-10% of the tank ID would

scale to 2.1-3.0 ft. whereas an actual nozzle diameter of 1-2 inches is more likely. The proposed cold finger ID is 15%-28% of the tank ID, which scales to 4.5-8.4 ft and has a surface area that appears to be about 25% of the tank surface area, which is impractical. Further, it is suggested that the wall cooling or "broad area cooling" elements can best be addressed with larger scale ground testing.

• The proposed reduced gravity drop tower testing appears to be of limited value.

Initial Experiment Direction

It is strongly believed an experiment can be devised which will more strongly benefit the CFM community and expedite data delivery. Further, the emphasis on zero boiloff is considered premature. A suggested approach is to focus the initial experiment on reduced gravity fluid mixing. Initial testing could be with clean tanks and be used for basic code validation. Perhaps carefully selected, representative obstacles could be deployed within the tank during the mission after the "clean tank" testing. The suggested objective would be to discern unmixed areas that could lead to elevated temperatures and inadequate or marginal subcooling in actual applications. The capability to make geometry and liquid level changes while on-orbit would add substantial value, improve experiment efficiency. Further comments on the proposed experiment instrumentation are offered in Appendix C.

Appendix B-11
Existing FLOW-3D Analytical Models and Activities

As an example, much of the proposed development and validation work has already been done using the commercially available FLOW-3D software. Many of the comments could be applied to the CFX code and perhaps to other codes as well. The FLOW-3D CFD solver had been in existence and continually improved since 1987. For example, before modification of FLOW-3D under the Pressure Control Data Correlation (PCDC) contract NNM05AB18C, the code already had the proven capabilities for natural convection flow, turbulence, wall heating, liquid slosh, and surface tension all in 3 dimensions and with complex geometries.

Recent PCDC contract progress in 2005 and 2006 includes comparison of tank pressurization and thermodynamic vent system results for LH2 and LN2 in normal and low gravity. Ullage gases being addressed are hydrogen and nitrogen vapor (GH2 and GN2) plus non-condensable helium (He) gas. The recent low-gravity validation using S-IVB data demonstrated pressurization accuracy within 3.5% of the flight data and ullage temperature accuracy within 6% of the flight data for the 5000 second LH_2 self-pressurization period at about 10^{-4} g's. These results are documented in AIAA paper 2006-5258.

Specific comments regarding the current national capability for simulating each significant phenomenon/issues to be examined by the listed in section 4.2.1 of the proposal is the following:

1. The dynamic interaction between the intermittent forced jet flow and the
natural/thermocapillary convection in 1g and microgravity.
Demonstrated through the PCDC contract which addressed both axial jet and spray bars mixers (2003 & 2005)

2. The effect of the combined flow on the interfacial mass transfer.
Demonstrated with 2003 & 2005 PCDC models but the relative effects of forced versus natural convections were not compared - but the capability exists.

3. Determination of the relevant transport time constants for pressurization,
destratification and pressure reduction in both the 1g and microgravity environments.
Time constants were estimated for MSFC's multipurpose hydrogen test bed (MHTB) under the PCDC contract in 2003 and 2005. The validation work shows good pressurization accuracy for all but the smallest ullage volumes. Time constants accuracies for the depressurization and destratification were limited by spatial resolution and simulation run time constraints.

4. The existence and extent of thermocapillary convection in 1g and microgravity due to wall contact or due to presence of the non-condensable gas in the vapor.
This has not been performed under the PCDC contract, however, it can be simulated with the current tool set. In order to simulate thermocapillary effects with FLOW-3D suitable resolution at the interface is required. The code already has the wall heating and temperature dependent properties needed. Also, FLOW-3D is widely used in the ink jet printer industry which has similar temperature dependent surface-tension dominated effects to that in a cryogenic low-gravity tank.

5. The effect of a non-condensable gas in the vapor region on the evaporation/condensation process.
This is the subject of the most recent efforts on the 2005 PCDC contract. In March 2006 the non-condensable ullage modification to FLOW-3D was completed providing the capability to simulate a cryogenic liquid with its own vapor and a non-condensable component. Currently, Boeing is modeling MHTB and Solar Thermal Upper Stage Technology Demonstrator (STUSTD) ground tests with He and GH2 or GN2 ullage gases and comparing the predictions to measured data. This current phase of the PCDC contract ends in March 2007.

6. The parametric range that natural convection and jet turbulences become an important factor affecting interfacial transport and tank pressurization in 1g.
In the PCDC contract different natural convection flows are created with various wall heat leaks. Two different TVS flow rates are simulated from each a spray bar and axial jet mixer. A k-epsilon turbulence model predicts turbulent effects both in the natural convection boundary layer and also at the forced convection jet inlets.

7. The impact of boil-off due to sudden heterogeneous or homogeneous nucleation and bubble growth.
This has not been previously simulated with the current tool set, however, there are features within FLOW-3D that can allow explosive boiling simulations. A superheat temperature difference may be input into FLOW-3D that prolongs vaporization beyond the saturation temperature. The model can initially be set to a specified superheat of say 20 degrees then boiling can be triggered by quickly ramping down the tolerable superheat in the model.

8. The dynamic interaction among an intermittent forced jet flow, a weakened natural convection and a pronounced thermocapillary convection in microgravity.

As described in #4 above thermocapillary effects can be simulated with enough computational cells using the current FLOW-3D tool "as is." The effect of adding varying forced or natural convection in the tank increases the model complexity and simulation run times but is expected to be achievable.

9. The effect of phase distribution (vapor location) on tank pressurization and pressure control.
This has been demonstrated and is inherently included in the low-gravity MHTB simulations reported in 2005.

10. The dynamic impact of g-jitter and impulse acceleration (frequency, magnitude, and direction) on vapor location and tank pressurization
The effects of vibration and highly dynamic environments on liquid motion are routinely included in propellant slosh models and have been since the early 1990's. This capability is already included in the standard release version of FLOW-3D.

Thus, based on the comments above it is recommended that the experimenters consider using the existing FLOW-3D-based tools that NASA has been developing for cryogenic tank modeling. As an alternative, the CFX code may eventually prove to have advantages, however, most experience is currently centered on FLOW-3D.

Appendix B-2
Related Avenues for Elevating CFM Technology Readiness

Full-Scale Flight Vehicle Experiments

Small scale orbital testing with a simulant liquid, although very helpful, cannot possibly address all the CFM issues. However, it should be recognized that opportunities exist for NASA to immediately begin to take advantage of the two flying cryogenic upper stages, Centaur and Delta IV. Non-intrusive type experiments can be used acquire large scale orbital CFM data on a relatively low cost and timely basis. Such flight demonstrations could range from simply adding flight instrumentation to potentially modified flight sequences and inclusion of improved hardware to support reduced boil-off. The use of multiple upper stage flights annually would allow NASA to answer many CFM questions cost effectively and develop accurate, relevant environment simulation tools that can be used to design future cryogenic stages in a time frame that supports the lunar missions.

Compilation of Existing Data

It is recommended that NASA initiate support for the assimilation of relevant open source CFM flight/test data into a comprehensive useful guide. Such a guide or report would be extremely useful to the entire CFM community, including industry, academia, and the government (NASA and DOD).

Appendix B-3
Instrumentation Comments

Particle Based Instrumentation Comments

Although visualization of the velocity fields and temperature fields would be of great value for validation, there may be risks with the particles influencing results. The present reviewer is not an expert on particle-based instrumentation but believes that the presence of particles could influence the thermal and momentum boundary layers which are more sensitive in reduced gravity. It would be unfortunate if the experiment were built and conducted in space only to have the results flawed.

Two recent flight experiments come to mind where there were similar problems. The recent magnetic liquid acquisition experiment on the KC-135 used iron particles in water to simulate a magnetically responsive fluid; here the low-gravity environment caused the liquid and entrained iron particles to coat the tank walls. The iron being opaque blocked the view of the liquid gas interface making the video data essentially worthless. A second experiment that I recall used surfactants in water to reduce the surface tension to achieve the dynamic scaling needed; here the surfactants in low-gravity formed a froth that limited the visualization of the liquid motion.

One suggestion is to consider a focusing Schlieren system for the flow visualization. A focusing Schlieren will visually indicate lines of constant density gradient which when viewed in time can indicate velocity and temperature. It requires nothing inside the tank, only transparent windows at opposite sides of the test section.

Another possibility is to instrument one side of the tank with intrusive devices like thermocouples or thermisters and leave the other side of the tank bare. If the tank is heated symmetrically the effects of the sensors on the flow field may be deduced.

Temperature Measurements

It would be advantageous to have more internal radial temperature measurements, thus not just at the wall. It is recognized that it is difficult to do non-intrusively, but in low-gravity the temperature fields can be quite dynamic and more sensors between the walls and tank center may be advantageous for validation.

NASA Goddard Comments

10/31/06

1. We agree with the panel's summary comments on the ZBOT proposal. In particular, we would again emphasize the following:

   a. the need for focusing on the important zero g thermal behavior rather than zero boiloff in particular. There are systems that combine active and passive thermal control, but don't necessarily eliminate boil-off, that may be advantageous. Thermal design of cryopropellant tanks (although with active cooling) should have very high priority in technology development for Exploration. It is not clear that the proposed solution, circulating liquid through a cooled heat exchanger, has any greater merit than properly designing the thermal system with active and passive elements to prevent any part of the tank from reaching temperatures that would correspond to unacceptably high pressures.

   b. the use of commercially available codes wherever possible to increase the likelihood of the analysis software being used in the future. Working with the commercial developer can lead to proper integration of the new physics.

      2. We disagree with the panel comment that active cooling is not relevant to any near- or intermediate-term exploration (i.e., lunar) programs. The recent Propellant Options Team report states that cryopropellants will be needed for the LSAM Descent Module and may be advantageous for the Ascent Module. Given the open questions on loiter times and lunar outpost missions, active cooling must be pursued in support of the lunar missions as well.

3. One issue that was touched on briefly by a reviewer, but that we believe needs to be made much more forcibly is the need for a stronger case that the experiment can be scaled to the relevant parameter space. The experiment is different in dimensional scale by more than a factor of 30. The temperature is more than an order of magnitude higher than that of LH2. Presumably, many of the fluid properties such as heat of vaporization, specific heat, thermal conductivity, viscosity, etc., are also very different. The proposal does not make any attempt to demonstrate that non-dimensional parameters such as Reynolds number, Weber number, etc, are close enough to those in a full sized cryogenic tank that the tests are in a relevant region of the parameter space, and thus can be expected to observe the correct phenomena. The scaling information should be folded in with designing the experiment to obtain useful engineering data when scaled to a real system.

4. Finally, we have the following specific comments on the proposed experiments:

   a. The apparent heat flow leakage from analysis of the ground test results needs to be dealt with in the flight experiment. A better thermal insulation system for the experiment is required, especially for longer duration experiments.

   b. Appendix B-2: We agree that the capability for real hydrogen/oxygen on orbit experiments needs to be explored. See Dave Chato's final report on the Experiments for the Maturation of Deep Space Refueling Technology. This does not eliminate the need for the

proposed experiment. Such experiments would obviously be probing a relevant region of the parameter space, except that the heat loads would be much higher than in a cryogen tank designed for long term storage.

We were surprised and disappointed that the reviewers do not seem to know about Chato's final report which was released this year. (See the compilation of existing data comment.) It means that this report's existence was not well advertised.

c). On Appendix B-3, we agree with the comments on particle based measurements. It certainly needs to be demonstrated and a backup plan developed in case of problems like the ones mentioned before proceeding to implementation. We also agree with the proposed plan to measure the radial temperature distribution and check for interference of the thermometers with measurements. This could very well be the backup plan for the particle based thermometry.

APPENDIX C

Response to the ZBOT Review Panels' Comments

The Zero Boil-Off Tank (ZBOT) Experiment

Response to the ZBOT Review Panels' Comments

PI: Mo Kassemi
National Center for Space Exploration Research
NASA Glenn Research Center
Cleveland, Ohio 44135

Co-I: David Chato
NASA Glenn Research Center
Cleveland, Ohio 44135

The ZBOT Science & Engineering Teams: Bill Sheredy (Project Manager, NASA GRC), David Plachta (Project Scientist, NASA GRC), Steve Barsi (Research Associate, CWRU/NCSER), Chris Lant (ZIN Project Lead, ZIN Tech), Kevin Magee (ZIN Technical Lead, ZIN Tech)

The HQ Review Panel: Leon Hastings (NASA MSFC), John Hochstein (University of Memphis), Gary Grayson (Boeing), Bernard Kutter (Lockheed Martin)

The Goddard Review Panel: Susan Breon, the Cryogenics and Fluids Branch Members (NASA Goddard)

February 7, 2007

The Zero Boil-Off Tank (ZBOT) Experiment

Response to ZBOT Review Panel

We are very grateful for the time and effort invested by the Review Panel in producing a comprehensive, detailed, and thoughtful technical assessment of our proposal. We are glad that the panel was of the general opinion that the proposed small scale simulant fluid ISS flight experiment "*could be used to significantly assist the cryogenic fluid management (CFM) engineering community*". We have carefully reviewed all the comments and concerns of the review panel and have made a valiant attempt to revise the proposed experiment and the associated modeling effort in order to adhere to the reviewers' suggestions. We are confident that this process has resulted in a more focused and technically strong experiment and modeling effort with both scientific and engineering relevance and potential for important tangible impacts for NASA and the general CFM community.

In what follows we first list the Review Panel's comments and suggestions as extracted from the panel report (10/1/06). Next, we provide an item-by-item and detailed response to these comments. We then go over the additional comments and suggestions included in a review (10/31/06) performed by the Cryogenic Team at NASA Goddard and provide additional responses to address their concerns.

The Review Panel Comments:

The main comments and concerns of the Review Panel are extracted from the panel report (10/1/06). They were also explained and expanded upon during a subsequent teleconference in October 2006, and are as follows:

1. The CFM community would be better served by a significantly simplified experiment with more selective objectives.
2. The engineering data and objectives need to be strengthened in the proposal.
3. The experiment fidelity must be sufficient to support analytical code validation, but scaling to actual tank geometries and thermodynamic/fluid conditions need to be more carefully addressed, including definition of scaling limits inherent in experiments like that proposed.
4. CFD modeling activities should take full advantage of existing/proven analytical modeling capabilities and be designed for incorporation in already existing commercial CFD codes so that improvements can be made available as "Public Domain" information.
5. Rename the program to remove the emphasis on a single concept or aspect of CFM, i.e. Zero Boil-Off.
6. Consider envisioning the experiment hardware as an orbital test facility that can be utilized for multiple flights that address a series of CFM issues, some of which are to be defined as CFM technology continues to mature.
7. Focus the initial flight test on the issue of reduced gravity propellant mixing.

Response to Review Panel Comments

1. *The CFM community would be better served by a significantly simplified experiment with more selective objectives.*

We agree with the panel that the proposal as it stands is very broad-based. Indeed, because the proposal was written to cover a range of CFM issues and to be inclusive of different and sometimes conflicting ideas within the general CFM community, there is a real danger that the research effort will become diffuse and lack incisive focus. In order to remove this important shortcoming we decided to considerably reduce the original scope of the proposal and focus on the elements that the panel recommended as the first priority for the exploration mission. The eliminated elements are still quite important but less urgent and can be hopefully addressed by future targeted ISS experiments.

According to the Review Panel, long duration cryogenic storage is enabled by four elements; (a) Modeling; (b) Thermal isolation; (c) Pressure control; and (d) Active cooling. They find the first three elements relevant to essentially any cryogenic mission employing both passive and active storage but the last element only pertinent to active storage. The panel is of the opinion that since active storage is most likely only needed in further down the road missions such as the Mars expedition, its elements and issues are secondary in priority to elements and issues of passive storage that have more immediate applications in the near term NASA expeditions.

In agreement with the logic of the Review Panel's comments, we have decided to greatly simplify the proposed experiment by primarily focusing the research effort on the three suggested elements of passive pressure control – that is: (a) thermal isolation; (b) forced jet mixing; and (c) modeling. Therefore, the comprehensive active cooling study will be deferred to future ISS experiments and flight opportunities. This, in turn, implies the exclusion of the following sub-elements and their associated hardware: (a) cold finger cooling; (b) broad-area (wall) cooling; (c) cold finger cooling with intermittent mixing; and (d) broad-area (wall) cooling with intermittent mixing. Furthermore, all the ground-based and ISS non-condensable pressurization and pressure control studies and their associated hardware developments will also be eliminated, again, with the hope that they will be addressed by some targeted experiments in future. Finally, in order to further reduce the overall cost of the project and eliminate any possible redundancies, the ground-based drop tower mixing studies will not be considered at this time.

2. *The engineering data and objectives need to be strengthened in the proposal.*

The Review Panel had the following explicit suggestions with regard to strengthening the engineering relevance of the proposal:

a. *The cited references do not reflect the extent of pressure control engineering data that already exist. Comparison with available large-scale cryogenic ground test data and flight vehicle tests with and without helium pressurization must be made.*

   We believe that benchmarking against the existing large scale ground-based and flight tank pressurization test data should be an integral part of our model validation and verification process. This is especially true since we hope that the model that will be developed and validated as part of this research will serve as a valuable tool for tank

scale-up design operations in future. We are thankful to the panel for providing us with a list of relevant experiments and references. We will carefully go over each individual experiment and the associated test data for our validation effort. At this point we intend to perform the following large scale validation case studies from the list provided by the panel: LH2, LN2, and LO2 with and without helium pressurization.

b. Perform mixing tests with different fill levels.

We intend to perform an array of tests at two or three different fill levels (50%, 75%, and 90%). How the different fill levels will be attained is still subject to engineering design and decision. There are two competing engineering scenarios. In the first scenario, sealed tanks at different fill levels will be flown and sequentially inserted into the MSG test facility for each series of experimental runs. In the second scenario, the MSG facility will be equipped with a reservoir and associated fluid support loops to fill and empty the test cell to the desired pre-selected levels on orbit. There are pros and cons associated with each scenario but the final choice will be made early on and solely based on engineering efficiency as assessed during the initial experimental bread-boarding.

c. *Include mixing tests with carefully selected representative obstacles in order to discern the possibility of unmixed areas that could lead to elevated temperatures or inadequate or marginal subcooling during actual applications.*

From an engineering point of view, changing the internal geometry by inserting baffles into the test cell on-orbit produces tremendous complexities in the hardware that, in fact, runs against the ultimate desire of the panel to simplify the experiment. Thus, if the on-orbit filling scenario is selected changing geometry will not be possible. However, if the sealed tank scenario is adopted (as defined above), equipping one of the sealed tanks at a given fill level with inserted baffle structures is quite conceivable and will be definitely considered.

d. The nozzle position of ½ tank diameter is unrealistic.

The nozzle was inserted deep into the tank solely to visualize and study the entrainment vortices that may form at the outlet of the nozzle during forced mixing. We fully appreciate the Review Panel's concern that this causes an unrealistic engineering configuration, especially, for the lowest fill level case. But from a science and code/model validation point of view, we still believe that it is essential to visualize the flow at the jet outlet for different flow rates and observe and study the formation and nature of the entrainment vortices. This will provide valuable microgravity data, especially, since due to the recommended modifications the experiment is now truly focused on the microgravity jet mixing behavior. However, if the sealed tank version is adopted, we will address the panels concern by keeping the nozzle in its original (deep) position only for the high fill level test cells where there is still considerable distance between the nozzle tip and the ullage interface, and we will position the nozzle in the bottom of the test cells for the lower fill level tests.

e. The nozzle diameter 10% of tank diameter is unrealistic.

This point is well taken but it is not possible to preserve the nozzle to tank diameter ratios between the sub-scaled experiment and the actual tank unless a point source jet flow is

implemented in the test cell, which from an engineering perspective is not a possibility. The engineering team has concluded that a 3% jet to tank diameter ratio is the minimum possible ratio. We will strive to achieve this with our hardware design. Although, this is not an exact rendering of the actual situation, by proper adjustment of jet velocities we can still cover all the relevant jet Reynolds number and jet Weber number mixing and interface interaction regimes. (Please also see the response to item 4 below). However, The CFD models are not subject to hardware restrictions. Even if the nozzle is quite small, it can still be essentially modeled. From a conceptual point of view, the important parameters are the momentum flux and the flow regime of the jet both of which can be properly characterized by adhering to the relevant Weber and Reynolds numbers in the model.

f. *The proposed cold finger dimensions are impractical from a scaling point of view*.
The cold finger tests and hardware have been eliminated

3. *The experiment fidelity must be sufficient to support analytical code validation, but scaling to actual tank geometries and thermodynamic/fluid conditions need to be more carefully addressed, including definition of scaling limits inherent in experiments like that proposed.*

Scaling to an actual flight tank is an important aspect of ZBOT. It is generally well known that a complete geometric and dynamic similitude between a small simulant fluid experiment, such as ZBOT, and a large scale tank with cryogenic fluid is difficult. Unfortunately, the Microgravity Science Glovebox (MSG) facility aboard the International Space Station (ISS) does not allow for a larger test cell and the stringent ISS safety requirements makes flying even specially designed environmentally-friendly refrigerant fluids such as PNP (candidate ZBOT test fluid) extremely difficult. Thus, ISS experiments with actual cryogens are not in the realm of possibility. In this light, the approach ZBOT has taken to overcome this inherent shortcoming is to use the sub-scale and simulant fluid experiment to validate and verify the CFD model and then use the CFD model for scaling-up to the actual flight cryogenic storage system.

For the CFD tank model developed as part of this research effort to be truly validated and verified for the scale-up task, it must be benchmarked not only against the ground-based and microgravity data that are collected as part of this project, but also against considerable amount of ground-based and flight data that have been accumulated as a result of years of engineering prototyping and system validation experiments. In this regard, actual flight data are a rare and valuable commodity and it will be used for model validation as much as possible. Although we have to still be mindful that the existing flight test data, correspond to cases with much higher heat loads than required by current tank designs for the lunar architecture and where active mixers were not employed.

As mentioned, it is difficult for the proposed experiment to match the performance of the full scale hardware exactly, as is generally true with most subscale tests. This is the classical dilemma of model testing. Even a geometrically scaled model of actual flight hardware (which is impossible because the flight hardware has not been designed) may behave inaccurately, being laminar where the full scale flow is turbulent or being dominated by surface tension effects when the full scale system is not. Of course, the classical solution to this problem is dimensional analysis and use of non-dimensional numbers. Usually, it is more important to be in a similar regime than to match the magnitude of the dimensionless parameters exactly.

For stratification and natural convection, the important non-dimensional parameters are Grashof (Gr) and Rayleigh numbers (Ra). Table 7 shows a comparison between the ZBOT experiment and a 1m hydrogen tank with a heat load of about 1.5 watts (similar to proposed designs for the Crew Exploration Vehicle and Lunar Lander Ascent Module)

Table 7: Convection Comparison

G-Level (m/sec^2)	Gr, Hydrogen Tank (based on tank radius)	Gr, ZBOT (based on tank radius)	Ra, Hydrogen Tank (based on tank radius)	Ra, ZBOT (based on tank radius)
$9.81(10^{-4})$	$1.4x10^8$	$1.4x10^6$	$1.7x10^8$	$1.1\ x10^7$
$9.81(10^{-6})$	$1.4x10^6$	$1.4\ x10^4$	$1.7\ x10^6$	$1.1\ x10^5$

In any case, for Gr numbers which tend to be quite large, a variation of 1-2 orders of magnitude is not significant as both flows will be still in the same regime. The Ra numbers that represent the ratio of the natural convective to conductive heat transfer are even closer.

Bond number governs the shape of the free surface. For both ZBOT and a 1 m hydrogen tank, the Bond numbers are less than one leading to similar spherical equilibrium free surface shapes. The fact that the Bond number is less than one for both the ZBOT experiment and the 1m hydrogen tank in microgravity, also suggests that the interfacial dynamics and ullage breakup is governed by a balance between inertia and surface tension forces as represented by the Weber number.

Thus, for studying jet spread and mixing and its interaction with the ullage, the key dimensionless quantities are jet Reynolds and Weber numbers, as many prior investigators have also pointed out. Since both of these parameters depend on velocity, they cannot be varied independently with the same test fluid. Nevertheless, the present experiment is capable of covering a broad range. Table 8 shows the Reynolds and Weber numbers achievable with the ZBOT experiment. (Note: Reynolds number is based on nozzle diameter and Weber number is based on jet diameter at the free surface). Of particular importance is the ability to cover the various low-g mixing flow regimes that will be present in a real tank configuration. Hasan et al. (1996) found at We < 1 there was little disturbance to the free surface, at We 3-5 a geyser formed on the free surface but was constrained, at We > 5 the geyser was unconstrained, resulted in ullage breakup and a re-circulating flow pattern developed. Similarly, as shown in Table 8, ZBOT will study the full range of Reynolds number regimes from laminar, through transitional, to full turbulent flow.

Table 8: ZBOT Flow Regimes

Fill Ratio		75% full	95% full
Average Jet Speed (cm/s)	Re	We	We
1	179	0.004	0.002
2	357	0.017	0.008
5	893	0.108	0.051
10	1786	0.430	0.204
20	3572	1.721	0.815
25	4465	2.690	1.274

4. *The CFD modeling activities should take full advantage of existing/proven analytical modeling capabilities and be designed for incorporation in already existing commercial CFD codes so that improvements can be made available as "Public Domain" information.*

The comments and sentiments of the Review Panel with regard to the numerical modeling are quite valid and indeed very close to our own heart. The numerical modeling proposed here will not be akin to *reinventing the wheel* and will not produce a piece of code or a numerical model that will gather dust at a corner of a government laboratory. Our modeling group is unique at NASA Glenn Research Center in its close relationship over the past 20 years (since 1987) with the commercial CFD code companies. We were among the first license holders for FIDAP and FLUENT and have watched and indeed helped in many ways for these companies and others like CFD-ACE grow to the prominence they enjoy today. In the past, we have helped the developmental efforts of FIDAP, FLUENT, CFD-ACE and CFX through NASA supported SBIRs and contracts that were mostly monitored by our group. Currently, and for many years, we have been license-holders for FIDAP, FLUENT, CFD-ACE, CFX, FLOW3D and ADINA. During these years, our common modeling practice with the CFD codes, especially with FIDAP and FLUENT, has been to: (1) work with the code that is the best fit (as is) to solve the problem at hand; (2) enhance the capabilities of the code when needed, through in-house theoretical, computational, and UDF code/model development to better solve the problem at hand; and (3) encourage the commercial code company to incorporate (hard-code) the NASA developed models into their commercial CFD package. As a result, several important models presently in FIDAP and FLUENT in the areas of chemical vapor deposition, crystal growth, and radiation heat transfer were first developed and beta-tested by our group at Glenn. This is precisely the path that we intend to take with regard to the phase change and multiphase flow capabilities that will be developed and validated as part of the proposed research effort.

We have chosen FLUENT as the work horse for our computational work due to several distinct computational advantages. CFX is also still under serious consideration because of some of its inherent salient features. For many of our sub-models such as natural and Marangoni convection, species transport, turbulent natural convection, and turbulent forced jet, we intend to use FLUENT, as is, or with limited in-house development and computational intervention. However, we intend to develop the two-phase flow and phase change theory and model, entirely on our own based on the state-of-the-art scientific knowledge extracted from archival literature and independent from any existing commercial code capability or implementation. We intend to rigorously validate the phase change theory and model using the high fidelity ground-based and microgravity data acquired during this research effort. The validation process is complete and comprehensive only if it is inclusive of scale-up issues. Therefore, we will further validate the model against existing ground-based and flight engineering data obtained from actual tank prototype tests with real cryogens. Finally and most importantly, in order for the validation verification process to have archival and lasting value, it is important that the theory, the complete and detailed mathematical formulation, the computational implementation, the ground-based and microgravity data and experiment,

and the validation & verification process, be all individually peer-reviewed. It is also important that the peer review be accomplished through prominent and archival scientific mediums directly dealing with the scientific premise of the model (e.g. Journal of Fluid Mechanics, Physics of Fluids, etc) so that it bears the full extent of prominent and expert scientific scrutiny. The validated & verified model and the associated code and its underlying mathematical and theoretical formulation will then be available to the engineering and scientific community at large and can be incorporated into any CFD code such as FLUENT, CFX and FLOW3D for the benefit of the entire CFD and CFM communities.

With regard to code validation & verification, an important point must be emphasized and understood. Today, most of the multipurpose CFD codes, especially, the prominent ones mentioned above, have an impressive array of predictive capabilities. From a developmental point of view, these capabilities can be divided into two categories. First are capabilities that have been extracted from years of benchmarking and archival published work. Among these are, for example, the k-ε or k-ω models for turbulence, the Boussinesq model for natural convection or the mathematical formulations for surface tension driven Marangoni convection and contact line dynamics. Thus, when one refers to, for example, the k-ε turbulence model of FLUENT, it is a well known entity with well established supporting theory, definitive parametric limits of applicability, and precisely documented physical and computational virtues and pitfalls. This is an outcome of almost a quarter century of computational and experimental benchmarking and peer-reviewed evaluation and assessment by the thermal/fluids community.

The second category of capabilities in the multipurpose codes are those that have been formulated, developed, and implemented by the code company usually in response to the request of an individual user or a group of users for some niche application. As such, its theoretical background, the details of its mathematical formulation and its computational implementation are unknown and have not been subject to peer-reviewed scrutiny and proper scientific validation by the larger CFD or fluid physics communities. Often, these formulations are equipped with arbitrary engineering coefficients or parameters that have no measured or universally determined value. As such they can be arbitrarily specified, varied, or adjusted by the end-user to provide agreement with certain specific prototype tests. This might be fine for the immediate needs of a given engineering project or application. However, it is far from proper and systematic validation because it lacks generality.

Many of the sub-models of our tank problem such as natural and Marangoni convection, species transport, turbulent natural convection, turbulent forced jet, fall straight into the first category. For modeling these phenomena, as mentioned before, we intend to use FLUENT, as is, or with limited in-house development and integration. Needless to say, even well scrutinized capabilities such as the traditional engineering turbulence models provided by the CFD codes such as FLUENT must be still validated and verified – not for integrity of formulation and implementation because those have been peer-reviewed - but for proper usage and application for the problem at hand. Otherwise the error that is generated due to inappropriate application in one sub-model can propagate to other areas and will thereby skew the overall validation verification process.

For example, our own sub-model benchmarking of the various turbulent models provided by FLUENT for the cryogenic tank problem against published experimental benchmark data has revealed that the k-ε turbulent model of FLUENT does a very good job of predicting the spread of the turbulent mixing jet, but it is quite inadequate for modeling turbulent natural convection driven by very thin boundary layers at the tank wall. This is due to its strong reliance on a strict law of the wall, On the other hand, our benchmarking has also indicated that the k-ω turbulent model, because of its flexible law of the wall approach, is excellent for predicting the turbulent boundary layer driven natural convection in the tank but it is, indeed, quite poor in determining the turbulent jet spread. Thus, for the storage tank problem at hand, where both turbulent natural convection and a turbulent mixing jet co-exist, Menter's Shear Stress Transport (SST) turbulent model that is an innovative blend of the k-ε and k-ω models seems to be best suited. FLUENT and several other CFD codes provide the option of choosing the k-ε, k-ω, and Menter's SST turbulence models to their users. But expert judgment and careful and patient sub-model benchmarking are still needed to make the proper choice.

The phase change capabilities of Fluent, CFX and Flow3D all fall within the second category. That is, they have been developed for a niche application or specifically for a group of customers. The detailed physics, mathematical framework, and numerical formulations associated with these capabilities have never been adequately and widely published and they have not been properly peer-reviewed. Consequently, on one hand, these niche capabilities have not benefited from years of peer-reviewed scrutiny and scientific development, unlike the above mentioned turbulence models, for example. And on the other hand, the underlying assumptions and simplifications inherent in their formulation may not always be apparent to the end user. Thus, with regard to a niche or customized modeling capability such as liquid-vapor phase change, it is always wise and prudent not to be more confident than the code developers themselves. For example, the best person to cautions us against an absolute reliance on the phase change capability provided by FLOW3D is Flow Science's president and main developer, Tony Hirt, who after describing the Flow3D's phase change model (Flow3D report FSI-01-TN57) concludes: "*It is hoped that this model will prove itself useful in that it does account for the exchange of energy between a liquid and a vapor, whether or not the rate is exactly accurate may be of secondary importance*".

In summary, we believe that you cannot expect that the entire CFM community to be satisfied or limited to the use of a certain phase change capability/model provided by a certain commercial code, especially, when the theory and numerical computations associated with this capability is currently subject to intense research and scientific debate within the thermal/fluids community. Thus as mentioned before, we intend to develop the two-phase flow and phase change theory and the associated interfacial heat and mass transfer model entirely on our own based on the state-of-the-art scientific knowledge extracted from archival literature and independent from any existing commercial code capability or implementation. The underlying theory, the complete and detailed mathematical formulation, the computational implementation, the ground-based and microgravity data and experiment, and the validation verification process, will all be made available in the open literature and subject to pertinent scientific and engineering peer-review. As part of the present project, the validated & verified model will then be incorporated into FLUENT or CFX. Moreover, the associated code and its underlying

mathematical and theoretical formulation will be available to the CFM community and to the engineering and scientific communities at large to be incorporated by individual users or commercial code developers into any commercial or in-house CFD code.

5. *Rename the program to remove the emphasis on a single concept or aspect of CFM, i.e. Zero Boil-Off.*

The science and engineering teams are in many ways attached to the name ZBOT, but will consider and discuss this in the immediate future.

6. *Consider envisioning the experiment hardware as an orbital test facility that can be utilized for multiple flights that address a series of CFM issues, some of which are to be defined as CFM technology continues to mature.*

We are in full support of an orbital test facility that can be utilized to accommodate multiple microgravity tank experiments addressing various aspects and problems of CFM. In fact, as mentioned at several instances, we hope that those elements of ZBOT that were removed to increase the focus of the present experiment can be ultimately revived in the near future in the form of a series of experiments to be performed on such an orbital CFM facility. But unfortunately, these programmatic considerations are outside the scope and beyond the means and premise of the present proposed effort.

We are also in support of the two other ideas put forward in the same spirit by the panel: (a) assimilation of relevant open source CFM flight/test data into a comprehensive useful guide; and (b) non-intrusive flight demonstration tests on the flying cryogenic upper stages such as Centaur and Delta IV. Again, these suggestions although quite sound and of essential value to NASA, are outside the scope and means of the present work.

7. *Focus the initial flight test on the issue of reduced gravity propellant mixing.*

As mentioned above in our response to item 1, the present experiment is greatly simplified by primarily focusing the research effort on the three suggested elements of passive pressure control: thermal isolation, forced jet mixing of bulk liquid, and modeling. As a result all the studies, requirements and hardware associated with the other broader aspects of the original proposal have been eliminated. The eliminated items are as follows:

1. Cold finger cooling
2. Intermittent mixing with cold finger cooling
3. Broad area (wall) cooling
4. Intermittent mixing with Broad area (wall) cooling
5. Non-condensable pressurization studies
6. Non-condensable pressure control studies
7. Drop-Tower mixing studies

The resulting setup will still consist of a pressurized test cell, since no venting is allowed on the ISS. The test cell has to be maintained in thermal isolation from the rest of the

MSG. The liquid jet temperature must be controlled to provide consistent and relevant comparisons possible.

Response to NASA Goddard Review

We are grateful to the Goddard team for their time and effort in reviewing our proposal and for their comments and suggestions. We were glad to see they were, for the most part, in agreement with the assessments of the Review Panel. This made our task of revising the experiment much easier. There is a great deal of commonality between the comments and suggestions of the two review teams. Therefore, in the interest of time and space, whenever we feel that a particular suggestion of the Goddard team has already been adequately addressed by our response to the Review Panel we will simply refer to that particular item or items of our previous response.

The NASA Goddard Comments:

The main comments and concerns of the Goddard panel as extracted from the Goddard Review Report (10/31/06) are as follows:

1. We agree with the panel's summary comments on the ZBOT proposal. In particular, we would again emphasize the following:
   a. The need for focusing on the important zero g thermal behavior rather than zero-boil-off in particular. There are systems that combine active and passive thermal control, but don't necessarily eliminate boil-off, that may be advantageous. Thermal design of cryo-propellant tanks (although with active cooling) should have very high priority in technology development for Exploration. It is not clear that the proposed solution, circulating liquid through a cooled heat exchanger, has any greater merit than properly designing the thermal system with active and passive elements to prevent any part of the tank from reaching temperatures that would correspond to unacceptably high pressures.
   b. The use of commercially available codes wherever possible to increase the likelihood of the analysis software being used in the future. Working with the commercial developer can lead to proper integration of the new physics.

2. We disagree with the panel comment that active cooling is not relevant to any near- or intermediate-term exploration (i.e., lunar) programs. The recent Propellant Options Team report states that cryo-propellants will be needed for the LSAM Descent Module and may be advantageous for the Ascent Module. Given the open questions on loiter times and lunar outpost missions, active cooling must be pursued in support of the lunar missions as well.

3. One issue that was touched on briefly by a reviewer, but that we believe needs to be made much more forcibly is the need for a stronger case that the experiment can be scaled to the relevant parameter space. The experiment is different in dimensional scale by more than a factor of 30. The temperature is more than an order of magnitude higher than that of LH2. Presumably, many of the fluid properties such as heat of vaporization, specific heat, thermal conductivity, viscosity, etc., are also very different. The proposal does not make any attempt to demonstrate that non-dimensional parameters such as Reynolds number, Weber number, etc, are close enough to those in a full sized cryogenic

tank that the tests are in a relevant region of the parameter space, and thus can be expected to observe the correct phenomena. The scaling information should be folded in with designing the experiment to obtain useful engineering data when scaled to a real system.

4. Finally, we have the following specific comments on the proposed experiments:
    a. The apparent heat flow leakage from analysis of the ground test results needs to be dealt with in the flight experiment. A better thermal insulation system for the experiment is required, especially for longer duration experiments.
    b. Appendix B: We agree that the capability for real hydrogen/oxygen on orbit experiments needs to be explored. See Dave Chato's final report on the Experiments for the Maturation of Deep Space Refueling Technology. This does not eliminate the need for the proposed experiment. Such experiments would obviously be probing a relevant region of the parameter space, except that the heat loads would be much higher than in a cryogen tank designed for long term storage. We were surprised and disappointed that the reviewers do not seem to know about Chato's final report which was released this year. (See the compilation of existing data comment.) It means that this report's existence was not well advertised.

5. On Appendix C, we agree with the comments on particle based measurements. It certainly needs to be demonstrated and a backup plan developed in case of problems like the ones mentioned before proceeding to implementation. We also agree with the proposed plan to measure the radial temperature distribution and check for interference of the thermometers with measurements. This could very well be the backup plan for the particle based thermometry.

Response to NASA Goddard Comments

Our item-by-item response to the NASA Goddard comments is as follows:

1. *We agree with the panel's summary comments on the ZBOT proposal. In particular, we would again emphasize the following:*
    a. The need for focusing on the important zero g thermal behavior rather than zero-boil-off in particular. There are systems that combine active and passive thermal control, but don't necessarily eliminate boil-off, that may be advantageous. Thermal design of cryo-propellant tanks (although with active cooling) should have very high priority in technology development for Exploration. It is not clear that the proposed solution, circulating liquid through a cooled heat exchanger, has any greater merit than properly designing the thermal system with active and passive elements to prevent any part of the tank from reaching temperatures that would correspond to unacceptably high pressures.
    b. The use of commercially available codes wherever possible to increase the likelihood of the analysis software being used in the future. Working with the commercial developer can lead to proper integration of the new physics.

The proposal has been significantly revised to primarily focus the effort on thermal isolation, mixing of bulk liquid, and modeling. For the details please refer to item #1 and item #7 of our response to Review Panel. However we have to point out, that due to safety considerations and restrictions on the ISS, any study that we perform, including the mixing studies, must be carried out without venting. Thus we still have a pressurized vessel where any boil-off must be contained within the tank and cannot be vented.

Each active cooling mechanism has its own inherent advantages and disadvantages. We have made no judgment calls on this issue. Indeed, the original proposal was aimed at comparing, from a transport point of view (not technology point of view), four different cooling modes: (a) Intermittent jet cold finger; (b) Cold finger alone; (c) Broad area (wall) cooling (d) Broad area (wall) cooling with mixing. However, as mentioned above, these elements and the associated comparisons have now been eliminated in favor of simplifying the experiment.

Finally, please refer to item #4 of the response to the Panel Review with regard to the CFD modeling approach taken by the project.

2. *We disagree with the panel comment that active cooling is not relevant to any near- or intermediate-term exploration (i.e., lunar) programs. The recent Propellant Options Team report states that cryo-propellants will be needed for the LSAM Descent Module and may be advantageous for the Ascent Module. Given the open questions on loiter times and lunar outpost missions, active cooling must be pursued in support of the lunar missions as well.*

Again, we do not disagree with these comments and they are well taken. But active cooling strategies were eliminated from this effort following the Review Panel's suggestion in order to simplify the experiment. We have also come to believe and are convinced that simplifying the experiment and increasing its focus on mixing is wise and extremely important and beneficial to the ultimate success of the research, especially, with the imposed time and budgetary constraints. Hopefully, active cooling strategies such as broad area cooling can and will be dealt with in some future ISS experimental opportunity or ground-based research. However, since even in our modified experiment, we still have to thermally isolate the tank and control and fix the temperature of the liquid jet for consistency of mixing test runs, it is conceivable to run several of the mixing tests with the temperature of the jet fixed at one or two sub-cooled levels. In this way some valuable cooling data can be also obtained without any additional complexity in the hardware or the experiment.

3. *One issue that was touched on briefly by a reviewer, but that we believe needs to be made much more forcibly is the need for a stronger case that the experiment can be scaled to the relevant parameter space. The experiment is different in dimensional scale by more than a factor of 30. The temperature is more than an order of magnitude higher than that of LH2. Presumably, many of the fluid properties such as heat of vaporization, specific heat, thermal conductivity, viscosity, etc., are also very different. The proposal does not make any attempt to demonstrate that non-dimensional parameters such as Reynolds number, Weber number, etc, are close enough to those in a full sized cryogenic*

tank that the tests are in a relevant region of the parameter space, and thus can be expected to observe the correct phenomena. The scaling information should be folded in with designing the experiment to obtain useful engineering data when scaled to a real system.

Please refer to items #2 and #3 of our response to the Review Panel.

4. *Finally, we have the following specific comments on the proposed experiments:*

a. *The apparent heat flow leakage from analysis of the ground test results needs to be dealt with in the flight experiment. A better thermal insulation system for the experiment is required, especially for longer duration experiments.*

b. Appendix B: We agree that the capability for real hydrogen/oxygen on orbit experiments needs to be explored. See Dave Chato's final report on the Experiments for the Maturation of Deep Space Refueling Technology. This does not eliminate the need for the proposed experiment. Such experiments would obviously be probing a relevant region of the parameter space, except that the heat loads would be much higher than in a cryogen tank designed for long term storage.

The ZBOT thermal design is under review and subject to early experimental bread-boarding. The design team is exploring several improvements to the thermal design including MLI blankets and thermal optical coatings, as well as changing from high conductivity aluminum piping to stainless steel.

We are aware of the findings of Chato since he serves as a Co-PI on the ZBOT team. We would also like to see a real hydrogen/oxygen experiment and do not believe that conducting ZBOT prevents the possibility of carrying such experiments in future.

5. *On Appendix C, we agree with the comments on particle based measurements. It certainly needs to be demonstrated and a backup plan developed in case of problems like the ones mentioned before proceeding to implementation. We also agree with the proposed plan to measure the radial temperature distribution and check for interference of the thermometers with measurements. This could very well be the backup plan for the particle based thermometry*

We have three important bread-boarding experiments that will be completed before the RDR. These tests will assess: (a) the extent of thermal isolation; (b) the effect of foreign gas leakage into the sealed tank; and (c) the effect of the PIV particles. But contrary to the concerns expressed by the reviewers, we feel that the main source of concern is not whether the PIV particles affect the convective boundary layer as they are coated, less than ten microns, and density-matched, but whether they affect pressurization by acting as nucleation sites that promote homogeneous boiling.

The reviewer's comments with regard to using Schlieren techniques as a non-intrusive diagnostic technique for flow and temperature measurements are only partly valid when applied to the present experiment. We have a great deal of experience with Schlieren techniques in prior microgravity research ground-based fluid physics investigations such as *Bubble Dynamics on Heated Surfaces*. First, it is difficult to extract

local temperature data from Schlieren images because it is an optical technique that produces index of refraction interferograms produced by integrating the effect of temperature variations on the index of refraction along the laser viewing path. Conceptually, extraction of temperature data is sometimes possible through a mathematical operation known as Abel transformation. But in practice this is very hard to accomplish.

In our prior work (Kassemi & Rashidnia, Physics of Fluids, 2001), we found it easier to work backwards. That is, to compute numerical index of refraction interferograms by using an inverse Abel transform of the detailed temperature distributions provided by our Finite Element model. In other words, we incorporated the Schlieren diagnostic technique into our finite element model. The results were excellent and provided superb validation of the model by the experimental data.

This process, however, is only possible under certain strict geometric and symmetry conditions that are absent in the present experiment. In addition, it is only possible to extract velocity information from a sequence of Schlieren images for thermal and fluid fields that are steady. Again, this is a condition that does not hold in the present situation. Moreover, Schlieren techniques are optically more sensitive and require flat optical quality windows that complicate our safety requirements in light of the ISS safety panel's stringent pressure vessel and structural safety codes. Finally, from an engineering implementation perspective, PIV is based on a mature diagnostic technology that has been flown successfully several times on the shuttle as part of other microgravity fluid physics experiments and used in Drop Tower experiments. The ZBOT engineering team has valuable experience with the PIV instrumentations associated with the previous flight and drop tower hardware. Since both of these are not the case with regard to Schlieren, the developmental time for a flight experiment might be prohibitively longer.

In conclusion, the inherent advantage of the Schlieren technique as a diagnostic tool is that its interaction with the fluid is completely optical. But it seems, that in the view of all the above-mentioned considerations, moving to a Schlieren technique is unwise because of its unfavorable cost and developmental time, the added risk, and potential for lower performance compared to the PIV technique.